The Brain Response to Peripheral Inflammation

Alison McColl
BSc (Hons)

Submitted in fulfilment of the requirements for the degree
of Doctor of Philosophy

Institute of Infection, Immunity and Inflammation
College of Medical, Veterinary and Life Sciences
University of Glasgow

October 2015

Abstract

Communication between the immune system and the central nervous system (CNS) is becoming increasingly topical as evidence suggests the two systems are intricately linked. Although the brain is considered an 'immune-specialised' tissue, it is not free from the influences of the periphery. Recent data indicate that peripheral immune stimulation can significantly affect the CNS, and patients with chronic inflammatory diseases, including rheumatoid arthritis (RA) and psoriasis, are often further burdened by the onset of neuropsychiatric conditions such as major depressive disorder (MDD), schizophrenia and anxiety. However, despite increases in our understanding, the precise mechanisms underpinning this relationship remain unclear. Therefore, the aim of this thesis is to investigate the communication pathways that exist between the immune system and the nervous system and to enhance our understanding of this bidirectional relationship.

Using a well-characterised animal model of psoriasis-like skin inflammation, I have investigated the effects of cutaneous, peripheral inflammation on the brain. Psoriasis-like skin inflammation was induced in female C57BL/6 mice via the repeated application of Aldara cream to the shaved dorsal skin. Twenty-four hours after the fifth application, the transcriptional response in the brain was assessed and compared with mice treated with an aqueous control cream, using Affymetrix GeneChip arrays. The induction of target genes, identified using microarray analysis, was confirmed in an independent model using QPCR and was compared to the gene induction following a number of other inflammatory models, including a sterile model of cutaneous inflammation.

Transcriptional profiling techniques allowed me to identify a number of differentially expressed genes in the brains of Aldara- and Imiquimod (IMQ)-treated mice when compared with the brains of control mice. This response included a range of interferon-stimulated genes (ISGs) and chemokines that were not induced in the peripheral blood leukocytes (PBL), and occurred independently of an overt cytokine response in the PBL. The brain ISG and chemokine response was not detected following a sterile model of cutaneous inflammation or following the intraperitoneal administration of Imiquimod.

The central induction of a number of chemokines prompted the evaluation of immune cell infiltration into the brain parenchyma. In addition, the functional consequences of topical Aldara treatment, and the involvement of inflammatory chemokines, were determined by assessing dentate neurogenesis and burrowing behaviour in wild-type and ACKR2-deficient mice.

The transcriptional response following cutaneous IMQ-induced inflammation is indicative of a peripherally triggered inflammatory response in the brain. In addition, the data described in this thesis demonstrate a functional consequence of peripheral immune stimulation and suggest that cutaneous inflammation could modulate the recruitment of leukocytes to the brain. These data highlight a potential mechanism of TLR-dependent communication between the periphery and the brain that could be mediated through the activation of the afferent vagus nerve.

Table of Contents

List of Tables

List of Figures

Acknowledgments

I would firstly like to thank my two supervisors Professor Jonathan Cavanagh and Professor Gerry Graham for all their advice, encouragement and guidance throughout the course of my PhD project. This thesis would not have come to fruition without all your help and continued motivation. I would also like to thank the Dr. Mortimer and Theresa Sackler Foundation for providing the scholarship that funded this research project.

I would like to extend a big thank you to Dr Carolyn Thomson. You were there to guide me through the lab when I first arrived all those years ago and have taught me most of what I know now. I am glad we have become good friends, despite your tendency to throw causal insults my way, and I will never forget (or get over) ELISA days!

It has been a privilege to be a member of the Chemokine Research Group and the Sackler Group throughout my PhD and I must offer my thanks to every member, past and present, for every helping hand, for every after work pizza and beer, for every scientific debate and for every afternoon gossip! There are many of you in the lab who deserve a special mention of gratitude for making those terrible science days more bearable and for ensuring my PhD was littered with many a hilarious tea break, particularly on a Friday afternoon. Jen, Kenny, Simone, Louise, Kayleigh, Kay, Carolyn, Louis, Trish, Steven, Felix and Emma M- I hope we will continue to enjoy plenty of laughs together in the future and many more messy nights out!

To all my 'non-science' friends and my wonderful in-laws, thank you for all your support and encouragement. A special thanks to my amazing cousin-in-law Karen, for having the patience of a Saint whilst enduring all my moans!

Thank you to my best friend, Magnus. You taught me the importance of doing the things you love and if it wasn't for you I wouldn't be where I am now (I would be an accountant…). I wish you were here to celebrate this moment with me, but I am grateful for all the amazing times we shared and for the memories I have. I know you would be proud of me xxx.

I would also like to say a huge thank you to my wonderful family; my parents Anne and Malcolm, my brother Graham and my grandparents, Evelyn and Peter and Malcolm and Alice. You have all helped make me the person I am today and I hope you are proud of my achievements. You have always made sure I wanted for nothing and have supported the decisions I made, even if we didn't always see eye to eye. I am eternally grateful for all the help you have given me, from supporting my many trips abroad to helping me through University, even when it seemed like I would be an eternal student, so thank you. Grandpa Fergie, I don't know which of us will be more relieved that you no longer have to ask me if I have finished writing my dissertation yet. Happy reading!

Finally, to my lovely husband Ian. Thank you for giving me the opportunity to change your perception of 'tax-dodging students' when we met in the Garage all those years ago. I hope you have come to realise just how wonderful we all are! Thank you for showing (feigning) an interest in all the lab talks, posters, thesis chapters and general science chat I have made you endure and for all the home-cooked dinners you made the nights I was working late. Who knew you were capable of more than frozen food and microwave meals?! On a serious note, your support and friendship means the world to me and you always know how to make me laugh, even in the midst of writing when life felt like a hardship. I will always appreciate what we have. Love you lots, like plant pots.

Author's Declaration

I declare that the work described in this thesis is original and, except where explicit reference is made to the contribution of others, was generated entirely as a result of my own efforts. None of the data included in this thesis has been submitted for any other degree, either at the University of Glasgow, or at any other institution.

Signature: ....

Printed name: Alison McColl

List of Abbreviations

5

5-HT	Serotonin

A

Ab	Antibody
ACh	Acetylcholine
ACKR	Atypical chemokine receptor
ACTH	Adrenocorticotrophic hormone
AD	Alzheimer's disease
APC	Antigen presenting cell
ATP	Adenosine triphosphate

B

BBB	Blood-brain-barrier
BCR	B cell receptor
BCSFB	Blood-cerebrospinal fluid-barrier
BDI	Beck depression inventory
BDNF	Brain derived neurotrophic factor

C

CLR	C-type lectin receptor
CMV	Cytomegalovirus
CNS	Central nervous system
CRH	Corticotropin-releasing hormone

CRP	C-reactive protein
CSF	Cerebrospinal fluid
CTL	Cytotoxic T lymphocyte
CVO	Circumventricular organs

D

DAMP	Danger-associated molecular pattern
DAPTA	D-ala-peptide T-amide
DARC	Duffy antigen receptor for chemokines
DAVID	Database for annotation, visualization and integrated discovery
DC	Dendritic cell
DCX	Doublecortin

E

EAE	Experimental autoimmune Encephalomyelitis
EDTA	Ethylenediamine tetraacetic acid
ELISA	Enzyme linked immunosorbent assay
EtOH	Ethanol

F

FDR	False discovery rate

FGF	Fibroblast growth factor		IFIT	IFN-induced protein with
				tetratricopeptide repeats
G			IFITM	IFN-inducible
GC	Glucocorticoid			transmembrane
GCR	Glucocorticoid receptor		IFN	Interferon
gp120	Glycoprotein 120		IFNAR	IFN-α receptor
			IFNGR	IFN-γ receptor
H			IFNLR	IFN-λ receptor
HADS	Hospital Anxiety and		Ig	Immunoglobulin
			IL	Interleukin
	Depression Scale		IMQ	Imiquimod
Ham-D	Hamilton rating scale for		ISF	Interstitial fluid
			ISG	Interferon-stimulated
	depression			
HCl	Hydrochloric acid			gene
HIV	Human immunodeficiency virus			
			K	
HPA	Hypothalamic-pituitary-		KA	Kynurenic acid
			KP	Kynurenine pathway
	adrenal			
HSPC	haematopoietic stem/		KYN	Kynurenine
	progenitor cell			
			L	
I			L	Litre
i.c.v	Intracerebroventricular		LCMV	Lymphocytic
				choriomeningitis virus
IBD	Inflammatory bowel		LEC	Lymphatic endothelial cell
	disease		LPS	Lipopolysaccharide
ICAM	Intracellular adhesion		LRR	Leucine rich repeats
	molecule		LTA	Lipoteichoic acid
IDO	Idoleamine 2,3-			
	dioxygenase			

M

MDD	Major depressive disorder
MgSO4	Magnesium sulphate
MHC	Major histocompatibility complex
MS	Multiple sclerosis
MTC	Multiple testing correction

N

NA	Noradrenaline
NaCl	Sodium Chloride
NaOH	Sodium Hydroxide
NaHCO3	Sodium bicarbonate
NET	Neutrophil extracellular trap
NK	Natural killer
NLR	NOD-like receptor
NO	Nitric oxide
NTC	No template control

O

O.D	Optical density
OPC	Oligodendrocyte precursor cell

P

PAMP	Pathogen-associated molecular pattern

PASI	Psoriasis area and severity index score
PBL	Peripheral blood leukocyte
PBS	Phosphate buffered saline
PC	Principle component
PCA	Principle component analysis
pDC	Plasmacytoid dendritic cell
PGE2	Prostaglandins of the E2 series
PKC	Protein kinase C
PKR	Protein kinase receptor
PM	Perfect match
PNS	Peripheral nervous system
PRR	Pattern recognition receptor
PSGL-1	P-selectin glycoprotein ligand 1
PVM	Perivascular macrophage
PVN	Paraventricular nucleus

Q

QA	Quinolinic acid
QPCR	Quantitative polymerase chain reaction

R

RIN	RNA integrity number
RLR	RIG-1-like receptor
RMA	Robust multi-array average
ROS	Reactive oxygen species

S

SAA	Serum amyloid A
s.c	Subcutaneous
SDF-1	Stromal cell-derived factor 1
SFV	Semliki forest virus
SSRI	Selective serotonin reuptake inhibitor

T

TBI	Traumatic brain injury
T_{CM}	Central memory T cells
Th	T helper
TIR	Toll/ interleukin-1 receptor
TLR	Toll-like receptor
Tm	Memory T cells
Treg	Regulatory T cell
Trp	Tryptophan

U

UV	Ultraviolet

V

VCAM	Vascular cell adhesion molecule
VSV	Vesicular stomatitis virus

W

WNV	West Nile virus

Z

ZAP	zinc-finger antiviral protein

Chapter 1

Introduction

1 Introduction

1.1 Inflammation and depression

Major depressive disorder (MDD) and other psychiatric illnesses, including schizophrenia and anxiety, are a significant burden to our society. These conditions are not only associated with a negative psychosocial outlook but they are also a growing concern for the economy, as the cost of long-term treatment and loss of earnings is extensive[1-3]. Neuropsychiatric diseases are commonly associated with chronic inflammatory conditions and appear to have a close, and often co-morbid, relationship with inflammation and, in particular, with inflammatory cytokines[4-6]. However, the mechanisms underpinning this relationship are largely unknown and it remains to be understood how inflammation in the periphery can influence the brain and lead to the onset of neurological conditions. To try to understand this relationship, studies have been performed in which peripheral inflammation was induced in rodents to analyse the onset of sickness behaviours and depressive-like symptoms[7, 8]. However, in addition to many unanswered questions remaining, most of these studies have used potent systemic inflammatory stimuli that are not representative of the human, tissue-specific conditions that correlate with neuropsychiatric disorders. Therefore, the aim of this thesis is to investigate the brain response to tissue-specific, peripheral inflammation and to try to identify the mechanisms driving this relationship. It is hoped that in doing so, new therapeutic targets can be identified and novel treatment strategies can be established.

This introduction will provide an overview of the relevant components of the immune system and central nervous system (CNS), before going into detail about the current literature with regards to the mechanisms and implications of communication between the brain and the periphery.

1.2 The immune system

We live in a world surrounded by microorganisms which we come into contact with on a daily basis. The term microorganism refers to bacteria, viruses, parasites and fungi, and whilst a lot of these pose no threat to a healthy

individual, many have the potential to cause disease and are thus referred to as pathogenic microorganisms, or pathogens. Pathogens are often kept 'at bay' by a number of physical and chemical barriers, including epithelial barriers and mucous membranes of the gastrointestinal tract and respiratory system. However, should these barriers be breached, the immune system acts as our internal defence system ready to respond to, and neutralise, any threat. If a pathogen enters the tissues or circulation, it will encounter cells of the innate immune system. The innate immune system is considered the first line of defence and is always primed for a rapid response. As such, innate cells are constantly circulating between the blood, tissues and lymph, acting as a surveillance system to detect infection by pathogens[9]. In such circumstances, these first responders will target the pathogen for removal using a number of mechanisms, and will induce the recruitment of additional effector cells to the site of infection. If an infectious organism resists the initial defences of the innate response, these cells are also able to initiate an adaptive immune response. Unlike the innate immune system, which is both rapid and dynamic, an adaptive immune response takes days to develop and is there to support the innate immune system should it become overwhelmed. The adaptive immune response relies on lymphocytes to mount a pathogen-specific response through the activation of an array of T cell subsets and the generation of a diverse antibody repertoire. Uniquely, the adaptive immune system is able to generate immunological memory via highly specialised antigen receptors. Thus a faster, stronger, response will be mounted if the same pathogen is encountered in the future. The innate and adaptive immune systems work in concert to identify and overcome infectious agents, whilst minimising the damage caused to the body. These systems are essential to our survival and both will be discussed in more detail in the following sections.

1.2.1 Innate immune system

As mentioned, the innate immune system is considered to be the first line of defence and is always ready to mount a response when a pathogen has breached the body's physical barriers. This response, unlike that of the adaptive immune system, is non-specific and does not lead to long term immunological memory. The acute, innate, inflammatory response is characterised by a number of physical changes including pain, redness and oedema that are the result of

vascular dilation in the local area[10, 11]. This vasodilation causes an increase in blood flow but a decrease in blood velocity and thus allows an influx of leukocytes that will clear the pathogens and repair the area. In addition, the release of clotting factors will prevent the internal spread of a pathogen or serve to minimise blood loss depending on the nature of the insult.

1.2.1.1 Cells of the innate immune system

There are many cell types that are hallmarks of the innate immune system, including neutrophils, macrophages, dendritic cells (DCs) and natural killer (NK) cells[10]. With the exception of NK cells, which are of lymphoid lineage, innate cells are generated from myeloid progenitor cells derived from multipotent haematopoietic stem cells of the bone marrow[12].

Neutrophils

Neutrophils are considered the first immune cell to be recruited to sites of damage or microbial infection[10]. As first responders, neutrophils have a multi-faceted approach to fighting infection, including phagocytosis, cytokine secretion and degranulation[13]. Another mechanism that neutrophils have evolved to combat pathogens is the release of neutrophil extracellular traps (NETs). First descried by Brinkmann et al. in 2004[14], neutrophils can release their granule contents along with chromatin to form long fibres, or NETs, through the process of NETosis[15]. NETs help contain pathogens and inactivate their 'virulence factors' that they use to modify the function of host cells. They also contain several proteins that can kill or inhibit microbes[16].

Monocytes

Large reservoirs of monocytes reside in the spleen and bone marrow and circulate through the blood[17]. Upon sensing appropriate signals, monocytes can extravasate through the endothelium and into the tissues where they differentiate into either macrophages or monocyte-derived DCs. Monocytes therefore serve to replenish the pool of tissue-resident cells in both steady state and inflammation.

Macrophages

Macrophages reside in various tissues throughout the body and their turnover is reliant on derivation from infiltrating monocytes. However, with the deletion of several transcription factors, some tissue-resident macrophages may have the capacity to self-renew[18]. Macrophages, like neutrophils, ingest and consume dead cells, host cell debris and foreign material through the process of phagocytosis, and are also able to present antigen to cells of the adaptive immune system[10]. Under steady state conditions, macrophages produce large amounts of IL-10 in order to maintain tissue homeostasis; however when they sense danger, through an array of pattern recognition receptors (PRRs) or in response to certain cytokines, macrophages become activated. Activated macrophages have been divided into two subsets based on their function in aiding specific T-helper (Th) responses, however these M1 and M2 macrophages are not mutually exclusive and have demonstrated a degree of plasticity in their ability to switch from one to the other in response to environmental signals of the local milieu[19, 20].

Dendritic Cells

DCs possess extensive dendrites that are efficient in sampling the local environment in the search for pathogens. DCs share many of the antimicrobial qualities of neutrophils and macrophages and are important for innate immune defence. However, they are best known for their role as professional antigen presenting cells (APC). DCs are present in almost all tissues and organs and are capable of migrating out of the tissue, through the lymphatic vessels and into organised lymphoid tissues where they can present antigen to T cells[10]. As such, DCs are important for the activation of an adaptive immune response[21]. Increasing literature has highlighted the heterogeneity of this group of cells and a number of different classifications of DC subsets now exist based on their function and location; however the various classifications and their specific functions will not be discussed further and are reviewed by Merad et al[22].

Natural Killer Cells

NK cells are able to identify, and target, infected host cells and are activated in response to interferons (IFNs) and macrophage-derived cytokines[10]. NK cells produce perforin, allowing them to perforate local infected cells, and subsequently use these pores to insert granzymes into the target cell and induce apoptosis[23]. This is important with regards to virus-infected cells to insure that they are degraded from the inside, rather than being lysed and their potentially harmful contents exposed to the environment.

1.2.1.2 Pattern recognition receptors

It is important that the innate immune system can readily identify pathogens and other harmful agents. Should the immune system make an incorrect judgement, a misdirected immune response would be harmful to the host, as is the case in many autoimmune disorders. As such, the innate immune system has developed a method of identification that relies on a number of pattern recognition receptors[10, 24]. PRRs have evolved to recognise repeating patterns of molecular structure that are only found in pathogens, called pathogen-associated molecular patterns (PAMPs), as well as endogenous molecules released from damaged cells known as danger-associated molecular patterns (DAMPs)[25]. Binding of PRRs can lead to a number of responses depending on the type of receptor and the nature of binding. These include the induction of phagocytosis, chemotaxis to the site of infection, the production of effector molecules and the initiation of adaptive immunity[26]. There are four classes of PRR families; NOD-like receptors (NLRs), retinoic-acid inducible gene (RIG)-1-like receptors (RLRs), C-type lectin receptors (CLRs) and Toll-like receptors (TLRs)[25]. These families, along with their respective ligands, are outline in Table 1-1. NLRs and RLRs, which are found in the cytoplasm, are essential for recognising virus infected cells and result in the production of anti-viral IFNs[27]. CLRs are membrane bound receptors characterised by the presence of a carbohydrate-binding domain. CLRs recognise carbohydrate structures of bacteria, viruses and fungi[28]. With regards to this thesis, TLRs are the most important PRRs and are discussed in detail here.

Toll- like receptors

Arguably one of the most important features of the innate immune system is the TLR family. Charles Janeway coined the term PRR and first hypothesised that cells devised a mechanism of pathogen recognition in 1989[29, 30], but it wasn't until almost 10 years later that this system was identified. TLR4 was the first to be described as a human ortholog of *Drosophila* Toll, based on the presence of the Toll/interleukin-1 receptor (TIR)[31] motif. It is the extracellular leucine rich repeats (LRRs) of TLRs that allow these type 1 transmembrane glycoproteins to bind to PAMPs. As highlighted in Table 1-1, TLRs are found on both the plasma membrane and the membrane of endosomes/lysosomes, allowing them to recognise both intra- and inter- cellular PAMPs. Upon ligation of TLRs with their corresponding ligand, the TIRs will dimerise and will undergo a conformational change that is required for the recruitment of downstream signalling molecules[32, 33]. This triggers an intracellular signalling cascade that culminates in the transcription of genes encoding necessary mediators, such as inflammatory cytokines and chemokines. With the exception of TLR3, all TLRs signal in a MyD88-dependent manner to activate NF-κB and other transcription factors via a number of protein kinases; however some TLRs, including TLR4 and TLR7, have also developed alternative, MyD88-independent signalling pathways[33, 34]. TLRs recognise PAMPs and DAMPs not only to initiate an innate immune response. Through MyD88 deficiency, it has been shown that TLR signalling is necessary for mounting an effective Th1 adaptive immune response[35].

Table 1-1 PRRs, their cellular localisation and their known ligand

Pattern Recognition Receptor	Localisation	Ligand
TLRs		
TLR1	Plasma Membrane	Triacyl lipoprotein
TLR2	Plasma Membrane	Lipoprotein
TLR3	Endolysosome	dsRNA
TLR4	Plasma Membrane	LPS
TLR5	Plasma Membrane	Flagellin
TLR6	Plasma Membrane	Diacyl lipoprotein
TLR7 (hTLR8)	Endolysosome	ssRNA
TLR9	Endolysosome	CpG-DNA
TLR10	Endolysosome	Unknown
TLR11	Plasma Membrane	Profilin
TLR12	Plasma Membrane	Profilin
NLRs		
NOD1	Cytoplasm	iE-DAP
NOD2	Cytoplasm	MDP
RLRs		
RIG-1	Cytoplasm	Short dsRNA, 5'triphosphate dsRNA
MDA5	Cytoplasm	Long dsRNA
LGP2	Cytoplasm	Unknown
CLRs		
MINCLE	Plasma Membrane	SAP130
Dectin-1	Plasma Membrane	B-Glycan
Dectin-2	Plasma Membrane	B-Glycan

1.2.2 Adaptive immune system

The adaptive immune system is not as evolutionarily ancient as the innate immune system. Present only in vertebrates, the adaptive immune system is a lymphocyte-dependent, specific response and therefore takes days to develop[10]. The adaptive immune system combats pathogens which have overcome the innate immune response, using more 'pathogen-specific' targeting. Initiating an adaptive immune response relies on the presentation of pathogenic antigens in the context of major histocompatibility complex (MHC), along with a specific set of co-stimulatory molecules and cytokines, to T cells in the secondary lymphoid organs[36]. Antigen presentation subsequently activates the differentiation of a number of T cells, some of which have the potential to initiate the production of a pathogen-specific humoral (antibody) response. One key advantage of the

adaptive immune response is that it leads to immunological memory. As mentioned, this highly specialised phenomenon means that subsequent encounters with a pathogen will induce a much stronger and faster response.

1.2.2.1 Cells of the adaptive immune response

T cells

The field of T cell biology has been an area of great interest in recent years and has led to a marked expansion in our understanding. As such, many different subsets of T cells have now been identified that are characterised and grouped based on their diverse effector functions and molecular phenotype. The main groups are naïve T cells, cytotoxic T lymphocytes (CTL), regulatory T cells (Treg), memory T cells (Tm) and helper T cells (Th), and within each group more than one subset may exist[10]. To go into detail about all the subsets and their corresponding functions would be lengthy, and is not of specific relevance to this thesis, therefore a very brief overview will be given.

Most effector T cell subsets will differentiate from CD4$^+$ naïve T cells into Th cells, and their fate will depend on the cytokines present during polarisation[37, 38]. Amongst these subsets are the well-characterised Th1, Th2 and Th17 cells as well as Th22 and Th9 effector cells, which have been more recently described[39]. Th22 cells, although yet to be fully defined, have already been implicated in a number of inflammatory skin diseases[40-42], whereas Th9 cells produce IL-9 and are thought to be involved in the defence against extracellular parasites including nematodes[43-45]. The differentiation of CD8$^+$ cells into effector T cells is somewhat more straightforward. These cells will become CTLs and will produce perforin, granzymes and IFNγ to direct the killing of infected or transformed cells[46]. As such, they are particularly important with regards to viral infections and cancer immunology.

B cells and antibodies

B lymphocytes are formed in the bone marrow and are characterised by the possession of a B cell receptor (BCR), which exhibits specificity to one particular Ag[10]. B cells are not able to penetrate target cells directly so they are not useful

for virus-infected cell targeting or cancerous transformed cells. Instead, B cells are responsible for the production of large volumes of Ag-specific antibodies (Ab), or immunoglobulins (Ig), which are released into the circulation[47]. B cells can either be short lived Ab-producing cells that survive only a few days, long-lived plasma cells that compete for a space in survival niches in the bone marrow and spleen, or memory B cells that continue to circulate in the blood. The immunological memory conferred by long-lived plasma cells and memory B cells allows for rapid antibody secretion during secondary infections.

1.2.3 Cytokines of the innate and adaptive immune system

Cytokines are protein messengers that together act as an intercellular communication pathway[10]. They can be produced by both immune- and non-immune cells (including endothelial cells and fibroblasts) and they evoke a variety of biological activities by binding to receptors on responsive target cells[48]. Cytokines can be both pro- and anti- inflammatory and any one cytokine can act on many different cell types. Cytokines can act on the cell that produced them (autocrine), on nearby cells (paracrine) or, in some cases, on distant cells (endocrine). Cytokine is the name given to these proteins as a superfamily; however other names can be given based on particular cell targets or presumed functions of the individual cytokines. For example, lymphokines are cytokines produced by lymphocytes (T and B cells)[49] whereas the term interleukin (IL) refers to proteins produced by leukocytes that regulate immune responses[50]. As this thesis relates to the immune response in experimental models of inflammation, we will focus only on cytokines relevant to immune function and leukocyte migration.

1.2.3.1 Inflammatory Cytokines

There are three classic inflammatory cytokines that are characteristic of early immune activation; IL-1ß, IL-6 and TNFα. These cytokines act in autocrine, paracrine and endocrine manners to amplify and maintain the immune response[10]. Inflammatory cytokines influence the accelerated release of leukocytes from the bone marrow reserves and TNF upregulates vascular adhesion molecules on the endothelium, promoting the extravasation of circulating leukocytes into the inflamed tissues[11, 51]. In addition, inflammatory

cytokines are able to activate leukocytes, and non-immune cells, to produce more inflammatory proteins, thereby enhancing the local response. IL-1 and TNF are endogenous pyrogens which stimulate prostaglandin synthesis leading to a rise in body temperature[52]. This fever response can help evade thermosensitive pathogens and can also speed up certain metabolic processes. Inflammatory cytokines, specifically IL-6, are also able to induce the synthesis of acute-phase proteins by hepatocytes in the liver[53, 54]. These include C reactive protein (CRP), fibrinogen and serum amyloid A (SAA) protein, all of which are thought to promote the inflammatory response and the elimination of microbes.

Inflammatory cytokines can also induce a number of changes to subjective experience and behaviour to allow an ill individual to reorganise their priorities during acute inflammation[55]. These changes, which include fever, lethargy, hyperalgesia, social withdrawal and increased anxiety, are the result of a reorganisation of actions and perceptions and are together called sickness behaviours[56]. The involvement of these cytokines in the induction of sickness behaviours is evident from a number of studies[6, 8, 57], the details of which will be discussed in section 1.6.2.

1.2.3.2 Interferons

First discovered in 1957 by Isaac and Lindenmann[58], IFNs represent a number of proteins that are secreted by cells and are so called on the basis of their ability to interfere with viral proliferation in cells. IFNs were the first of the cytokines to be discovered and were among the first to be used therapeutically. There are three groups within the IFN family, differentiated by their receptor complexes; type I-, type II- and type III IFNs. To date, there are nine type I IFNs, four type III IFNs and only one type II IFN, IFNγ[59].

IFNγ production is restricted mainly to immune cells but it binds to the widely expressed IFN-γ receptor (IFNGR) and plays a number of important roles in immune regulation[60]. These include the activation of macrophages, the facilitation of Ag presentation and the differentiation of Th1 effector cells. Thus IFNγ is an important mediator of both the innate and adaptive immune systems. The importance of this type II IFN is demonstrated using genetic strains in which IFNγ production, or signalling, is inhibited[61]. Deficiency leads to increased

susceptibility to a number of intracellular pathogens, as well as loss of tumour control[62-64].

There are seven classes of Type I IFNs; IFNα, of which there are 13 human subtypes, IFNß, IFNκ, IFNε, IFNo, IFNδ and IFNτ[65]. All type I IFNs bind to the IFN α/ß receptor (IFNAR) and together exhibit a greater degree of complexity as they can have different effects in response to different pathogens. For example, Type I IFNs induce a protective inflammatory response to pathogens such as *Escherichia Coli* and *S. pneumonia*[66]. However, they have been shown to increase susceptibility to the likes of *L. monocytogenes*[67-69], *Salmonella enterica*[70] and *Staphylococcus aureus*[71] by supressing the innate immune response. This range of activity is primarily due to the multiple cellular responses that can result from the activation of IFN-stimulated genes (ISGs) and their downstream effectors[72]. Amongst other functions, Type I IFNs have the ability to mediate cellular damage and inflammation, induce differentiation and migration and inhibit proliferation and angiogenesis[73, 74].

Type III IFNs are the most recent to be discovered and are known to bind to the IFN-λ receptor (IFNLR) expressed on epithelial cells, but are not as well characterised as type I and II IFNs[75]. There are three type III IFNs; IFNλ1, IFNλ2 and IFNλ3, although a fourth member of the group, IFNλ4, has been recently described[76]. Type III IFNs are thought to share a number of common biological functions with type I IFNs, including anti-proliferative and anti-viral properties, which is perhaps surprising as type I and type III IFNs are produced in response to different stimuli and bind different receptors expressed on different cell types[75].

Interferon Stimulated Genes

The production of IFNs, as the result of PRR ligation, leads to the activation of the JAK-STAT signalling pathway and the transcription of a broad set of genes called interferon stimulated genes[77]. Hundreds of these genes have been identified using oligonucleotide arrays, however few have been extensively characterised in terms of their effector functions and those that have are mainly reliant on *in vitro* data[78]. *In vivo* experimentation, even with the use of knock-out mice, has been hindered by the redundancy of the ISG family, which has made it more difficult to decipher the specific functions of an individual gene.

Broadly however, ISGs and their products exhibit many antiviral functions and together they are able to interrupt almost any step of the viral lifecycle[79]. Those that have been further investigated include the IFN-inducible transmembrane (IFITM) family, that block endolysosomal-mediated virus entry into cells[80, 81], SOCS proteins and USP18 that are negative regulators of IFN signalling and zinc-finger antiviral protein (ZAP)[82, 83], and the IFN-induced protein with tetratricopeptide repeats (IFIT) family, the OAS-RNaseL pathway, and PKR which all interfere with viral translation[80, 84].

1.2.4 Chemokines

Chemokines, or chemotactic cytokines, are a family of cytokines that are defined by the presence of a highly conserved cysteine motif[85]. To date, more than 50 chemokines and receptors have been identified making the chemokine family the largest family amongst cytokines. Chemokines have been divided into four subfamilies based on the number and spacing of their conserved cysteine motif and are named CCL, CXCL, XCL and CX3CL (Figure 1-1)[86]. In 1987, the chemoattractant activity of CXCL8 in the recruitment of neutrophils was established, and subsequently chemokines have become best known for their ability to mediate directed chemotaxis[87-90]. Chemokines are classically involved in the regulation and migration of leukocytes; however they have been widely implicated in a number of other essential processes including angiogenesis[91], embryogenesis[92] and tissue repair[93]. Between 1995 and 1996 chemokines were also implicated in the pathogenesis of HIV when it was discovered that CCR5 and CXCR4 act as co-receptors for viral entry into host cells[94-98]. A chemokine receptor binding to its cognate ligand leads to a classical signalling cascade and downstream cellular changes. As well as being divided based on their structure, chemokines can be divided into two groups based on the context in which they function. Homeostatic chemokines are involved in a number of essential processes that help maintain the body in its steady state, whereas inflammatory chemokines are upregulated during an immune response and ensure the trafficking of leukocytes to and from sites of infection. However, it is important to note that this classification is not absolute as a number of chemokines exhibit dual-functions.
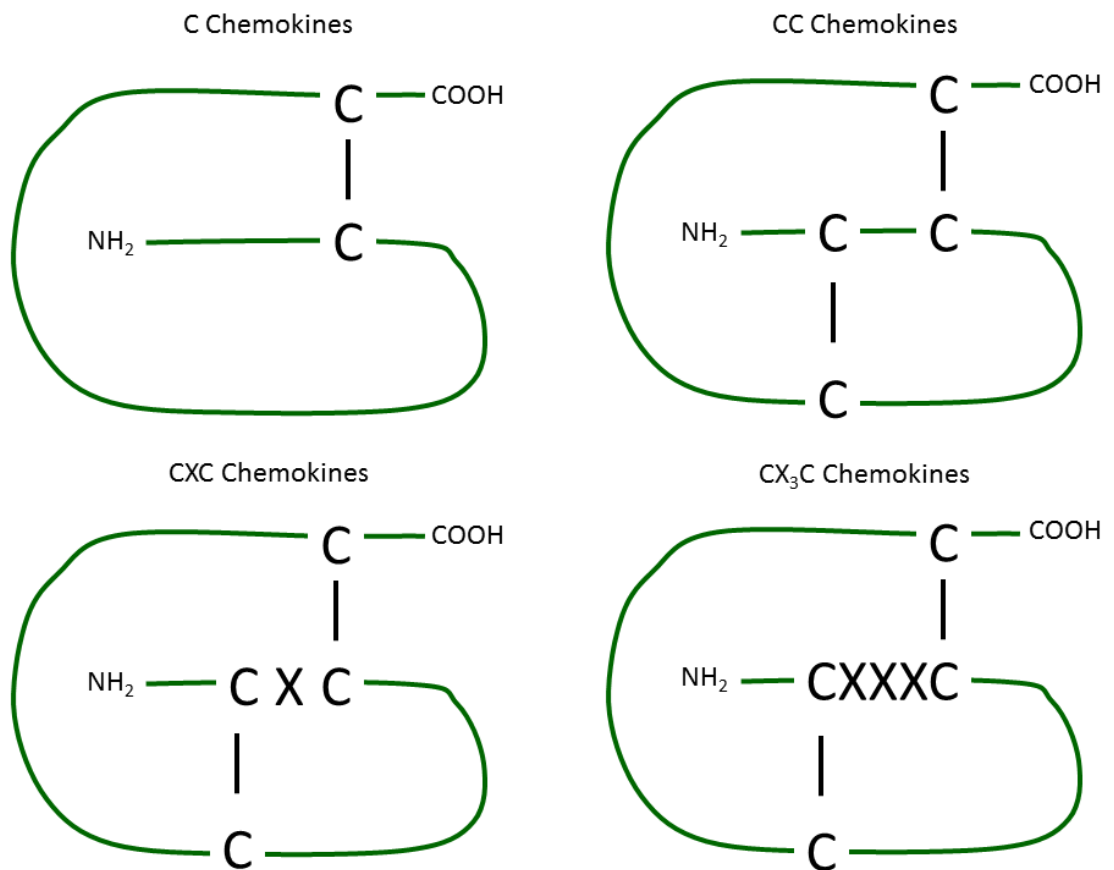
Figure 1-1 Structure of the conserved cysteine motif of the chemokine family
The chemokine family is based on the presence of a conserved cysteine motif. The four sub-groups of the chemokine family are so named based on the number and spacing of the cysteine residues as shown.

1.2.4.1 Homeostatic chemokines

Homeostatic chemokines are constitutively expressed in the steady state and are essential for regulating a number of key developmental and homeostatic functions. These include, but are not limited to, the homing of haematopoietic stem cells to their bone marrow niches[99], the direction and distribution of immature lymphocytes within lymphoid organs[100] and the control of stem and progenitor cell migration during organ development[92]. For example, CCL19 and CCL21 are constitutively expressed in the secondary lymphoid organs and, through their receptor, CCR7, serve to mediate interactions between DCs and T cells within lymphoid follicles[101, 102]. Such interactions are essential for regulating the immune system in the steady state and the importance of these chemokines is confirmed in the phenotypes of mutant mice. Mice deficient in CCR7 present with disruption in the spatial organisation of lymphoid organs, as well as a disruption in T cell and DC migration and an impaired ability to mount

an antigen-specific inflammatory response[102-104]. The CXCL12:CXCR4 axis is another important relationship with regards to homeostatic function. CXCL12, also known as stromal cell-derived factor 1 (SDF-1), was the first chemokine to evolve and is highly conserved across many species[105]. CXCL12 is essential for development as mice deficient in CXCL12, or its receptor CXCR4, die perinatally as the result of abnormalities in cerebellar neuronal migration and haematopoiesis[106, 107]. In addition to its involvement in development, CXCL12 regulates a number of essential steady-state processes in the mature CNS, and functions to maintain haematopoietic stem/progenitor cell (HSPC) homeostasis[108].

1.2.4.2 Inflammatory chemokines

Inflammatory chemokines are significantly upregulated in response to infection and inflammation, and are best known for their role in regulating the migration of appropriate leukocytes to sites of inflammation[109]. The chromosomal clustering of inflammatory chemokines suggests that they evolved rapidly in response to new pathogens, for example CC chemokines ligands 1-5 are found on chromosome 17, whereas CXC chemokine ligands 1-11 are clustered on chromosome 4[110]. Generally, inflammatory chemokines bind many receptors, conferring greater promiscuity than their homeostatic counterparts, which are normally restricted to just one or two receptors. For example, CCL5, which is of relevance to this thesis, binds three receptors, CCR1, CCR3 and CCR5[85]. This means that any cell type expressing any one of these receptors, which includes specific monocyte and T cell subsets, will be responsive to this chemokine ligand. Thus the expression of any inflammatory chemokine will result in the recruitment of a range of different cell types. Similarly, chemokine receptors are not necessarily restricted to any one chemokine ligand. Chemokines CXCL9-11 are IFN-inducible genes that all bind to the same receptor, CXCR3[85]. This receptor is predominantly expressed on activated T cells and so these chemokines are normally secreted during Th1 cell-mediated immune responses[111].

1.2.5 Chemokine receptors

Chemokines exert their function by binding to chemokine receptors. Chemokine receptors are G protein-coupled receptors which contain a seven transmembrane-spanning domain (Figure 1-2)[10]. All chemokine receptors have an approximate length of 350 amino acids and consist of an extracellular N-terminus and an intracellular C-terminus[109]. The N-terminal end, which binds to the chemokine, is important for ligand specificity, whereas the C-terminal end confers the intracellular signalling cascade following ligation. The DRYLAIV motif, found on the second intracellular loop of the receptor, is important for the coupling of G-proteins, which are necessary for mediating downstream signalling[112]. To date, 18 chemokine receptors have been identified which, like chemokines, are divided into four sub-families (CCR, CXCR, XCR and CX_3CR) based on the ligands they can bind to[113]. Chemokine receptors will only bind to ligands from one sub-family; however they can bind to several individual chemokines within that family. Receptors, like the ligands, can be divided into two groups based on their function; homeostatic and inflammatory. Inflammatory receptors bind to many different ligands, for example CCR5 and CXCR2 can both bind to as many as seven different ligands[85]. In contrast, homeostatic chemokine receptors are more faithful, often binding only one or two ligands. The full complexity of chemokine: receptor interaction is shown diagrammatically in Figure 1-3.
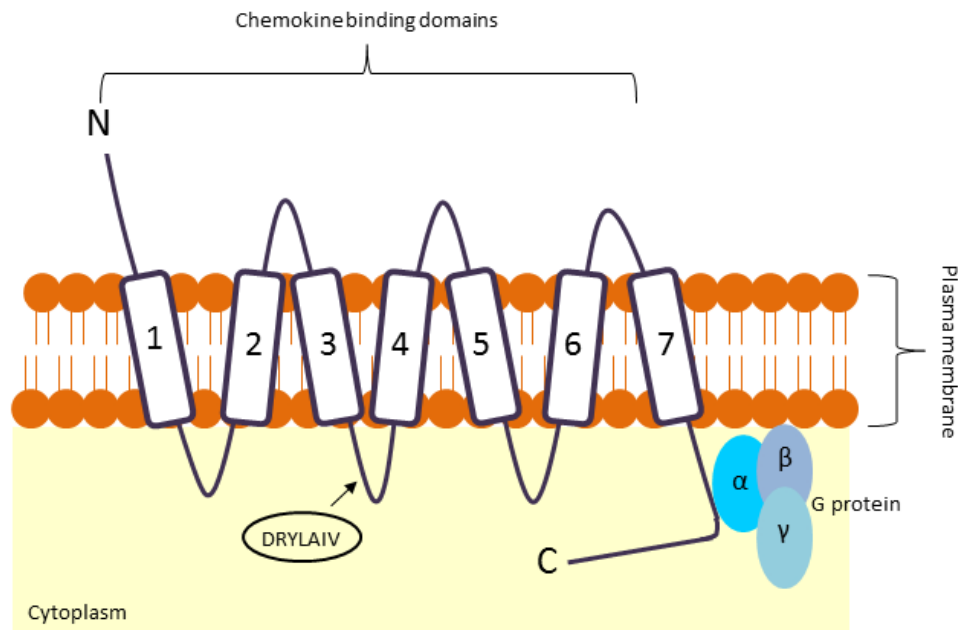
Figure 1-2 Schematic of a chemokine receptor
Chemokines exert their functions through ligation with chemokine receptors, which are seven transmembrane-spanning G protein-coupled receptors. Interactions involve multiple regions of the ligand and the receptor, with particular relevance for the N-terminal domains.

1.2.5.1 Atypical chemokine receptors

In addition to the chemokine receptors already mentioned, there are four receptors that are considered 'atypical' due to their lack of classical downstream signalling[114]. These atypical chemokine receptors (ACKRs) are called Duffy antigen receptor for chemokines (DARC), D6, CXCR7 and CCRL1, although a standard nomenclature has recently been developed and they are now known as ACKR1, ACKR2, ACKR3 and ACKR4, respectively[115]. ACKRs have a seven transmembrane spanning domain structure; however they are unable to couple with G-proteins due to the missing, or modified, DRYLAIV motif of the second intracellular loop[116]. Although ACKRs are considered 'silent', Boronni et al and Rajagopal et al have recently reported that ACKR2 and ACKR3, respectively, are able to signal downstream in a ß-arrestin-dependent, G-protein-independent manner[117, 118]. However, this signalling is unable to induce the classical cellular responses we see as the result of ligand binding to other chemokine receptors, such as cellular migration. ACKR1 and ACKR2 bind a large number of chemokine ligands that are exclusively inflammatory in function. As such, these ACKRs fine

tune chemokine ligand gradients by scavenging, storing or transpresenting ligand[116].

ACKR2

ACKR2, formerly known as D6, is one of four atypical chemokine receptors and is expressed on lymphatic endothelial cells (LECs), trophoblasts and some leukocytes[119, 120]. It binds many CC chemokines (Figure 1-3), all of which are classically inflammatory in nature. Upon ligation, ACKR2 will internalise and destroy its ligand before circulating back to the cell surface[121]. For this reason, its effects are considered anti-inflammatory, acting as a scavenger to clear inflammatory chemokines from the local milieu[120]. This proposed role of ACKR2 has been supported by a number of studies in a range of disease models. For example, ACKR2-deficient mice have been shown to be more susceptible to a range of skin based inflammatory pathologies[122], including chemically induced skin tumours[123].

With regards to the CNS, ACKR2 is highly expressed in the dentate gyrus of the hippocampus, a region of the brain that is classically associated with adult neurogenesis. However, its role in this location is unclear, with no clear abnormalities being seen in the ACKR2-null mice.
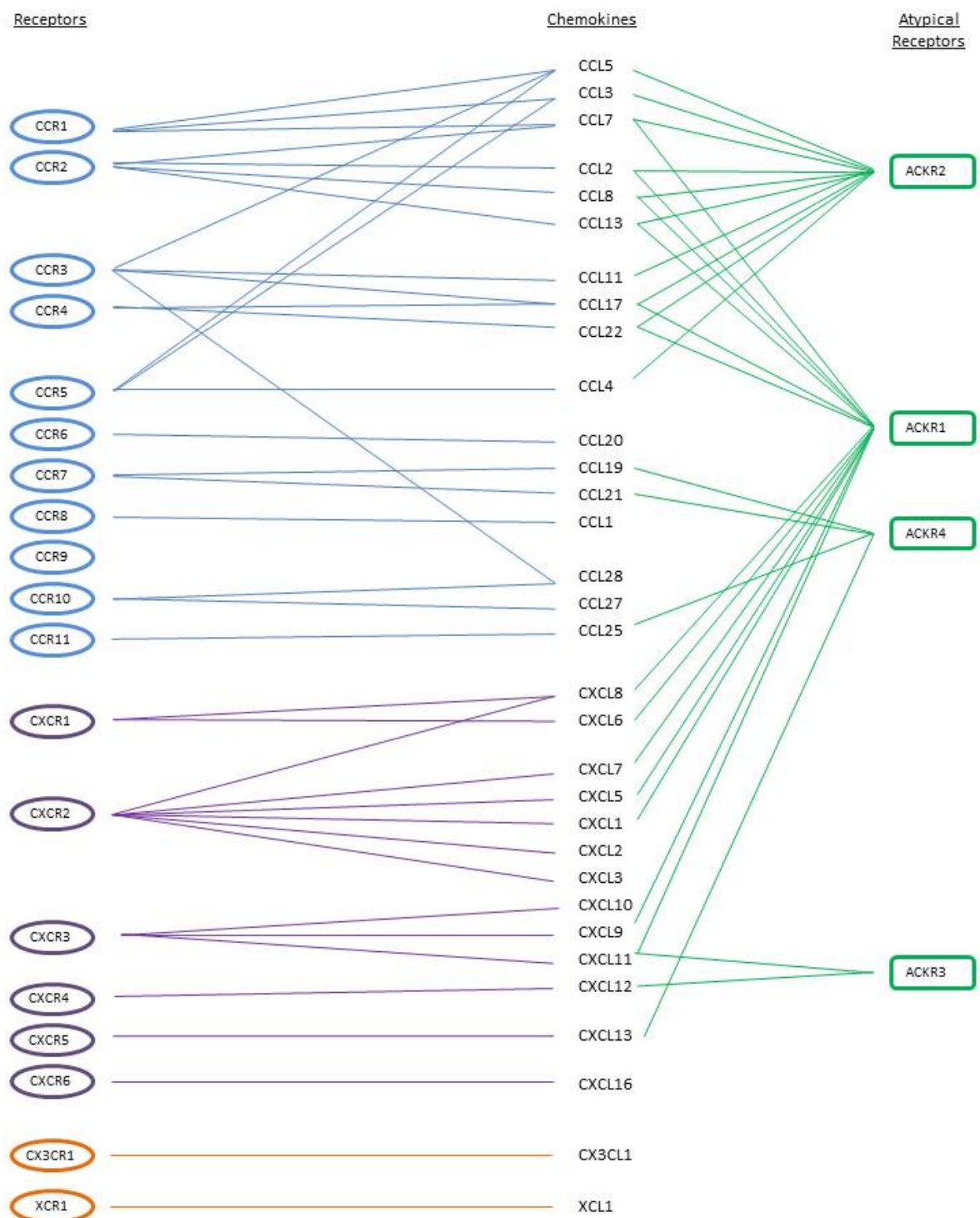
Figure 1-3 Complexity of chemokine family interactions
Chemokine receptor: ligand interactions and atypical chemokine receptor: ligand interactions, highlighting the complexity and promiscuity of the chemokine family. The colour corresponds to specific receptor subfamilies: CCR (blue), CXCR (purple), CX3CR/ XCR (orange) and ACKR (green).

1.2.6 Chemokines in disease

Chemokines and chemokine receptors are essential for the coordinated movement of leukocytes during inflammation and infection. During an acute response, the work of the chemokine family is, predominantly, beneficial to the host. However, in some cases of chronic inflammation or infection, chemokines can be detrimental and are therefore implicated in the pathogenesis of many diseases. The role of chemokines in CNS inflammation, which is particularly relevant to this thesis, is discussed in more detail in Section 1.4.3. In order to demonstrate the importance of chemokines, their role in some of the most prominent chemokine-mediated diseases is discussed here.

Human immunodeficiency virus (HIV)

HIV was isolated for the first time in 1983[124]; however it took over a decade for the mechanisms of transmission to be identified. To gain entry into host cells, the HIV-1 envelope glycoprotein 120 (gp120) must bind to CD4, along with one of two chemokine receptors that function as co-receptors[125]. CXCR4 and CCR5 were identified as the co-receptors that facilitate HIV entry into host cells after it was discovered that CCL3, CCL4 and CCL5, produced by CD8^{+} cells, were HIV-suppressive factors[94-98, 126, 127]. HIV-1 variants that use only CCR5 for entry are called R5, whereas those that use only CXCR4 as a co-receptor are referred to as X4. If a virus can use both chemokines as co-receptor, they are considered to be dual tropic and are called R5/X4[128]. During early infection, R5 tropic viruses dominate and are preferentially transmitted between hosts, whereas X4 viruses are more common during the later stages of the disease when patients progress towards AIDS[129].

A small percentage of the population have a naturally occurring mutation in the gene encoding for CCR5, called CCR5Δ32. Around 1% of the Caucasian population of European origin are homozygous for this 32bp deletion and are resistant to HIV as they do not express a functional CCR5 required for viral entry into host cells[130]. This mutation does not appear to have any adverse effects in healthy humans; however people possessing this mutation are thought to be more susceptible to severe forms of WNV[131].

Multiple sclerosis (MS) is an autoimmune disease characterised by the loss of motor and sensory functions as a result of demyelination and axonal damage[132]. MS can be either progressive or relapsing-remitting, with the latter characterised by periods of remyelination and amelioration; however MS will ultimately lead to paralysis. The pathogenesis of MS has been widely studied through the use of animal models, the most common of which is experimental autoimmune encephalomyelitis (EAE). This model is induced using myelin specific Th1 and Th17 cells, produced in response to immunisation with myelin oligodendrocytes glycoprotein (MOG) in combination with adjuvant, and is characterised by the influx of inflammatory leukocytes into the CNS[133].

Chemokines are important in the pathogenesis of MS and EAE, as discussed in Section 1.4.3. In brief, many chemokines and their receptors are highly upregulated in the brains of MS patients and in EAE mice. Mice deficient in the chemokine receptors CCR1, CCR2 and CCR6 display increased resistance to EAE, experiencing delayed onset of disease[134, 135]. However, Gaupp et al have suggested that the promiscuity of chemokines means CCR2 deficiency is compensated for with the increased expression of other chemokines[136].

1.3 Components of the central nervous system

The central nervous system consists of the brain and spinal cord, which are protected by the skull and vertebral column, respectively, along with three layers of membrane called the meninges. The CNS is the processing centre for the nervous system and it is responsible for relaying information to, and from, the peripheral nervous system. The brain controls both a number of very basic functions, including appetite, temperature regulation and coordination of movement, as well as more sophisticated functions such as cognition and memory. The CNS was once considered "immune-privileged", meaning it was isolated from events in the periphery, including those of the immune system. Nowadays, the CNS is thought to be "immune-specialised", the main difference being that people no longer consider the CNS separate from the rest of the body but rather unique, or specialised. This is for several reasons; it is protected from the periphery by a number of barriers, including the blood-brain-barrier (BBB)

and the blood-cerebrospinal fluid-barrier (BCSFB)[137] (Section 1.3.2), under steady-state conditions, it contains fewer APCs than other peripheral tissues[138] and, until very recently, it was thought to lack a lymphatic network[139, 140].

1.3.1 Cells of the central nervous system

1.3.1.1 Neurons

All cells in the nervous system interact with neurons and they are therefore considered the basic unit of the system. Neurons consist of a cell body containing the nucleus and organelles, branching dendrites, which communicate with neighbouring neurons and an axon, along which electrochemical nerve signals are conducted. There are three types of neuron, sensory neurons, motor neurons and interneurons, which differ in structure and location, but all function to carry nerve signals. Individual axons called nerves, along which information is transmitted, are protected by a layer of Schwann cell-produced myelin, which increases transmission speed. As mentioned earlier, the breakdown of myelin is a hallmark of multiple sclerosis, a debilitating neurodegenerative disease[132]. Neurons are generally considered to be terminally differentiated and unable to renew, highlighting the importance of their protection. However, it has been shown that adult neurogenesis does occur within specific brain regions[141, 142]. This will be discussed further in section 1.6.4.

1.3.1.2 Glia

Glial cells are distinguishable from nerves as they are not directly involved in synaptic transmission and electrical signalling, although they do function to support neurons in this role. In addition, glial cells modulate the response to neural injury, maintain the ionic milieu of nerve cells and provide a scaffold for certain aspects of neural development. The three subtypes of glia are discussed below.

Microglia

Representing around 10% of the adult brain cell population, microglia are tissue-resident macrophages that are found throughout the parenchyma. Like macrophages, microglia are phagocytic cells which possess the capacity to

become activated in response to various triggers and express low levels of many classic macrophage markers, including CD45, CD11b, F4/80 and MHC[143]. However, unlike conventional myeloid immune cells, terminally differentiated parenchymal microglia are thought to be derived from cells originating in the yolk sac in an IRF8- and PU.1- dependent manner, and are present in the embryonic brain from as early as E9.5[144]. Conventional CNS-microglia, derived from blood monocytes, can be found around the boundaries of the brain, for example in the choroid plexus, the meninges and the perivascular space[145]. Microglia are the only immune cells found within the parenchyma and are responsible for monitoring the intraneuronal space, which they do so by screening the local environment for damage every few hours with motile processes. When damage is sensed, perhaps via adenosine triphosphate (ATP) release by neighbouring cells or extracellular calcium, microglia enter an activated state and, like macrophages, can polarise towards M1- or M2- like phenotypes[146].

Microglia express many PRRs, including TLRs 1-9 and various scavenger receptors, and are thus able to respond to a wide range of pathogens, both viral and bacterial[147]. PRR ligation in microglia induces the synthesis of a number of pro-inflammatory cytokines including IL-1β, IL-6, IL-12 and TNFα as well as inflammatory chemokines[147]. Activated microglia are able to kill neurons directly or indirectly through the actions of these pro-inflammatory mediators. Their broad and generalised response to pathogens means that microglial activation is a hallmark of most CNS pathologies. To ensure that microglial activation itself is regulated, interactions between the neuronal CD200 receptor and the microglial CD200 ligand maintains microglia in a quiescent state[148, 149]. Mice deficient in CD200 show signs of spontaneous microglial activation and a disordered arrangement[150]. CX3CL1 is also thought to play an important role in maintaining microglia in a quiescent state under homeostatic conditions[151]. Cross-talk between neurons and microglia in a CX3CL1-dependent manner is thought to regulate neurogenesis (Section 1.6.4), synaptic plasticity, motor learning and cognitive function[152]. Aged rodents present with a reduced level of CX3CL1 expression, along with a reduction in neurogenesis and an increase in inflammation. When supplemented with CX3CL1, hippocampal neurogenesis is restored and microglia return to a resting state[153].

Astrocytes

Astrocytes, which are restricted to the brain and the spinal cord, are the most numerous and heterogeneous glia in the brain and are found in the extracellular spaces between neurons. In the healthy CNS, astrocytes are primarily responsible for maintaining a homeostatic chemical environment within these spaces in order to support neuronal signalling, and do so by regulating the concentration of substances including potassium ions[154, 155]. The expression of membrane neurotransmitter receptors, their ability to remove excess glutamate and their secretion of a number of gliotransmitters means that astrocytes are important for regulating neurotransmission and synapse function[156]. In addition, their close proximity to blood vessels, and their ability to produce proteins such as prostaglandins of the E2 series (PGE2) and nitric oxide (NO), allows them to control blood flow as well as to regulate energy exchange between the blood and surrounding cells[157, 158].

In the event of CNS injury or disease, astrocytes undergo a number of functional and cellular changes that together comprise the process of reactive astrogliosis. During reactive astrogliosis, astrocytes can lose, or gain, certain functions which can consequently exert either beneficial or detrimental effects on the environment, including glial scar formation[159]. Many intercellular components are capable of triggering reactive astrogliosis. These include, but are not limited to, inflammatory cytokines, TLR ligands, neurotransmitters, purines, reactive oxygen species (ROS), hypoxia and products of neurodegeneration, such as ß-amyloid[160-162]. All of these factors can be released by other CNS cells in response to a variety of insults. Activated actrocytes produce monocyte and neutrophil chemoattractants including CCL2, 3, 4 and 5 and CXCL1 and 2 respectively[161, 163]. Astrocytes may also upregulate adhesion molecules upon TLR ligation which, due to their anatomical location, can promote the ingress of circulating leukocytes from the perivascular space into the parenchyma.

Oligodendrocytes

Mature, myelin-producing oligodendrocytes derive from oligodendrocyte precursor cells (OPC) and are responsible for coating axons with the protective layers of membrane that are together called the myelin sheath[164]. Found only in

the CNS, oligodendrocytes can contribute to the myelination of several axons. Oligodendrocytes share many similarities with Schwann cells; however Schwann cells are found in the peripheral nervous system (PNS) and can myelinate only a single axon[165]. Myelin, which is distributed across the length of axons, with the exception of certain areas called the 'Nodes of Ranvier', provides electrical insulation and speeds up action potential propagation[166]. Therefore, disturbances in the myelin sheath, as the result of injury or disease, can have a profound effect on normal neural transmission[167, 168].

1.3.2 Barriers in the brain

As mentioned previously, the CNS is considered to be immune-specialised, in part due to the physical barriers that isolate it from the periphery. These barriers differ in terms of their anatomical location and cellular properties, and are discussed here.

1.3.2.1 The blood-brain-barrier

The BBB, found along the capillaries, is a highly selective barrier that protects the brain from noxious chemicals, variations in blood composition and breakdown of concentration gradients[169]. The BBB restricts the entry of certain molecules into the parenchyma based on their size and polarity.

The cellular components of the BBB are the cerebral capillary endothelial cells, pericytes and astrocytic feet (also known as glia limitans); however the most important functional component is the endothelial tight junctions which serve as a diffusion barrier. BBB endothelial cells are distinct from their peripheral counterparts for a number of reasons. They possess a relatively low number of vesicles, they lack fenestrae, have higher electrical resistance and they have evolved specialised transport systems[170]. Molecules and some cells can traverse the BBB either through the endothelial cell (transcellular passage) or between the cells (paracellular passage). Both the passive diffusion of neutral lipophilic substances (with a molecular weight less than 450) and the active transport of small and large hydrophilic molecules occurs transcellulary. In addition, many essential nutrients that are not able to diffuse are transported by specialised membrane proteins. Conversely, ions and solutes diffuse paracellulary down a

concentration gradient through the tight junctions[171]. These tight junctions are found between neighbouring endothelial cells and mediate gate function; preventing substances with a molecular weight greater than 180 from traversing the BBB through paracellular diffusion[172, 173].

In the healthy individual, most toxic substances and antigens are unable to traverse the BBB due to its tightly constrained intercellular junctions ; however its permeability increases during inflammation. This dysregulation, which allows the influx of leukocytes and causes brain oedema, is a characteristic of a number of CNS pathologies, including the archetypical neurodegenerative disease, MS[174, 175].

1.3.2.2 The blood-cerebrospinal fluid-barrier

Cerebrospinal fluid (CSF), secreted primarily by the choroid plexus, is important for buoyancy and protecting the brain, maintaining chemical balance and clearing waste and toxins[176]. Adults will normally have a total volume of between 80 and 150ml of CSF, which is continually being produced and reabsorbed, and which circulates within the ventricular system of the brain[177, 178].

The BCSFB comprises the choroid plexus epithelial cells, found in the vascular tissue of all cerebral ventricles, and the arachnoid membrane of the meninges[179]. The barrier is formed by epithelial cells and the tight junctions that link them. This barrier allows the free movement of small molecules across the endothelial cells of the choroid plexus capillaries through fenestrations and intercellular gaps. The BCSFB allows not only free diffusion, but also mediates facilitated diffusion and the active transport of molecules into the CSF.

CSF production is driven by the active ion transport of sodium into the lateral ventricles, creating osmotic pressure that draws in water to the CSF space[180]. Electroneutrality is maintained by negatively charged chlorine ions which follow positively charged sodium ions. Thus CSF contains higher concentrations of sodium and chlorine than plasma, which are the main ionic constituents of CSF.

1.3.2.3 The circumventricular organs

The circumventricular organs (CVO) are structures that allow the passage of polypeptide hormones out of the brain without disrupting the BBB[181]. Characterised by their small size, high permeability and fenestrated capillaries, CVOs are found around the third and fourth ventricles of the brain. The fenestrated nature of the endothelium means that microglia and neurons may be exposed to circulating mediators directly. Several hypothalamic peptide hormones leave the brain through the CVOs and go on to affect the anterior pituitary, or act peripherally following release into the circulation[181]. These include a number of hormones involved in the HPA axis (section 1.6.1) as well as vasopressin and oxytocin. In addition to regulating the secretion of hormones out of the brain, CVOs allow other substances to trigger changes in brain function. Hormones that are unable to cross the BBB can sometimes exert their actions on CVO neurons which span the BBB and project into the brain parenchyma.

1.3.2.4 The meninges

The meninges are a triple layer of membrane that surrounds the brain and spinal cord. The outer membrane, called the dura mater, is fixed to the skull and forms a protective sac around the inner membrane. The inner membrane, or leptomeninges, is formed by two thin membranes called the arachnoid mater and the pia mater[182]. The meninges are filled with CSF and are best known for offering protection to the CNS. Not only do they constitute a physical barrier around the CNS, but the fluid-filled cavity within the meninges cushions the brain from damaging events. The meninges are also thought to be important for maintaining CNS homeostasis and are able to secrete a number of trophic factors such as growth factors and cytokines, including fibroblast growth factor (FGF) 2, CXCL12 and retinoic acid[183-185]. During embryogenesis, the meninges are essential for correct CNS development, although the exact mechanisms by which they contribute remain to be fully understood.

1.3.3 Immune surveillance and antigen drainage

Although the CNS is protected by the BBB and BCSFB, the healthy brain is under continual surveillance. The sentinel duties of a limited number of cells involved

in immune surveillance under steady-state conditions ensures that homeostasis is maintained[186].

As mentioned in Section 1.3.1.2, microglia are one of the key cell types involved in immune surveillance of the CNS. Due to their expression of a number of PRRs, microglia are sensitive to a wide range of insults and their activation leads to the production of pro-inflammatory agents that heighten the inflammatory response. Thus, microglia are able to efficiently sample the local environment and respond effectively to danger.

Present in small numbers, leukocytes including T cells, macrophages and DCs patrol specialised areas of the CNS, outwith the parenchyma, for harmful agents. These are all possible sites of extravasation and include the non-fenestrated vascularised stroma of the BCFSB surrounded by choroid plexus epithelial cells, the perivascular space and the postcapillary venules that enter the parenchyma directly. Perivascular macrophages are a minor, bone-marrow derived, CNS population found within the perivascular spaces adjacent to small and medium blood vessels[187]. PVMs can shroud local blood vessels with long processes and are activated in response to neural injury or death as well as cytokines or LPS in peripheral blood. Upon becoming activated, these cells can synthesise IL-1 production and function as APCs[188]. DCs, although not detected in the parenchyma, are abundant throughout the meninges and choroid plexus of healthy rodents and humans, and are found at low levels in the CSF[189-192]. The strong upregulation of MHC and co-stimulatory molecules in the CNS following infection and other CNS pathologies suggests that many cells in the CNS possess the ability to present antigen[193]. However, around 80% of immune cells found in the CSF are T cells, the majority of which are CD4$^+$ central memory T cells (T$_{CM}$), whose passage into the CSF is facilitated by CCR7, CXCR3, L-selectin and a number of other adhesion molecules[194]. T$_{CM}$ cells remain in the CSF for several hours sampling antigen presented on central APCs, before returning to the bloodstream. Activation of T$_{CM}$ cells by encountering their specific antigen initiates a neuroinflammatory response through T cell effector functions[194].

Some reports have suggested that resident memory T cells can remain in the CNS for up to a year after initial infection, far longer than T$_{RM}$ cells in other peripheral organs, suggesting the CNS is isolated from recirculating memory

pools[195, 196]. This is most commonly reported following viral infection and it is therefore possible that the CNS has a specialised ability to retain CD8$^+$ T$_{RM}$ cells that are primed to respond to a secondary insult with their cognate antigen[197]. It is also possible that low levels of activated T cells can enter the brain parenchyma. Wekerle et al have used encephalitogenic T cells to show that activated T cells are able to cross the BBB in Lewis rats, whereas naïve T cells cannot[198]. If these cells do not find their antigen they simply traffic back into the blood or die.

Prior to June 2015, it was presumed that the CNS lacked a lymphatic network; however, using injectable tracers such as Indian ink[199] and quantum dot 655[200], routes by which antigens and cells can traffic out of the brain were identified[201]. In animals and humans, CSF, containing free antigen, drains from the subarachnoid space to the nasal mucosa and cervical LNs via a number of channels that pass through the cribriform plate of the ethmoid bone[202]. Conversely, interstitial fluid (ISF) and solutes from the brain parenchyma drain to the cervical LNs via a separate route, first by diffusion through the extracellular spaces and then along the walls of the cerebral capillaries and arteries[203]. Recently, studies by Louveau et al attempted to investigate the mechanisms of meningeal immune surveillance and uncovered the existence of a functional CNS lymphatic network[140]. Using sophisticated techniques, whole mount meningeal immunohistochemistry revealed the presence of classical Prox1$^+$ CD31$^+$ LYVE-1$^+$ Podoplanin$^+$ VEGFR3$^+$ CCL21$^+$ lymphatic endothelial cells lining the dural sinuses. Furthermore, ligation studies suggest a physical connection between meningeal lymphatic vessels and the deep cervical LNs. The presence of T cells, B cells and DCs in meningeal lymphatic vessels under normal conditions suggests this system participates in steady-state immune cell trafficking through the CNS. The discovery of this network has led to the re-evaluation of the mechanisms of immune surveillance in the CNS and could implicate malfunctioning meningeal lymphatics in a variety of neurological diseases[204]. To ensure that the CNS responds appropriately to insult, cells must be able to monitor the local environment and present antigen to T cells when an adaptive immune response is required. It is clear that there are a number of systems in place that allow continual immunosurveillance and antigen drainage,

demonstrating that, in addition to its complex physical barriers, the cells of the CNS represent a tightly controlled surveillance system.

1.4 Chemokines in the CNS

Chemokine expression throughout the brain differs depending on the context in which it is assessed. Many chemokines, particularly homeostatic chemokines, are essential during development and continue to be important throughout life for maintaining a number of steady state functions[205]. Of course, during inflammation and CNS disease, the chemokine repertoire changes as inflammatory chemokines are produced by activated cells[206]. In addition, all major cell types in the brain have been shown to express a range of chemokine receptors and possess the ability to produce a number of chemokines themselves[207]. This suggests there is an independent chemokine signalling circuit within the brain, indicating that their role within the CNS may extend beyond localised immune cell mobilisation.

1.4.1 Development

Appropriate cellular migration and organisation is essential for the developing CNS and relies upon a number of chemokines that have been shown to play a role in regulating such processes. The most prominent of these chemokines is CXCL12, and its receptor CXCR4, which have already been mentioned briefly. CXCL12, considered the primordial chemokine, is extensively expressed throughout the developing CNS[208]. Its importance is demonstrated in mice deficient for CXCL12 or CXCR4, which die perinatally and often present with developmental abnormalities of the brain, specifically disorganisation of the cerebellum. Cerebellar development in the normal embryo is an organised process of CXCL12-dependent migration and maturation of precursor cells which results in the formation of cerebellar granule neurons[208]. Without the guidance from this chemokine, migration is impaired and the granule neurons form ectopically. As well as regulating the migration of granule progenitors, CXCL12 is thought to hold them in a proliferative environment and facilitate their proliferation by interacting with a particular mitogen, Sonic hedgehog[209]. Thus, not only does the CXCL12-CXCR4 interaction ensure the appropriate organisation of the cerebellar granule neurons, they also regulate proliferation. In a similar

fashion, the granule layer of the dentate gyrus is impaired in CXCR4 KO mice and fails to develop properly[210]. These mice do possess dentate granule neurons; however they are fewer in number and can be found ectopically within the normal migratory stream, which extends from the dentate neuroepithelium. This suggests that the absence of CXCR4 has an effect on both the proliferation and migration of the precursor cells. Although heavily implicated in development, CXCL12 and CXCR4 continue to be expressed by granule neurons and precursor cells in adult animals, suggesting that the role of this chemotactic pair does not cease with development[211].

CXCR2 has also been implicated in spinal cord development by mediating the migration of oligodendrocyte precursors. These precursor cells originate in the ventricular zone and migrate to the white matter where they proliferate and differentiate[212]. Their arrest in the white matter is thought to be dependent on CXCL1 signalling through its receptor CXCR2 as the spinal cords of CXCR2 null mice exhibited a reduction in the number of oligodendrocytes, many of which were found abnormally clustered at the periphery[213].

1.4.2 Homeostasis

The expression of certain chemokine receptors and ligands in the brain continues into adulthood irrespective of the presence of inflammatory stimuli, suggesting that these chemokines may have a role in maintaining certain brain processes in the steady state.

A number of studies have suggested a role for chemokines in regulating several neuroendocrine functions such as feeding, temperature and water balance[207, 214, 215]. A drawback of a lot of these studies is that they involved either injection of lipopolysaccharide (LPS) or injection of a chemokine directly and are therefore not 'steady-state'. However, the fact that an inflammatory stimulus or an increase in expression can induce a change in these functions suggests that chemokines are homeostatic regulators. For example, CXCL8, CCL3, CCL4 and CCL5 have all been shown to induce hyperthermia[216-219] and CXCL8, CXCL10, CCL2 and CCL5 can reduce short term food intake when injected intracerebroventricularly (i.c.v)[220, 221].

It has also been suggested that certain chemokines could function as neurotransmitters. To help define neuropeptide ability as neurotransmitters, a list of five criteria was established to which they should comply. The list stipulates that they should be localised at nerve terminals, they should co-localise with other neurotransmitters at the nerve terminal vesicles, they should show release following membrane depolarisation, they should exhibit electrophysiological effects and the receptors for the peptide should be expressed both pre- and post-synaptic[222]. Although chemokines do not adhere to all five of the stipulations, they do present a strong case for acting as neurotransmitters. It has been shown in rats that CXCL12 and CCL2 are able to co-localise with both cholinergic and dopaminergic neurons, depending on the brain region of interest[223, 224]. The spatial distribution of chemokine receptors in relation to the cells that synthesise their ligands suggests that they must be released by nerve endings or dendrites. For example, CX3CR1, located on neurons and microglia, is stimulated by its ligand CX3CL1, which is expressed only by neurons[225]. In cultured mouse hippocampal and hypothalamic neurons, Guyon et al showed that CXCL12 can directly modulate voltage-dependent membrane currents, the effects of which can be blocked using the CXCR4 antagonist AMD3100[226]. In addition, patch-clamp recording of cultured rat spinal cord neurons showed that CCL2 could regulate neurophysiology by modulating GABAergic neurotransmission[227]. Together, these findings demonstrate that chemokines can have electrophysiological effects in the CNS. Chemokine receptors can be expressed on pre-synaptic neurons that also synthesise the ligand. Like classical neurotransmitters such as dopamine, the dual expression of both a ligand and its cognate receptor by the same neuron suggests some kind of autocrine function. Interestingly, Callewaere et al showed that, in rats, CXCL12 not only co-localises with arginine vasopressin, but also inhibits its release from hypothalamic dendrites through autocrine mechanisms involving pre-synaptic CXCR4[228].

1.4.3 Infection and inflammation

In the event of inflammation or disease, either within the CNS or in the periphery, the chemokine repertoire in the brain is altered. The primary role of chemokines during neuroinflammation is facilitating the transmigration of leukocytes across the physical barriers of the brain[229]. In this way, using the

process which is described in detail in section 1.5.1, certain inflammatory chemokines have been shown to induce the infiltration of certain leukocyte subsets. For example, CCL2, CCL3, CCL4 and CCL5 induce the activation and chemotaxis of T cells and monocytes[230-232]. In addition, blocking certain chemokines and receptors changes the leukocyte repertoire within the CNS[231, 233]. Although to an extent chemokine involvement in CNS inflammation appears to differ between pathologies and may be specific to the nature of the insult, there is a degree of overlap and certain conditions have provided a generalised insight into chemokine involvement in neuroinflammation.

Michlmayr et al have used models of viral encephalitis to show that many, but not all, inflammatory chemokines are upregulated in the brains of treated mice[234]. They report that, 7 days following infection with Semliki forest virus (SFV), inflammatory chemokine ligands, in particular CCL2, CCL5, CXCL9 and CXCL10, are significantly upregulated, in some cases with a 90-fold increase. This expression pattern coincides with the influx of a number of leukocyte cell types into the brain, including NK cells, myeloid cells, B cells and, most notably, CD3$^+$ T cells. Using a series of chemokine receptor blockers, they showed that this cellular migration into the CNS was mainly reliant on the actions of CCR5, CCR2 and CXCR3. Others have reported, both *in vivo* and *in vitro*, that at earlier time points following infection, inflammatory chemokines are secreted by activated, or virally infected, cells in the CNS including astrocytes, microglia and endothelial cells[235, 236]. Moreover, neutrophil infiltration is said to occur in several viral models through the CXCR2/CXCL1 axis[237, 238]. This reportedly heightens CNS inflammation by increasing the permeability of the BBB[239].

It is well documented that leukocyte infiltration is a pivotal event in the pathogenesis of MS. Several chemokines have been shown to help mediate this process through their expression on the vascular endothelial lumen[240]. Studies have reported the incidence of CCR7$^+$ cells in MS lesions, which are likely infiltrating in response to the ligands CCL19 and CCL21[241]. There is still some debate regarding the phenotype of these cells; however 90% of leukocytes in the CSF of MS patients are thought to be CCR7-expressing central memory T cells. Elevated levels of CCL2, CCL3, CCL4, CCL5, CCL7, CCL8, CXCL1, CXCL9 and CXCL10 have been described in MS, and the corresponding mouse model experimental autoimmune encephalomyelitis[240]. The expression pattern of these

proteins is thought to differ temporally and spatially adding to the complicated nature of the disease. With regards to EAE specifically, CCL2 is thought to be of particular importance. One of the major cellular infiltrates in EAE is monocytes, which are recruited into the CNS in a CCR2-dependent manner, and which are able to differentiate into microglia[242]. Many studies have confirmed the involvement of CCR2 and CCL2 using KO mice[136, 243-245]. However, reports have suggested that depleting monocyte infiltration is compensated for by supplementary neutrophil infiltration, indicating that chemokines work in concert to ensure that a range of leukocyte subsets can access the brain parenchyma[136].

Although very little has been done to investigate the chemokine repertoire in the CNS in response to peripheral inflammation, D'Mello et al have reported that monocytes are recruited into the brain during hepatic inflammation. They have shown that cerebral microglia, activated by peripherally induced TNFα, recruit monocytes in a CCL2:CCR2-dependent fashion[230].

Together, reports suggest that CNS inflammation, and perhaps also peripheral inflammation, leads to increased expression of many chemokines and cytokines which can mediate cellular influx into the brain. Chemokines and their receptors are therefore potential therapeutic targets for the regulation of inflammatory pathologies of the CNS.

1.5 Routes of immune-to-brain communication

Under homeostatic conditions, the barriers described in section 1.3.2 are sufficient to ensure that the CNS environment is protected and maintained. However, it must be possible for the CNS to respond to inflammation in the periphery, otherwise the manifestation of sickness behaviours in response to systemic infection would not occur. There are many different routes by which the immune system can communicate with the brain[6]. Most, at least on some level, can be mediated by inflammatory cytokines and the secondary mediators that they induce[5, 246]. The different methods of communication will be described below.

1.5.1 Leukocyte infiltration

Inflammation normally requires the extravasation of leukocytes from the blood into the tissue through the endothelial cell barrier, which occurs via a multi-step process called the leukocyte adhesion cascade[247]. Inflammatory cytokines, including IL-1ß and TNFα, LPS and histamine activate the endothelium resulting in the release of selectins[51]. The prototypical interaction is between P-selectin, which is released from Wiebel-Palade bodies and platelet granules, and the carbohydrate structure P-selectin glycoprotein 1 (PSGL-1) found on activated leukocytes. This interaction leads to the rolling of leukocytes along the surface of the endothelium. Immobilised chemokines expressed on the surface of the endothelium will bind leukocytes that express the corresponding receptor, initiating an intracellular signalling cascade which results in a conformational change and the activation of integrins. These cell-surface integrins will bind to cell adhesion molecules expressed by endothelial cells, including intracellular adhesion molecule 1 (ICAM-1) and vascular cell adhesion molecule 1 (VCAM-1), and will result in the firm adhesion of selected leukocytes. Finally, these leukocytes will undergo diapedesis and will transmigrate across the endothelium into the tissues, either directly through the cells or through the junctions between them. Entry into the CNS normally relies on transcellular migration alone due to the tight junctions found between the endothelial cells of the BBB[248].

Under steady state conditions, this process is tightly regulated by the BBB and BCSFB and few leukocytes are able to enter the parenchyma. However, in the event of peripheral or central inflammation, this selection process becomes more relaxed. Leukocyte infiltration and BBB disruption are classic hallmarks of many inflammatory conditions of the CNS including MS, stoke, traumatic brain injury (TBI) and viral encephalitis[249-252]. Mechanisms regulating BBB permeability and cellular infiltration are incompletely understood, but are thought to involve the effects of inflammatory cytokines and chemokines on BBB endothelial cells.

Many of the findings regarding leukocyte infiltration into the brain have implicated factors involved in normal cellular migration, suggesting an increase in activity rather than a change in mechanism. In the steady state, the adhesion molecules ICAM-1 and VCAM-1 are barely detectable in normal brain cells;

however they are upregulated on endothelial cells and glia under a number of inflammatory conditions including stroke, LPS challenge and TBI[253, 254]. *In vivo* and *in vitro* studies using ICAM-1-deficient mice have shown a definitive role for ICAM-1 in facilitating leukocyte migration into the CNS following TBI[255]. It is thought that ICAM-1 signalling induces cytoskeletal alterations in brain endothelial cells that facilitate a change in the BBB permeability. In a mouse model of acute cytokine-induced meningitis, increased BBB permeability and leukocyte accumulation in the CSF are seen. However, both of these phenotypes are almost completely abolished when the model is applied to mice doubly deficient in P- and E-selectin[256]. The upregulation of cellular adhesion molecules on brain endothelium and trafficking leukocytes appears to be induced by inflammatory agents and cytokines directly. Wong et al have used primary cultures of human brain microvessel endothelial cells to show that treatment with LPS or inflammatory cytokines upregulated ICAM-1 in a concentration- and time-dependent manner[257]. Similarly, Roe et al used cultures of human brain microvascular endothelial cells to show that infection with West Nile virus (WNV) upregulated ICAM-1, VCAM-1 and E-selectin expression and enhanced leukocyte adhesion[252]. In MS, Th1 inflammatory cytokines, including IFNγ, TNFα, IL-1ß and IL-6, are involved in the pathogenesis of the disease and can activate the expression of endothelial cell adhesion molecules[258]. Together, these findings suggest that inflammatory components promote the interaction of leukocytes with brain endothelium by inducing elevated adhesion molecule expression.

Some studies have suggested that changes in BBB permeability and facilitated leukocyte transmigration may involve alterations in tight junction integrity[259, 260]. Indeed, the breakdown of tight junctions has been noted in the vicinity of MS lesions[249], and in vitro studies have shown that stimulation of cultured endothelial cells with serum isolated from relapsing MS patients provokes a downregulation of occludin and VE-cadherin, proteins that are important for tight junction integrity[261].

Whatever the mechanism, there is a plethora of literature indicating that leukocyte infiltration into the CNS is a key process during many inflammatory conditions. The consequence of this appears to differ depending on the nature of the insult. A model of TBI in Wistar rats found T cell infiltration and microglia activation to be indicative of the acute response and were capable of

contributing to the classic brain oedema often seen following such injury[262]. In stroke, there is mounting evidence to suggest that post-ischemic tissue damage in the brain is mediated by infiltrating leukocytes, including neutrophils[263], macrophages (and activated microglia)[264] and T cells[265, 266]. However, Fassbender et al have shown that infiltrating cells may not actually influence infarct size following transient occlusion of the middle cerebral artery[267]. Using histology and flow cytometry, these cell types were shown to have differing temporal recruitment patterns[268, 269] which may explain the conflicting data concerning their effects if timing is a crucial variable. Determining whether or not leukocyte infiltration is beneficial or detrimental in stroke is difficult since, although these cell types have a damaging effect to the local tissue, immune cells are also important for the removal of dead neurons from the ischemic core and for promoting astrocytosis[250].

1.5.2 Cytokine transport

The BBB provides a physical barrier between the brain and the periphery and is characterised by its highly selective nature. Under steady state conditions, the BBB uses specialised transport mechanisms to mediate the transendothelial migration of certain proteins and peptides, ensuring that the CNS is not flooded by humoral neurotransmitters and blood elements[179].

During CNS inflammation, cytokines can be directly secreted in the CNS by TLR activation in an array of cell types. However, it is also possible for cytokines circulating in the periphery, including those produced by cells at the CVOs and choroid plexus, to enter the brain by active transport. This has been demonstrated in a number of studies using radiolabelled inflammatory cytokines that have been induced in the periphery[270-273]. Their active transport across the BBB into the parenchyma occurs without disruption of the BBB itself, demonstrating that this mechanism of transport does not rely on a loss of structure. Peripheral administration of large quantities of unlabelled cytokine leads to the rapid saturation of this transport system, suggesting that this cytokine-specific transport mechanism is not the only route of communication between the periphery and the brain[273].

Inflammation can influence the permeability of the BBB, with leukocyte influx being a characteristic of many CNS pathologies. Breakdown of BBB integrity, perhaps mediated through astrocytic activation, is thought to aid in the pathogenesis and progression of many neurological diseases, including seizure disorders[274], Alzheimer's disease (AD)[275] and MS[174]. The function of active cytokine transporters, which normally operate at low levels, can also be altered by pathological conditions. Interestingly, stroke and spinal cord injury both lead to an increase in activity of the TNFα transporter[272, 273].

1.5.3 Humoral pathway

The humoral pathway of communication is slower than the neural pathway and involves cells found within the CVOs and brain endothelial cells. Blood-borne proteins, including inflammatory cytokines, are able to activate brain endothelium directly to relay information across the BBB, or they can activate specific brain regions independently of the BBB, namely the CVOs[276].

Circulating cytokines are able to activate cells found within the BBB, specifically brain endothelial cells and perivascular macrophages (PVMs)[277]. Stimulation of these cells by inflammatory agents will lead to the release of secondary mediators such as PGE2, which are able to diffuse freely across the BBB[278]. In addition to activating BBB components, circulating proteins are able to enter into the parenchyma at areas lacking an intact BBB, namely the CVOs. As discussed previously (section 1.3.2.3), hormones which are capable of activating the hypothalamic-pituitary-adrenal (HPA) axis may come into direct contact with neurons and microglia due to the fenestrated nature of the endothelium[181]. The activation of neurons at the CVOs can be confirmed by c-Fos induction[279, 280]. In addition to neuronal activation, activated microglia can initiate a wave of stimulation to neighbouring structures, spreading the response throughout the brain parenchyma[281].

1.5.4 Neural pathway and the cholinergic anti-inflammatory pathway

Immunity is coordinated by neural circuits that operate reflexively. The afferent arc, consisting of nerves that sense injury or inflammation, activates the efferent neural circuits that modulate immune responses and the progression of

inflammatory disease[282]. The vagus nerve is the main nerve of the parasympathetic division of the autonomic nervous system which regulates metabolic homeostasis. The vagus nerve exits the brain from the medulla oblongata and descends vertically within the carotid sheath postlateral to the carotid arteries. From there, the branches of the vagus nerve innervate the gut and peripheral organs including the lungs, spleen, kidneys and liver. It controls heart rate, gastrointestinal motility and secretion, hepatic glucose production and other visceral functions[283]. It is also a major constituent of the inflammatory reflex; a physiological mechanism that functions on the path between immunity and metabolism. Recent evidence has shown that the efferent vagus nerve can control local and systemic inflammatory responses using a process termed "the cholinergic anti-inflammatory pathway"[284].

The vagus nerve can be activated by inflammatory cytokines. In addition, the afferent branches of the vagus nerve contain macrophages and DCs in the perineural sheath that express TLRs and can be activated by PAMPs[282]. Much of the information regarding the role of the vagus nerves in immune-to-brain transmission comes from vagotomy experiments. Many people have used rodent models to show that intraperitoneal injections of LPS can stimulate c-fos expression in neurons[285]. However, when vagotomys are performed under the diaphragm, so as not to disturb cardiac and pulmonary function, expression of this early activation gene is attenuated. This has also been shown by Marvel et al in a model of reversible inactivation of the vagus nerve using anaesthetic. They found that non-responsiveness of the dorsal vagus complex blocked the social withdrawal and c-fos upregulation normally seen in LPS injected rats[286]. These findings suggest that the neuronal activation of the brainstem, the hypothalamus and limbic structures that normally follows peripheral intraperitoneal LPS stimulation is dependent on vagus nerve transmission[287]. In addition, surgical transection of the vagus nerve in rodents, preventing immune signalling at peripheral nerve endings, is able to attenuate sickness behaviours caused by peripheral immune stimulation[56, 288, 289]. However, this suppression is thought to be dose-dependent and can be overcome with the administration of a large dose of IL-1β[290]. In this manner, the administration of cytokine can induce fever and sickness behaviour by bypassing neural circuitry and acting through the CVOs via the humoral pathway.

The actions of the neural pathway are thought to be mediated through the production of acetylcholine (ACh) from the stimulated afferent arm[291]. Acetylcholine, an important neurotransmitter and neuromodulator, signals through two different kinds of receptor; muscarinic and nicotinic[292]. RNA analysis of these receptors shows that they are expressed on mixed populations of lymphocytes as well as other cytokine producing cell types, most of which are also capable of producing acetylcholine[293]. Via post-transcriptional mechanisms, acetylcholine can suppress the production of a number of pro-inflammatory cytokines, including TNF and IL-1ß, by LPS- stimulated human macrophage cultures[294].

Although this is clearly an important mechanism of immune-to-brain communication, it seems to be more essential for some processes than for others. For example, vagotomised LPS- or IL-1ß- injected rodents may have attenuated sickness behaviours, but they do still present with a fever response[295]. These results confirm that the neural pathway is not the only communication pathway between the immune system and the brain. It seems likely that the afferent arc is particularly important for relaying information to the brain in response to mild to moderate peripheral inflammation.

1.6 CNS responses to peripheral stimulus

The major routes of immune-to-brain communication have been highlighted in the previous section and demonstrate that peripheral components of the immune system, namely inflammatory cytokines, are able to stimulate the CNS. There are a number of ways in which the brain will respond to such stimuli, activating a central response to try to eliminate the threat; however there are also several routes through which peripheral stimulation can mediate behavioural changes which may, in severe cases, result in the onset of neuropsychiatric disorders. The routes implicated, although presented as independent pathways, likely work in parallel and will be discussed in detail.

1.6.1 The HPA axis

The hypothalamic-pituitary-adrenal axis is a major part of the neuroendocrine system and is based on the feedback interactions of three endocrine glands; the

hypothalamus, the pituitary gland and the adrenal glands[296]. The HPA axis regulates many essential processes such as energy exchange, the immune system, digestion and mood. In addition, the HPA axis is responsible for directing the response to stress through the production of glucocorticoids (GCs)[222]. The stress system is always active and is characterised by circadian variations, but in circumstances where physical or emotional stressors exceed a critical threshold, the activities of the stress system intensify. This response is necessary to try and reinstate homeostasis by instigating behavioural adaptations, the redistribution of energy and inhibition of the inflammatory response. Being able to appropriately and efficiently respond to stress confers a survival advantage by controlling the 'fight or flight' response[297].

As shown diagrammatically in Figure 1-4, when physical or psychological stress is experienced, corticotropin-releasing hormone (CRH) is produced by the paraventricular nucleus (PVN) of the hypothalamus. This acts on the anterior pituitary gland, stimulating the production and release of adrenocorticotrophic hormone (ACTH), which in turn activates the adrenal glands. The adrenal glands subsequently release GCs (cortisol in humans or corticosterone in rodents), as well as stimulating the production of other stress hormones including noradrenaline and adrenaline[222]. GCs bind glucocorticoid receptors (GCRs) which are ubiquitously expressed throughout many tissues and on almost all immune cell subsets. As well as controlling growth and metabolism, GCs can act as neuromodulators and exert inhibitory effects on the immune system[298]. For example, through either direct inhibition or inhibition of key transcription factors, GCs can interfere with the production of a number of inflammatory cytokines, including IL-1β and IL-6[299]. Glucocorticoids not only inhibit inflammatory cytokines, but they also upregulate the synthesis of anti-inflammatory cytokines including IL-10. In addition, it has been shown that GCs can increase the phagocytic potential of macrophages to stimulate the clearance of debris and other harmful elements[300]. The combined actions of the HPA axis result in a potent anti-inflammatory response that aims to return the body to its homeostatic state. Should the HPA axis become impaired in some way and homeostasis lost, a chronic stress response may ensue leading to the onset of neuropsychiatric symptoms. This is often indicated in patients suffering from depression, who present with raised levels of cortisol[301].

Whilst the HPA axis works to control inflammatory responses by modulating cytokine production, this system itself is sensitive to a number of inflammatory cytokines. This is interesting as long-term sufferers of MDD have elevated levels of inflammatory cytokines, which may be the driving force behind chronic HPA axis activation[302, 303]. Several studies have demonstrated an important role for inflammatory cytokines in the hyper-activation of the HPA axis and the severity of MDD[5, 304]. Moreover, using either direct administration of Il-1 into rats or by using viral infection, studies have shown that IL-1 is able to stimulate the production of CRH, which in turn will upregulate ACTH[305]. Andreis et al have shown that this effect is mediated through the direct action of IL-1ß on the adrenal gland[306].
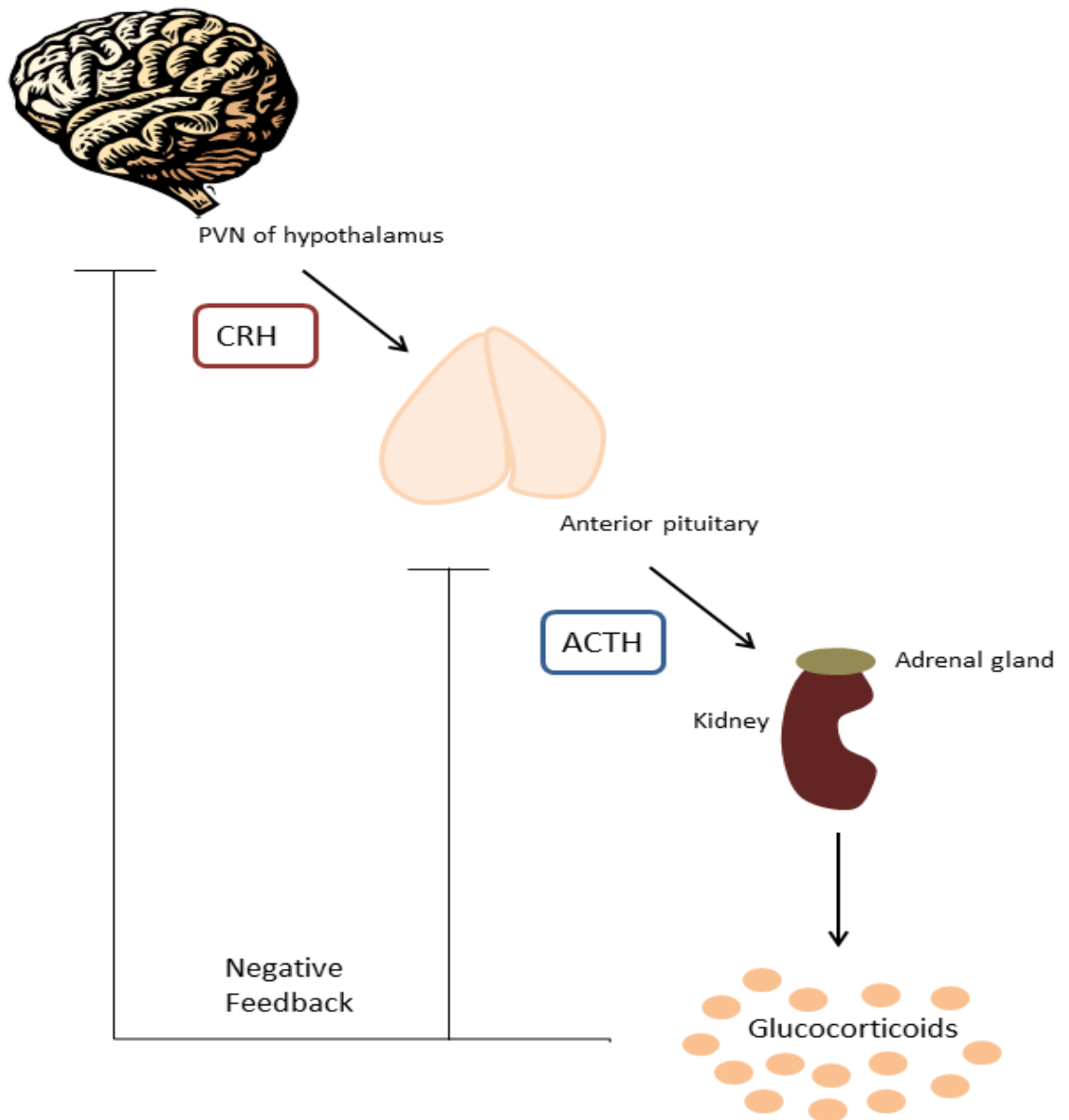
Figure 1-4 The HPA axis
Stress induces the production of CRH from the PVN of the hypothalamus. This, in turn, stimulates the release of ACTH from the pituitary gland which activates the adrenal glands of the kidneys to produce glucocorticoids. The HPA axis works as a negative feedback loop, whereby glucocorticoids suppress further production of CRH and PVN by the hypothalamus and pituitary, respectively.

1.6.2 Neurotransmitter modulation

The monoamine neurotransmitters dopamine, serotonin (5-HT) and noradrenaline (NA) are released from neurons in the CNS and the periphery[222]. They are thought to be involved in a wide range of physiological and homeostatic functions including learning and memory, concentration and attention and blood pressure regulation. The relationship between monoamines and depressive

disorders were seen with the use of a monoamine oxidase inhibitor, which was originally developed for other purposes, but was quickly found to have anti-depressive effects and, as such, drugs that augment the effects of monoamines are often used in the treatment of psychiatric conditions. The current treatment for MDD is the use of selective serotonin reuptake inhibitors (SSRIs). However, 30% of patients do not respond to each given treatment which suggests that monoamines alone do not explain the pathogenesis of MDD[307].

Tryptophan (Trp) is a circulating essential amino acid that serves as the precursor to many metabolic pathways[308]. Trp may be used for the synthesis of 5-HT, although around 90-95% of it is metabolised via the kynurenine (KYN) pathway (KP). This pathway facilitates the oxidative degradation of Trp into KYN, which is able to cross the BBB and enter the parenchyma where it can be metabolised by microglia, astrocytes and perivascular macrophages[309]. Metabolism of KYN is compartmentalised depending on the cell type and can lead to the production of both neurotoxic and neuroprotective substances. Kynurenic acid (KA), which is favoured by astrocytes, is thought to be neuroprotective, whereas quinolinic acid (QA), the preference of microglia, causes oxidative stress and is thought to be neurotoxic[310]. Microglia and infiltrating macrophages are the only cell types in the CNS that possess all the necessary enzymes for QA production[311], and studies have suggested that QA production is the favoured path in patients suffering neuropsychiatric disorders[312, 313] or acute inflammation[314]. The oxidation of Trp which is the initiating step in the KP is catalysed by the enzyme idoleamine 2,3-dioxygenase (IDO). IDO can therefore control the levels of 5-HT and stimulate the production of neuromodulators, both positive and negative[315].

Trp, as an essential amino acid, is important for the survival of many infectious microbes and its consumption is frequently seen during infection. Therefore the breakdown of Trp is actually a variant of the antimicrobial response which restricts its availability for infectious agents[316]. It has been shown that a number of factors involved in immunity can influence the levels of IDO. Pro-inflammatory cytokines including, IL-2, IFNγ and TNFα, as well as secondary mediators such as PGE2, are potent activators of IDO, whereas the cytokines IL-4 and IL-10 inhibit IDO[317]. Regulatory DCs and macrophages, which favour tolerance, express IDO as an immunosuppressive mechanism to catabolise Trp

degradation[318]. IDO expression is thought to be induced by IFNγ produced by activated T cells, which subsequently induces IDO-dependent arrest or apoptosis of T cells in a negative feedback fashion[319]. Patients suffering from MDD metabolise Trp at a higher rate than non-depressed controls, and a number of inflammatory conditions have been linked with higher expression of IDO[320].
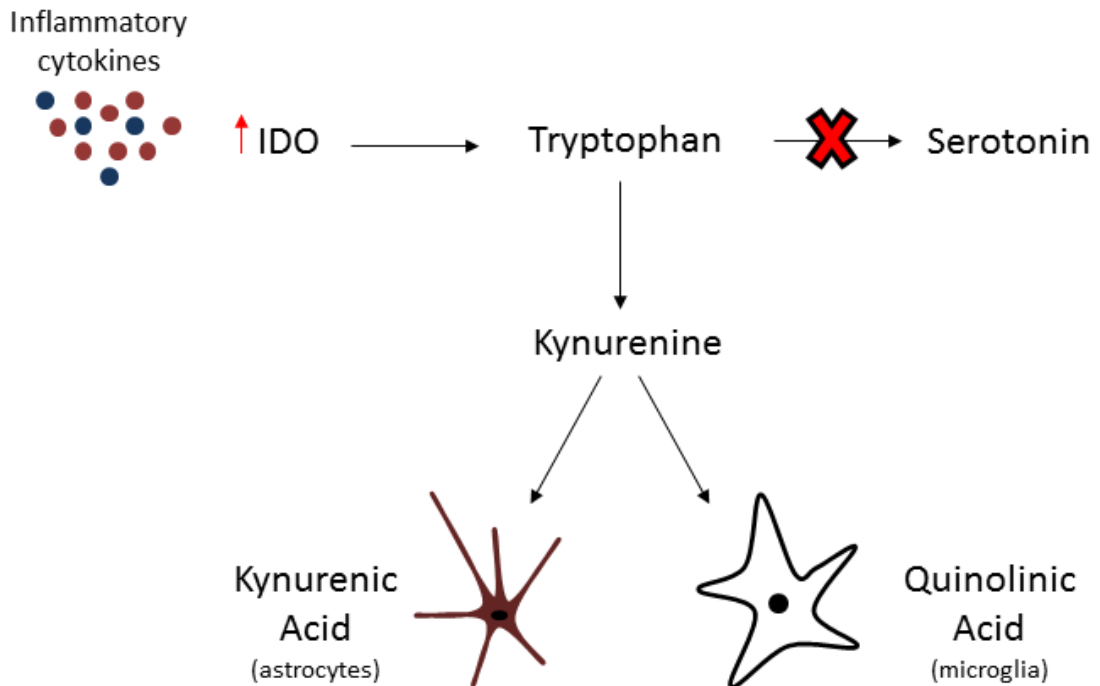
Figure 1-5 The kynurenine pathway of tryptophan degradation
IDO, which is upregulated by a number of inflammatory cytokines, is an enzyme which catalyses the oxidation of TRP into KYN. KYN is then further metabolised into either KA, which exhibits neuroprotective properties, or QA which is neurotoxic. This pathway, initialised by the actions of IDO, prevents TRP from facilitating the production of serotonin, an important neurotransmitter.

1.6.3 Peripheral inflammation and behavioural changes

There is now an abundance of literature that links inflammation with changes in behaviour. These findings come from both human and animal studies and involve a number of arms of the inflammatory response. Along with human clinical data, in which chronic inflammatory diseases are associated with the onset of neuropsychiatric conditions including depression and anxiety, there are also rodent studies which have shown the same correlation using administration of immune stimuli and assessment of sickness behaviours[5, 55, 246, 321, 322]. Numerous behavioural tests for rodents have been developed and, although a degree of

scepticism will always remain with regards to the interpretation of the 'mood' of rodents, these have allowed us to specifically test the effects of inflammation on behavioural changes.

It is now broadly accepted that rodents receiving inflammatory stimuli experience the onset of sickness behaviours, which serve as an 'immunological' model of MDD. The peripheral administration of recombinant cytokines or inflammatory cytokine inducers, such as LPS, triggers the classic symptoms of sickness including fever, reduction in food intake and activation of the HPA axis[7, 55, 56]. Set-point body temperature is controlled by neurons in the preoptic hypothalamus; however pyrogenic cytokines can mediate changes to instigate a fever response. To do this, cytokines, which cannot freely pass through the BBB, must be able to communicate with the brain. I have already highlighted the numerous methods of communication between the periphery and the CNS (Section 1.5), be it neural, humoral or via the activation of the HPA axis, which could mediate the behavioural adaptations presented with immune modulation.

With regards to human clinical data, there are a number of non-CNS diseases in which cytokine administration or cytokine blockage is used as a form of treatment. This has provided scientists with a suitable cohort for studying the effects of inflammatory cytokines on neurological wellbeing. The treatment of Hepatitis C patients with IFNα has implicated cytokine therapy in the onset of neuropsychiatric disorders including depression, anxiety and anger/hostility[323]. Kraus et al found that 35% of patients receiving IFNα treatment experienced the onset of clinically relevant depressive symptoms using the well-validated Hospital Anxiety and Depression Scale (HADS)[324]. They found that this was exacerbated when treatment was combined with the anti-viral drug Ribavirin, although a more recent evaluation by Udina et al showed a lower depression onset rate of 1 in 4[325]. These neuropsychiatric symptoms described by Kraus et al subsided in 15% of patients 4 weeks after IFNα treatment was terminated[324]. However, other studies have reported the incidence of interferon-induced depression as being anywhere between 0% and 90%[326, 327]. Similar findings have been reported in a double-blind study involving IFN-α treatment of patients with malignant melanoma, whereby the authors suggest that different mechanisms may govern the different manifestations that fall under the 'umbrella' of cytokine-induced sickness behaviours[328]. Psoriasis is another peripheral disease

that is commonly associated with the onset of neuropsychiatric symptoms such as depression, as well as substance abuse and suicidality. Published in The Lancet in 2006, Tyring et al noted some interesting findings from a phase III clinical trial involving the treatment of psoriasis patients for a 12 week period with the anti-TNF drug Etanercept[329]. 50% of patients experienced an improvement in their secondary symptoms of depression, measured using the Hamilton rating scale for depression (Ham-D) and the Beck depression inventory (BDI)[329]. These improvements in depressive symptoms did not significantly correlate with an improvement in psoriatic disease score as measured using the psoriasis area and severity index score (PASI). This suggests that TNFα is, on some level, associated with the neurological symptoms that are often presented by psoriasis patients. In addition to the knowledge gained from specific diseases, Reichenberg et al have performed studies in which humans were injected with endotoxin. Administration of LPS or Salmonella was found to induce depressive mood, anxiety, reduced food consumption and mild fever, phenotypes that were directly proportional to the levels of circulating inflammatory cytokines[322, 330].

1.6.4 Neurogenesis and plasticity

Adult neurogenesis, which was identified in human tissue for the first time in 1998[141], occurs primarily at two specific sites within the brain. These are the subgranular layer of the dentate gyrus of the hippocampus and the subventricular zone of the lateral ventricle, although recent reports have suggested there may be new neuron formation in other areas[142]. In mice, it takes several days to weeks for new cells in the granule layer of the dentate gyrus to be fully incorporated into hippocampal circuitry and express mature neuronal markers, going through a four stage process of proliferation, migration, differentiation and survival[331]. This process is thought to take significantly longer in humans and non-human primates. There is still some debate regarding the function and necessity of new neurons but, due to their increased plasticity in comparison with mature neurons, they are thought to have a role in maintaining brain regions by replacing dead or dying cells. Furthermore, neurogenesis is positively correlated with increased cognition, memory and spatial learning[332, 333]. Specifically, mice with increased levels of neurogenesis were found to excel in pattern separation tasks[332]. However, very recent publications have suggested that increased neurogenesis erodes memory, likened to the phenomenon of

infantile amnesia, which coincides, with the highest period of neuronal turnover[334, 335].

1.6.4.1 Inflammation and neurogenesis

Several studies have shown that peripheral inflammation, MDD, ageing and neurodegenerative diseases can have a negative impact on the degree of adult neurogenesis[336], which can be evaluated using either BrdU or doublecortin (DCX) immunostaining. Interestingly, a proportion of sufferers of MDD or other psychiatric conditions present with reduced hippocampal volume, measured using magnetic resonance imaging (MRI)[337, 338]. This reduction in volume is thought to inhibit neurogenesis and restrict neuronal plasticity. In agreement, Malberg et al have reported that long term anti-depressant treatment of rodents leads to a significant increase in adult neurogenesis in the hippocampus[339] as does voluntary exercise, running and environmental stimulation[340, 341]. Sufferers of chronic depression also have reduced levels of brain derived neurotrophic factor (BDNF), an important factor in the regulation of synaptic plasticity[342], which is rescuable with anti-depressant treatment[343]. It is thought that BDNF is particularly important during the stress response as it confers cognitive flexibility and the ability to adapt to environmental change[344]. Microglia can be both supportive and harmful to neurogenesis depending on their activation state[345]. In steady state conditions, ramified microglia ingest dying neurons in a manner that avoids the release of DAMPS, preserving brain homeostasis[346]. In addition, microglia are thought to release several factors that promote the proliferation and survival of new neurons. However, central or peripheral administration of LPS leads to microglial activation and a decrease in new neuron survival[347]. The survival of neurons negatively correlated with the number of activated microglia, an effect that could be blocked with the administration of the microglial inhibitor, minocycline[348].

Together, these findings highlight just how much of an effect immune-mediated processes can have on adult neurogenesis, an event that appears to be important for cognitive function, memory and plasticity.

1.7 Peripheral inflammation and the CNS

There are unquestionable correlations between long term sufferers of chronic inflammatory illnesses of the periphery and a decline in mental health and quality of life. However, it has been very difficult to identify the biological mechanisms of these symptoms due to the outdated assumption that the CNS is devoid of influence from the periphery. As mentioned previously, the use of cytokine therapy has now provided solid evidence that certain diseases normally associated with the periphery can have a measurable and reversible biological effect on an individuals' psyche.

1.7.1 Psoriasis

Although there are many chronic inflammatory diseases associated with the onset of neuropsychiatric conditions, psoriasis is of particular relevance to this thesis and will be focused on as a representative peripheral disorder with a negative correlation with MDD.

Psoriasis is a debilitating, recurrent skin disease that affects around 2% of the Caucasian population. The most common type of psoriasis is characterised by silver plaque-like formations on the skin that are variform, sharply demarcated, raised and itchy. A strong genetic risk factor for psoriasis has been identified[349-352] and it is thought that the disease responds to a number of triggers including stress, infections, smoking and injury. The immune component of psoriasis was first noted with the success of treatment with general immunosuppressive drugs including cyclosporine and methotrexate and it was subsequently thought that psoriasis was driven by IFNγ-producing Th1 cells. However, it was later found that DCs and keratinocytes in psoriatic lesions overproduced IL-23[353], which in turn implicated Th17 cells as the main drivers of the disease. IL-23 is considered the "master regulator" of the Th17 pathway and is essential for the survival and proliferation of these cells. As such, it is now known that T-cell mediated hyperproliferation of keratinocytes, thought to be driven primarily by IL-23-dependent Th17 cell-produced IL-17 and IL-22, induces the classic pathology seen in psoriasis[354]. Recently, a new subset of T cells has emerged which, like Th17 cells, produce IL-22, but they do not produce IL-17 or IFNγ[41]. These cells, subsequently name Th22 cells, are found in high levels in inflammatory skin

lesions and are characterised by their expression of homeostatic chemokine receptors, CCR4 and CCR6[40, 355]. IL-22 induces keratinocyte proliferation and epidermal hyperplasia and promotes the production of antimicrobial mediators[356]. As such, Th22 cells are now defined as pivotal in the pathology of psoriasis and are a new potential target in this, and many other, inflammatory skin diseases.

In addition to the effects of psoriasis itself, there is also a high risk association between psoriasis and other inflammatory conditions including arthritis and inflammatory bowel diseases (IBD)[357]. More than 10% of psoriasis patients also present with arthritis. As mentioned, psoriasis is one of many chronic inflammatory disorders that are strongly associated with debilitating neurological side effects. It is therefore an interesting disease to study with regards to co-morbid associations and neurological correlations.

1.7.2 Animal models of peripheral inflammation

There are very few successful animal models of chronic peripheral inflammation that exhibit a true reflection of a human disease. Of the models that have been developed, most are of course used to study the pathology itself and thus focus on the affected tissue, and perhaps the response in the periphery, rather than the response in the CNS. Most of the peripheral inflammation models that have been used to study the CNS response have relied upon the systemic injection of inflammatory agents and have failed to reflect a specific disease state. Rather, they utilise the ability to activate the systemic immune system by introducing bacterial components directly into the blood. Although this allows us to visualise the response in the CNS, it is not as applicable to discerning the relationship between peripheral diseases and neuropsychiatric disorders in humans, as these comorbidities are often presented with tissue-specific chronic disorders.

1.7.2.1 The Aldara model of skin inflammation

Aldara cream is a prescription drug that is used topically for the treatment of actinic keratosis[358], genital warts[359] and superficial basal cell carcinoma[360]. Aldara cream contains 5% imiquimod (IMQ) as its active component, which activates TLR8 in humans and TLR7 in rodents. Over a short period of time, its

application to the skin causes a localised skin inflammation[361, 362], and can trigger flare-ups in psoriasis patients[363], and it has now been developed by scientists into a commonly used rodent model of psoriasis-like skin inflammation.

The earlier animal models of psoriasis relied on either transgenic mice or xenotransplantation, both of which are costly and time consuming[364]. The mouse model of IMQ induced psoriasis on the other hand is favoured for its simplicity and is characterised by epidermal hyperplasia, acanthosis and leukocyte infiltration that are thought to be mediated through the IL-23/ IL-17 axis[365]. Mirroring human psoriasis, IL-23 and Th17 cell-associated cytokines are upregulated in lesions in the skin, and blockade of IL-23 is able to supress the inflammation[366]. Plasmacytoid DCs (pDCs), which express high levels of TLR7[367] and infiltrate the skin in a CCL2-dependent manner following IMQ application[368], are considered by some to represent the main source of the type I IFN response seen in this model[369, 370]. However, others have reported that pDCs are dispensable for the localised effects to IMQ[371]. The initial skin response is associated with the upregulation of inflammatory cytokines in the skin, including IL-1β and IL-6, along with neutrophil infiltration and keratinocyte activation[372].

Interestingly, Aldara cream contains another active component in addition to the TLR7/8 ligand IMQ. Isostearic acid, which is present in the vehicle, has been shown to activate the inflammasome via NALP3 pathway independently of IMQ and can induce the production of the inflammatory cytokines IL-1β and IL-18[372]. Although some of the early effects of Aldara are thought to involve both active components, the requirement for TLR7 ligation and MyD88 signalling suggests a primary role for IMQ in driving the full response[371, 372].

This model provides a pathology very similar to that seen in human psoriasis, and allows us to investigate the effects of peripheral, tissue-based inflammation on brain biology to try to identify possible mechanisms that underpin the relationship between chronic inflammatory conditions and neuropsychiatric disorders.

1.8 Justification and thesis aims

Having ruled out the previous misconception that the brain is isolated and protected from the periphery, it is clear that immune activation outwith the CNS can have a profound effect on the brain. The importance of this relationship has been highlighted in a number of studies in which the inflammatory cytokine profile has been manipulated. As such, it is clear that inflammation originating in the periphery can have a very fundamental effect on the neuropsychological state of patients. However, much remains to be elucidated with regards to the biological mechanisms underpinning this relationship. Using a well-characterised animal model of psoriasis-like skin inflammation, it is hoped that we can increase our understanding of how the immune system and the central nervous system are linked. Developments in this field have the potential to allow for better directed treatment that will improve both chronic inflammatory illness and neurological wellbeing.

As such, the primary aim of this thesis is:

- To investigate the effect of peripheral inflammation on the brain using a well characterised model of psoriasis-like skin inflammation.

As this thesis progressed, further specific aims were established. Once we had identified the distinct transcriptional response in the brains of treated mice, we sought to determine, in more detail, the mechanisms driving the response to skin-based inflammation. This was done using a range of peripheral inflammatory models, both TLR-dependent and TLR-independent, or 'sterile'. We also aimed to determine whether transcriptional chemokine expression in the brain could induce immune cell recruitment and we sought to evaluate what role, if any, atypical chemokine receptor ACKR2 had in the brain response to cutaneous inflammation (using ACKR2 knock-out mice). Finally, we wanted to understand whether peripheral inflammation could induce a functional output. The two parameters we chose to examine were behaviour, due to the well-described relationship between inflammation and sickness behaviour, and neurogenesis. Neurogenesis is sensitive to many other inflammatory insults and this, along with the much-localised expression of ACKR2 at known sites of adult neurogenesis, highlighted neurogenesis as an interesting function to assess in our studies.

Chapter 2

Materials & Methods

2 Materials and Methods

2.1 General materials & reagents

Plastics: All plastics were purchased from Gibco (Invitrogen, Paisley UK) or BD Biosciences (Oxford, UK) unless stated otherwise.

Tips: All tips were sterile filter tips purchased from Starlab

EDTA: 186.1g ethylenediaminetetraacetic acid (EDTA) (Sigma Aldrich) and 20g sodium hydroxide (NaOH, Sigma Aldrich) was dissolved in 900ml distilled H_2O (dH_2O), and adjusted to pH8 using hydrochloric acid (HCl, Sigma Aldrich). This was subsequently made up to 1 litre (L) using dH_2O.

1% acid alcohol: 1% concentrated HCl was added to 100ml of 70% Ethanol (EtOH)

Citrate buffer (0.1 M): 2.1g citric acid monohydrate (Sigma Aldrich) was dissolved in 700 ml dH_2O. 2M NaOH was added to adjust the solution to pH6. The total volume was made up to 1L of buffer with addition H_2O.

Eosin Y solution: 1% Eosin Y (Cell Path) was added to tap water

ELISA wash buffer: 1x Phosphate buffered saline (PBS) (Invitrogen) was mixed with 0.5% Tween 20 (Sigma Aldrich)

Tris-acetate EDTA (TAE) Buffer: A 50x stock solution of TAE buffer was made by dissolving 242g Tris base (Sigma Aldrich) in 750ml dH_2O. 57.1ml glacial acetic acid (Sigma Aldrich) and 100ml 0.5M EDTA was then added and the buffer was made up to 1L with dH_2O. Before use, stock buffer was diluted 1:50 in dH_2O.

Scott's tap water: 3.5g sodium hydrogen carbonate (NaHCO3) and 20g magnesium sulphate (MgSO4) were added to 1L of distilled H_2O. Thymol (Sigma) was added to prevent mould formation.

10x Tris Buffered Saline with Tween 20 (TBST): For 1L of buffer, 24.23g Tris base (200mM), 87.66g sodium chloride (NaCl, 1.5 M) and 10ml Tween® 20 (1%)

were added to 800ml of distilled H_2O. The solution was adjusted to pH 7.6 using concentrated HCl and diluted 1/10 to obtain 1x TBST.

2.2 *In Vivo* Procedures

2.2.1 Animals

C57BL/6 WT mice were either bred at the Central Research Facility at the University of Glasgow or purchased from Harlan Laboratories. GGDKB mice (ACKR2 KO mice) were bred at the Biological Services Unit at the Beatson Institute, University of Glasgow and were transferred to the Central Research Facility prior to being put on procedure. All mice were given at least one week to acclimatise to the facility before being used and were maintained in specific pathogen free conditions. Mice were age and sex matched and used between 6 – 9 weeks of age. All experiments received ethical approval and were performed under the authority of UK Home Office Licences.

2.2.2 Induction of Peripheral Inflammation

2.2.2.1 Aldara Model

C57BL/6 female mice were shaved on their dorsal skin. 24 hours later mice were treated with either Aldara cream (MEDA, 5%v:v Imiquimod, 1/3 of a sachet per mouse, 80mg) or aqueous control cream (Boots, UK, Liquid paraffin B.P. 6% w/w, White Soft Paraffin B.P. 15% w/w, Purified Water, Emulsifying Wax, Chlorocresol 0.1% w/w) of the same quantity which was applied to the area of shaved skin. Treatment was repeated every 24 hours for 5 days. Mice were weighed after each application. Mice were euthanised 24 hours after the final application by CO_2 inhalation.

2.2.2.2 Aldara Timecourse Model

C57BL/6 female mice were were treated with Aldara cream as described. Mice were euthanised by CO_2 inhalation 24 hours following the first, third or fifth application of Aldara depending on their group (D1, D3 and D5, respectively).

2.2.2.3 TPA Model

C57BL/6 female mice were shaved on their dorsal skin. 24 hours later mice were treated with either 12-O-Tetradecanoylphorbol-13-acetate (TPA) (Sigma, 150µl 100µM per mouse) or equivalent volume acetone (VWR International) which was applied to the area of shaved skin. Treatment was repeated every 24 hours for 5 days. Mice were weighed after each application. Mice were euthanised 24 hours after the final application by CO_2 inhalation.

2.2.2.4 TPA Timecourse Model

C57BL/6 female mice were treated with TPA (150µl 100µM per mouse) as described. Mice were euthanised by CO_2 overdose 24 hours following the first, third or fifth TPA application depending on their group (D1, D3 and D5, repectively).

2.2.2.5 Soluble Imiquimod Model

C57BL/6 female mice were injected intraperitoneally (I.P) with either soluble Imiquimod (Source Bioscience, 100µl 1mg/ml per mouse) or equivalent volume PBS. Treatment was repeated every 24 hours for 5 days. Mice were weighed after each application. Mice were euthanised 24 hours after the final application by CO_2 inhalation.

2.2.2.6 Topical Imiquimod Model

C57BL/6 female mice were shaved on their dorsal skin. 24 hours later they were treated with 80mg aqueous control cream supplemented with 5% v:v soluble Imiquimod, or equivalent volume aqueous control cream alone. Treatment was repeated every 24 hours for 5 days and mice were weighed after each application. Mice were euthanised 24 hours following the final application by CO_2 inhalation.

2.3 Tissue Isolation following *In Vivo* Models

2.3.1 Perfusion

The right atrium of the heart was cut to allow blood to drain into the chest cavity without compromising the circulation. Perfusions were performed by injecting 20ml of PBS, warmed to 37°C, into the left ventricle of the beating heart using a 23G needle.

2.3.2 Isolation of plasma from peripheral blood

Mice were culled by CO_2 inhalation. An incision was made in the right atrium and blood was collected in a 1ml syringe flushed with EDTA. Blood was immediately transferred to a 1.5ml eppendorf tube containing 20µl EDTA. Plasma was isolated by centrifugation at 300g for 10 mins. Taking care not to disturb the pellet, plasma was transferred to a fresh 1.5ml eppendorf tube before being centrifuged again at 10,000g for 5 mins. Platelet-free plasma (supernatant) was collected and was stored in a fresh 1.5ml eppendorf tube at -80°C.

2.3.3 Isolation of leukocytes from peripheral blood

Mice were culled by CO_2 overdose; a recognised schedule 1 technique. An incision was made in the right atrium and blood was collected in a 1ml syringe flushed with EDTA. Blood was immediately transferred to a 1.5ml eppendorf tube containing 20µl EDTA. After the removal of the plasma, cells were incubated in a 15ml falcon tube in 5ml of 1X red cell lysis buffer (Miltenyi) for 10 mins at room temperature. Tubes were centrifuged for 10 mins at 300g to allow the cells to pellet, and the supernatant was poured off. Cells were washed with 10ml PBS, centrifuged as before and then transferred to a fresh 1.5ml eppendorf tube. Cells were washed for a final time with 500µl PBS and centrifuged at 600g for 3 mins. The supernatant was poured off and the pellet was resuspended in 350µl of RLT buffer. PBL samples were stored at -80°C until they were processed for RNA purification.

2.3.4 Brain Dissection

Following perfusion, mice were decapitated and the skin on the head was cut back to reveal the skull. Scissors were carefully inserted under the interhemispheric fissure and the skull was cut open. Forceps were used to pull the skull apart allowing for the brain to be dissected out. The olfactory bulb, brainstem and the meninges were carefully removed. Dissected brains were either submerged in formalin for 24 hours prior to processing or were 'snap-frozen' in liquid nitrogen and stored at -80°C.

2.3.5 Skin Dissection

Following perfusion, an incision was made along the base of the shaved and treated area of the dorsal skin of the mice. Skin was gently lifted away from the underlying muscle and the patch of treated skin was cut off. This area was cut in two and one half was 'snap-frozen' in liquid nitrogen and stored at -80°C. The other half was laid out flat on filter paper (epidermis-side up) to prevent it from folding, and was then inserted into a bijoux containing 10% neutral buffered formalin. Tissue was fixed overnight in formalin before being processed, as described later.

2.3.6 Recovery of Spleens

The spleens of perfused mice were extracted and were stored in PBS on ice. Subsequently, spleens were weighed and photographed.

2.4 Gene Expression Analysis

2.4.1 Lysate preparation and phase separation of animal tissue

Tissue samples were homogenised in 1ml of QIAzol Lysis Reagent (Qiagen) using a TissueLyser LT (Qiagen) homogeniser for 10 minutes. Lysate was then incubated for 5 minutes at room temperature before 0.2ml chloroform was added. Tube was shaken vigorously by hand, incubated for 2-3 minutes and then centrifuged at 12,000g for 15 minutes at 4°C. The colourless upper phase (containing the RNA) was transferred to a fresh eppendorf tube prior to RNA extraction.

Cells were lysed in 350μl (>1 x 10^5 cells) of RLT buffer and stored at -80°C until required. Prior to RNA purification, cells were thawed and were passed through a QIAshredder (Qiagen) by centrifugation at full speed for 1min.

2.4.2 RNA extraction using silica-gel membrane technology

RNA was extracted following the RNeasy Mini Kit protocol (Qiagen) as described in the manufacturer's handbook. RNA was precipitated by adding 1 volume of 70% EtOH in RNase-free H_2O. RNA from each sample was collected by centrifugation through an RNeasy spin column (Mini Kit). Genomic DNA was digested on-column as described in the protocol. Briefly, a stock solution of DNase I enzyme (in buffer RDD, diluted 1/8) was prepared and 80μl was added to each sample and incubated for 15mins. Spin columns were washed several times to remove any protein impurities and then air dried. RNA was eluted from the columns in30- 50μl RNase-free H_2O.

2.4.3 Assessment of RNA Integrity

The quality of RNA was assessed by the University of Glasgow Polyomics Facility using a Bioanalyzer 2100 (Agilent) on a Nano chip in accordance with manufacturer's instructions. All chips and reagents used were supplied in the RNA 6000 Nano kit (Agilent). Nuclease-free H_2O was used to dilute the RNA to the following concentration:

Nano chip

Total RNA	5-500 ng/ml
mRNA	25-250 ng/ml

To prime the chip, the micro-channels were filled with a sieving polymer matric and fluorescent dye. Pressure was applied using a priming syringe (supplied) to disperse the gel-dye mix throughout the microfluidics of the chip. 9μl was also applied to an additional 2 wells as described in the protocol.

After priming, 5μl of RNA 6000 marker was applied to each of the wells. Subsequently, 1μl of RNA 6000 nano-ladder was pipetted into the ladder well and 1μl of each diluted RNA sample was added to each of the sample wells.

Chips were vortexed briefly to mix contents and then RNA was separated in a microchannel according to size using the Bioanalyzer 2100.

2.4.4 Affymetrix GeneChip Arrays

Microarray assays were performed by the Sir Henry Wellcome Functional Genomics Centre at the University of Glasgow. The quality of total RNA samples was assessed using an Agilent 2100 Bioanalyzer in accordance with manufacturer's instructions. 1µg of purified total RNA was amplified by *in vitro* transcription and converted to sense-strand cDNA using a WT Expression kit (Ambion). cDNA was then fragmented and labelled using an Affymetrix GeneChip WT Terminal Labelling kit. Fragmented cDNA samples were quality-checked using the 2100 Bioanalyzer and then hybridized to Affymetrix GeneChip Mouse Gene 1.0 ST Arrays. Procedures were carried out as described by the manufacturers.

Data were pre-processed and analysed using GeneSpring GX software and were normalised using RMA 16. Prior to analysis, background correction was performed. Background correction is arguably the most important step in probe level processing and is a non-linear correction performed on a chip-by-chip basis. Background signal may be caused by non-specific binding and optical noise and needs to be accounted for in order to determine the true signal intensity. The Affymetrix GeneChip array used in this study utilises an innovative design and includes 17,000 generic background probes that cover the full range of GC content. The modified GC-RMA algorithm was selected as the favoured method to correct this array for background noise. Using the signal intensity from the 17,000 anti-genomic probes to determine the background, the GC-RMA algorithm corrects for it using three sequential steps:

1. Optical background correction: to account for optical noise introduced by the scanner that measures the hybridisation efficiency

2. Adjustment of probe intensity through non-specific binding using the background probe signal intensities

3. Adjustment of probe intensity through gene-specific binding where the signal intensities are corrected for the effect of PM probe affinities.

Essentially, by following these three steps, the median signal intensity of the background probes possessing an equal GC content is subtracted from the signal intensity of the probe set. This provides what is considered to be the true signal intensity.

Normalised and corrected data was subsequently analysed using unpaired t-tests to determine the significance of each gene in Aldara-treated mice compared to control mice. P-values were adjusted for multiple comparisons using the Benjamini Hochberg multiple comparison method. Microarray profiling data were deposited in the National Center for Biotechnology Information Gene Expression Omnibus database with the series entry identifier GSE72214. Functional clustering was performed using the Database for Annotation, Visualization and Integrated Discovery (**DAVID**) v6.7.

2.4.5 cDNA Synthesis from RNA

RNA was converted to complementary DNA (cDNA) using Precision nanoScript RT kit (Primerdesign). Following quantification using a Nanodrop (ThermoFisher), RNA was diluted to equal concentrations (100-2000ng, depending on experiment) with RNase-free H_2O. The following components were added to 200µl thin-walled PCR tubes and incubated at 65°C for 5 minutes:

RNA (100-2000ng)	9µl
Oligo DT Primer Mix	1µl
Total Reaction Volume	10µl

The reactions were cooled to room temperature, allowing the primers to anneal to the RNA. The following components were added from a master mix:

10X Reaction Buffer	2µl
dNTP mix (25mM each dNTP)	1µl
100mM DTT	2µl
dH$_2$O	4µl
Reverse Transcriptase	1µl
Total Reaction Volume	20µl

A '-RT' control was included during cDNA synthesis in which the reverse transcriptase enzyme was substituted with 1µl of nuclease- free H$_2$O. Reactions were incubated for 10 minutes at 25°C to extend the primers then for 20 minutes at 65°C to synthesise cDNA. The reactions were then terminated by incubating at 75°C for 15 minutes. cDNA was diluted 1/10 with distilled H$_2$O and stored at -20°C.

2.4.6 Polymerase chain reactions

Polymerase chain reactions (PCRs) were performed using pre-made red PCR master mix (Rovalab) as described below:

Red PCR mastermix	45µl
Forward primer	0.5µl
Reverse primer	0.5µl
Template cDNA	1-2µl
Nuclease-free H$_2$O*	
Total Volume	50µl

*Reaction made up to 10µl in H$_2$0.

PCR reactions were run in a thermocycler set for the following programme:

1. 95°C 3 minutes
2. 95°C 15 seconds ⎫
3. 60°C 15 seconds ⎬ 35-40 cycles
4. 72°C 45 seconds ⎭
5. 72°C 5 minutes
6. 4°C forever

2.4.6.1 Gel electrophoresis of PCR products

Following PCR reactions, products were separated on a 2% agarose gel containing ethidium bromide. To make the gel, the appropriate quantity of agarose (Sigma) was weighed out and dissolved in TAE buffer by heating in a microwave. Ethidium bromide was added to the solution before it was poured into a gel cassette. 'Combs' were used to create wells of an appropriate size and the gel was left to set. Once samples were loaded, the gel was left to run in TAE buffer for approximately 1hr at 100 volts. PCR products were visualised under ultraviolet (UV) light using an Alpha 2200 Digital UV-Visphoto Imager (Alpha Innotech). In order to verify the size of the products, samples were run alongside one of two DNA ladders; Hyperladder I for products <10 kilo bases (kb) or Hyperladder IV (both Bioline) for products <1000 base pairs (bp).

2.4.7 Quantitative Real-Time PCR

2.4.7.1 Primer design

In order to detect and quantify genes of interest using SYBR green quantitative real- time PCR (qRT-PCR), two sets of primers were designed. 'Inner' primers, or QPCR primers, were necessary for the amplification of the target gene whereas the 'outer' primers (Table 2-2) were designed to function as standard templates. Standard primers flank the amplicon targeted by the qRT-PCR primers, along with 20bp's either side, amplifying this region. Primers were designed using Primer3 Input software version 4.0.0 (http://primer3.ut.ee/), adhering to the following conditions to ensure their specificity and efficiency.

Specification for QPCR primers:

Primer size	18 to 24 bp (20bp optimal)
Melting temperature (Tm)	59.5°C to 61°C (60°C optimal)
GC content	40% to 65% (50% optimal)
Max self-complementarity	3 (≤2 optimal)
Max 3' complementarity	1
Amplicon size	≤150bp

Standard primers were designed to the same stringent criteria, however the amplicon size could range from 100bp to 2000bp and, if need be, the self-complementarity could be increased to 5.

2.4.7.2 Primers preparation for quantitative PCR

Primers were synthesised by Integrated DNA Technologies (IDT, Belgium) by standard DNA synthesis and desalination, to remove any impurities. Standard and QPCR primers were resuspended in nuclease- free H_2O to a concentration of 100μM and forward and reverse primers were subsequently mixed 1:1 to obtain a final primer concentration of 50μM. The specificity of the primer sequences was assessed using Basic Local Alignment Search Tool (http://blast.ncbi.nlm.nih.gov/ Blast.cgi), before being confirmed by PCR using cDNA known to contain the region of interest. All reconstituted primer pairs were stored at -20°C

Table 2-1 Primer sequences used for RT-PCR

Gene	Forward Sequence	Reverse Sequence
TBP	5' TGC TGT TGG TGA TTG TTG GT 3'	5' AAC TGG CTT GTG TGG GAA AG 3'
CXCL10	5' GCT CAA GTG GCT GGG ATG 3'	5' GAG GAC AAG GAG GGT GTG G 3'
Gbp2	5' CCA AGC GAG ATG CCT TTA TC 3'	5' TTC TTC TTC CAG GGG TCC A 3'
Gbp3	5' ACC CAT TTG TCT GGT GGA AA 3'	5' GAG GCT GTG CTA TCT GCT CAA 3'
Gbp4	5' CCT CTT CCT CTT TCT TCT TCC TTT 3'	5' GTG TTT CTA TGG GGG TGT GG 3'
Gbp6	5' AAA CAC ACT CCC TCT CCC AGT 3'	5' TGA AGC CAG TCA ACA TCC AG 3'
Ifit1	5' ACC ATG GGA GAG AAT GCT GAT GGT 3'	5' TGA TGT CAA GGA ACT GGA CCT GCT 3'
Ifitm3	5' CGC TCC ATC CTT TGC CCT TCA GTG 3'	5' GCC CCC ATC TCA GCC ACC TCA T 3'
Igrm1	5' AGT TCA GCA GGT AGC CCA GA 3'	5' TCA GCC TCA GTT TCC AGT CC 3'
Irf7	5' GAA GAG GCT GGA AGA CCA ACT 3'	5' AGA TAA AAC GCC CTG TGC TG 3'
Lgals3bp	5' ATT CCT GTG TCC CCT CCT TC 3'	5' GTG AGT GCT GGC TGA AAC CT 3'
Oasl2	5' AGA AAG GGA TGG GAA CAG GTG GCT 3'	5' GGGTCGGGGACTAAGCAGGGTT3'
Rtp4	5' GCA TCT TTG GGT GAG AAG GT 3'	5' ATG GGG AGG AAC TCT TTG GT 3'
Sp100	5' CAT CAT TTT CCT TGG CTG GT 3'	5' CAT TTT GGT TGG TCC TTG CT 3'
Stat1	5' GAA AAA CGC TGG GAA CAG AA 3'	5' CGA CAG GAA GAG AGG TGG TC 3'
CCL3	5' CAG CCA GGT GTC ATT TTC CT 3'	5' CAG GCA TTC AGT TCC AGG TC 3'
CCL5	5' CTG CTG CTT TGC CTA CCT CT 3'	5' ACA CAC TTG GCG GTT CCT T 3'
CCL9	5' CTC ACA ACC ACG GAC CTA CA 3'	5' CAC TGG GGA AGA CCA AAG AA 3'
CXCL13	5' CAT ACC CAA CCC ACA TCC TT 3'	5' GCC TGT TCT CAA ATA GCC TTT C 3'
CXCL16	5' TGC TGA CCC TTT GCC TCT AC 3'	5' GGC TGG CTT GGA CTA AAT AAC A 3'
CCR5	5' TTT GTT CCT GCC TTC AGA CC 3'	5' TTG GTG CTC TTT CCT CAT CTC 3'

Table 2-2 Standard sequences used for RT-PCR

Gene	Forward Sequence	Reverse Sequence
TBP	5' GAG TTG CTT GCT CTG TGT GCT G 3'	5' ATA CTG GGA AGG CGG AAT GT 3'
CXCL10	5' CGA TGG ATG GAC AGC AGA GAG CCT 3'	5' GAC AAG GAG GGT GTG GGG AGC A 3'
Gbp2	5' TTT GTG GGC TTC TTT CCA AC 3'	5' CTT TGC TGC CTC TGT GAG TG 3'
Gbp3	5' CCC CAG AGA GGA CAA AGT GA 3'	5' ACC CCC AGA GAA CAG AGA AAG 3'
Gbp4	5' TTG GTT TTG TGA GGG CAT TT 3'	5' ATC AGT AAA GGG GAG GCA GT 3'
Gbp6	5' GTC TTC TCT TCC CCC ACC TC 3'	5' GGC TCC CAA TAA AAC CGC AC 3'
Ifit1	5' GCA AGA GAG CAG AGA GTC AAG GCA 3'	5' GCA GGG TTC ATT TCC CCA GTG AGC 3'
Ifitm3	5' TCT GAG AAA CCG AAA CTG CCG CA 3'	5' TGT AGG GAG GGG CAA GGA GGG A 3'
Igrm1	5' CTG CTC CAC TAC TCC CAA C 3'	5' CTC TCC AGC CCA AAA ACA AA 3'
Irf7	5' CTG TGA CCC TCA ACA CCC TAA 3'	5' GAG CCC AGC ATT TTC TCT TG 3'
Lgals3bp	5' TGG TCA TAC GCC CCT TCT AC 3'	5' CAC AGG AAA TCC CAC AGG AC 3'
Oasl2	5' AGA AAG GGA TGG GAA CAG GTG GCT 3'	5' GGG TCG GGG ACT AAG CAG GGT T 3'
Rtp4	5' AGA CAG TGC TTG GCA GGT TC 3'	5' CTA TGG GGA AGG GCA TTT TT 3'
Sp100	5' CCG AAT GGG TCA TCC TTA GA 3'	5' TCT TTT TCT GCG TCG TTG TG 3'
Stat1	5' CCT ATG AGC CCG ACC CTA TT 3'	5' GGA AGC AGG TTG TCT GTG GT 3'
CCL3	5' CCA CGC CAA TTC ATC GTT 3'	5' TAT GCA GGT GGC AGG AAT GT 3'
CCL5	5' CCC TCA CCA TCA TCC TCA CT 3'	5' TCA GAA TCA AGA GGC CCT CTA TCC 3'
CCL9	5' GCC CTC TCC TTC CTC ATT CT 3'	5' GCC CTC TCC TTC CTC ATT CT 3'
CXCL13	5' AAC GCT GCT TCT CCT CCT G 3'	5' CCA TCT CGC AAA CCT CTT GT 3'
CXCL16	5' CGC CTA CAG CAA GAG TGG A 3'	5' AAG AGT GTT CCC CAA GAG CA 3'
CCR5	5' ACC CAT TGA GGA AAC AGC AA 3'	5' CCT CTG AGG GGC ACA ACA AC 3'

2.4.7.3 Generation of standard templates

The expression levels of target genes can be quantified by comparing them against a standard curve. This was generated by performing a PCR reaction (described in section 2.4.6) using cDNA known to contain the target amplicon, the products of which were separated using gel electrophoresis (2.4.6.1). The relevant band, whose size corresponded with that of the desired product, was subsequently cut from the gel using a scalpel. The bands were then purified using a QIAquick Gel Extraction Kit (Qiagen) in accordance with the manufacturer's instructions and the quantity of DNA was assessed using the

Nanodrop 1000. The following calculation was used to assess the absolute number of amplicon copies:

$$\text{Copies (per µl)} = \frac{\text{(Concentration (g/µl) X Avogadro's Constant)}}{\text{Molecular weight of amplicon}}$$

where the molecular weight of the amplicon is equal to the size of the amplicon in base pairs, multiplied by 660 Daltons, the average molecular weight of one base paired nucleotide. Purified standards were diluted in 1×10^{-2} TE buffer and stored at -20°C until use.

2.4.7.4 Quantitative real-time PCR

qRT-PCR was performed using a Prism® 7900HT Sequence Detection System (Applied Biosystems) in accordance with manufacturer's guidelines. qRT-PCR amplifications were performed in triplicate within wells of a 96-well or 384-well PCR plate (both StarLab). Along with biological samples, each plate was performed with the addition of a –RT (2.4.5) and non- template control (NTC). NTCs were void of cDNA, substituting nuclease- free H_2O in its place. Each reaction contained the following:

	96-Well	384-Well
SYBR® Green FastMix[1]	7.5µl	5µl
RNase-free H_2O	5.7µl	3.85µl
Forward Primer[2]	0.15µl	0.075µlReverse
Primer[2]	0.15µl	0.075µl
cDNA (from a 1/10 dilution[3])	1.5µl	1µl

---

[1] Purchased from Quanta Bioscience
[2] Primers listed in Table 2-1
[3] Diluted in nuclease-free H_2O prior to experiment

2.4.9 Determining relative gene expression

QPCR results were analysed using Sequence Detection System 2.4 software, whereby an absolute copy number for each target gene was generated based on the values of the standard curve. Comparative studies were previously performed in our lab to evaluate housekeeping gene expression across different tissues and found that tata binding protein (TBP) was the most consistent within the brain. Therefore, to eliminate variations caused by differences in starting RNA concentrations, the absolute copy numbers were normalised against TBP as follows:

Normalised Copy Number = Target Gene Copy Number ÷ TBP Copy Number

Subsequently, the normalised copy number was then used to calculate magnitudes of fold change by comparing treatment groups against relevant control groups.

2.5 Protein Expression Analysis

2.5.1 Enzyme-linked immunosorbent assay

Cytokine levels in murine plasma were analysed using Duoset enzyme- linked immunosorbent assay (ELISA) Development System kits (R&D Systems). Frozen samples were thawed thoroughly before use, and were diluted appropriately using the relevant reagent diluent. The protocol was followed as outlined in the manufacturers' handbook using half volume plates (Costar, Corning International), so all sample and reagent volumes used were half of that outlined in the protocol. Plates were read using a TECAN plate reader to provide optical density (O.D) readouts which were then converted to protein concentration values based on the standard curve of known quantities.

2.5.2 Histology

2.5.2.1 Tissue Preparation

Samples for histological analysis were dissected as previously described. Samples were immediately submerged in formalin and kept at room temperature for 24 hours before being processed.

2.5.2.2 Tissue Processing

Following fixation in neutral buffered formalin for 24 hours, tissues were processed using an automated Shandon Citadel 1000 processor (ThermoFisher), whereby they were dehydrated over increasing concentrations of ethanol, submerged in xylene and infiltrated with paraffin wax (see details below).

1. 70% Ethanol   1 hour
2. 90% Ethanol   1 hour
3. 95% Ethanol   1 hour
4. 100% Ethanol   1x 1 hour, 1x 2 hours, 1x 2.5 hours
5. Xylene   2x 1 hour and 1x 1.5 hours
6. Molten paraffin wax 2x 4 hours (60-65°C)

Following processing, samples were inserted into metal moulds and embedded in paraffin wax using a Shandon Histocentre 3 (ThermoFisher). Wax blocks were subsequently cooled on an integrated cold plate until set hard, and were stored at room temperature until use.

2.5.2.3 Tissue Sectioning

Sections of skin and brain, at 5μm and 7μm thickness respectively, were cut using a Shandon Finesse 325 microtome (ThermoFisher). Cut sections were floated onto a water bath at a temperature of 40°C to smooth out wrinkles before being adhered to Microslide Superfrost Plus slides (VWR International). Slides were left on a Raymond A Lamb Hotplate (ThermoFisher) set to 55°C for approximately 1 hour to dry. Slides were stored at room temperature until use.

2.5.2.4 Haematoxylin & eosin (H&E) staining

Tissue sections were deparaffinised by being submerged in absolute xylene (VWR International) for 3 minutes before being rehydrated across a gradient of 100% and 70% ethanol solutions for 20 seconds each. Sections were rinsed in running water for 2 minutes before being transferred to Haematoxylin Z Stain (CellPath) for 6 minutes. Sections were rinsed under running water for 2 minutes, differentiated in 1% acid alcohol for 30 seconds and then rinsed again. Sections were immersed in Scott's tap water for 2 minutes and were then rinsed, prior to

being counterstained in Putt's Eosin (CellPath, diluted 1:4 with dH$_2$O) for 6 minutes. Sections were rinsed for a final 2 minutes and were then dehydrated along a gradient of 70%, 90% and 100% ethanol solutions for 20 seconds each. Finally, sections were placed in absolute xylene for 3 minutes before being mounted in DPX (Leica Biosystems).

2.5.2.5 Doublecortin (DCX) Fluorescent Staining

Brains were cut sequentially along the midsaggital plane (from the inside to the outside) to 7µm thick sections. Sections were deparaffinised in absolute xylene for 5 minutes before being dehydrated across a gradient of 100%, 90% and 70% ethanol solutions for 2 x 3 minutes each. Sections were rehydrated in H$_2$O for 5 minutes before being washed in TBST for 5 minutes. Antigen retrieval was performed using citrate buffer, in which the sections were boiled for 8 minutes. Slides were left to cool for 15 minutes at room temperature, before being washed in H$_2$O and TBST for 5 minutes each. Sections were blocked for 1 hour at room temperature using 20% normal horse serum (Vector Laboratories) in TBST containing 4 drops of Avidin (Vector Laboratories) block, before being washed again in TBST. Primary antibody (Polyclonal goat anti-mouse DCX (Santa Cruz Biotechnology) 1:100/ 2.5% normal horse serum/ 2.5% mouse serum (Invitrogen) in DAKO diluent (DAKO) + 4 drops Biotin (Vector Laboratories) block/ml) or isotype (Goat IgG (Vector Laboratories) 1:2500/ 2.5% normal horse serum/ 2.5% mouse serum in DAKO)/ negative control was added to the slides and incubated overnight at 4°C. The following day, slides were brought to room temperature, washed twice in TBST and were incubated with the secondary antibody (Horse anti-goat IgG 1:200/ 2.5% normal horse serum/ 2.5% mouse serum in DAKO) for 30 minutes at room temperature. Cells were washed in TBST, incubated with FITC-Avidin D (1:500 in PBS, pH 8.0) (Vector Laboratories) for 40 minutes in the dark at room temperature, washed once again and then mounted with 2 drops of Vectashield Hardset containing DAPI (Vector Laboratories).

2.5.3 Luminex

Plasma samples from skin inflammation models were isolated as described previously, and were stored at -80°C until use. The mouse cytokine 20-plex panel was used, along with the extracellular protein buffer reagent kit (Life

Technologies), to determine the concentration of 20 cytokines in the plasma samples (Table 2-3). Assay was carried out in accordance with the manufacturer's instructions. Briefly, samples were diluted 1:4 with assay diluent and were added in triplicate to a 96-well filter plate coated with premixed beads, along with an appropriate standard curve and blanks. Plates were wrapped in tin foil and were left on a plate shaker at room temperature for 2 hours. Subsequently, plates were washed, Biotinylated Antibody mix was added and the plates were incubated for 1 hour at RT. Following another wash step, Streptavidin-RPE was added and plates were left shaking at room temperature for 30 minutes. Plates were washed for a final time before results were read using a Bio-Rad Bio-Plex machine and analysed with Bio-Plex Manager 4.1 software.

Table 2-3 Cytokines and chemokines analysed using Luminex

FGF Basic	IFN-γ	GM-CSF	IL-1α
IL-1β	IL-4	IL-2	IL-5
IL-6	IL-12	IL-10	IL-13
IL-17	KC	CXCL10	CCL2
CXCL9	TNF-α	CCL3	VEGF

2.6 Behavioural Models

2.6.1 Burrowing Model with Aldara Treatment

Burrowing tubes were commissioned to a local model maker who constructed twenty identical tubes to the dimensions and specification outlined in the Nature Protocol[373] and shown in Figure 2-1. 200g of normal food pellets were deposited into each tube, which were then placed individually into large cages, against the back right corner. Mice were acclimatised overnight in group cages, whereby one burrowing tube containing 200g of food was left in a cage of 5 mice overnight. The tubes were removed the following morning. Baseline tests were carried out at for a 2hr and a 24hr time-point. To do so, mice were individually caged and left between 2pm and 4pm. At 4pm the contents of each tube was weighed and

returned to the respective tube. Mice were then left overnight in their single cages until the next morning when the remaining food pellets were weighed again. Baseline texts were carried out 48hrs prior to mice being put on procedure. Mice were put on procedure and treated in the morning with either 80mg Aldara cream or equivalent control cream as described in section 2.2.2.1. Four hours later, coinciding with the 2hr baseline time period, burrowing tests were performed over 2hrs. Again, mice were caged individually in the same cage they had been in for the baseline tests and the remaining food was weighed at the end of the 2hr window. Mice were then returned to their group cages. Individual cages were cleared of burrowed food pellets between each test. Both the treatment and the burrowing tests were repeated for a total of 3 consecutive days to coincide with the peak of the Aldara treatment.
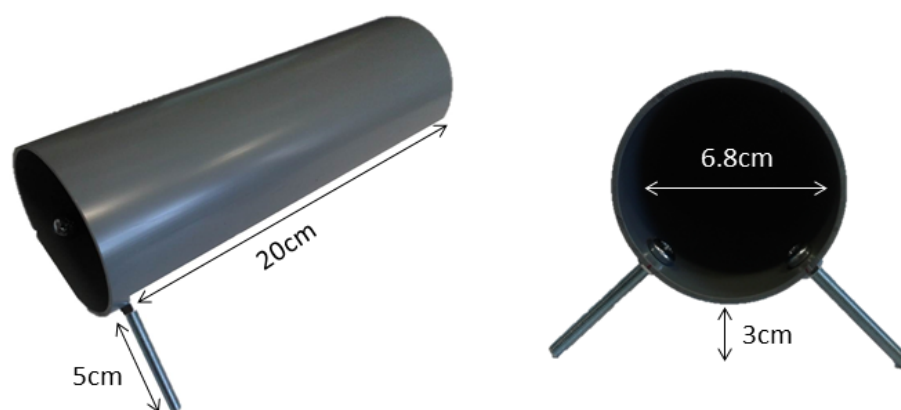
Figure 2-1 Burrowing Tubes
Behavioural analysis of treated mice was performed using a burrowing model of anhedonia. This required the use of burrowing tubes of a particular dimension and specificity, as shown.

2.6.1.1 Compound 21

CXCR3 Blocker, or Compound 21, a kind gift from Amgen Inc. (Thousand Oaks, CA, US), was first prepared as a stock solution by being dissolved in 100% DMSO to a concentration of 7.9mg/ml. This was stored at -20°C until further use. 500μl of 50% PEG400 (Sigma) and 500μl of dH$_2$O were added to 1ml of the Compound 21 stock solution. Water was added very slowly to prevent the compound from falling out of solution. Mice were injected subcutaneously (s.c) with 50μl (10mg/kg) of Compound 21 for four consecutive days, starting one day prior to

the initiation of Aldara treatment (24hrs after baseline tests). Control mice were treated with the vehicle minus Compound 21 at the same concentration.

2.6.1.2 Use of DAPTA

D-ala-peptide T-amide (DAPTA), a CCR5 antagonist, was dissolved in H_2O to a concentration of 1mg/ml. Mice were injected s.c with 200µl (1mg/kg) of DAPTA daily for four consecutive days, starting one day prior to the initiation of Aldara treatment (24hrs after baseline tests).

2.7 Statistical Analysis

Data were analysed using GraphPad Prism software (San Diego, CA). Depending on the experiment, analysis was performed using a Student's unpaired t test or a one- or two- way ANOVA with Bonferroni post-tests, as outlined in figure legends. A probability value (p-value) of $p < 0.05$ was considered statistically significant.

Chapter 3

Transcriptional profiling of the brain following cutaneous inflammation induction with Aldara

3 Transcriptional profiling of the brain following cutaneous inflammation induction with Aldara

3.1 Introduction

It is clear that events in the periphery can have a profound effect on the CNS. However, the mechanisms by which peripheral inflammation can influence the brain remain to be fully understood. Evidence suggests that immune components, particularly inflammatory cytokines, may mediate some of the neurological conditions that are often presented alongside chronic inflammatory diseases[5, 55, 302, 322]. These conditions include major depressive disorder, anxiety and schizophrenia[321, 374]. Trying to understand the relationship between inflammation and mood disorders in the human brain is difficult due to the obvious ethical and practical restrictions and for this reason many have turned to animal models. Animal models have helped confirm this correlation and have shown that immune activation in the periphery can induce a set of depressive-like behaviours called 'sickness behaviours'[55, 56, 375]. These behaviours are a way of conserving energy and are often short lived, coinciding with the duration of illness. However it is thought that in some cases, inflammation fails to resolve and these behaviours become chronic, resulting in the emergence of long term mood disorders. Generally speaking however, animal models used to try to further our understanding in this respect have relied on rather crude methods of instigating large scale systemic inflammation, rather than focusing on disease models that are arguably more reflective of human conditions. This makes it difficult to gauge just how relevant these studies are with regards to the relationship that exists between the immune/inflammatory system and the CNS in humans. In addition, the models that have been studied have so far failed to reveal the underlying mechanisms of this co-morbid relationship and as such, further investigation is required.

The aim of this thesis was to investigate the effects of peripheral inflammation on the brain using a tissue- specific model of peripheral inflammatory disease that reflects the human disease, psoriasis. Aldara cream, described in detail in section 1.6.2.1, has been shown to induce psoriasis- like skin inflammation when applied repeatedly to the dorsal skin of mice[363]. Extensive reviews of this model suggest that it is one of the most accurate mouse models of human psoriasis as it

functions through the IL-17/ IL-23 axis[366, 376]. This, along with its simplicity and reproducibility, made it an appropriate model to use for this study. The aim of this chapter was to investigate if and how the Aldara model of psoriasis-like skin inflammation affects the brain in control and Aldara treated mice. To do so, Affymetrix GeneChip arrays were used to derive a full transcriptional profile of the brain. In addition, a basic behavioural test was performed to determine whether or not Aldara treatment can induce a functional CNS phenotype.

3.2 The Aldara model of skin inflammation

To induce the psoriasis-like pathology, Aldara cream was applied daily to the shaved dorsal skin of 6-8 week old female c57BL/6 mice. This was repeated over 5 consecutive days. Alternatively, age and sex matched mice were treated with a water based control cream. Mice were terminally anaesthetised 24 hours after the final application and tissues harvested for analysis.

3.2.1 Model Validation

Prior to carrying out microarray analyses, the suitability of Aldara as an inducer of reproducible skin inflammation was confirmed. To do this, mice treated with Aldara cream, or control cream, every 24 hours were weighed following each application. In addition, spleens were collected, weighed and measured. Dorsal skin samples from the area of application were removed from the mice after the final application, sectioned and stained with H&E. Consistently, mice treated with Aldara cream lost a significant amount of weight compared with control cream treated mice (Figure 3-1A). This loss was apparent 24 hours following the first treatment and was most pronounced between the third and fifth treatments. Between the fourth and fifth applications, the Aldara treated mice showed signs of recovery; however their weight remained lower than the control group. The spleens of the treated mice were consistently larger than those of the control mice, often more than twice the weight and size (Figure 3-1B-C). Finally, H&E staining of the skin sections revealed a psoriasis-like skin inflammation in mice treated with Aldara. This was characterised by epidermal hyperplasia, dermal thickening and inflammation and flaking of the skin (Figure 3-1D). These results demonstrate that, in agreement with the literature, Aldara cream induced a psoriasis- like skin inflammation at the site of application. The

corresponding weight loss and splenomegaly suggest that this model is also associated with a systemic response. To investigate this, 24hr after the fifth application of Aldara cream, plasma was isolated from mouse whole blood obtained by cardiac puncture. ELISA was used to assess the protein expression of three prominent inflammatory cytokines, IL-1β, IL-6 and TNFα (Figure 3-2A-C). Plasma from LPS- treated mice was used as a positive control (Figure 3-2D). After the fifth application of Aldara, none of the cytokines were present in measurable concentrations in the plasma as all fell below the minimum detection level of the kits. The positive controls confirmed that the assay worked. However, the lack of cytokine induction seen in the periphery may be due to the timing of the analysis.
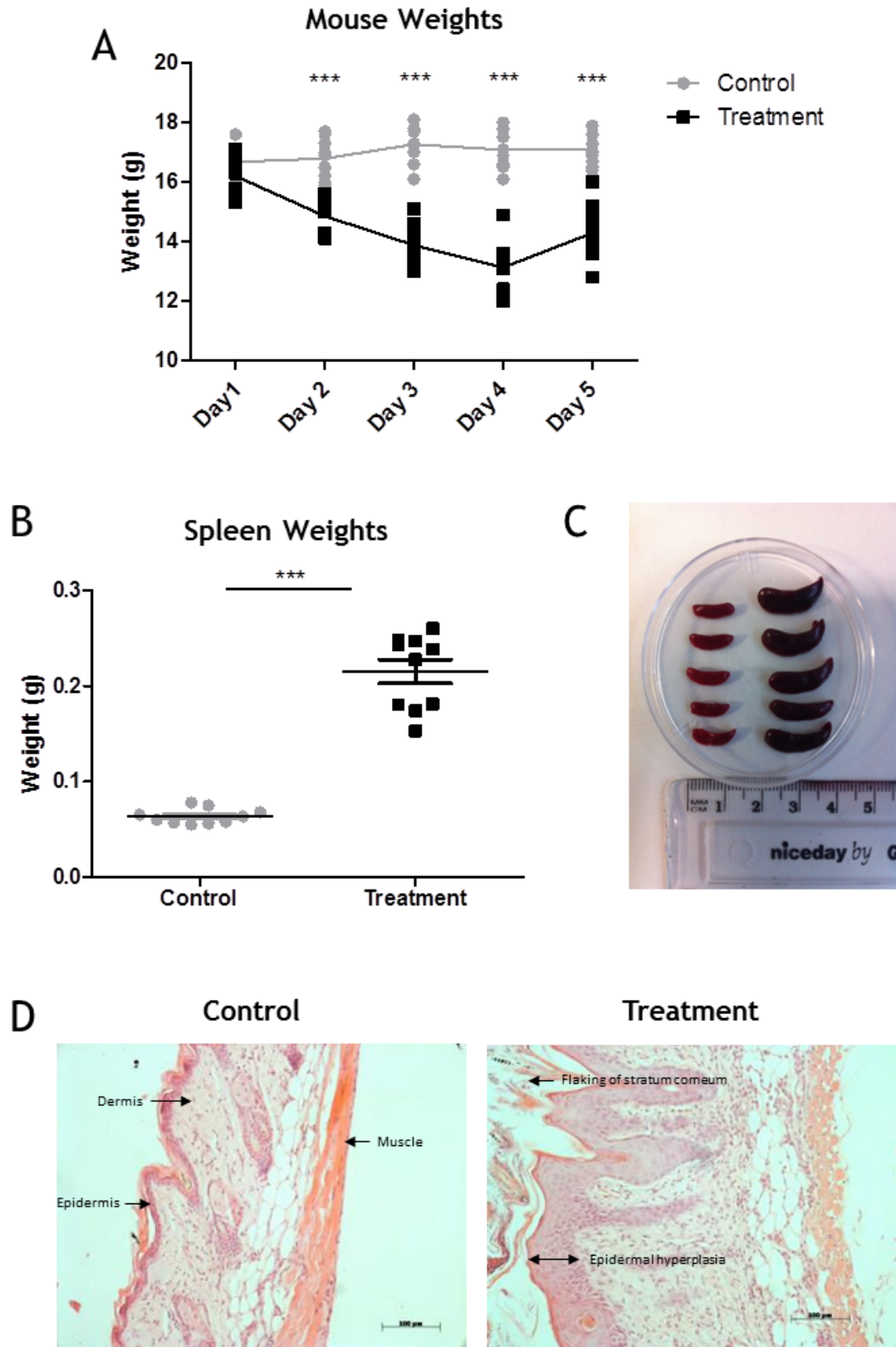
Figure 3-1 Evaluation of the phenotypic response to Aldara- induced skin inflammation
Mice treated with ~80mg Aldara cream, or equivalent volume control cream, were weighed following each application (A). In addition, spleens were removed and were weighed (B) and photographed (C). H&E staining was performed using 5µm thick sections of Aldara- or control-treated skin which were visualised at 200X magnification (D). (A & B) n = 10/ group from two independent experiments (C & D) n = 5/ group. Significance was measured using two-way ANOVA with Bonferroni multiple comparison post-tests *** = p ≤ 0.001.
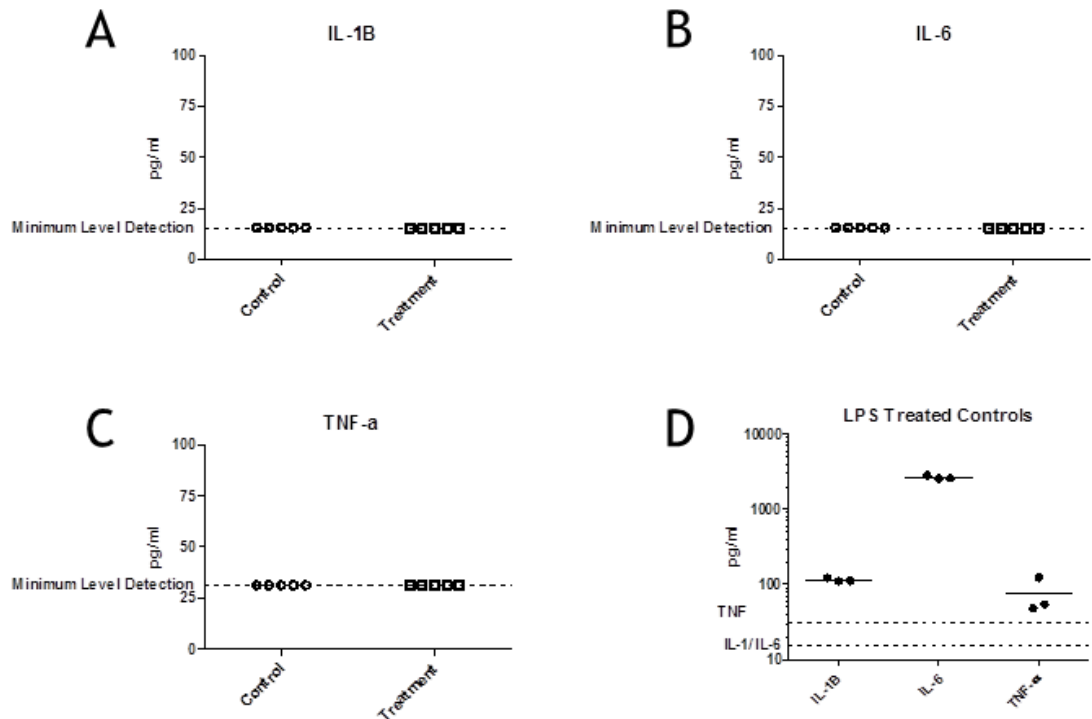
Figure 3-2 Expression of inflammatory cytokines in the plasma of Aldara-treated mice
Plasma was isolated from mice treated with ~80mg Aldara cream, or equivalent volume control cream, 24hrs after the fifth application. ELISAs were used to assess the expression of three key inflammatory cytokines, IL-1β (A), IL-6 (B) and TNF-α (C). To ensure the integrity of the assay, plasma from LPS- injected mice was included as a positive control. Group size of n = 5 for Control cream and Aldara- treated mice, n = 3 for LPS- treated mice. Minimum level of detection represents the lowest sensitivity for each kit.

3.2.2 Processing of RNA samples

RNA was extracted from the right hemisphere of brains taken from mice 24 hours after the fifth, and final, application of Aldara cream. Before microarray analysis could be performed, the integrity of the RNA samples was assessed. This analysis, which was performed by the University of Glasgow Polyomics facility, was done using an Agilent 2100 Bioanalyser, which assesses nucleotide fragments separated by size and evaluates them quantitatively on microfluidic chips via laser induced fluorescent detection (fluorescent units, FU). Screening each sample generates an electropherogram that allows RNA integrity to be visually assessed. In addition, using a mathematical algorithm, an RNA integrity number (RIN) can be generated. RIN is a software tool that has been designed to estimate RNA integrity based on the presence or absence of degraded RNA products and the ratio of 28S:18S ribosomal 'RNA species'. RIN values are between 1 and 10, where 1 is a completely degraded sample and 10 is a

perfectly intact sample. RIN software algorithm ensures repeatability of electropherogram interpretation by removing user-dependent visual interpretation. An example of an electropherogram from a completely intact RNA sample with an RIN of 10 is shown in Figure 3-3A. This eletropherogram contains three peaks which represent the RNA marker (1), the 18S rRNA (2) and the 28S rRNA (3). Very little background signal should be present outwith these three peaks as this would indicate the presence of RNA degradation products. The integrity of the RNA from each brain sample was assessed. One representative electropherogram of RNA integrity from control mice (B) and one from Aldara treated mice (C) are shown. The RIN of each sample is shown in Table 3-1. An RIN of 8 or above is considered sufficient for performing microarray analysis, thus all samples met the requirement. In addition, Table 3-1 shows the ratio of 28S to 18S rRNA species in each sample. In the mouse, a ratio >2 is considered good quality RNA, with an optimal ratio of 2.5. Therefore, the 28S:18S ratio, high RIN, low background and clear peaks demonstrate that all RNA samples were of high enough quality to proceed to microarray analysis.

Having confirmed the integrity of the RNA, samples were amplified by in vitro transcription and reverse-transcribed to generate sense-strand cDNA. This was then fluorescently labelled and fragmented. The Agilent 2100 Bioanalyzer can measure the efficiency of cDNA fragmentation using a DNA chip, which generates an electropherogram by measuring the fluorescence intensity over time.

Figure 3-3(D-E) show representative fragment electropherograms from control mice (D) and Aldara treated mice (E). Each shows one peak next to the DNA marker, denoted on the electropherogram by the number 1, indicating that the DNA fragments in each sample were of similar size. The speed with which they passed through the investigative electrophoretic microchannel suggested that the fragments were relatively small and together these data indicate that the RNA samples were of high quality and were successfully fragmented.
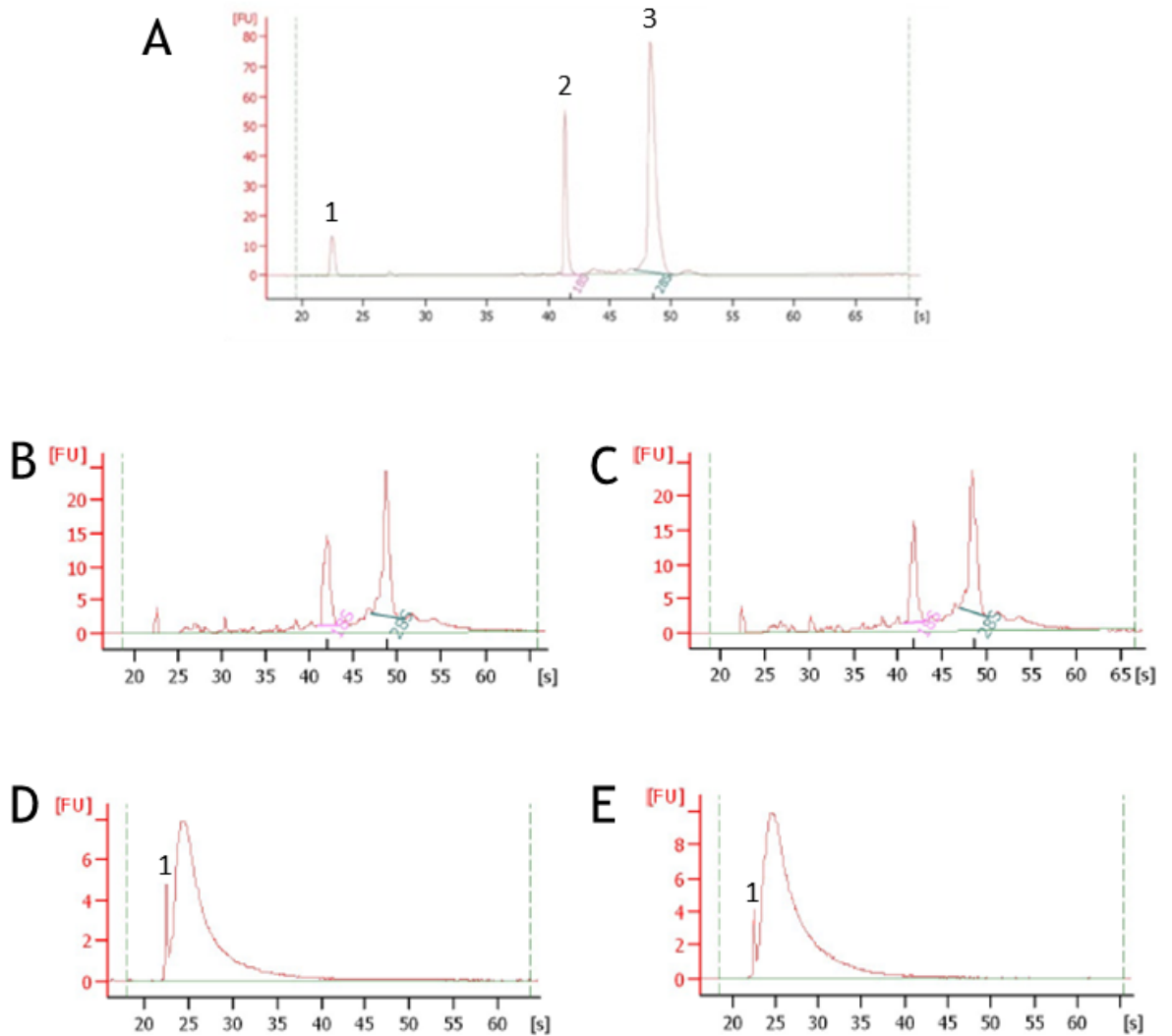
Figure 3-3 Electropherograms to show RNA integrity
RNA isolated from Aldara-treated brains and control cream-treated brains was prepared for microarray analysis. Prior to the array, RNA integrity and the efficiency of sense-strand DNA fragmentation were measured using an Agilent 2100 Bioanalyzer. An electropherogram was generated for each sample. This was used to assign an RIN value between 1 and 10. Data are shown as Fluorescent units (FU) over time. (A) Representative high integrity RNA sample with RIN of 10. (B-C) Integrity of whole brain RNA from; (B) control mice and (C) Aldara treated mice. (D-E) Fragmented DNA samples from (D) control mice and (E) Aldara treated mice. (B-E) Data are shown as one representative from each group. n=5/ group.

Table 3-1 RNA integrity of brain samples

Sample ID	RIN Value	Ribosomal 28s:18S ratio
Control 1	9	2.5
Control 2	8.9	2.5
Control 3	9.1	2.5
Control 4	9.1	2.5
Control 5	9.1	2.5
Treatment 1	8.8	2.5
Treatment 2	8.9	2.4
Treatment 3	9.0	2.4
Treatment 4	9.0	2.2
Treatment 5	8.9	2.4

3.3 Determining the effect of Aldara treatment on the transcriptional profile of the brain

To determine the transcriptional effect of cutaneous Aldara treatment on the brain, the transcriptional profiles of the brains from 5 Aldara treated mice were compared with those from the brains from 5 control cream treated mice. The Affymetrix GeneChip Mouse Gene 1.0 Array has been extensively validated and was selected for this transcriptomic analysis. This array provides a comprehensive expression profile, using 770,317 distinct probes distributed across the full length of about 28,853 specific coding transcripts.

3.3.1 Pre-processing of Affymetrix chip data using GeneSpring

Microarray experiments were carried out by the Glasgow Polyomics facility (http://www.polyomics.gla.ac.uk), a core University facility. In order to control the effects of systematic error from dye efficiencies, uneven hybridisation or other extraneous factors, whilst still retaining biological variance, the quality of the raw data was assessed and pre-processed with the following steps:

- Background correction: this is to adjust for the hybridisation effects that are not directly related to the interactions between the probes and the DNA. The details of this step are outlined in Section 2.4.4.

- Normalisation: this allows multiple chips to be compared with one another by removing systematic error and bias. This unifies the distribution of the perfect match values across the different chips, assuming that they have approximately the same distribution.

- Perfect match probe correction and summarisation: this summarises the 11 perfect match (PM) probe intensity values providing a normalised value of RNA expression for each gene.

Agilent GeneSpring GX software was used for pre-processing and data analysis, utilising a modified version of Robust Multi-array Analysis (RMA), RMA 16, for the normalisation and summarisation of probe-level intensity measurements.

3.3.2 Signal histogram of normalised data

Following data normalisation and prior to formal analysis of the array, sample hybridisation was monitored for differences in efficiency. This was to check for variations between the chips that may affect the quality and reproducibility of the array, which can result from user error or differences in chip manufacturing. To do so, fragmented cDNA is first added to a hybridisation control cocktail containing a set of 4 control transcripts; *BioB*, *BioC*, *BioD* and *cre*. These control transcripts are prepared to staggered standard concentrations of 1.5pM, 5pM, 25pM and 100pM, respectively. To ensure consistency of hybridisation efficiency between chips, the signal intensities of the four hybridisation control transcripts on each of the 10 GeneChips used in this study are plotted on the histogram shown in Figure 3-4, where the red lines represent the treatment samples and the green lines represent the control samples. The similar intensity values for the four hybridisation controls would suggest that there is little variation in hybridisation efficiency between each chip.
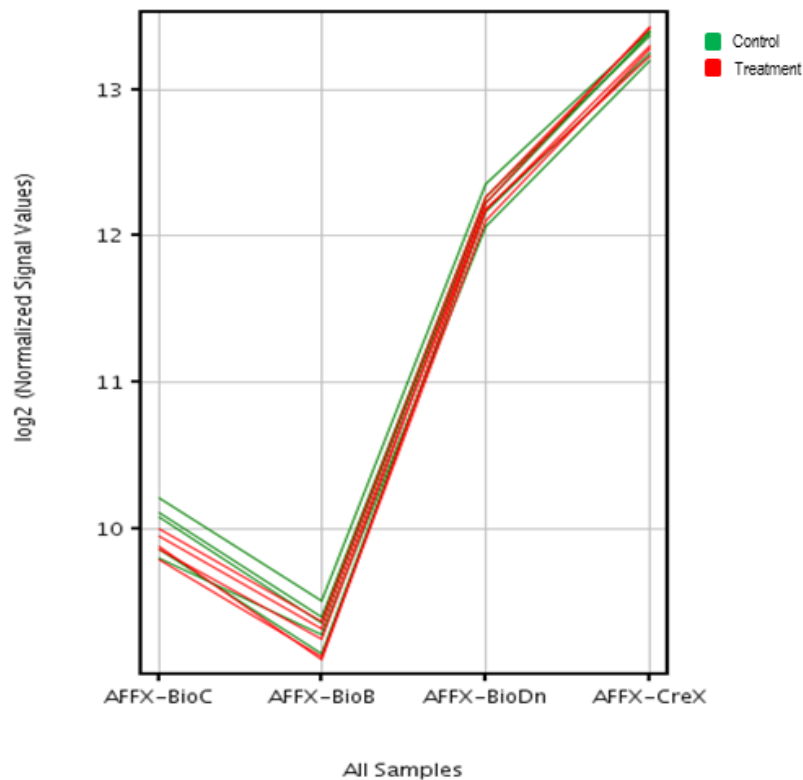
Figure 3-4 Signal histogram showing normalisation of microarray data
To determine the transcriptional response in the brain following Aldara treatment and control cream treatment, microarray analysis was performed. Labelled sense-strand cDNA, generated from amplified RNA samples as described, was hybridised to 10 different chips along with 4 control transcripts at known standard concentrations. Signal histograms were generated for sample and control hybridisation, allowing the signal intensities to be compared. The histogram shown here depicts the normalised signal intensities of the hybridization controls; bioB, bioC, bioD and cre. Each line on the histogram represents an individual GeneChip, where the red lines are the treatment samples and the green lines are the control samples.

3.3.3 Principle component analysis

Principle component analysis (PCA) is a level of analysis that identifies patterns in the observed differential transcriptomic data. PCA uses a mathematical method that allows multidimensional data from the array to be transformed into a lower dimensional output using a minimal set of variables, called principle components (PC). The resulting PCA graph allows for visual analysis to be performed so that trends in the data, and outlying samples, can be identified.

Figure 3-5 shows the PCA map of the normalised microarray data from this study. Each circle represents one sample and each colour represents a different group, where green is the control group and red is the Aldara treated group. The graph shows variation between samples within the same group, indicated by the lack

of tight clustering, which suggests that there are slight differences in the transcriptomic profile of the brains of both groups. None of the samples was identified as an outlier and thus all samples were included for subsequent analysis. The PCA graph shows a separation between the control and treatment groups, suggesting a differential gene response to the two different stimuli.
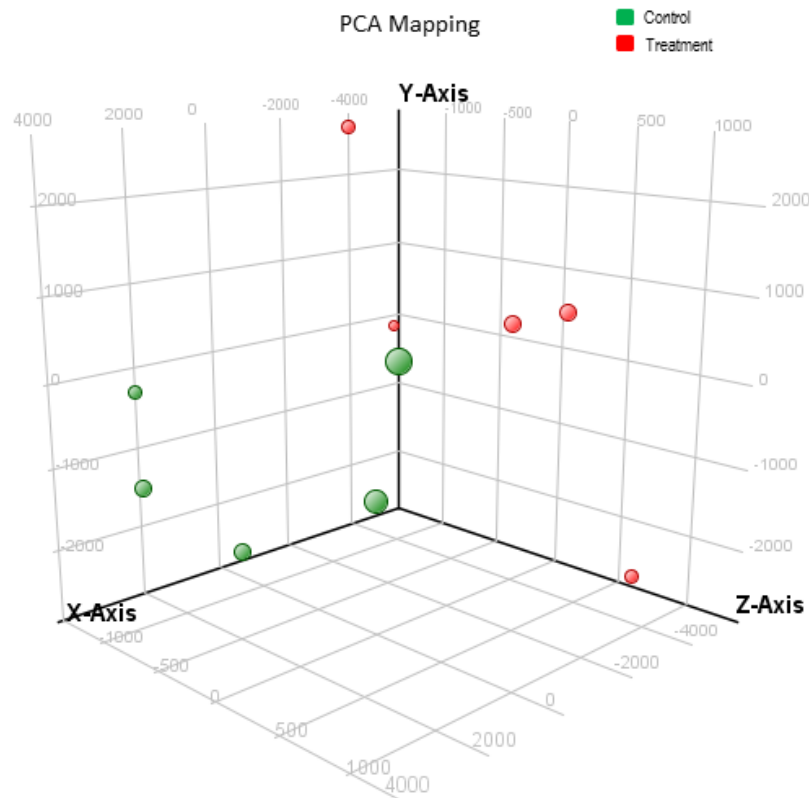
Figure 3-5 Principle component analysis mapping of microarray samples
To determine the transcriptional response in the brain following Aldara treatment and control cream treatment, microarray analysis was performed. Principle component analysis (PCA) was performed on normalised data from all samples included in the microarray study to identify trends in the data. Samples clustered in the same area are considered to be genetically similar. Each circle represents one sample and the different colours represent the different groups; where green is the control group and red is the Aldara treated group. n=5/group.

3.3.4 Analysis of Affymetrix GeneChip data

The various steps of quality control outlined above were applied to the GeneChip arrays to rule out sources of variation from differences in RNA quality, background signal noise and efficiency of hybridisation. As such, it can be assumed that any subsequent differences in signal intensity are representative of

differences in the transcriptional profile of the samples. In order to focus our investigation and to determine the biological relevance of transcriptional changes, differentially expressed genes had to be identified by order of significance. Thus, normalised signal intensities from the GeneChip array, generated using the GCRMA algorithm, were subject to statistical analysis.

3.3.4.1 Filtering entities on expression

Pre-processing the array chips using the RMA16 algorithm assigns the 28,853 entities with a normalised signal intensity value. As an additional control, and to remove background, each entity had to have a signal intensity value between 20% and 100%. By ensuring the entities outwith the upper 80% of all chip values were removed, background signal was eliminated. In addition, each entity had to satisfy this parameter in all five samples of each group in order to pass quality control and be included for analysis. The entities that remained following the filtration on gene expression are shown in the profile plot in Figure 3-6. This graph shows the normalised signal intensity of the entity, where the signal is normalised to the median value of that entity across all the samples, and allows entities with very high or very low signal values to be visualised on the same graph. The normalised signal intensity value of each entity is shown for both control samples and Aldara-treated samples. It is clear from the plot that the relative expression of many of the entities is much higher in the Aldara-treated samples, indicative of gene induction in these samples.
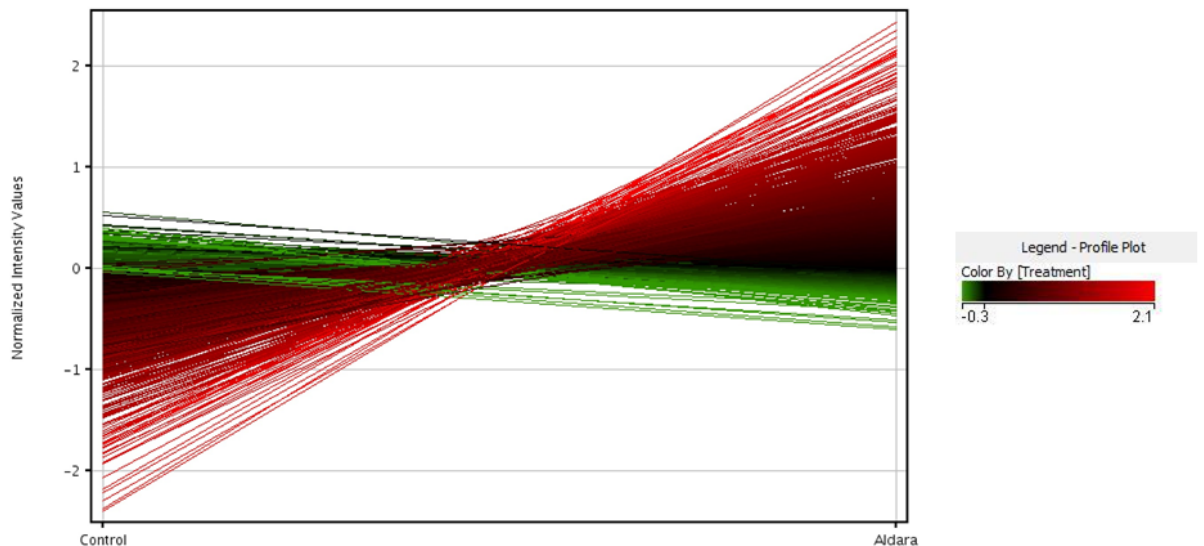
Figure 3-6 Profile plot showing normalised intensity values of entities following filtration
This graph shows the change in the signal intensity value of each entity in control samples (left hand side) and treatment samples (right hand side). Each line represents one entity and the colour of the line denotes the signal intensity of that entity in the treatment group, ranging from -0.3 to 2.1, as outlined in the legend.

3.3.4.2 Genes identified by GeneSpring as being differentially expressed in the brains of Aldara treated mice

Differentially expressed genes were identified using a paired t-test along with Benjamini-Hochberg multiple testing correction (MTC) with a false discovery rate (FDR) of 0.1.

MTC should be performed where possible in order to reduce the number of false positive results. Statistical analysis performed on large scale arrays like this one will use one test per entity. With many thousands of variables, and thus many thousands of tests being performed, the number of random events falsely being determined significant will increase. The p-value is the likelihood or probability of the null hypothesis being true and the more often the p-value is calculated from a single dataset, the higher the frequency of false positive results. For example, to analyse 1000 genes, 1000 statistical tests would be performed. If each has a p-value of 0.05, 50 of these genes would be considered false positives (0.05*1000). MTC is a statistical method that reduces the rate of error by taking into consideration the number of genes being tested, subsequently calculating a corrected p-value. Whilst MTC reduce the occurrence of false positives, they

also increase the chance of false negatives, thus the least stringent, Benjamini-Hochberg, MTC method was ideal for this relatively small study.

This method of statistical analysis generated a list of genes that were differentially expressed in the brains of the treatment group compared to the control group which satisfied a p-value ≤ 0.05. 7381 entities fell into this category; therefore a stringent fold change cut off ≥ 3 was applied to the dataset. The full list of genes that were differentially expressed in the brains of the treatment group, and which satisfied a p-value ≤ 0.05 and a fold change cut off ≥ 3 are listed in Appendix 1. In line with these criteria, 210 differentially expressed entities were found to be upregulated in the brains of the treatment group, which are shown in the volcano plot in Figure 3-7. In this plot, entities in red and green satisfied a p-value ≤ 0.05 and, in addition, the green samples were upregulated with a fold change ≥ 3. Since it was not feasible to validate all 210 genes, we next categorised them according to gene ontology.
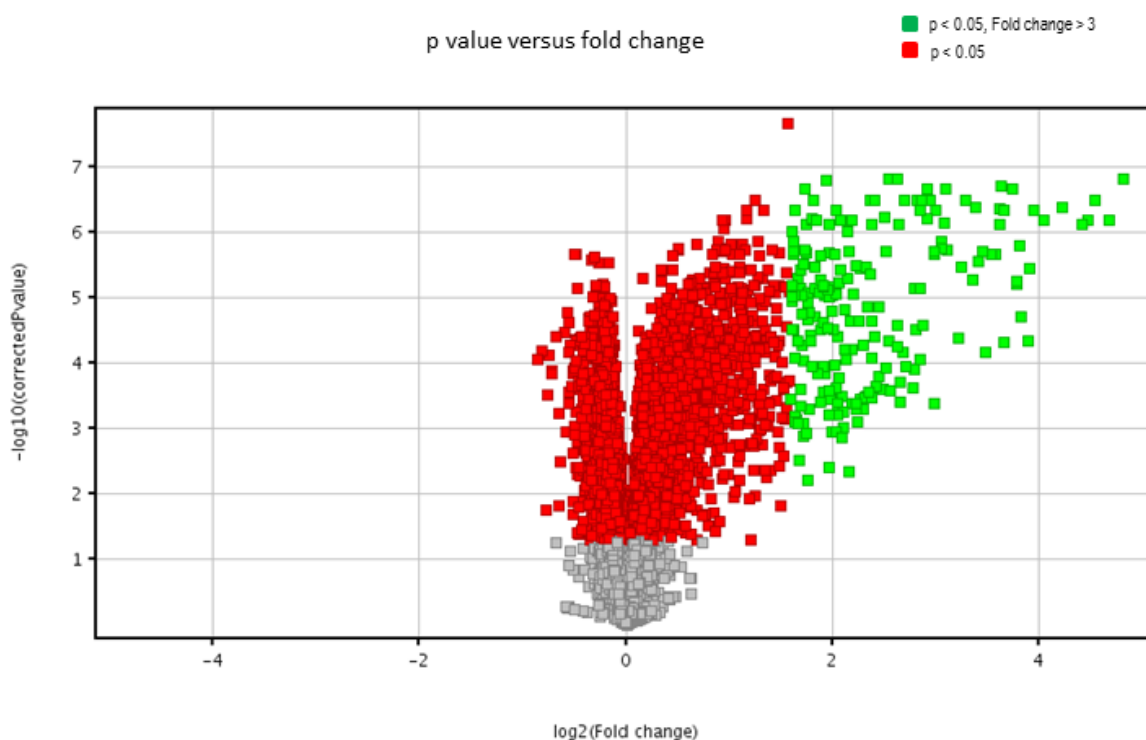
Figure 3-7 Volcano plot of microarray data
To determine the transcriptional response in the brain following Aldara treatment and control cream treatment, microarray analysis was performed. All of the entities evaluated in this array were plotted on a volcano plot that was generated using GeneSpring GX software. Red and green plots satisfy a p value ≤ 0.05 and, in addition, green plots adhere to a fold change cut off of 3 or above.

3.3.5 Gene ontology clustering using the Database for annotation, visualisation and integrated discovery (DAVID)

Following the statistical, and fold change, analysis of the brain samples, further analysis was performed to functionally group the genes which were differentially expressed in the treatment brains. This analysis can help define patterns in the differentially expressed genes by grouping them according to their function. Often, this type of analysis is more informative than studying each gene individually and may provide insight into the mechanisms involved in the brain response to Aldara treatment.

To apply biological relevance to the dataset of differentially expressed genes and to identify which groups of functionally related genes were enriched, gene ontology was assigned using the Database for Annotation, Visualization and Integrated Discovery (DAVID) Bioinformatics Resources. This publicly available software tool allows the visualisation of significantly enriched biological pathways based on the upregulated gene profile obtained from the microarray analysis. DAVID software uses a modified Fisher's exact test and Benjamini-Hochberg MTC to determine which groups of functionally related genes are enriched, and groups with a p value < 0.05 were considered to be specifically associated with the gene list. DAVID analysis takes into consideration that each gene is represented by more than one probe on the Affymetrix GeneChip and will only analyse each gene once, irrespective of how many times it appears in the gene list.

The most enriched pathways are shown in Figure 3-8, amongst which are 'Chemokine signalling pathway', 'Inflammation mediated by chemokine and cytokine signalling pathway' and 'Leukocyte transendothelial migration'. This strongly associates chemokines with the brain response and suggests that leukocyte migration into the brain may be mediating the distal response to Aldara treatment. In addition, the third most enriched process is 'Toll-like receptor signalling pathway', which may be the result of the TLR ligand, Imiquimod, directly stimulating cells in the brain.
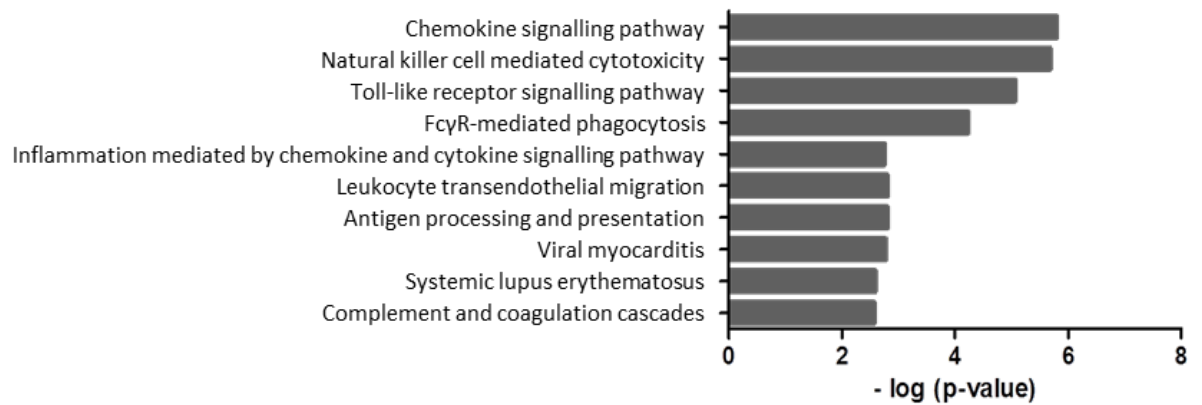
Figure 3-8 Top 10 enriched biological processes identified using DAVID software
Following microarray analysis, the list of differentially expressed genes in the brain were uploaded into DAVID software in order to identify enriched biological pathways. This figure shows the ten most enriched pathways in order of significance of the - log of their p-value.

3.3.6 Comparing the brain response in models of TLR-induced peripheral inflammation

Statistical analysis of the microarray dataset identified 210 differentially expressed genes in the brains of Aldara-treated mice that satisfied a p-value ≤ 0.05 and a fold change cut-off ≥ 3. As it was not feasible to validate this number of genes using individual QPCR, a subset of target genes had to be identified. Since 'Toll-like receptor signalling pathway' was one of the pathways found to be enriched in the brains of Aldara-treated mice, we compared our data set to that of other models of peripherally induced TLR stimuli. LPS challenge has been studied extensively in the context of the brain response to peripheral inflammation. In one such study by Thomson et al, microarray analysis was performed following I.P. LPS administration, which allowed for the identification of a panel of 24 differentially expressed genes in the brains of treated mice[377]. Upon comparing our dataset with theirs, we found that 23 out of the 24 genes were also induced following Aldara treatment (Figure 3-9), a number of which were ISGs. Since both TLR4 and TLR7 signalling can induce an IFN response, the ISGs were an appropriate focus for our investigation. Figure 3-10 shows the 15 ISGs in order of their fold change induction in the brain following Aldara treatment, presented as a heatmap which was generated using GeneSpring GX software. The fold change and p-value for each of the ISGs is shown in Table 3-2.
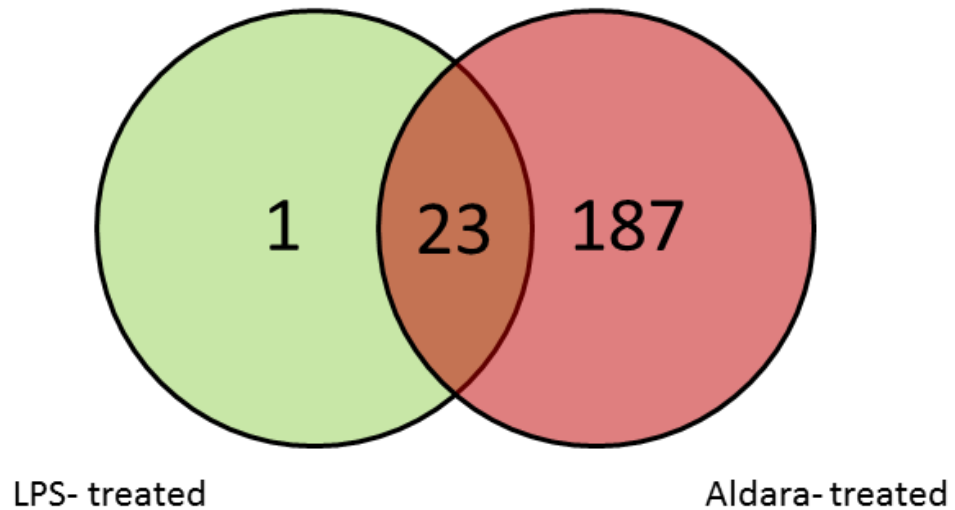
Figure 3-9 Venn diagram showing common genes between LPS and Aldara models
Differentially expressed genes identified in the brain following an LPS model of systemic
inflammation were compared to the list of differentially expressed genes generated following
microarray analysis of brains from Aldara treated mice. Interestingly, 23 out of the 24 genes
identified in the LPS model were also upregulated following the Aldara model, providing a focus for
investigation in this chapter.
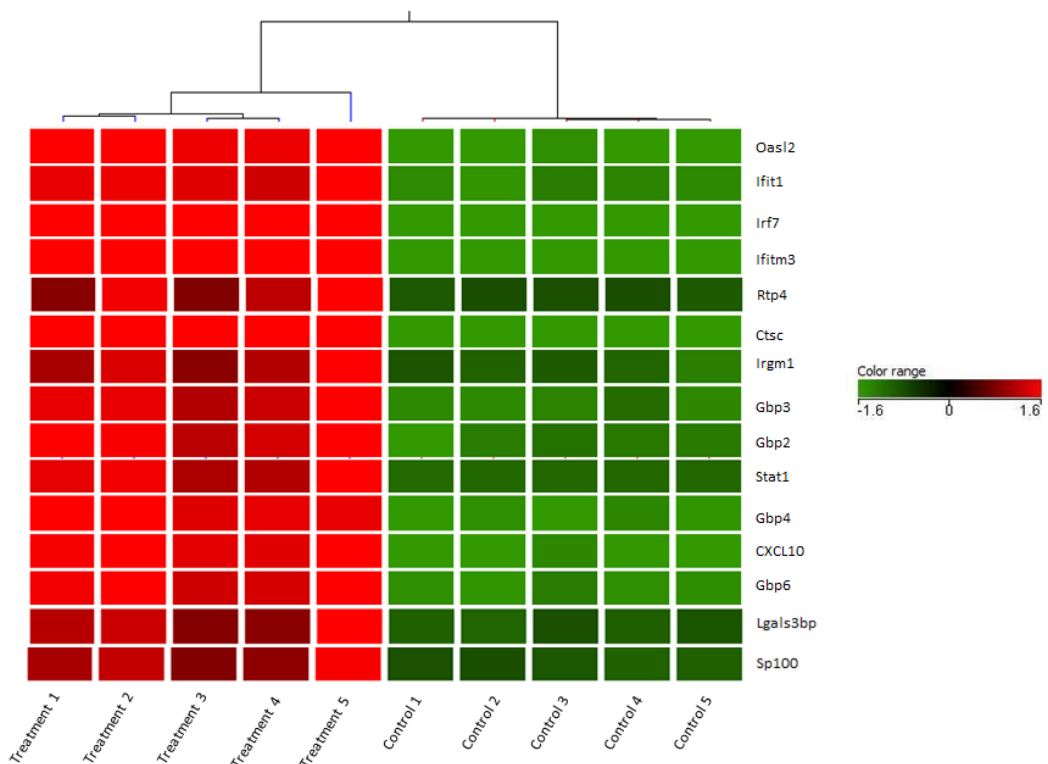
Figure 3-10 Heatmap of differentially expressed ISGs identified by microarray analysis
Microarray analysis was performed using RNA from brains of Aldara treated and control mice.
Following statistical analysis, the list of differentially expressed genes was compared to the list of
genes identified in the brain following systemic LPS stimulation. A heatmap was generated using
GeneSpring GX software to depict the 15 differentially expressed ISGs in Aldara treated and
control brains that were identified previously in an LPS model of systemic inflammation. The five
treatment samples are shown in red and the five control samples in green.

Table 3-2 A list of the 15 ISGs that were upregulated in the Aldara model

Symbol	Gene name	Fold change	p-value
Oasl2	2'-5' oligoadenylate synthetase-like 2	14.91	1.68E-08
Ifit1	interferon-induced protein with tetratricopeptide repeats 1	14.15	2.26E-07
Irf7	interferon regulatory factor 7	13.70	3.23E-08
Ifitm3	interferon induced transmembrane protein 3	7.91	6.25E-09
Rtp4	receptor transporter protein 4	7.32	3.52E-07
Ctsc	cathepsin C	7.22	2.65E-10
Irgm1	immunity-related GTPase family M member 1	6.98	4.35E-07
Gbp3	guanylate binding protein 3	6.91	3.71E-06
Gbp2	guanylate binding protein 2	6.51	3.34E-06
Stat1	signal transducer and activator of transcription 1	5.20	2.13E-06
Gbp4	guanylate binding protein 4	4.33	1.37E-06
CXCL10	chemokine (C-X-C motif) ligand 10	4.25	1.27E-04
Gbp6	guanylate binding protein 6	4.08	1.01E-05
Lgals3bp	lectin, galactoside-binding, soluble, 3 binding protein	4.06	3.03E-06
Sp100	Sp100 nuclear antigen	3.67	4.49E-07

3.5 QPCR analysis of the transcriptional profile in response to Aldara treatment

Microarray analysis provided the data set of genes that were differentially expressed in the brains of Aldara treated mice. To confirm the upregulation of these genes, individual SYBR Green QPCR was performed using RNA from an independent model of Aldara-induced skin inflammation. To focus our investigation, this was restricted to the 15 ISGs of interest that have been shown to be induced in the brains of mice challenged with systemic LPS, the majority of which were identified in the microarray.

3.5.1 QPCR validation of differentially expressed genes in the brain

Specific primer pairs were designed for each gene as described in section 2.4.7.1. SYBR Green QPCR was performed using RNA from brains from an independent Aldara model. With the exception of *Gbp4*, all of the ISGs evaluated were significantly elevated in the brains of Aldara treated mice compared with the brains of control mice (Figure 3-11). With regards to the significant genes, the upregulation ranged from around 2- to >60 fold induction, with *CXCL10* exhibiting the greatest induction of 64-fold.

3.5.2 QPCR validation of the peripheral blood response

To determine whether or not the ISG response was induced systemically, the ISG induction in the brain was compared with induction in peripheral blood leukocytes (PBL) using SYBR Green QPCR. If an ISG response was identified in the PBL, it may be that the expression seen in the brain was the result of a contaminating signal from the blood. Therefore, this part of the study would ensure that blood contamination was not a factor in the brain response. PBL were harvested from Aldara treated and control mice 24 hours following the fifth Aldara application. The results show that none of the ISGs assessed was significantly elevated in the PBL of the treatment group. The only genes to show an upward trend in the PBL were *Gbp3, IFITm3* and *Oasl2*, although the induction is very slight and not significant. Of note, several genes appeared to be downregulated in the PBL (Figure 3-11).

3.5.3 Comparison of central brain response with peripheral blood response

Having established the differential expression of the ISGs in the brain and the PBL by comparing them to control tissues using individual student's t tests, we next sought to determine the significance of the fold change induction when comparing between the two tissues. This was done using two-way ANOVA with Bonferroni multiple comparison post-tests. The fold change induction in the brain was significantly greater than the fold change induction in the PBL for all 15 ISGs examined (Figure 3-11), highlighting the differential response between the periphery and the brain.
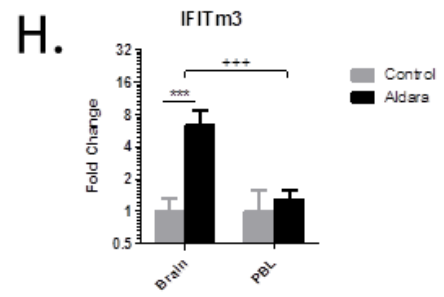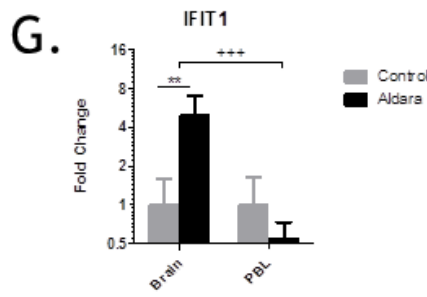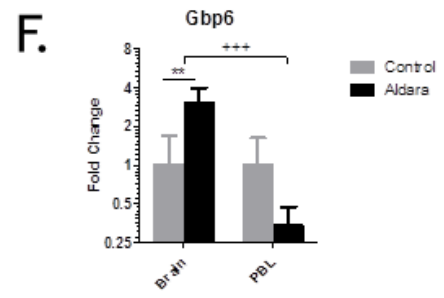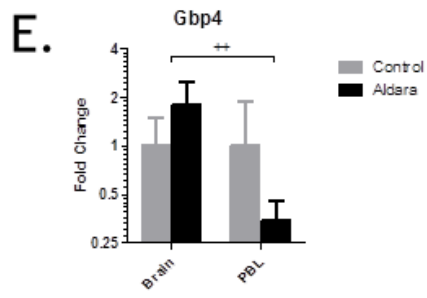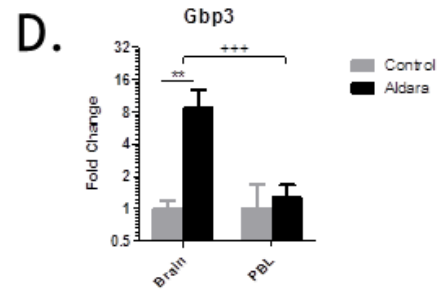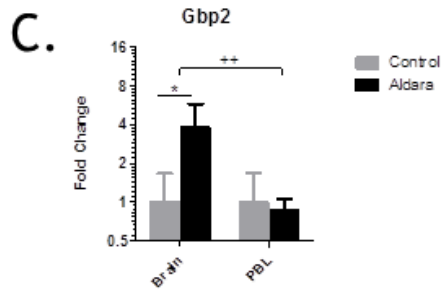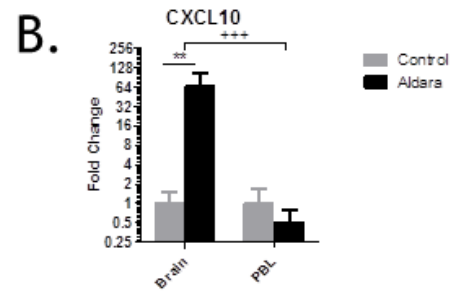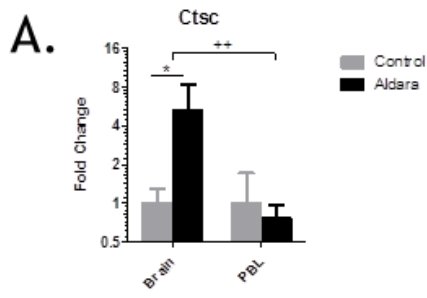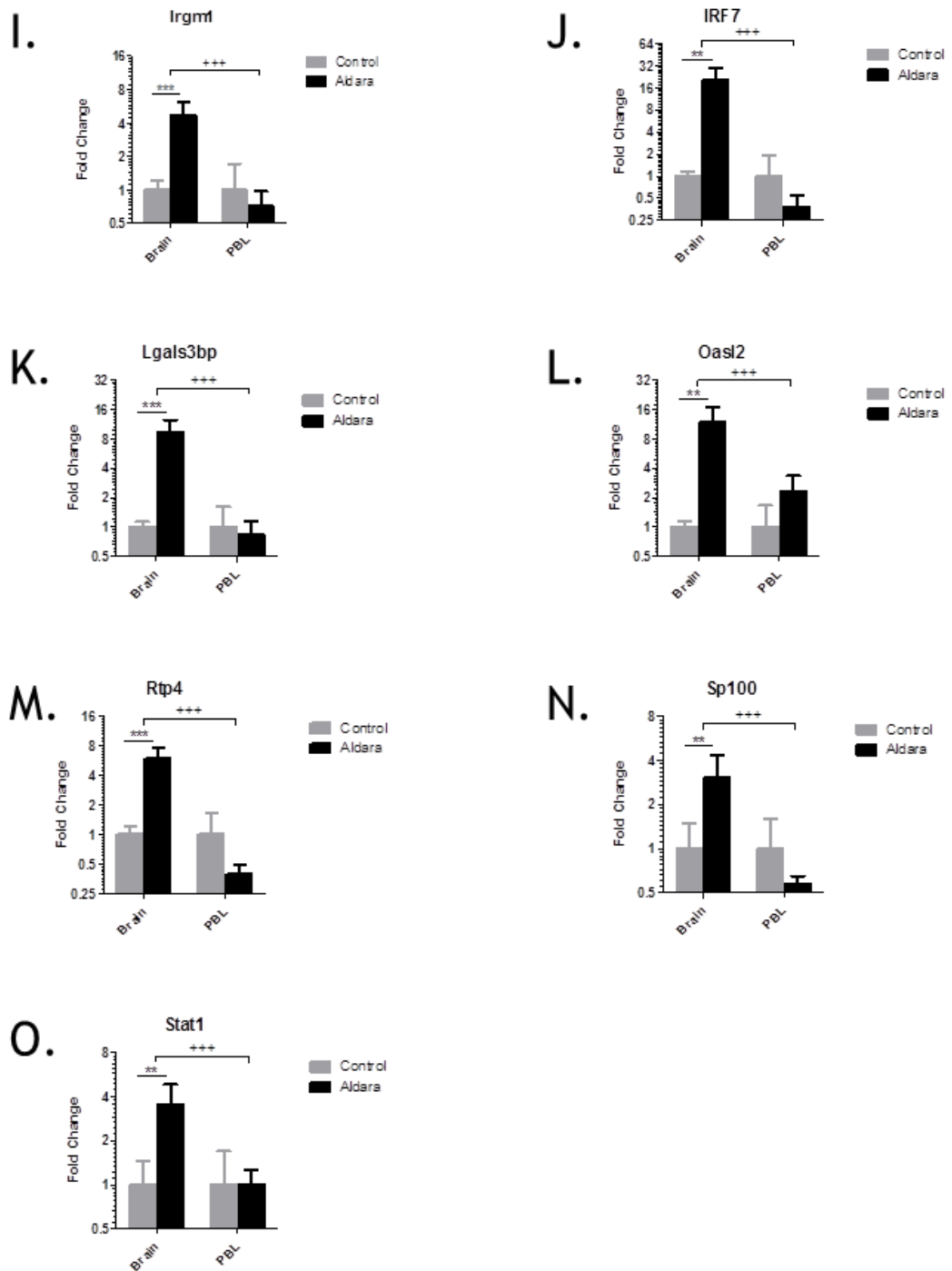
Figure 3-11 QPCR analysis of ISGs in brains and PBL
Mice were treated with 80mg Aldara cream or control cream every 24hrs for 5 consecutive days. Mice were euthanised 24hrs after the final application. Cardiac puncture was performed to retrieve PBLs and perfused brains were extracted. RNA was isolated from both tissues. QPCR analysis of the target ISG genes identified in the microarray was performed for both tissues (A-O). n= 5 mice per group. Significance was measured using individual students t test or two-way ANOVA with Bonferroni multiple comparison post-tests *** (+++) = p ≤ 0.001 **(++) = p ≤ 0.01 *(+) = p ≤ 0.05

3.6 Assessment of burrowing behaviour

Having identified a number of transcriptional changes in the brains of Aldara treated mice, it was important to determine what, if any, functional effect these transcripts may mediate. Neuroinflammatory components are key candidates for triggering the behavioural changes often presented in tandem with chronic inflammatory disorders of the periphery. To determine whether or not topical Aldara treatment could induce a functional output, a simple behavioural model was employed. This model used custom made burrowing tubes to assess the extent to which mice burrow during a 2 hour period following treatment[373]. Burrowing is an instinctive and natural behaviour in rodents. To test this behaviour, mice were first acclimatised to the presence of a burrowing tube overnight prior to baseline tests being carried out. The groups were then divided to ensure that the best, and worst, burrowers were split evenly between the two groups. Mice were treated at the same time each morning with 80mg of either Aldara cream or control cream as described previously and were then single housed for the testing period 4 hours later. Each single cage contained one burrowing tube prefilled with a fixed weight of food pellets. The mice were then left undisturbed to burrow at their leisure for a two hour period, before being returned to group cages. The weight of food remaining in each tube was recorded. Figure 3-12(A) shows the setup of the burrowing tube containing 200g of food pellets in a large cage before and after the burrowing test period. The weight of food left in the tube was significantly lower in the control group than the Aldara treated group, meaning that control mice 'burrowed' more of the contents than the Aldara treated mice (B). Both groups showed a range of burrowing activity during the baseline tests, however even after the first application, the activity of Aldara treated mice was significantly reduced. This trend continued over the three testing days with some mice failing to burrow at all after only one treatment. In contrast, control mice appeared to burrow more with time suggesting an improvement in this behaviour. When presented as a percentage of the baseline activity for each individual mouse, where the baseline burrowing is considered 100%, it is apparent that some of the Aldara treated mice do display enhanced burrowing activity. However, the burrowing activity of Aldara treated mice is increased to a lesser extent than that of the control mice (C). Similarly, one out of the five mice in the control group

burrowed less on day 3 than it did in the baseline tests; however the trend lines show a clear separation between the two groups. These results show that burrowing behaviour was impaired in Aldara treated mice, an effect that could be seen after only one treatment. The motor functions of these mice did not appear to be a factor as they displayed normal activity levels and the burrowing tubes were large enough that they did not come into contact with, and potentially irritate, the affected area of skin. However, motor functions were not directly tested.
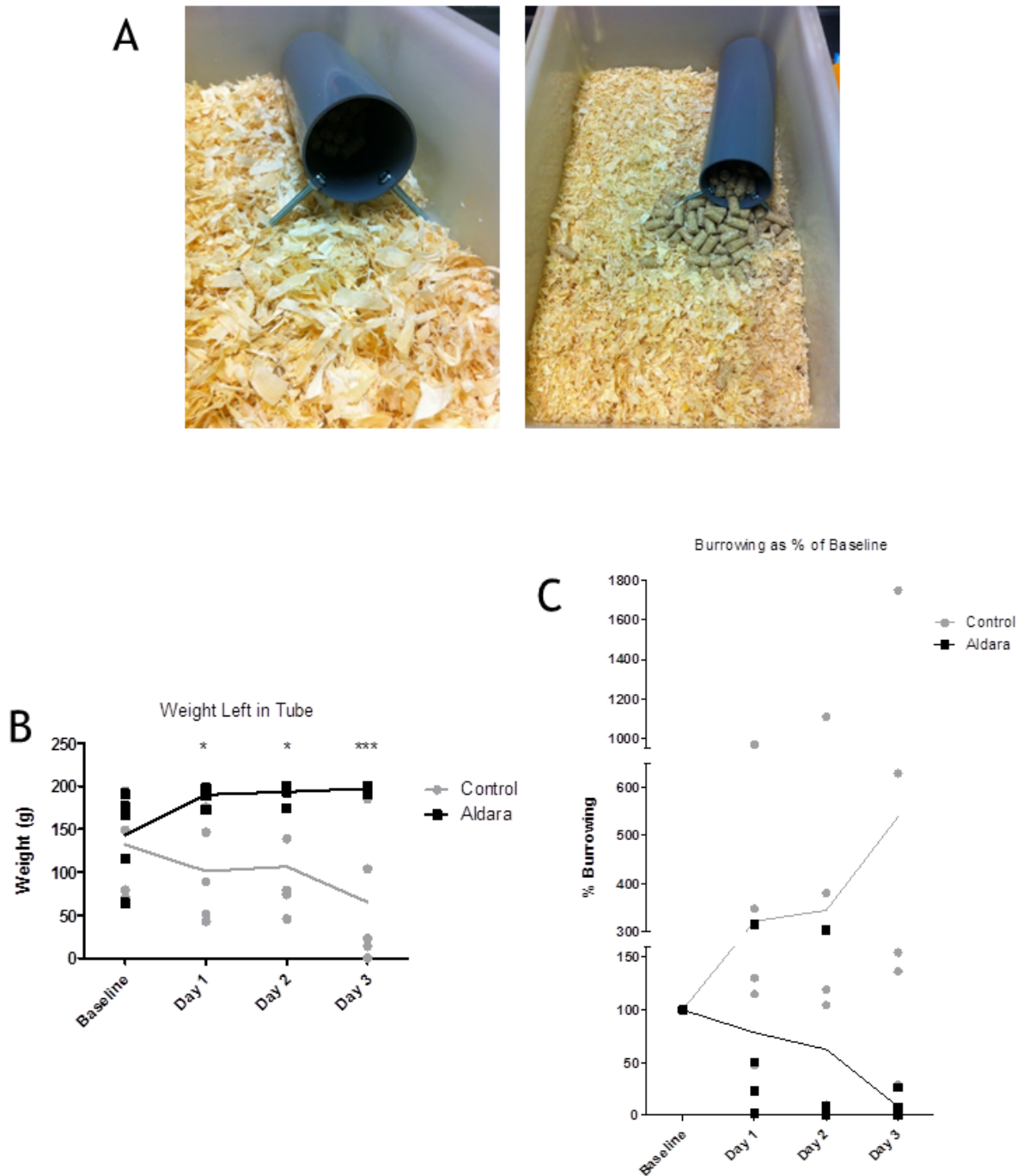
Figure 3-12 Burrowing activity of Aldara treated mice
Aldara treated or control treated mice were assessed for burrowing activity on three consecutive days. Four hours following treatment application, mice were single caged with a burrowing tube containing 200g of food pellets for 2 hours. At the end of this time point, mice were caged again in groups and the remaining weight of food pellets in the tubes was recorded. (A) shows the setup of the burrowing tubes before and after burrowing activity. The weight left in the tube following the 2 hour period is shown (B) or presented as a percentage of baseline tests, where baseline readings were considered 100% (C). n=5 per group. Significance was measured using two-way ANOVA with Bonferroni posttests *** = $p \leq 0.001$ *= $p \leq 0.05$.

3.7 Discussion

In order to determine the effect of peripheral, tissue-specific inflammation on the brain, the Aldara model of psoriasis-like skin inflammation was used[362]. This model, in which mice were treated with a daily dose of cutaneous Aldara cream, was first validated to ensure its reproducibility before microarray analysis of the brains was performed. This study identified a large number of differentially expressed genes in the brains of the treatment group, which satisfied a p-value ≤ 0.05 and a fold-change cut off of 3. Amongst the upregulated genes was a distinct panel of ISGs that have previously been identified in the brain in a model of peripheral LPS injection[377]. To determine the likelihood that this ISG response is a generic consequence of TLR driven peripheral inflammation, these ISGs served as the focus of this chapter. These genes of interest were validated in an independent Aldara model to confirm their induction in the brain and, in order to determine whether the response was systemic, the transcriptional profile of the PBL was also assessed. A basic behavioural model was used to determine whether, or not, Aldara treatment was sufficient to induce impaired burrowing activity, a behaviour that is instinctive to rodents.

QPCR analyses confirmed that all 15 ISGs, which were commonly upregulated in response to Aldara and LPS, were significantly induced in the brains of the Aldara treatment group. In addition, the fold change induction in the brain was significantly greater than the fold change induction in the PBL for all genes. This suggests that the response in the PBL differs in kinetics and magnitude to the response in the brain. Importantly, this also rules out the possibility of blood contamination in the brain being responsible for the transcriptional changes observed.

CXCL10 is the gene that exhibits the greatest fold change induction in the brain when analysed using QPCR. With an upregulation of almost 64-fold, its expression change is significant, allowing it the potential to play a prominent role in the CNS response to peripheral inflammation. CXCL10 is a classic ISG that is commonly expressed in the brain in response to a range of inflammatory stimuli, including traumatic brain injury (TBI)[251], EAE and MS[243, 378-380], and a number of viral infections[234, 381-383]. CXCL10 binds to the receptor CXCR3 and can mediate the migration of receptor expressing leukocytes. This mechanism has

been shown to induce the influx of leukocytes into the brain during inflammation. It is possible that, with such a strong induction in response to Aldara treatment, CXCL10 could be mediating the recruitment of leukocytes into the brain in this model. This is supported by the DAVID analysis which identified 'Chemokine signalling pathway', 'Inflammation mediated by chemokine and cytokine signalling pathway' and 'Leukocyte transendothelial migration' as significantly enriched biological pathways in the brain. Therefore, leukocyte infiltration into the CNS, as a consequence of Aldara-mediated peripheral inflammation, is plausible.

In addition to the transcriptional response, Aldara treatment also induced a functional response in the brain, in the form of impaired behaviour. Although this cannot be directly associated with the increased ISG production, the burrowing model has been shown to be sensitive to a number of treatments in which the inflammatory profile of the brain has been altered[384, 385].

The specific actions of Aldara cream, through which this brain response is mediated, remain unknown. However, Aldara cream works as a therapeutic agent due to its active component, IMQ, which binds to TLR7/8 and stimulates an IFN-driven anti-viral response.TLR7/8, which recognise single-stranded RNA, can signal canonically through MyD88 to activate the transcription factor NF-κB and lead to the production of inflammatory cytokines. In addition, it can also signal through an independent, IRF7-mediated pathway leading to the activation ISRE7 and the production of IFNα. These signalling pathways drive a specific anti-viral immune response that is characterised by the production of type I IFNs and is amplified by the transcription of ISGs[386]. This response has been described in a number of publications reporting human, primate and rodent studies, both *in vitro* and *in vivo*, and using natural as well as synthetic agonists[387-390].

It is therefore predictable that we see an IFN stimulated response following TLR7-mediated immune stimulation. However, what is surprising about the data from this study is that the ISG response appears to be localised in the brain, independently of an ISG response in the PBL. Furthermore, there was no evidence of an overt inflammatory cytokine response in the plasma. The presence of such a pronounced transcriptional response in the brain 24 hours

after the fifth application of Aldara suggests that the response in the brain is long-lived and perhaps ensues beyond the response in the periphery.

To our knowledge, the CNS response to topical Aldara treatment has not been examined before. However its active component, IMQ, has been used to investigate the brain response following various different routes of administration. Butchi et al. have shown that intracerebroventricular inoculation with Imiquimod in developing mice leads to microglia and astrocyte activation[391]. They have reported that protein levels of certain proinflammatory cytokines are upregulated in response to TLR7 ligation, along with a strong IFNß response. Damm et al. used IMQ to investigate how TLR ligation, and different routes of administration, can cause the manifestation of inflammation at distant sites, including the brain[7]. They found that a high dose of peripherally administered IMQ (subcutaneous and intraperitoneal) induced a milder brain-controlled illness response than other TLR ligands have been shown to, but did induce a moderate fever, peripheral and hypothalamic cytokine induction and inflammatory transcription factor activation. Although there was a marked upregulation of IFNs in the periphery, they reported no change in the levels of IFN in the brain. However, topical application to the skin was not investigated in either of these studies, nor did they evaluate the expression of ISGs, thus it is difficult to make direct comparisons with the analysis performed in this thesis.

In addition to the IMQ-based studies, others have shown an ISG response in the brain following different inflammatory stimuli; however the route of administration used in these studies is more direct, either through the nasal cavity or by intracranial injection. Wacher et al used intranasal West Nile Virus (WNV) and intracranial lymphocytic choriomeningitis virus (LCMV) to show the upregulation of several ISGs in the brain at different time-points[392]. Similarly, van der Pol et al used the intranasal administration of vesicular stomatitis virus (VSV) and cytomegalovirus (CMV) to demonstrate the upregulation of ISGs at four distinct sites throughout the brain, highlighting the long-range of IFN signalling. In addition, they showed that viral RNA was below the level of detection in some of the distant brain regions, indicating that the ISG response was not dependent on the localised presence of viral stimuli[393]. Analysis was also performed following the intravenous injection of VSV. Here, an ISG response was found in all tissues examined, including the brain, irrespective of the presence of virus

RNA. However it should be noted that only two ISGs, *OAS* and *IFIT2*, were analysed as being representative of the ISG response. The work by Thomson et al[377], upon which our selection of target ISGs was based, showed the induction of a distinct panel of ISGs in the brain in response to both acute and chronic LPS stimulation. In addition, this response was not mimicked in the PBL and could not be induced with the administration of inflammatory cytokines directly, or with an alternative TLR ligand, lipoteichoic acid (LTA). Interestingly, a commonality between Aldara and LPS is that their receptors, TLR7 and TLR4, respectively, both have an alternative, non-canonical, signalling pathway that can lead to the production of type I IFNs. It is therefore possible that the brain response we see in both of these models is the result of NF-κB-independent downstream signalling. There is considerable evidence linking type I IFNs to psychiatric disorders, including sequencing data that showed a significant association between MDD and genes involved in the IFN α/β signalling pathway[394] and the onset of MDD in patients with Hepatitis C and cancer following IFN treatment[323, 327, 328, 395-397]. Therefore, we hypothesise that TLR-mediated type I IFN production could lead to a distinct ISG response in the brain and the subsequent onset of behavioural deficits.

Although it is clear from the results that topical, cutaneous Aldara treatment can induce a distinct brain response, the mechanisms by which this response is mediated remain to be established. It may be possible that, provided IMQ was able to cross the BBB, the IFN response is induced by the direct activation of glial cells within the brain parenchyma. To our knowledge, no one has looked specifically at whether or not IMQ is able to do so, however the microarray did not show any evidence of an upregulated expression of IFN itself. If IMQ is not able to traverse the BBB, the response must be initiated first in the periphery, whereby peripherally-induced IFNs could be travelling to, and interacting, with the brain.

In summary, through studies described in this chapter we have identified a transcriptional profile in the brain in response to Aldara treatment. In addition, this treatment induces a behavioural abnormality that is associated with impaired neurological well-being. However, the mechanisms by which this response is driven remain to be established. We have yet to determine whether

this response is TLR-dependent, or what the role of the initial localised skin response is. Thus further investigation is required.

Chapter 4

Defining the mechanism of the brain response to peripheral cutaneous inflammation

4 Defining the mechanism of the brain response to peripheral cutaneous inflammation

4.1 Introduction

The results in Chapter 3 identified a brain response to peripherally induced cutaneous inflammation in the Aldara model of skin inflammation. However, the mechanisms involved in establishing this response remain unclear and many questions remain unanswered. For example, although the ISG response was consistent across two TLR-mediated models, LPS and Aldara, it is not clear if the brain response was TLR-dependent. During this study in 2013, Walter et al published a Nature Communications article showing that Aldara cream could also activate a TLR7-independent cutaneous immune response[372]. It was reported that isostearic acid alone, a component of the vehicle, could induce keratinocyte cell death and inflammasome activation. They concluded that the full immune response required both IMQ and isostearic acid, however, the systemic response was largely dependent on TLR7 and type I IFN signalling. These findings highlighted the importance of determining the separate contributions of IMQ and isostearic acid in generating the brain response described in Chapter 3.

The QPCR analysis of the PBL, and the ELISA analysis of the plasma, in Chapter 3 suggested that the brain response was occurring independently of a peripheral inflammatory response; however this was only analysed following 5 repeated applications of Aldara cream, which may be considered quite late in the response. Therefore, it may be that a peripheral response has driven the CNS response but that it is generated at a much earlier time point.

This Chapter set out to address these issues in an attempt to understand more about the mechanisms of the brain response to cutaneous inflammation. To do so, the TPA model of skin inflammation was first used[398]. TPA is a chemical irritant which activates protein kinase C (PKC) and, when applied repeatedly to the dorsal skin, induces a similar psoriasis-like phenotype to Aldara[398, 399]. However, TPA does not function through TLRs and is therefore considered a 'sterile' model of inflammation. Thus, using this model, we hoped to determine the involvement of TLR stimulation in the generation of the brain response. In

addition, to determine whether or not the brain ISG response could be the result of an ISG response in the periphery, present at an earlier time-point, a time course model of both Aldara and TPA was assessed. Finally, to understand the individual contribution of IMQ, an additional two IMQ models were analysed.

4.2 The TPA model of skin inflammation

To induce peripheral skin-specific inflammation, 12-O-Tetradecanoylphorbol-13-acetate (TPA) was applied daily to the shaved dorsal skin of 6-8 week old female c57BL/6 mice. This application was repeated over 5 consecutive days. As a control, age and sex matched mice were treated in a similar way with acetone vehicle. Mice were terminally anaesthetised 24 hours after the final application.

4.2.1 Model Validation

In order to compare the TPA response to the Aldara response examined in Chapter 3, the same parameters were assessed as a method of validating the model. Mouse weights were recorded following each application, spleens were collected to be weighed and photographed and H&E stained sections from the treated dorsal skin were analysed. Unlike Aldara treated mice, TPA treated mice did not lose any weight over the course of the treatment and in fact, like control mice, gained weight (Figure 4-1A). The mice did however show signs of splenomegaly as the spleens from the treated group were significantly bigger than the spleens from the control group and weighed almost twice as much (Figure 4-1B+C). When the H&E staining of the control and treated areas of skin was analysed, it was clear that TPA induced an inflammatory response characterised by epidermal hyperplasia, dermal expansion, erythema and inflamed lesions (Figure 4-1D). Again, ELISA analysis was used to assess the plasma concentrations of three key inflammatory cytokines, IL-1ß, IL-6 and TNFα (Figure 4-2A, B+C, respectively). All samples fell below the minimum level of detection of the ELISA kits for each of the three cytokines. To ensure the robustness of the assays, plasma from LPS-treated mice was included on each plate as a positive control (Figure 4-2D).
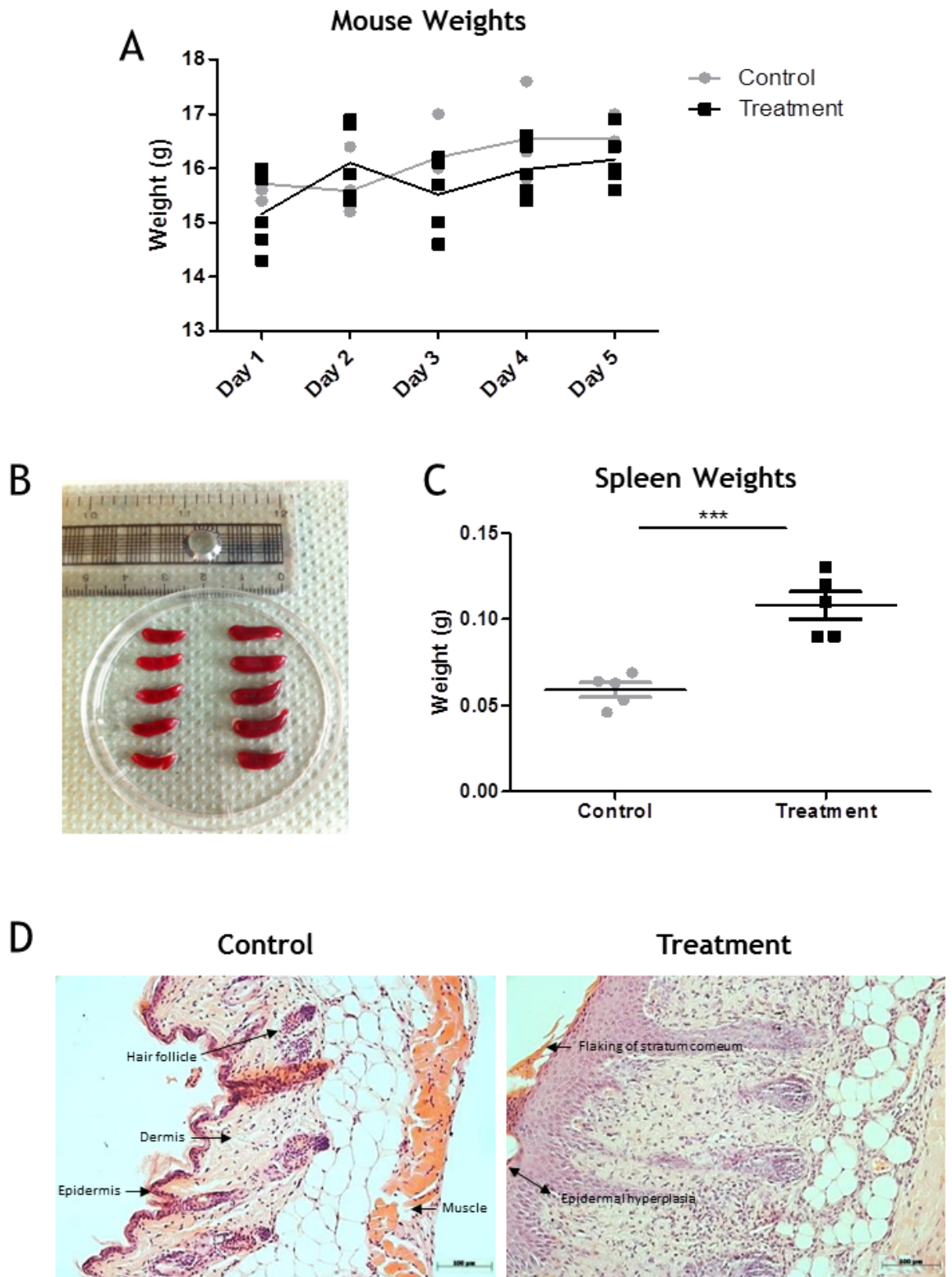
Figure 4-1 Evaluation of the phenotypic response to TPA induced skin inflammation
Mice treated with 150μl 100μM TPA, or equivalent volume acetone, were weighed following each application (A). In addition, spleens were photographed (B) and weighed (C). H&E staining was performed using 5μm thick sections of TPA- or acetone- treated skin which were visualised at 200X magnification. n = 5/group. Significance was measured using two-way ANOVA or student's t test. *** = p ≤ 0.001.
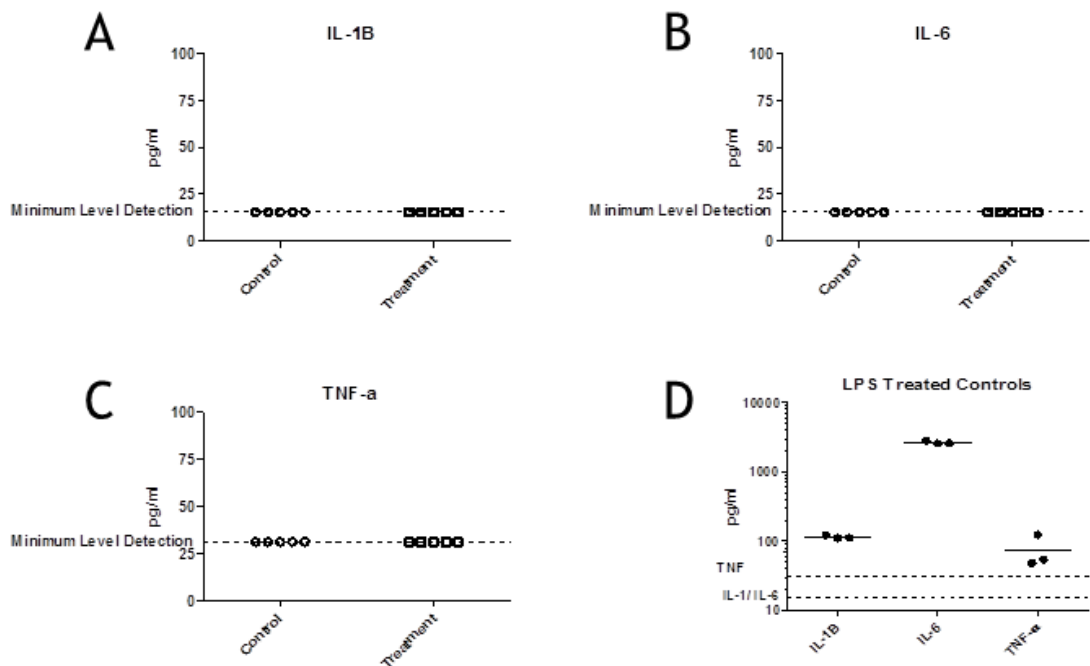
Figure 4-2 Expression of inflammatory cytokines in the plasma of TPA-treated mice
Plasma was isolated from mice treated with 150µl 100µM TPA, or equivalent volume acetone, 24hrs after the fifth application. ELISAs were used to assess the expression of three key inflammatory cytokines, IL-1β (A), IL-6 (B) and TNF-α (C). To ensure the integrity of the assay, plasma from LPS- injected mice was included as a positive control. Group size of n = 5 for TPA/acetone treated mice, n = 3 for LPS- treated mice. Minimum level of detection represents the lowest sensitivity for each kit.

4.2.2 QPCR analysis of ISG expression in response to TPA treatment

To determine the expression of the 15 target ISGs (described in Chapter 3) following TPA treatment, QPCR analysis was performed using RNA from brains and PBL isolated 24 hours after the final TPA treatment. Expression of each gene was normalised to the housekeeping gene, *TBP,* and each treatment group was compared to the corresponding control group, values from which were normalised to a fold change value of 1. The fold change induction of each gene in the brain and PBL is shown in Figure 4-3.

4.2.2.1 QPCR analysis of ISG response in the brain

The results of the QPCR analysis show that none of the ISGs was significantly upregulated in the brain in response to TPA treatment. All genes exhibited a fold

change induction of 1 or below. Four of the genes, *Ctsc, Gbp2, Gbp6* and *Stat1,* showed a significant downregulation of expression in the brains of TPA treated mice compared with the control brains. However, the CT values of some of the samples were high and close to what would be considered the level of detection, therefore it is difficult to determine if the downregulation was real or if it was the result of inaccuracy resulting from low expression. This inaccuracy could also account for the high standard deviation present in many of the groups. Regardless, it is clear that cutaneous TPA treatment fails to induce a similar ISG brain response to cutaneous Aldara treatment.

4.2.2.2 QPCR analysis of the ISG response in the peripheral blood

To determine whether or not TPA treatment induces a transcriptional response in the periphery, QPCR analysis was performed using RNA from the PBL. This comparison also ensured that the expression levels in the brain were not the result of blood contamination. Again, none of the ISGs were significantly induced in the PBL of the treatment group. Some of the genes, for example *Rtp4*, showed a difference, however these did not reach significance and the variation within these groups is high, again suggesting that the low expression levels have introduced inaccuracies. The expression of *Gbp4* in the PBL is significantly reduced following TPA treatment, with a fold change of 0.5 (Figure 4-3).

4.2.2.3 Comparison of brain response with the peripheral blood response

When comparing between the two tissues, it is obvious that neither exhibits a significant ISG induction following cutaneous TPA treatment. Only three genes are significantly differentially expressed between the brain and PBL; *Gbp2, Rtp4* and *Stat1* (Figure 4-3). With only very minimal fluctuations in expression and high standard deviation, it was apparent that the response to TPA treatment is minimal in comparison with the response to Aldara treatment described in Chapter 3.
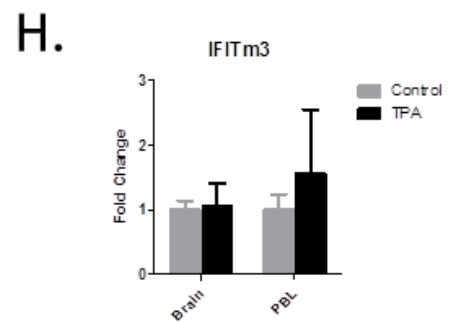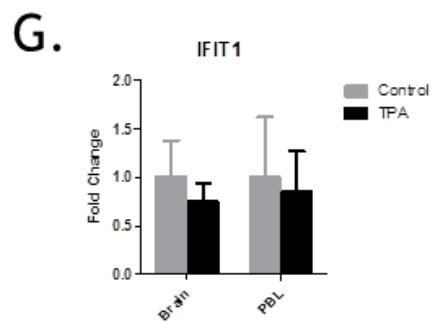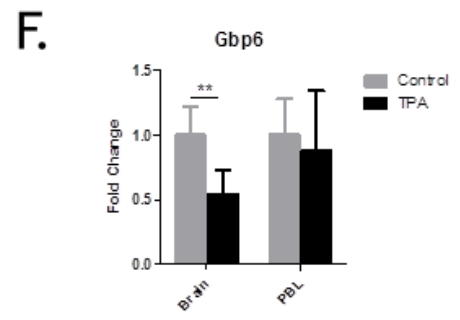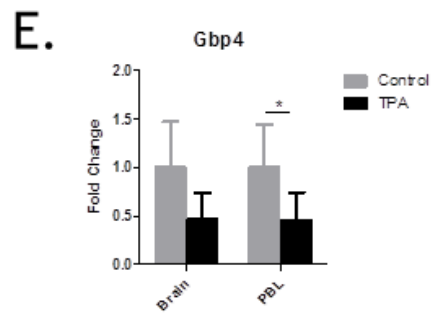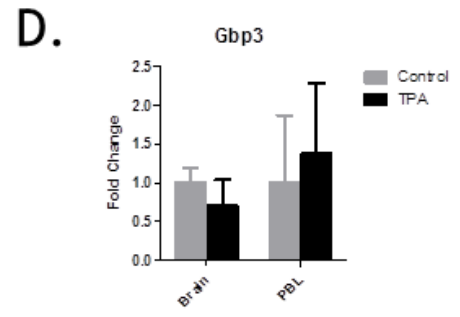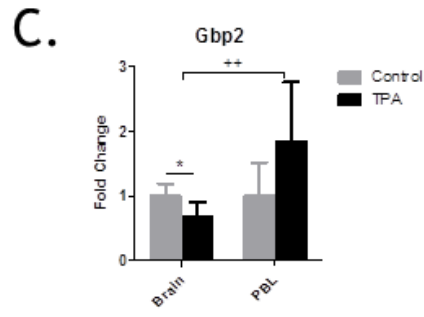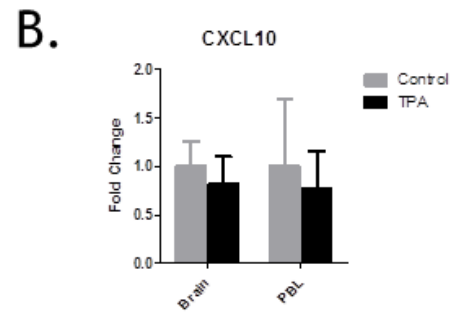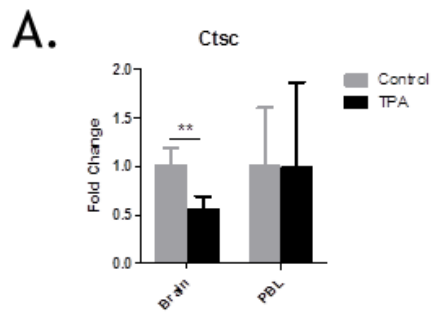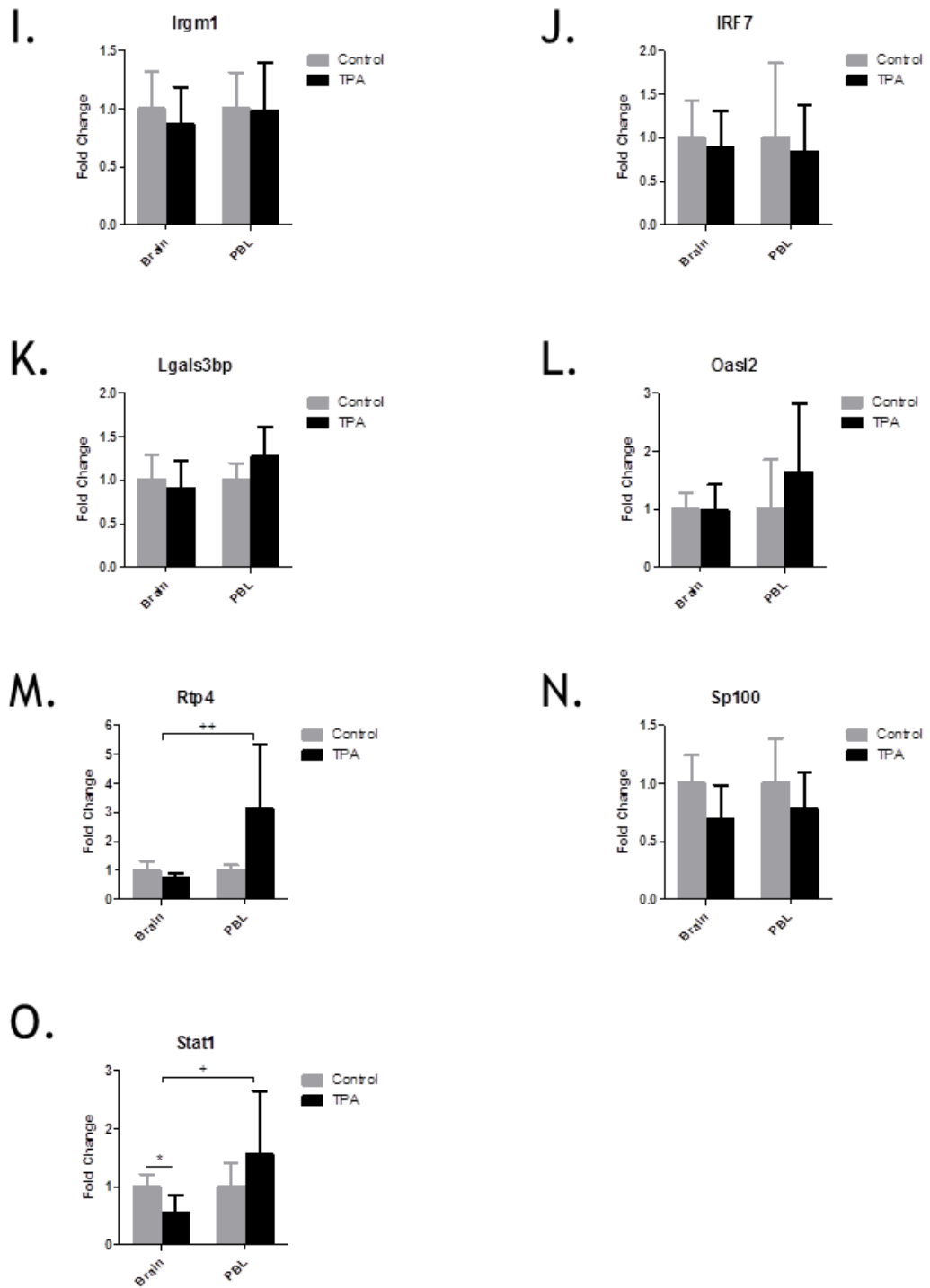
Figure 4-3 QPCR analysis of ISGs in brains and PBL following TPA treatment
Mice were treated with 150μl 100μM TPA, or equivalent volume of acetone, every 24hrs for 5 consecutive days. Mice were euthanised 24hrs after the final application. Cardiac puncture was performed to retrieve PBLs and perfused brains were extracted. RNA was isolated from both tissues. QPCR analysis of the 15 target ISG genes was performed for both tissues (A-O). n= 5 mice per group. Significance was measured using individual unpaired students t tests for individual tissues (control vs treated) or two-way ANOVA with Bonferroni multiple comparison post-tests for comparisons between tissues (PBL vs brain). *** (+++) = p ≤ 0.001 **(++) = p ≤ 0.01 *(+) = p ≤ 0.05

4.3 Temporal response following cutaneous Aldara treatment

Work described in Chapter 3 established that repeated treatment with Aldara cream induces a brain ISG response. This appears to be independent of an overt inflammatory response in the periphery. However, it may be that the brain response is driven by a peripheral response which is initiated at a much earlier time point and which has dissipated by the fifth application. To investigate this, a time course of Aldara treatment was used. 80mg of Aldara cream was applied daily to the shaved dorsal skin of 6-8 week old female c57BL/6 mice for 1, 3 or 5 applications. As a control, age and sex matched mice were treated with an equal quantity of water based control cream. Mice were terminally anaesthetised 24 hours after the final application.

Consistent with previous results, the Aldara treated mice lost a significant amount of weight over the course of the treatment, with the most significant weight loss occurring between the third and fifth applications. The mice had regained some of their weight by the end of the treatment period; however they remained significantly lighter than the control mice (Figure 4-4A). Areas of the treated dorsal skin were sectioned and H&E stained. The control skin remained uninflamed throughout the five day period; however the Aldara treated mice showed epidermal thickening even after one application. The skin inflammation was most pronounced after the third and fifth applications, where distinct epidermal hyperplasia was evident (Figure 4-4B).
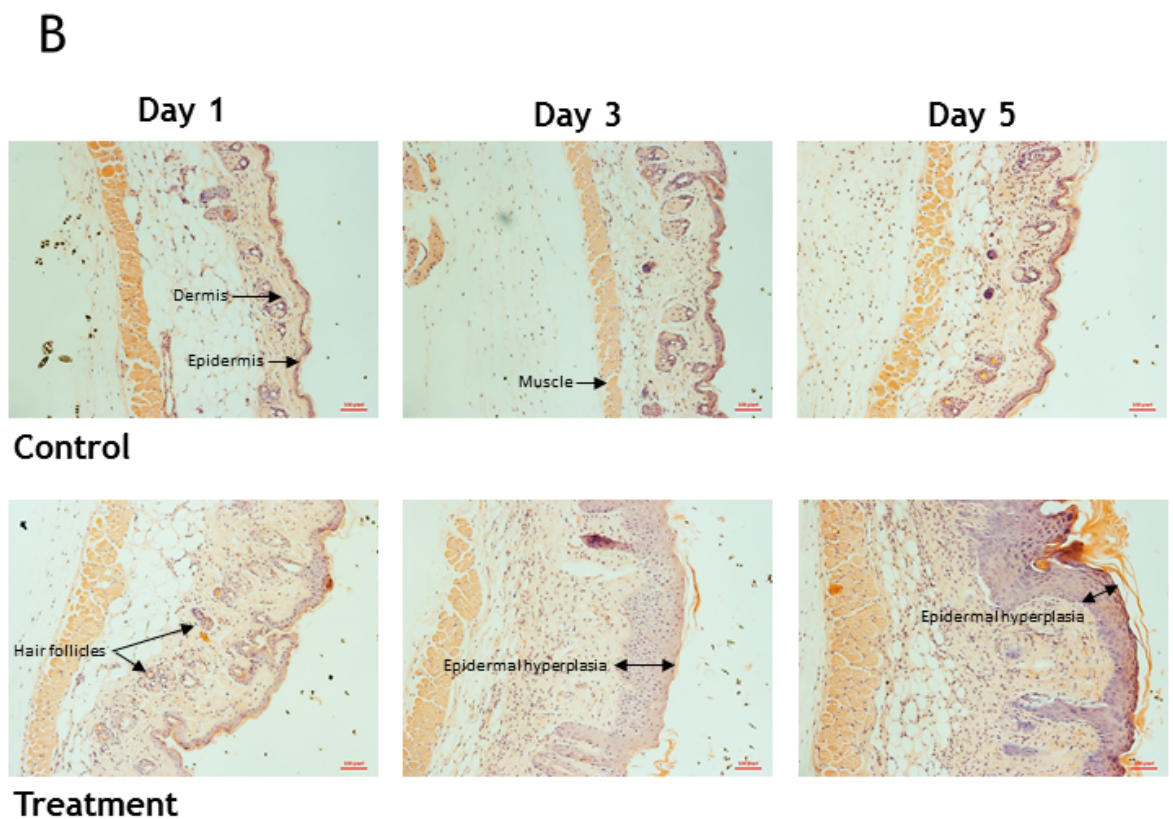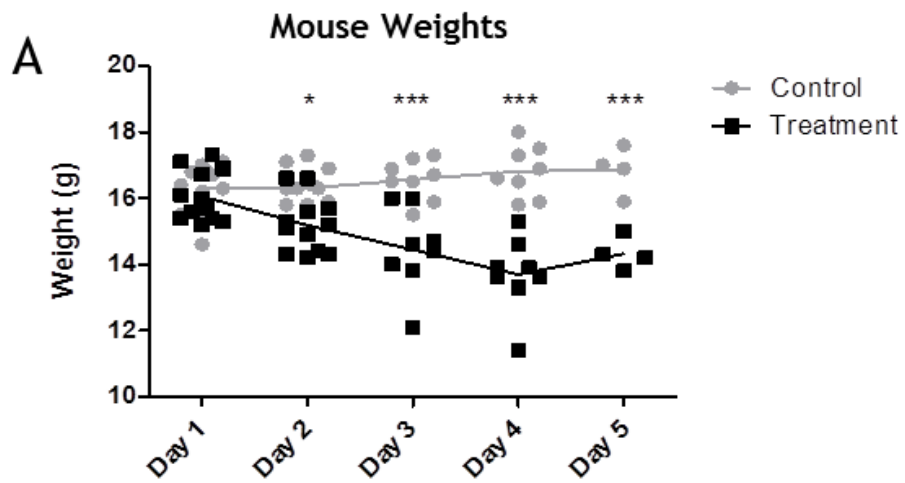
Figure 4-4 Model validation of Aldara time course
Mice were treated with 80mg of Aldara, or an equivalent quantity of control cream, for 1, 3 or 5 consecutive applications. Mice were weighed following each application (A). H&E staining was performed using 5µm thick sections of Aldara- or control cream- treated skin from each time point and sections were visualised at 200X magnification (B). n = 4/group. Significance was measured using two-way ANOVA *** = p ≤ 0.001 * = p ≤ 0.05

4.3.1 QPCR analysis of the transcriptional ISG profile at different time points in response to Aldara treatment

To assess the time course of the ISG response to Aldara treatment, SYBR Green QPCR analysis was performed using RNA from brains and PBL isolated 24 hours after 1, 3 or 5 treatments. Each gene was normalised to the housekeeping gene, *TBP*, and each treatment group was compared to the corresponding control group, which were normalised to a fold change value of 1. The fold change induction of each gene in the brain and PBL is shown in Figure 4-5

4.3.1.1 QPCR analysis of ISG response in the brain

The results of the QPCR analysis of the control and Aldara-treated brains show that all 15 genes are induced in the brain at day 3 following Aldara treatment when compared with the control brains. Although the response at day 1 was less pronounced than the other time points, six of the ISGs, *Gbp2*, *IFIT1*, *IFITm3*, *IRF7*, *Sp100* and *Stat1*, were significantly induced (Figure 4-5C,G,H,J,N and O, respectively). It is evident from the results that day 3 is the peak of the ISG response in the brain following cutaneous Aldara treatment, as all 15 ISGs were significantly induced. This ranged from a 20-fold induction to a striking 1000-fold induction for *CXCL10*, which was the most highly induced (Figure 4-5B). By day 5, all of the genes remained elevated in the brain and, with the exception of *IFIT1*, *Gbp2* and *CXCL10*; the expression levels were statistically significant compared with the controls. These data show that the brain response to Aldara treatment is initiated during the early stages of the model and persists throughout the time-course; however this response appears to peak after the third treatment before beginning to diminish. With the exception of *Sp100*, the induction at day 3 is significantly higher than it is at day 5, confirming that the response dissipated beyond day 3.

4.3.1.2 QPCR analysis of the ISG response in the peripheral blood

The QPCR analysis of the PBL from both Aldara-treated and control mice indicated the presence of an ISG response in the periphery at the earlier time points. 11 out of the 15 genes were significantly induced in the PBL of the treatment group compared with the control group at day 1. None of the ISGs expressed in the PBL was induced more than 20-fold. By day 3, only 4 genes

remained significantly induced; *Ctsc, CXCL10, Rtp4* and *Stat1*, and by day 5 this was down to only one gene; *IFITm3*. However, *IFITm3* was not significantly induced on day 3 and appeared to have fluctuated in the PBL over the time course. These data suggest that an early ISG response is induced in the PBL after the first treatment; however this response dissipates over time, and is minimal by day 5.

4.3.1.3 Comparison of central brain response with the peripheral blood response following Aldara treatment

When comparing the brain and PBL in Aldara-treated mice, there is a clear separation in the magnitude and temporal pattern of the two responses. The response in the brain is much stronger than in the PBL, with fold-change inductions in the hundreds or even thousands. Although there appears to be an initial PBL response at day 1, only with *Ctsc* is the fold change induction in the PBL higher than in the brain. Using statistical analysis, the induction of all 15 ISGs is significantly higher in the brain than in the PBL at day 3. By day 5, although all genes still show a fold change induction, this is only significant in comparison with the PBL for two of the genes; *Ctsc* and *Stat1*. By comparing these two tissues, it would appear that the PBL response differs in magnitude and temporal pattern to the brain response. This indicates that the strong response which lingers in the brain following cutaneous Aldara treatment cannot be attributed to the ISG response in the PBL.
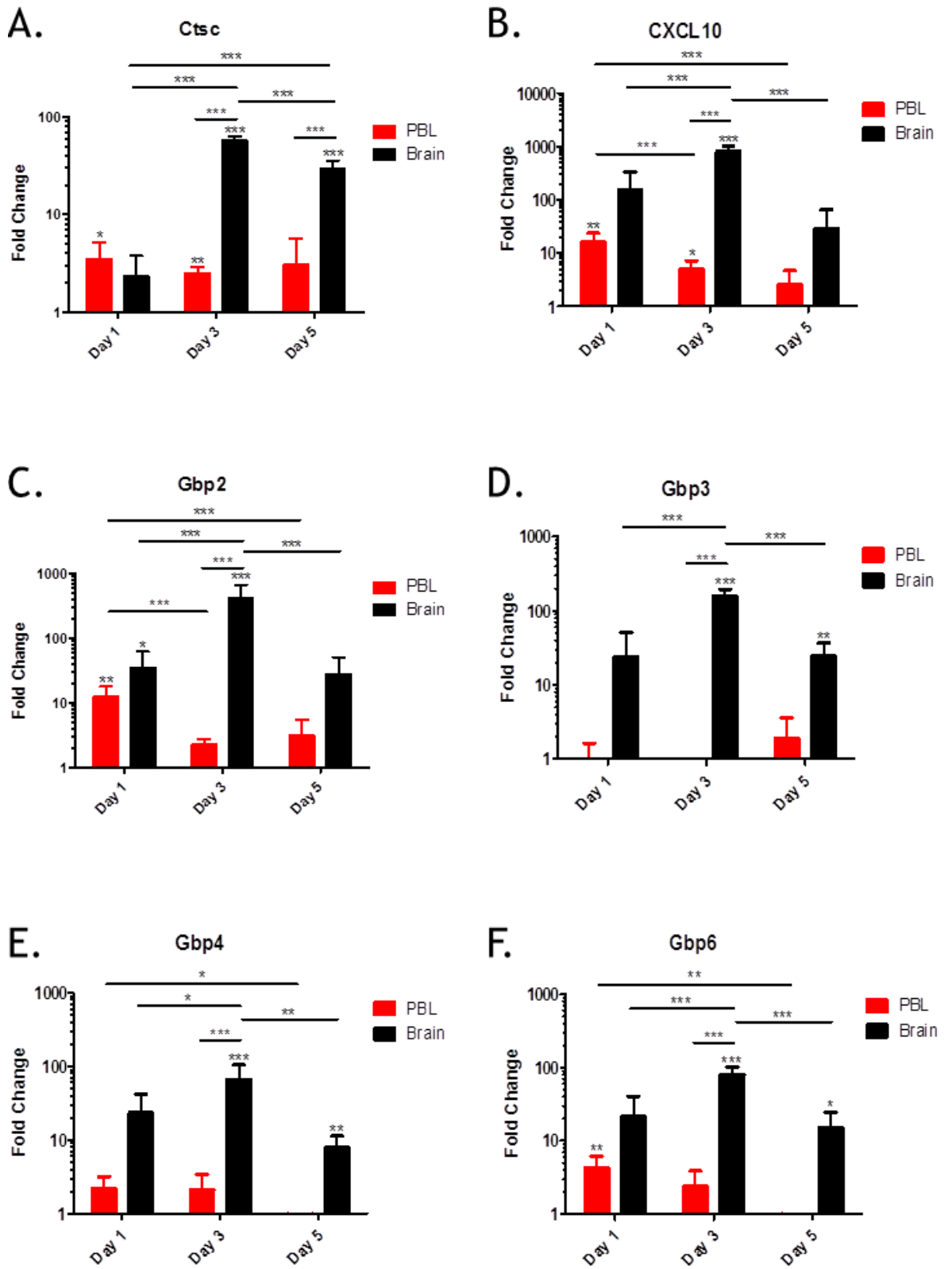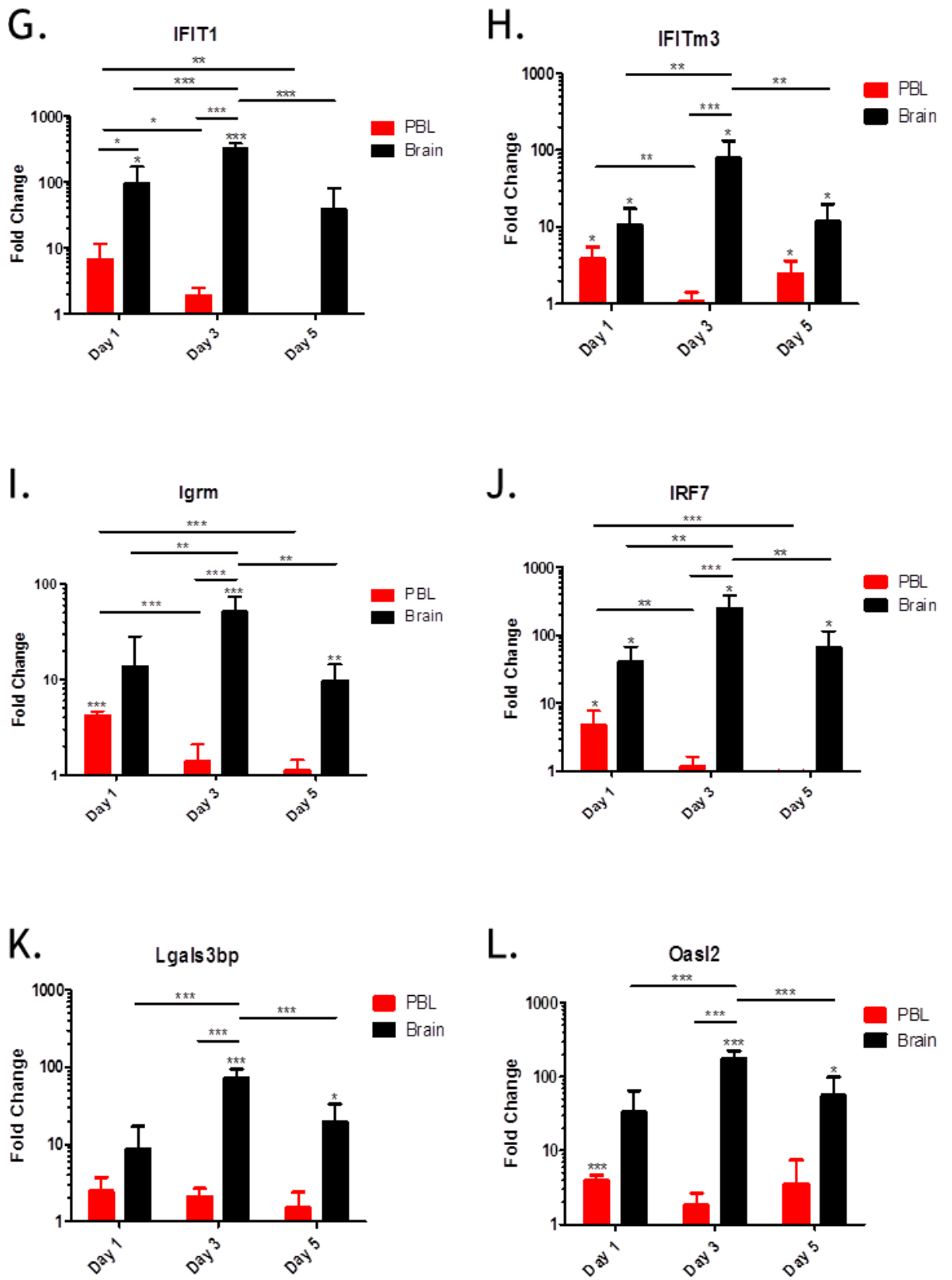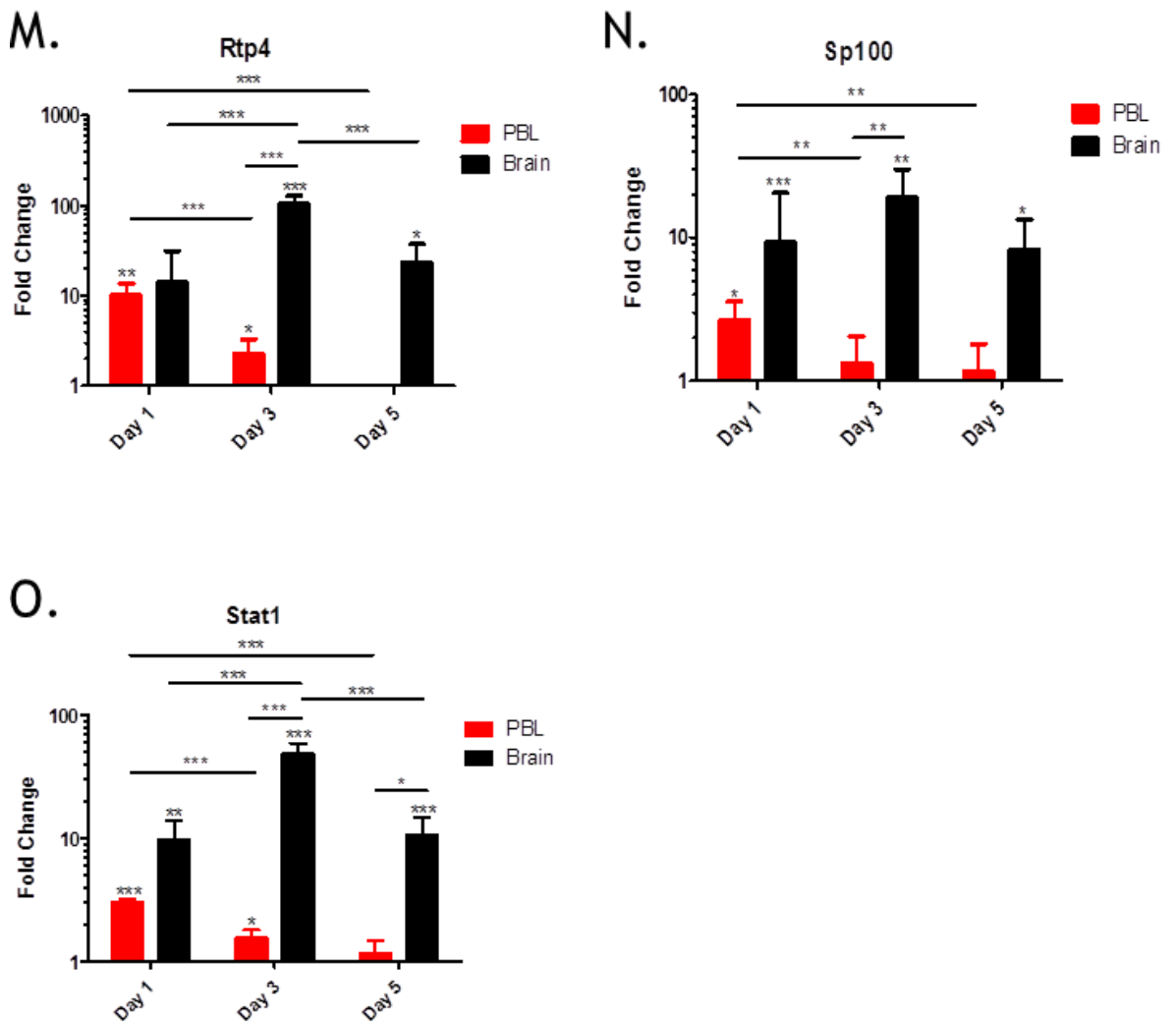
Figure 4-5 QPCR analysis of ISGs in the brain and PBL during the Aldara time course
Mice were treated with 80mg of Aldara cream, or an equivalent volume of control cream, every 24hrs for 1, 3 or 5 days. RNA was then isolated from the brain and PBL 24hrs after the final treatment. Gene expression analysis of (A) Ctsc, (B) Cxcl10, (C) Gbp2, (D) Gbp3, (E) Gbp4, (F) Gbp6 (G) Ifit1, (H) Ifitm3, (I) Irgm1, (J) Irf7, (K) Lgals3bp, (L) Oasl2, (M) Rtp4, (N) Sp100 and (O) Stat1 was performed using QPCR and was normalised to TBP. Data are expressed as fold change induction, relative to the controls, which have a fold change value of 1. Data represent the mean +/- SD. Significance was calculated for individual tissues (control vs treated, d1 vs d3 vs d5), between tissues (treated only, PBL vs brain) and between time-points (treated only, d1 vs d3 vs d5) using two-way ANOVA with Bonferroni multiple comparison post-test. *** $p \leq 0.001$. ** $p \leq 0.01$, * $p \leq 0.05$. n = 4/group

4.3.2 Luminex analysis of the temporal response following Aldara treatment

Luminex analysis was performed in order to determine the cytokine response in the plasma at the different time points following cutaneous Aldara treatment. The mouse 20-plex panel covered a range of key cytokines (Figure 4-6), chemokines and growth factors (Figure 4-7). In order to include the appropriate

number of technical replicates, where each sample was analysed in triplicate, samples were diluted 1:4 prior to analysis. However, as a result, many of the readings were below the level of detection of the assay. To enable statistical analysis, any sample which failed to obtain an expression value was assigned a concentration equal to the minimum level of detection for each protein. Three of the proteins failed to obtain a value for any of the samples included on the assay; therefore IL-1α, IL-10 and IFNγ were omitted from further analysis.

8 out of the 17 remaining proteins were significantly induced in the treated group when compared with the control group at day 1. These included 4 cytokines; IL-2, IL-5, IL-6, IL-12 (Figure 4-6B, D, E, F) and 4 chemokines; CCL2, CXCL1, CXCL9 and CXCL10 (Figure 4-7A, C, D, E). Several of these were highly expressed, at around 1000 pg/ml, including all four chemokines. By day 3, the expression of the cytokines failed to reach significance when compared to the controls, however CXCL1, CXCL9, CXCL10, VEGF and GM-CSF were significantly induced in the Aldara treated mice compared with control mice (Figure 4-7). At day 5, IL-1β and IL-17 levels were significantly higher in the control group compared with the treated group, indicating a downregulation following cutaneous Aldara treatment. The only proteins significantly induced in the Aldara treated mice at day 5 were VEGF and GM-CSF, the expression of which appeared to be higher than the control mice at the later time points in this model. Interestingly, IL-1β, IL-6 and TNFα were detected at day 5 in this assay despite being below the level of detection when investigated using ELISA earlier in this thesis. This was perhaps due to the increased sensitivity of the Luminex assay. In summary, the results of the Luminex analysis suggest that topical Aldara treatment can induce an early peripheral inflammatory response, characterised by the expression of cytokines and chemokines, which dissipates over the course of the treatment. This response appears to be temporally different to the central response.
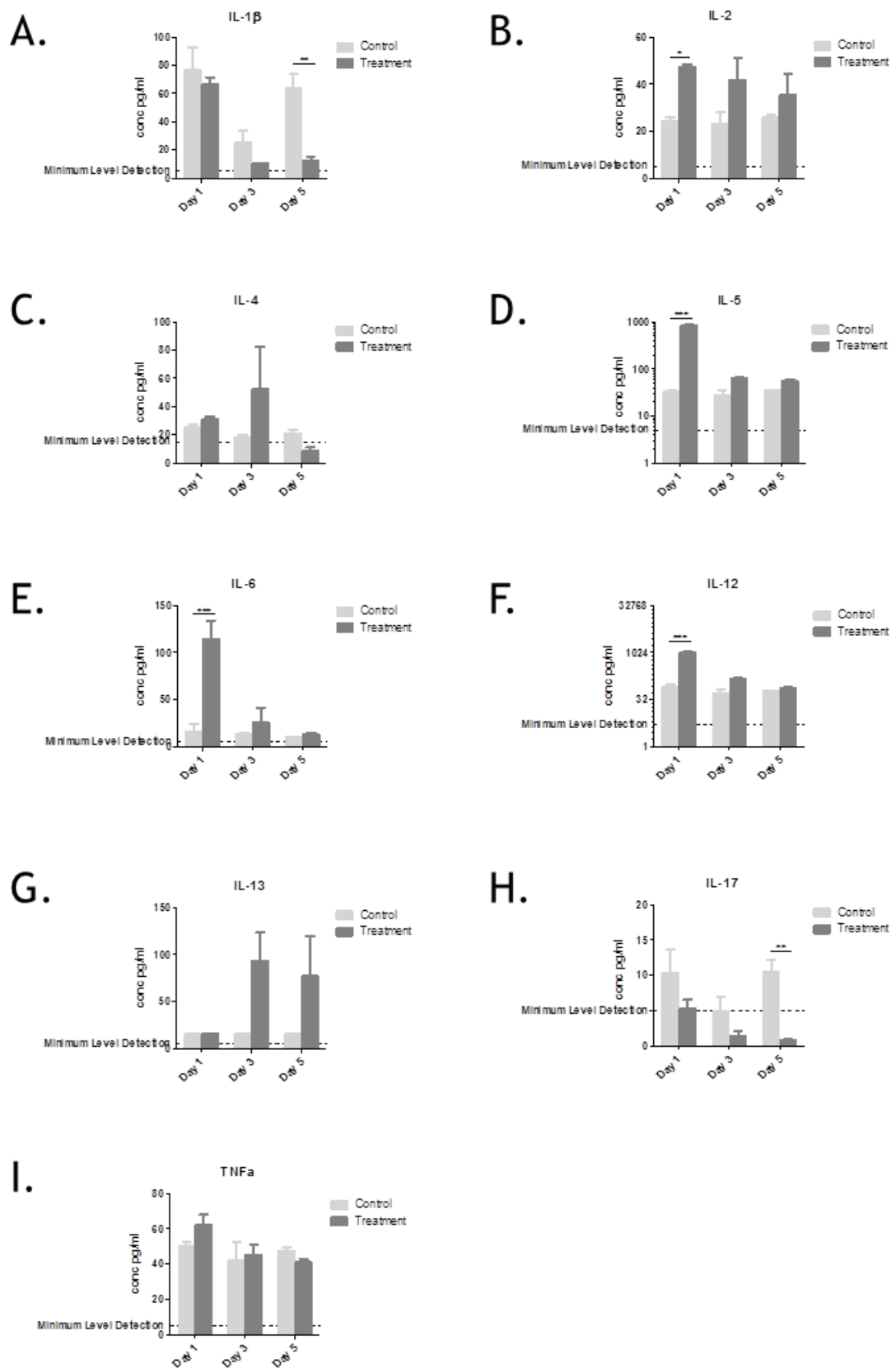
Figure 4-6 Cytokine expression in the plasma 1, 3 or 5 days following Aldara treatment
Mice were treated with 80mg of Aldara cream, or an equivalent volume of control cream, every 24hrs for 1, 3 or 5 days. Plasma was isolated 24hrs after the final treatment. Luminex analysis of (A) IL-1β, (B) IL-2, (C) IL-4, (D) IL-5, (E) IL-6, (F) IL-12 (G) IL-13, (H) IL-17 and (I) TNFα was performed. Data are expressed as concentration in pg/ml. Data represent the mean +/- SEM. Significance was calculated using two-way ANOVA with Bonferroni multiple comparison post-tests: *** $p \leq 0.001$. ** $p \leq 0.01$, * $p \leq 0.05$. n = 4/group
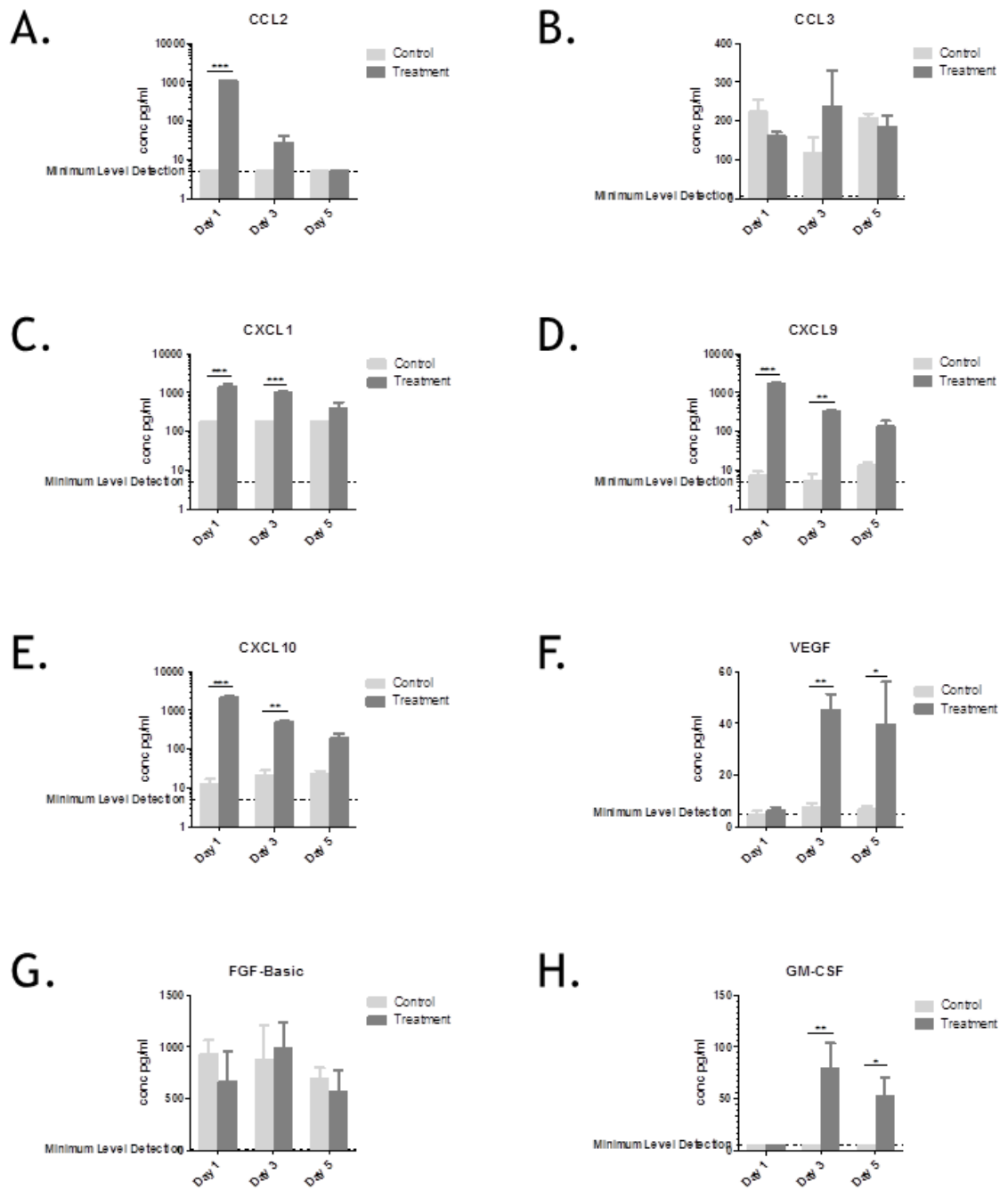
Figure 4-7 Chemokine/ growth factor expression in the plasma 1, 3 or 5 days following Aldara treatment

Mice were treated with 80mg of Aldara cream, or an equivalent volume of control cream, every 24hrs for 1, 3 or 5 days. Plasma was isolated 24hrs after the final treatment. Luminex analysis of (A) CCL2, (B) CCL3, (C) CXCL1, (D) CXCL9, (E) CXCL10, (F) VEGF (G) FGF-Basic and (H) GM-CSF was performed. Data are expressed as concentration in pg/ml. Data represent the mean +/- SEM. Significance was calculated using two-way ANOVA with Bonferroni multiple comparison post-tests: *** $p \leq 0.001$. ** $p \leq 0.01$, * $p \leq 0.05$. n = 4/group

4.4 Temporal response following TPA treatment

Analysis of the temporal response to Aldara treatment, described in Section 4.3, showed that topical Aldara treatment induced an early peripheral cytokine response, skin inflammation that worsened over the course of the treatment and a brain ISG response that peaked at day 3. Conversely, the TPA model of cutaneous inflammation failed to induce an ISG response in the brain after 5 applications. To determine whether or not the TPA model can induce a brain ISG response at earlier time-points, a time-course was set up. TPA was applied daily to the shaved dorsal skin of c57BL/6 mice for 1, 3 or 5 days. As a control, age and sex matched mice were treated with an equal quantity of acetone. Mice were terminally anaesthetised 24hrs following the final application and plasma and perfused tissues collected.

Mice did not lose any weight over the course of the treatment and, like acetone-treated control mice, TPA-treated mice gained weight with time (Figure 4-8A). H&E analysis of the treated dorsal skin sections showed that TPA treatment induced skin inflammation following just one application, indicated by epidermal hyperplasia, which worsened with repeated doses. Skin inflammation was most pronounced after the third and fifth treatments (Figure 4-8B).
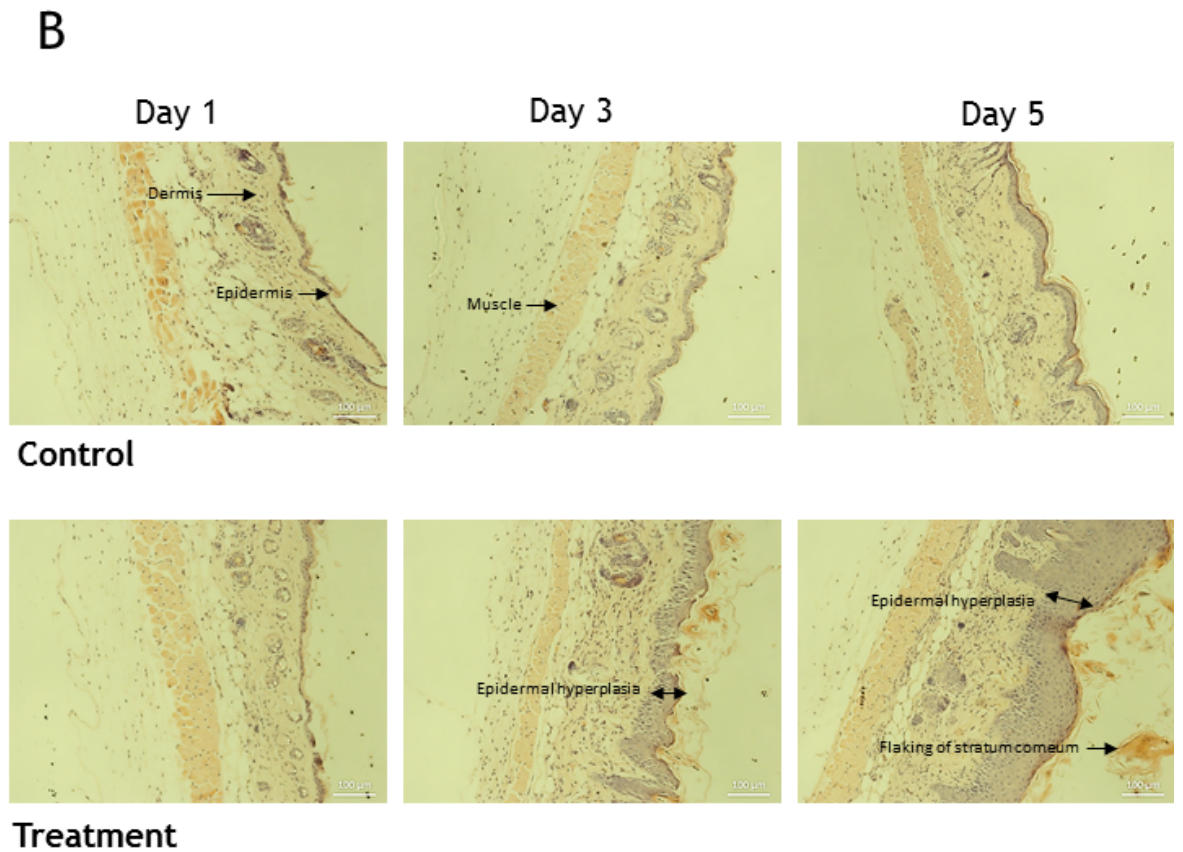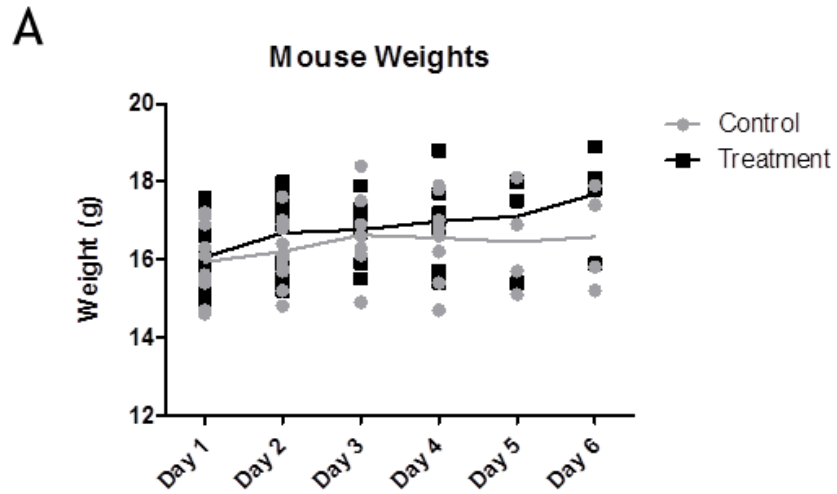
Figure 4-8 Model validation of TPA time-course
Mice were treated with 150µl 100µM TPA, or equivalent volume acetone, for 1, 3 or 5 consecutive applications. Mice were weighed following each application (A). H&E staining was performed using 5µm thick sections of TPA- or acetone- treated skin from each time point and sections were visualised at 200X magnification (B). n = 4/group. Significance was measured using two-way ANOVA

4.4.1 QPCR analysis of temporal ISG expression following TPA treatment

To assess the time course of the ISG response to TPA treatment, QPCR analysis was performed using RNA from brains and PBL isolated 24 hours after 1, 3 or 5 treatments. Each gene was normalised to the housekeeping gene, *TBP*, and each treatment group was compared to the corresponding control group, which were normalised to a fold change value of 1. The fold change induction of each gene in the brain and PBL is shown in Figure 4-9.

4.4.1.1 QPCR analysis of ISG expression in the brain

The results of the QPCR analysis of ISG expression in control and TPA-treated brains showed that this treatment failed to induce an ISG response in the brain at any of the time points examined. Only one gene, *Gbp3*, was significantly induced in the brains of the treated group and this was only at day 3. Several other genes, including *Irgm*, *Lgals3bp*, *Stat1*, *IFITm3* and *CTSC*, were downregulated in the brain in response to TPA treatment at various time points, but particularly at day 5. It is clear from these data that the brain ISG response following TPA treatment is minimal and, in fact, many of the genes appear to be downregulated. This is in stark contrast to the distinct ISG response seen following Aldara treatment.

4.4.1.2 QPCR analysis of the ISG response in the peripheral blood

The QPCR analysis of the PBL from both TPA-treated and control mice indicated the presence of a mild ISG response in the periphery (Figure 4-9). Only one gene, *Gbp4*, was significantly induced at day 1, however by day 3, 10 out of the 15 ISGs were significantly induced in the PBL of the treatment group compared with the control group (*CTSC*, *Gbp2*, *Gbp3*, *IFITm3*, *IFIT1*, *IRF7*, *Lgals3bp*, *Oasl2*, *Rtp4* and *Stat1*). This response was considered mild as none of the ISGs expressed in the PBL was induced more than 4-fold. By day 5, only one gene remained significantly induced; *Sp100*. These data suggest that TPA treatment can induce a moderate ISG response in the PBL, particularly at day 3; however the response is short lived.

4.4.1.3 Comparison of central brain response with the peripheral blood response following TPA treatment

When comparing the brain and PBL from TPA-treated mice, the ISG response appeared to be greater in the PBL than in the brain (Figure 4-9). The fold change induction of six of the genes; *CTSC*, *Gbp2*, *IFITm3*, *Oasl2*, *Rtp4* and *Stat1*, is significantly greater in the PBL than in the brain at day 3. Although the induction of ISGs in the PBL is not particularly strong, with fold-change inductions of 4 or less, many of the ISGs were downregulated in the brain, highlighting the difference between the peripheral and central response. Much of the ISG response in both tissues had dissipated by day 5, however two ISGs, Stat1 and Sp100, were significantly induced in the PBL compared with the brain. By comparing these two tissues, it appeared that the PBL response to TPA is stronger than the brain response to TPA, when evaluated using ISG induction. These findings are in contrast to the response following Aldara treatment, for which the opposite is true.
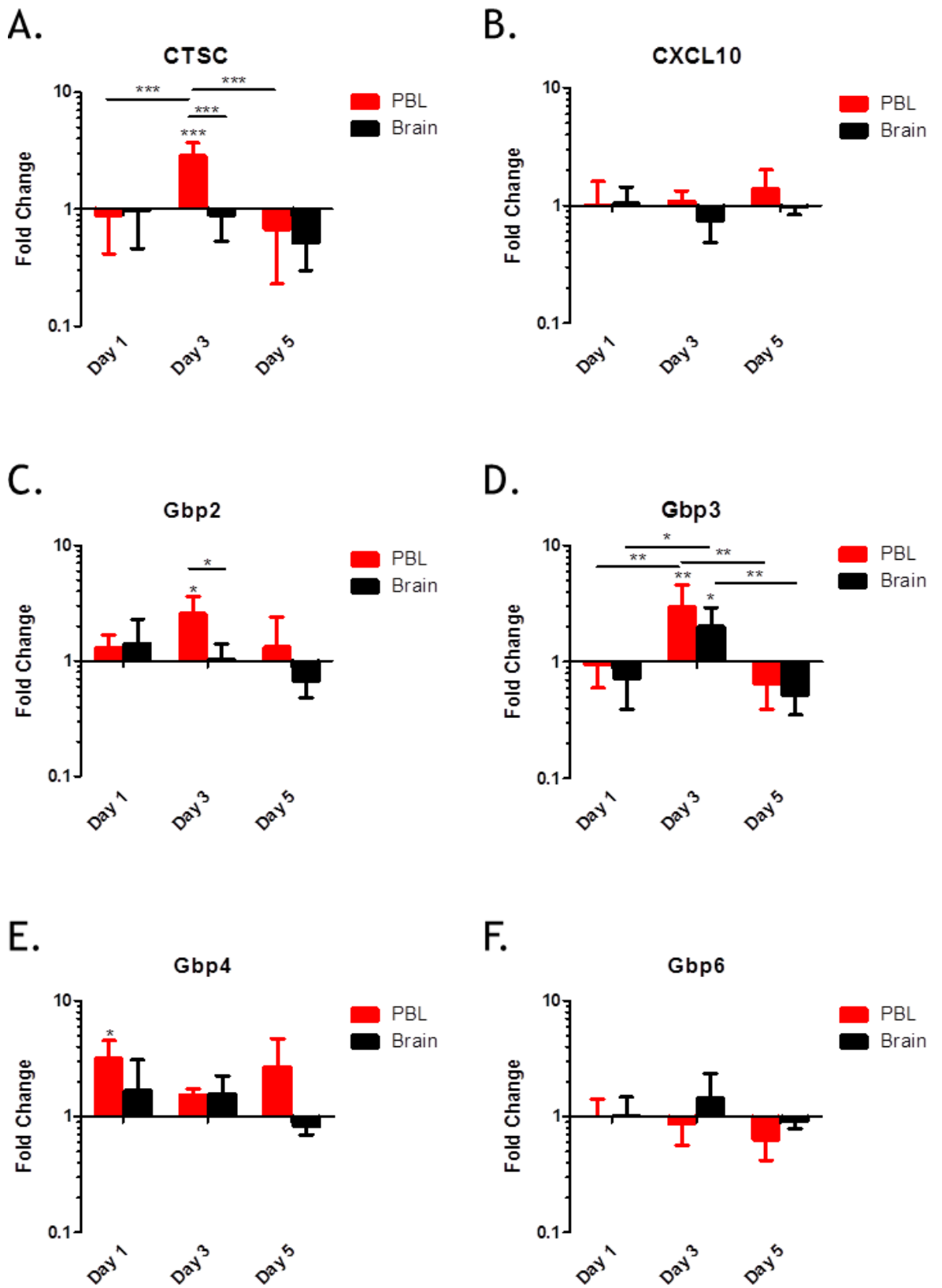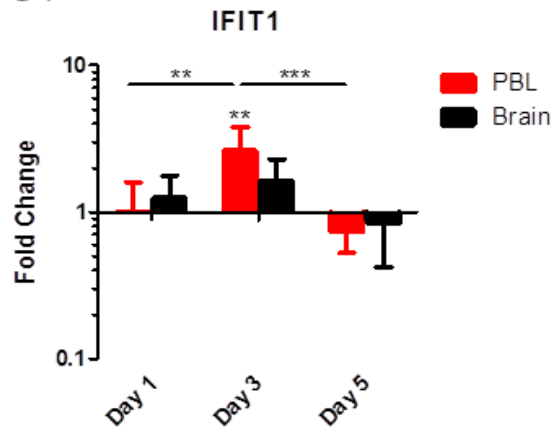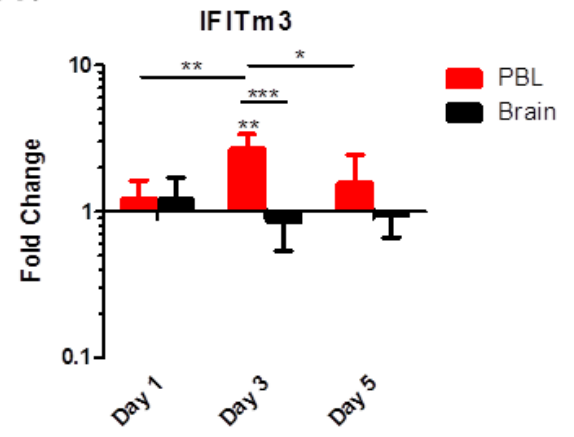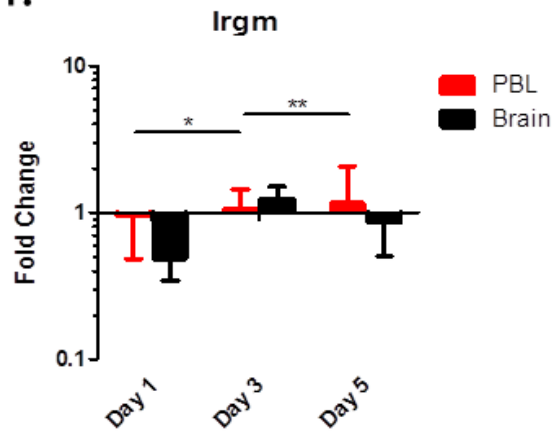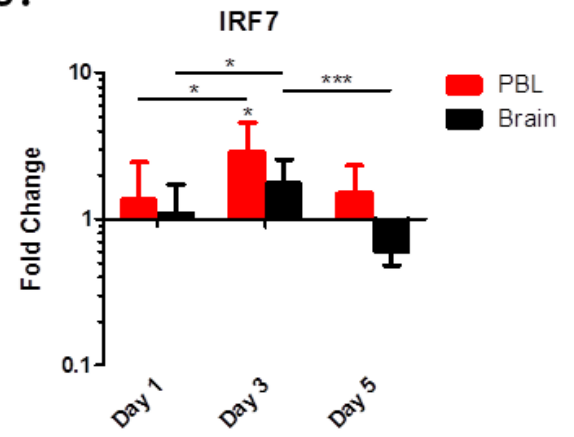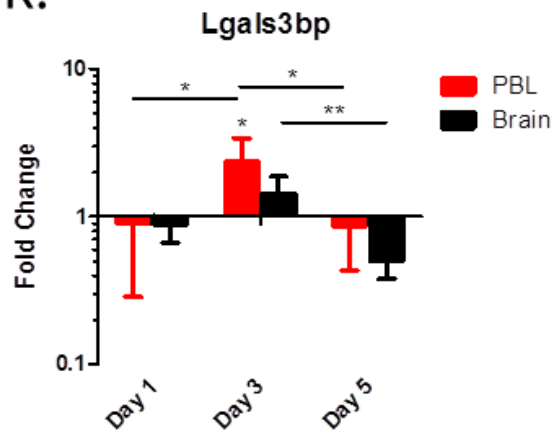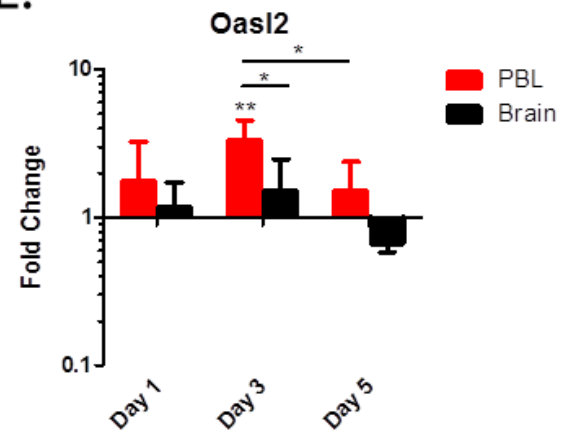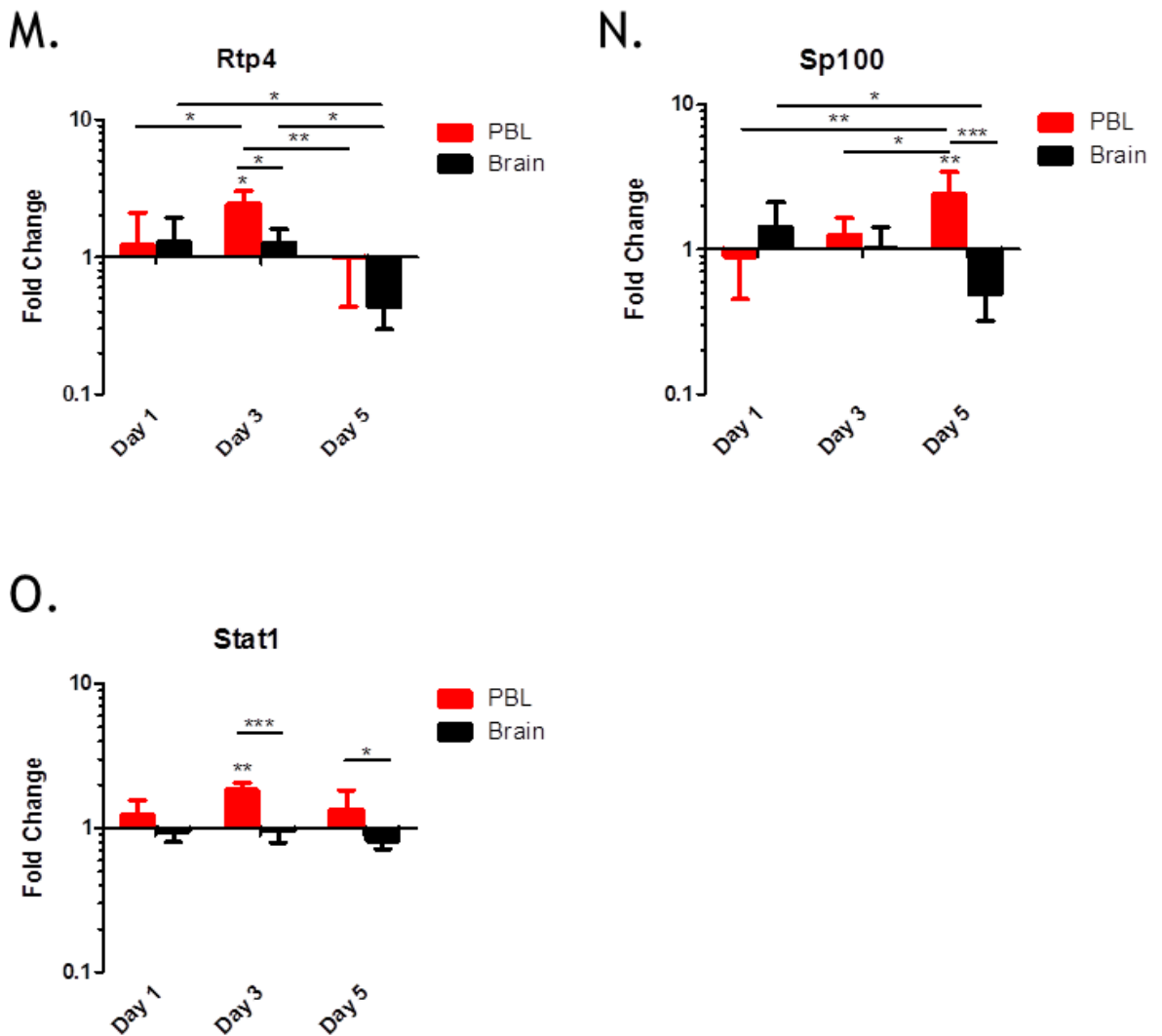
Figure 4-9 QPCR analysis of ISGs in the brain and PBL during the TPA time-course
Mice were treated with 150μl 100μM TPA, or equivalent volume of acetone, every 24hrs for 1, 3 or 5 days. RNA was then isolated from the brain and PBL 24hrs after the final treatment. Gene expression analysis of (A) Ctsc, (B) Cxcl10, (C) Gbp2, (D) Gbp3, (E) Gbp4, (F) Gbp6 (G) Ifit1, (H) Ifitm3, (I) Irgm1, (J) Irf7, (K) Lgals3bp, (L) Oasl2, (M) Rtp4, (N) Sp100 and (O) Stat1 was performed using QPCR and was normalised to TBP. Data are expressed as fold change induction, relative to the controls, which have a fold change value of 1. Data represent the mean +/- SD. Significance was calculated for individual tissues (control vs treated, d1 vs d3 vs d5), between tissues (treated only, PBL vs brain) and between time-points (treated only, d1 vs d3 vs d5) using two-way ANOVA with Bonferroni multiple comparison post-test. *** $p \leq 0.001$. ** $p \leq 0.01$, * $p \leq 0.05$. n = 4/group

4.4.2 Luminex analysis of the temporal cytokine response following TPA treatment

Luminex analysis was again performed to determine the cytokine levels in the plasma at the different time points following TPA treatment. As before, samples were diluted 1:4 prior to use in the assay. As a result, many of the cytokines were below the level of detection of the assay and in this case, IL-1α, IL-6, IL-10, IFNγ and GM-CSF were omitted from further analysis. The remaining eight

cytokines, five chemokines and two growth factors are shown in Figure 4-10 and Figure 4-11, respectively.

Only two of the cytokines, IL-5 and IL-13, were significantly induced following TPA treatment. The expression of IL-5 was significantly higher in the treatment group than in the control group at day 1 (Figure 4-10D), whereas the expression of IL-13 was significantly higher at both day 1 and day 3 (Figure 4-10F). None of the other cytokines was found to be significantly induced at any other time-point. TNFα was found to be significantly downregulated in the treatment group at day 5 when compared with the control group. With regards to the chemokines and growth factors, only CCL2 (Figure 4-11A) and CXCL10 (Figure 4-11E) were significantly induced at day 1 and day 3, respectively. CCL2 showed the highest induction following TPA treatment with an expression of around 200pg/ml after day 1. Together, these data suggest that TPA treatment does not induce a strong inflammatory response in the periphery. Although the expression of certain cytokines and chemokines at the earlier time points indicates a response, this appears to be mild and short-lived.
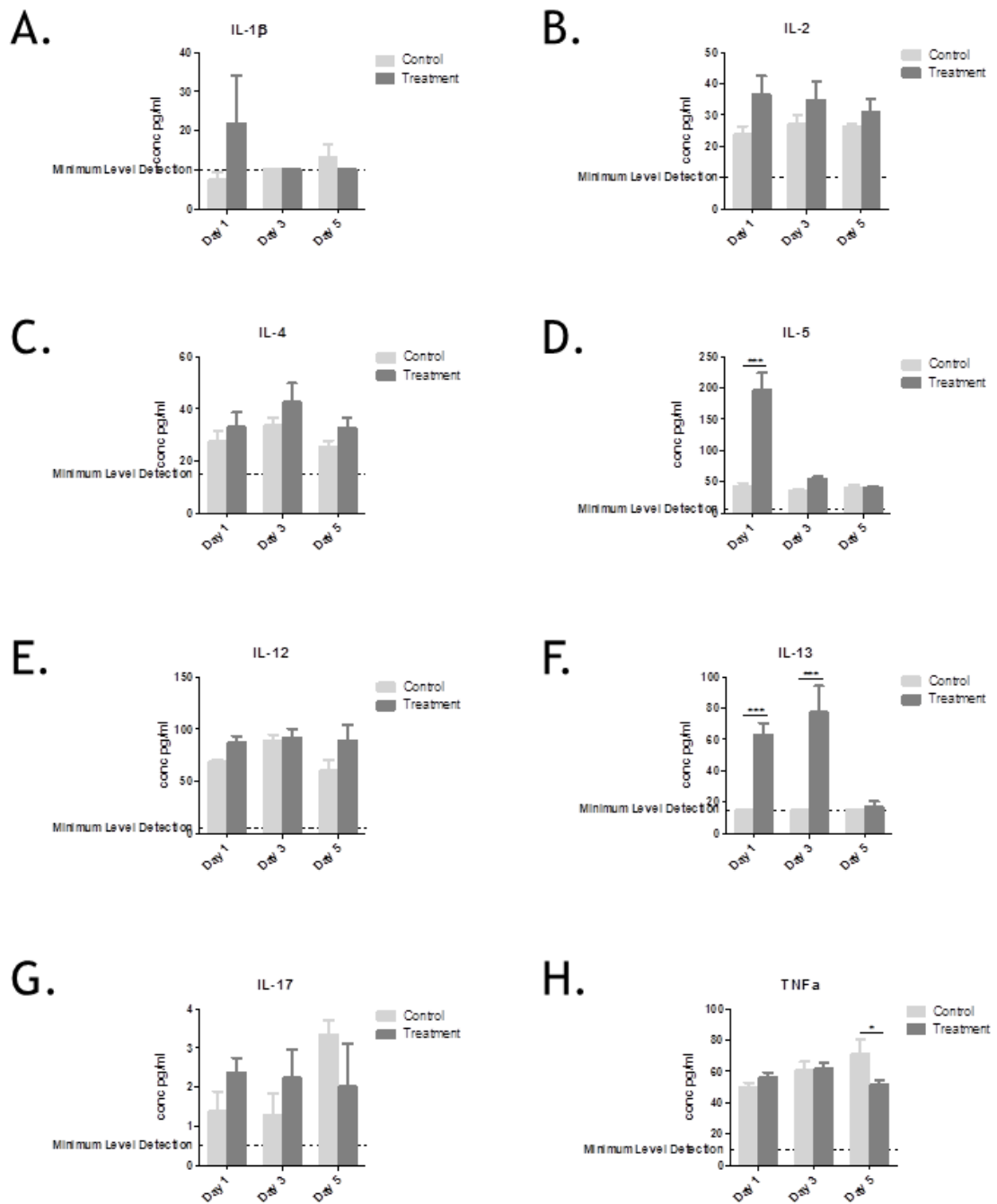
Figure 4-10 Cytokine expression in the plasma 1, 3 or 5 days following TPA treatment
Mice were treated with 150μl 100μM TPA, or an equivalent volume of acetone control, every 24hrs
for 1, 3 or 5 days. Plasma was isolated 24hrs after the final treatment. Luminex analysis of (A) IL-
1β, (B) IL-2, (C) IL-4, (D) IL-5, (E) IL-12 (F) IL-13, (G) IL-17 and (H) TNFα was performed. Data are
expressed as concentration in pg/ml. Data represent the mean +/- SEM. Significance was
calculated using two-way ANOVA with Bonferroni multiple comparison post-tests: *** $p \leq 0.001$. **
$p \leq 0.01$, * $p \leq 0.05$. n = 4/group
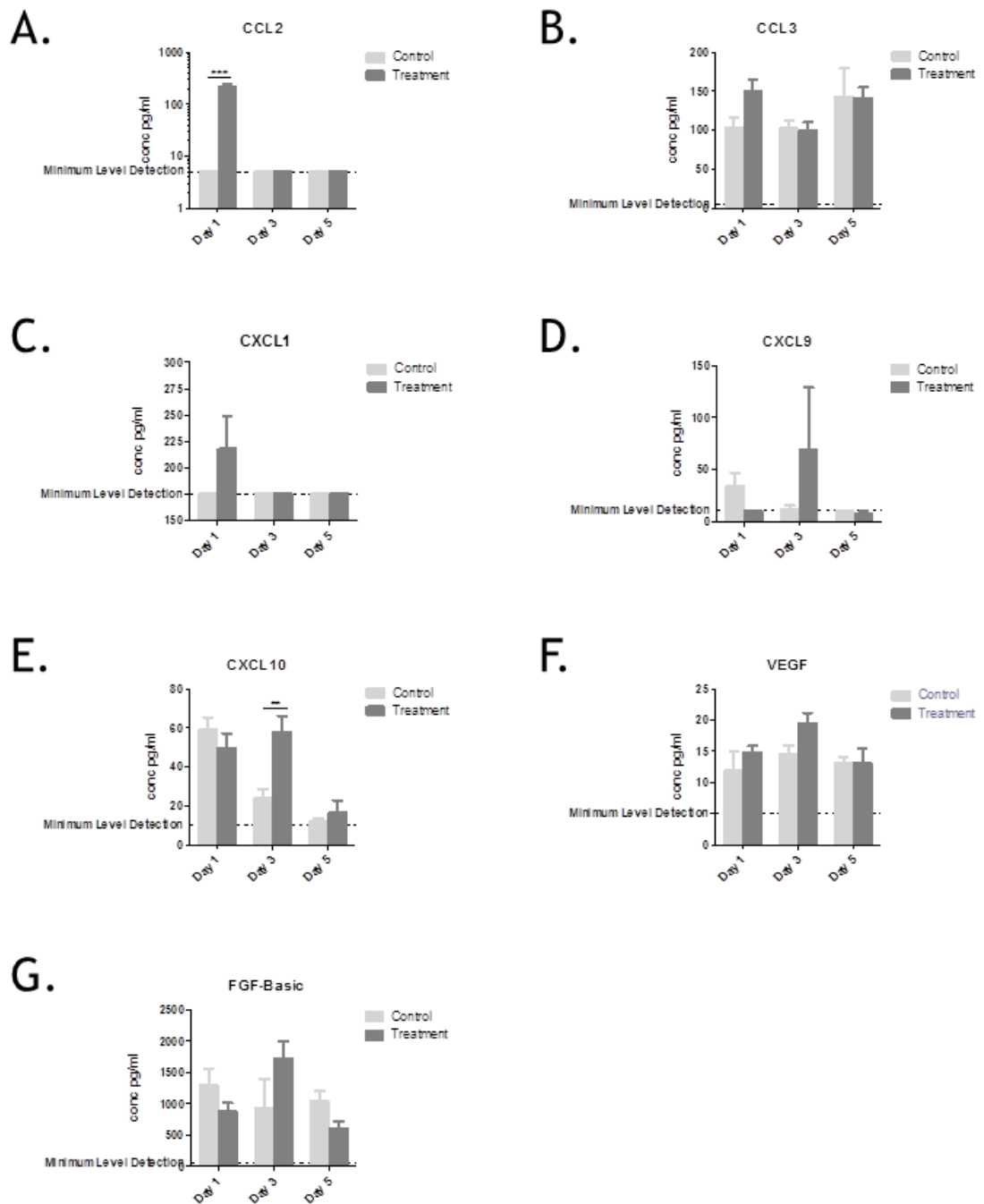
Figure 4-11 Chemokine/ growth factor expression in the plasma 1, 3 or 5 days following TPA treatment
Mice were treated with 150µl 100µM TPA, or an equivalent volume of acetone control, every 24hrs for 1, 3 or 5 days. Plasma was isolated 24hrs after the final treatment. Luminex analysis of (A) CCL2, (B) CCL3, (C) CXCL1, (D) CXCL9, (E) CXCL10, (F) VEGF and (G) FGF-Basic was performed. Data are expressed as concentration in pg/ml. Data represent the mean +/- SEM. Significance was calculated using two-way ANOVA with Bonferroni multiple comparison post-tests: *** $p \leq 0.001$. ** $p \leq 0.01$, * $p \leq 0.05$. n = 4/group

4.5 The response to systemic Imiquimod

Cutaneous Aldara treatment leads to the expression of a distinct, brain transcriptional ISG response. This response appears to peak after the third application and is induced independently of an overt inflammatory profile in the periphery. In addition, it has been shown that this response cannot be induced in the brain following a sterile, non-TLR-mediated, model of skin inflammation, TPA. Together, these findings suggest that the ISG response is TLR7-dependent as it is only induced following treatment with Aldara, which contains the TLR7 antagonist, Imiquimod. However, as mentioned above, studies have suggested that Aldara can mediate an immune response in a TLR7-independent manner, through the actions of isostearic acid[372]. Therefore, it is difficult to establish whether the brain response is generated as a result of the stimulation of TLR7 by IMQ or the activation of the inflammasome by isostearic acid. In an attempt to understand the effect of IMQ treatment alone, c57BL/6 mice were injected I.P with soluble IMQ every 24 hours for five consecutive days. Alternatively, control mice were injected I.P with an equal volume of saline. As before, the model was characterised by monitoring mouse weights throughout the treatment and evaluating spleen size 24 hours after the final administration.

Mice treated with I.P IMQ did not lose any weight over the course of the treatment and, consistent with the control mice, appeared to gain weight over time (Figure 4-12A). Although there was a slight difference in the spleen weights, this did not reach significance, and the administration of IMQ via this route did not cause splenomegaly (Figure 4-12B + C).
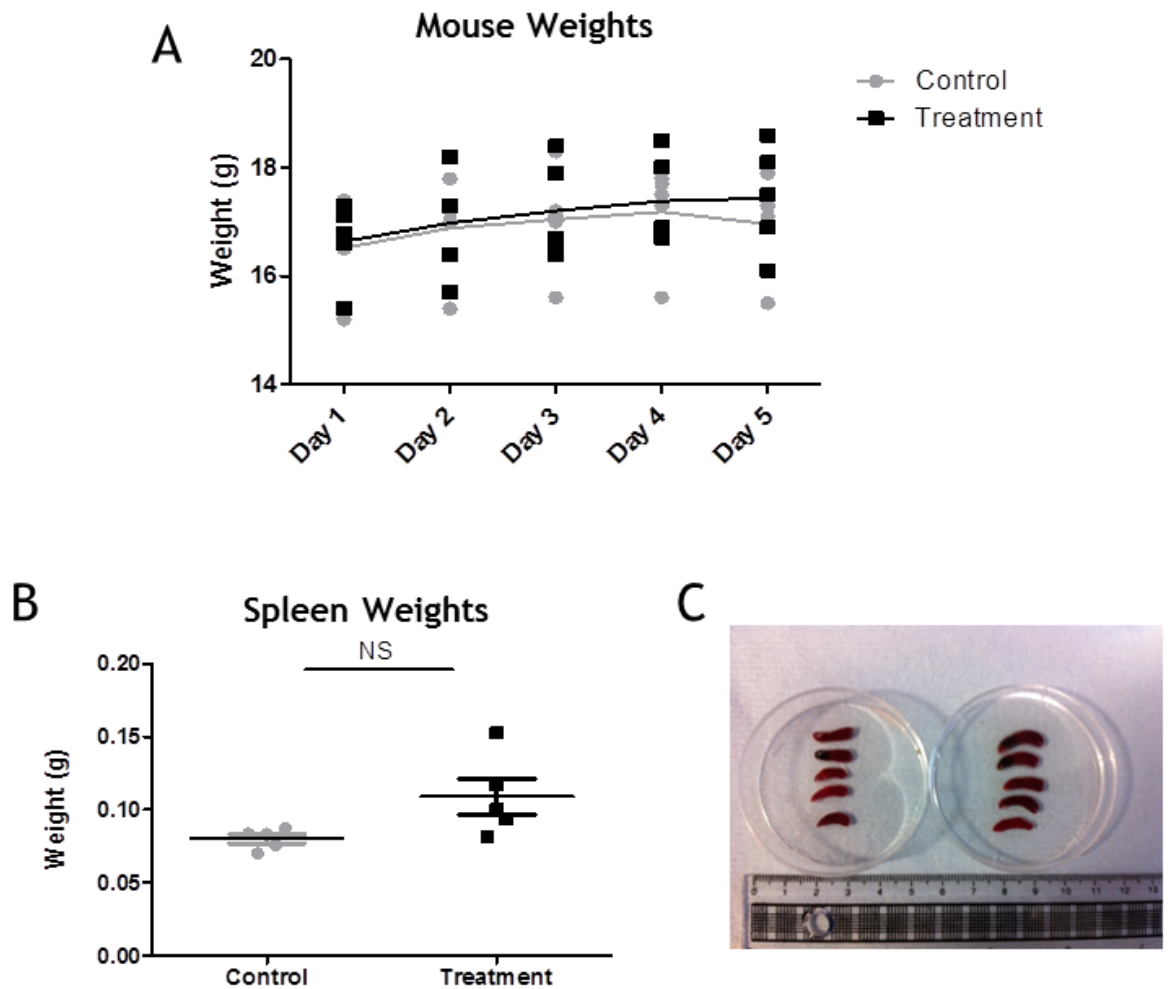
Figure 4-12 Evaluation of the phenotypic response following intraperitoneally administered Imiquimod

Mice were treated with 100µl 1mg/ml IMQ, or equivalent volume of PBS, every 24hrs for five consecutive days. Mice were weighed following each application (A). In addition, spleens were removed and were weighed (B) and photographed (C). n = 5/group. Significance was measured using two-way ANOVA (weights) or student's t test (spleens).

4.5.1 QPCR analysis of ISG expression in response to intraperitoneal Imiquimod

To determine whether or not I.P administration of IMQ could stimulate the expression of ISGs in the brain and the periphery, QPCR was performed using brains and PBL isolated 24 hours after the final injection. Each of the 15 ISGs was normalised to the housekeeping gene, *TBP,* and each treatment group was compared to the corresponding control group, which were normalised to a fold change value of 1. The fold change induction of each gene in the brain and PBL is shown in Figure 4-13.

4.5.1.1 QPCR analysis of the ISG response in the brain

The results of the QPCR revealed that only 6 out of the 15 ISGs were significantly induced in the brain following I.P IMQ administration. *Gbp3, IFIT1, IFITm3, IRF7, Lgals3bp* and *Rtp4* were all significantly induced in the brains of treated mice compared with the control brains; however the fold change induction was low in comparison to the induction following Aldara treatment and the maximum induction was 3-fold. Unlike the brain response following TPA, none of the genes was found to be downregulated in the brain following IMQ treatment. The brain response to I.P. IMQ appears to lie somewhere between the response to Aldara, where a strong ISG profile is seen, and the response to TPA, in which none of the ISGs was induced in the brain. It would appear from these results that I.P. IMQ treatment induced only a moderate ISG response in the brain.

4.5.1.2 QPCR analysis of the ISG response in the peripheral blood

With regards to the peripheral ISG response to IMQ treatment, 9 out of the 15 ISGs were significantly induced in the PBL, including many of the genes which were also induced in the brain. *Gbp6, IFIT1, IFITm3, Irgm, IRF7, Lgals3bp, Oasl2, Rtp4* and *Sp100* were all significantly induced in the PBL of the treated group when compared with the control group. Again, none of the ISGs was significantly downregulated in the PBL following IMQ treatment.

4.5.1.3 Comparison of central brain response with the peripheral blood response

Two-way ANOVA was performed to determine the significance of the differential expression of the ISGs between the brain and the PBL. 7 genes were significantly differentially expressed between the brain and the PBL; *Gbp3, Gbp6, IFIT1, Irgm, IRF7, Oasl2* and *Sp100*. With the exception of *Gbp3*, all of these genes were induced to a greater extent in the PBL than in the brain, suggesting that the peripheral ISG response to I.P. IMQ is greater than the central ISG response. Together, the results of the QPCR suggest that treatment with I.P. IMQ fails to induce an ISG response in the brain. This is in contrast to the data which show that treatment with topical Aldara, which contains IMQ as its active component, leads to a strong and distinct ISG response in the brain. It may suggest that the

transcriptional response is driven by IMQ-independent mechanisms, or that it is reliant on a cutaneous route of administration.
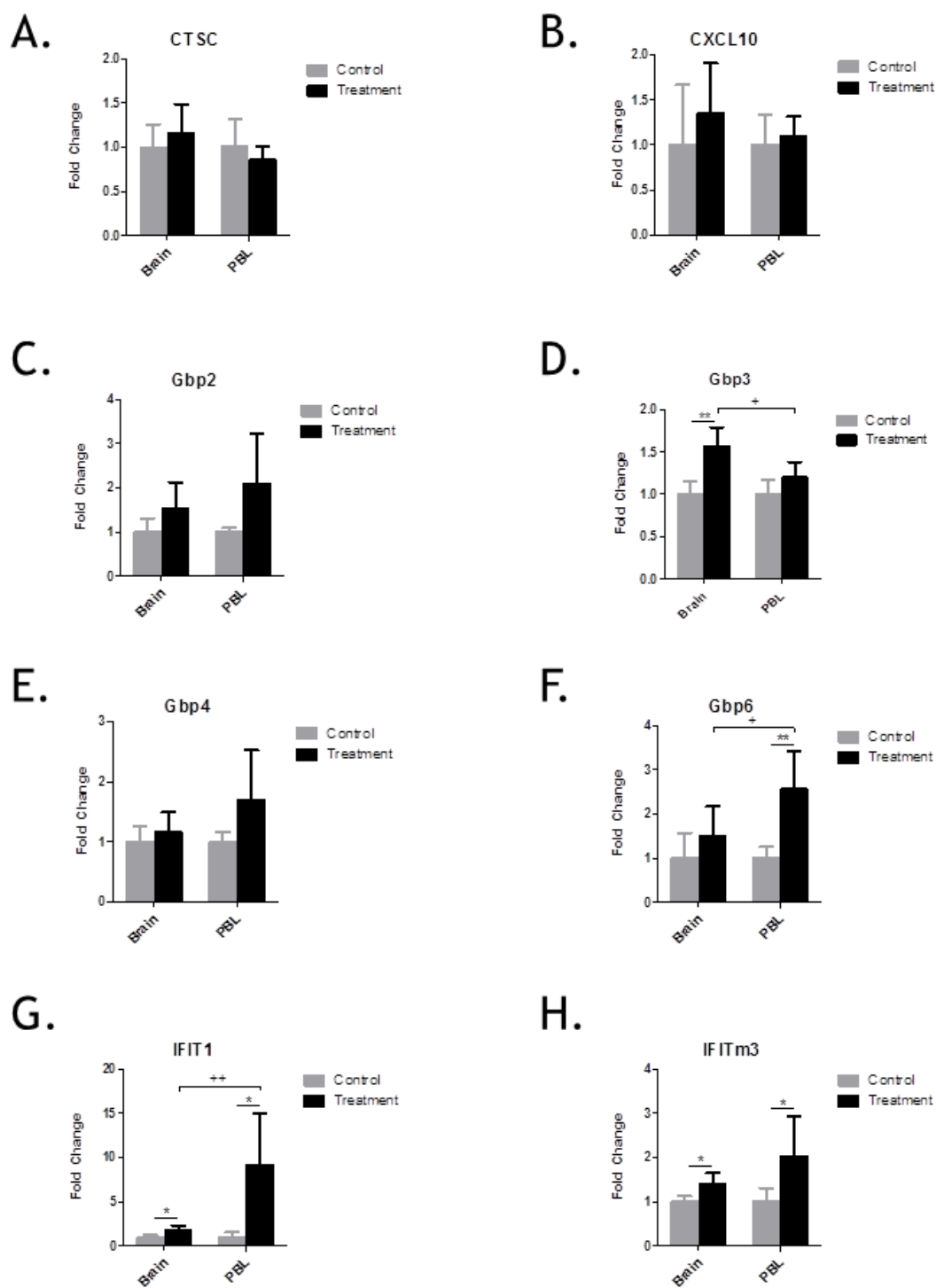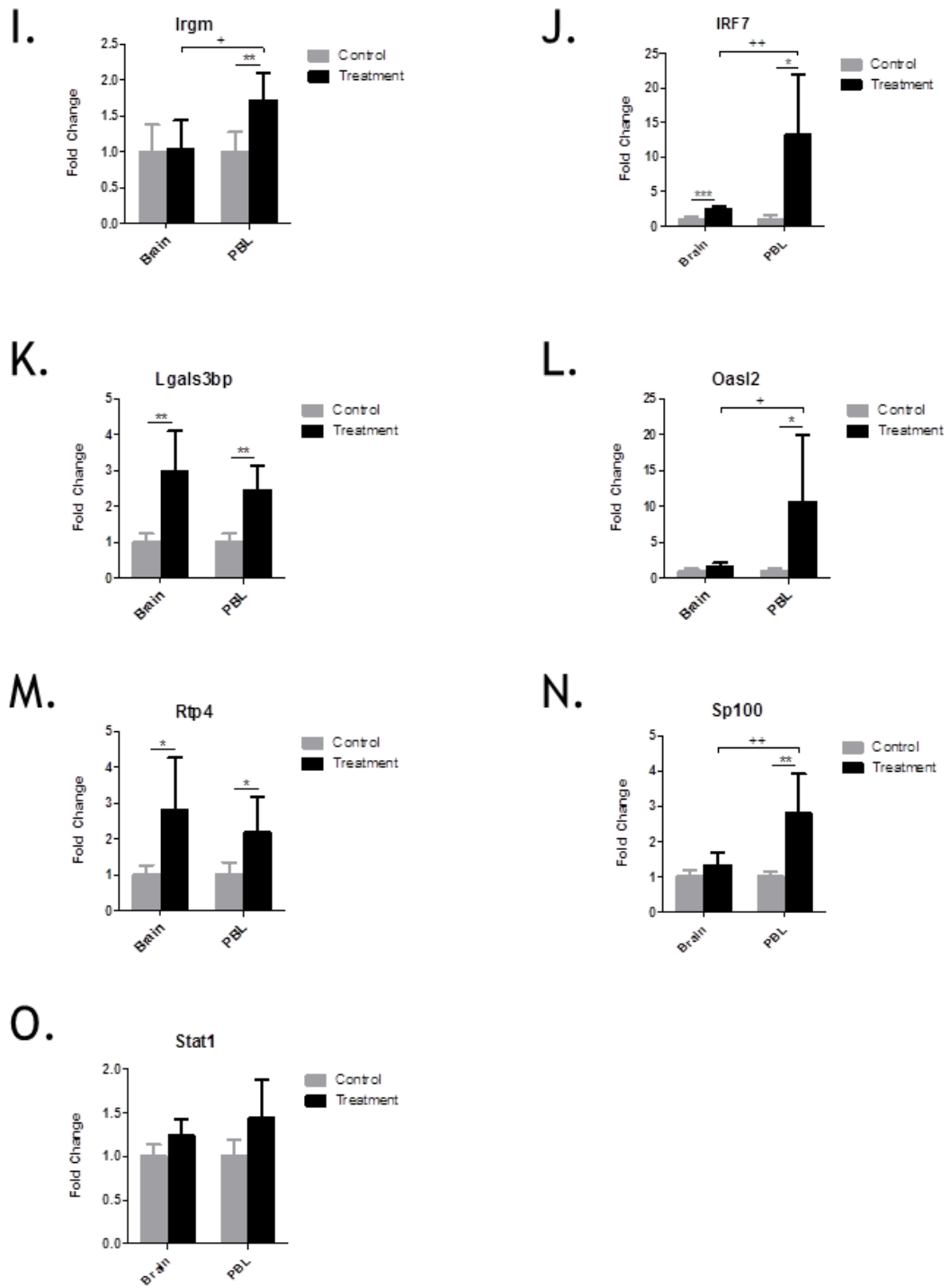
Figure 4-13 QPCR analysis of ISGs in brains and PBL following IMQ injections
Mice were treated with 100µl 1mg/ml IMQ, or equivalent volume of saline, every 24hrs for 5
consecutive days. Mice were euthanised 24hrs after the final application. Cardiac puncture was
performed to retrieve PBLs and perfused brains were extracted. RNA was isolated from both
tissues. QPCR analysis of the 15 target ISG genes was performed for both tissues (A-O). n= 5
mice per group. Significance was measured using individual unpaired students t tests for individual
tissues (control vs treated) or two-way ANOVA with Bonferroni multiple comparison post-tests for
comparisons between tissues (PBL vs brain). *** (+++) = p ≤ 0.001 **(++) = p ≤ 0.01 *(+) = p ≤ 0.05

4.5.2 Luminex analysis following intraperitoneal Imiquimod treatment

The results of the QPCR analysis showed that I.P. IMQ treatment leads to a higher ISG response in the PBL than in the brain and a higher PBL response when compared with the PBL response following topical Aldara application. To see if this was a direct result of a general inflammatory response in the periphery, Luminex analysis was again performed to determine cytokine expression in the plasma. As with previous Luminex data presented in this thesis, the samples were diluted 1:4 prior to use and, as a result, many of the readings were below the level of detection of the assay. In this case, IL-1α, IL-6, IL-10, IL-13, IFNγ, CXCL1, CCL2 and GM-CSF were omitted from further analysis. Levels of the remaining seven cytokines, three chemokines and two growth factors are shown in Figure 4-14 and Figure 4-15, respectively.

Interestingly, none of the cytokines examined was significantly induced in the plasma following I.P. IMQ treatment. Although certain cytokines, including IL-1β, IL-2 and IL-17 (Figure 4-14A, B + F), appeared to be increased in the treated group, there was a high degree of variability within the biological replicates, thus the inductions failed to reach significance. Two of the chemokines, CXCL9 and CXCL10 (Figure 4-15B + C), were significantly induced in the plasma following IMQ treatment. CXCL10, in particular, was highly upregulated with an expression value of around 250pg/ml. The results would suggest that the ISG response in the PBL, identified using QPCR, is not a direct result of a general inflammatory profile in the periphery, although it may be possible that a peripheral cytokine response is present earlier in this model.
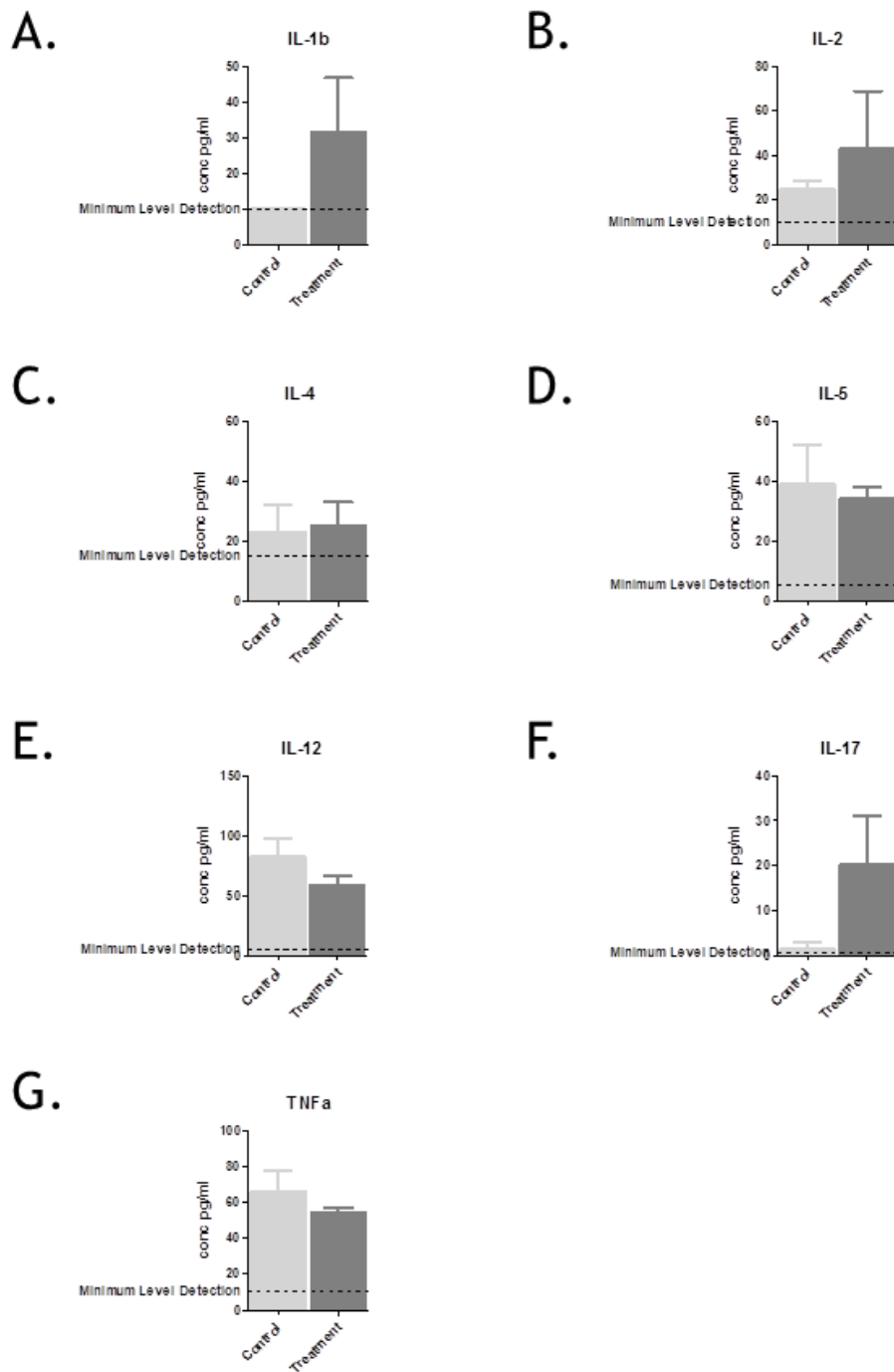
Figure 4-14 Cytokine expression in the plasma following intraperitoneal IMQ treatment
Mice were treated with 100µl 1mg/ml IMQ, or equivalent volume of saline, every 24hrs for 5 consecutive days. Plasma was isolated 24hrs after the final treatment. Luminex analysis of (A) IL-1β, (B) IL-2, (C) IL-4, (D) IL-5, (E) IL-12, (F) IL-17 and (G) TNFα was performed. Data are expressed as concentration in pg/ml. Data represent the mean +/- SEM. Significance was calculated using unpaired student's t tests: *** p ≤ 0.001. ** p ≤ 0.01, * p ≤ 0.05. n = 5/group
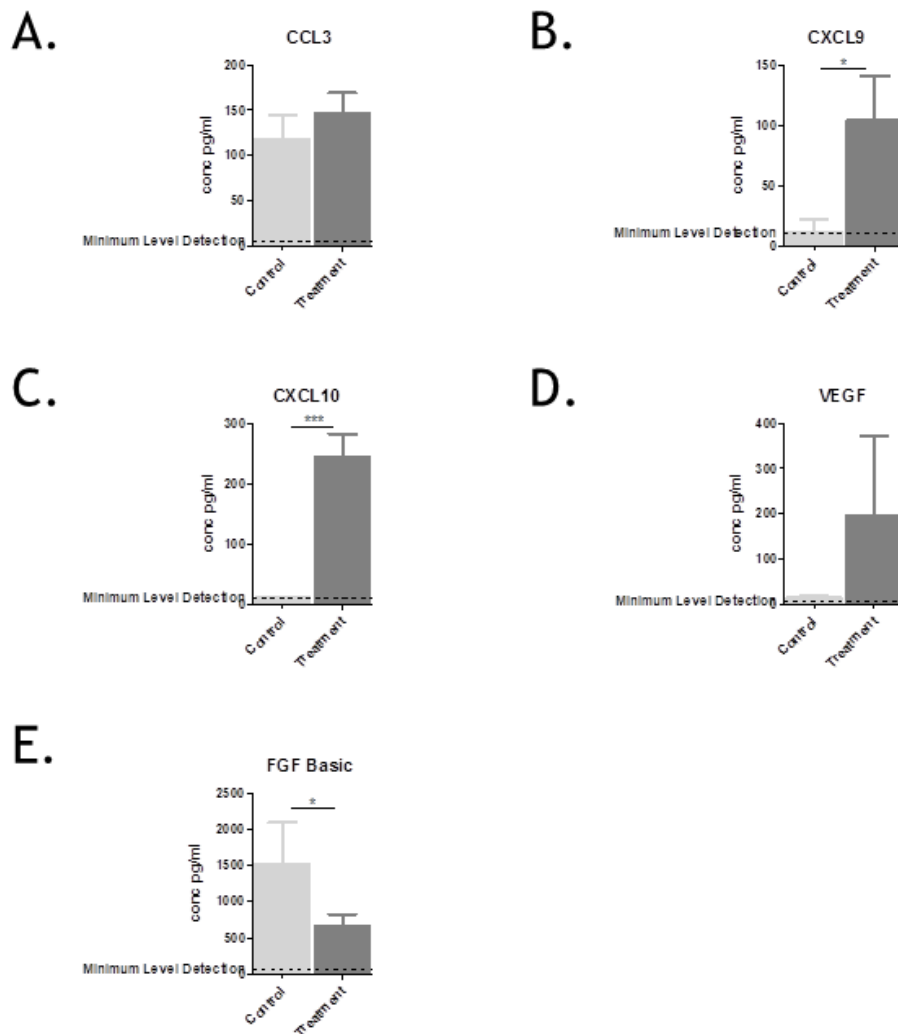
Figure 4-15 Chemokine/ growth factor expression in the plasma following intraperitoneal IMQ treatment

Mice were treated with 100μl 1mg/ml IMQ, or equivalent volume of saline, every 24hrs for 5 consecutive days. Plasma was isolated 24hrs after the final treatment. Luminex analysis of (A) CCL3, (B) CXCL9, (C) CXCL10, (D) VEGF and (E) FGF-Basic was performed. Data are expressed as concentration in pg/ml. Data represent the mean +/- SEM. Significance was calculated using unpaired student's t tests: *** $p \leq 0.001$. ** $p \leq 0.01$, * $p \leq 0.05$. n = 5/group

4.6 Topically applied Imiquimod as a model of skin inflammation

Results in Section 4.5.1, in which soluble IMQ was injected intraperitoneally, demonstrated that IMQ administered in this way was not sufficient to induce the brain ISG response that was seen following topical Aldara treatment. These results suggested that the central response may be driven by IMQ-independent mechanisms, perhaps via the actions of isostearic acid. However, using a different route of administration was not an ideal method of comparison, as the initial tissue response in the skin may be an important factor in the generation

of the remote response in the CNS. In order to test the importance of the local tissue response, soluble IMQ was first dissolved in PBS before being reconstituted into the water based, non isostearic acid containing, control cream. This was applied topically to the shaved dorsal skin of c57BL/6 mice daily for 5 consecutive days. As a control, mice were treated with an equal volume of aqueous control cream alone. This model eliminated the potential actions of other components found in the Aldara vehicle, and meant that any response would be the result of IMQ-induced mechanisms.

Mice were weighed daily following each application. Weights are shown as percentage of initial weight in Figure 4-16A, where the initial weight was considered 100%. IMQ treated mice lost a significant amount of weight, evident after the first application. Weight loss ceased and mice began to regain some of their weight after the third application, however they remained significantly lighter than the control mice. The IMQ- treated mice showed signs of splenomegaly, whereby their spleens weighed more than 2.5 times that of the control mice (Figure 4-16B + C). Surprisingly, the H&E analysis of the treated dorsal skin showed that topical IMQ failed to induce psoriasis-like skin inflammation.
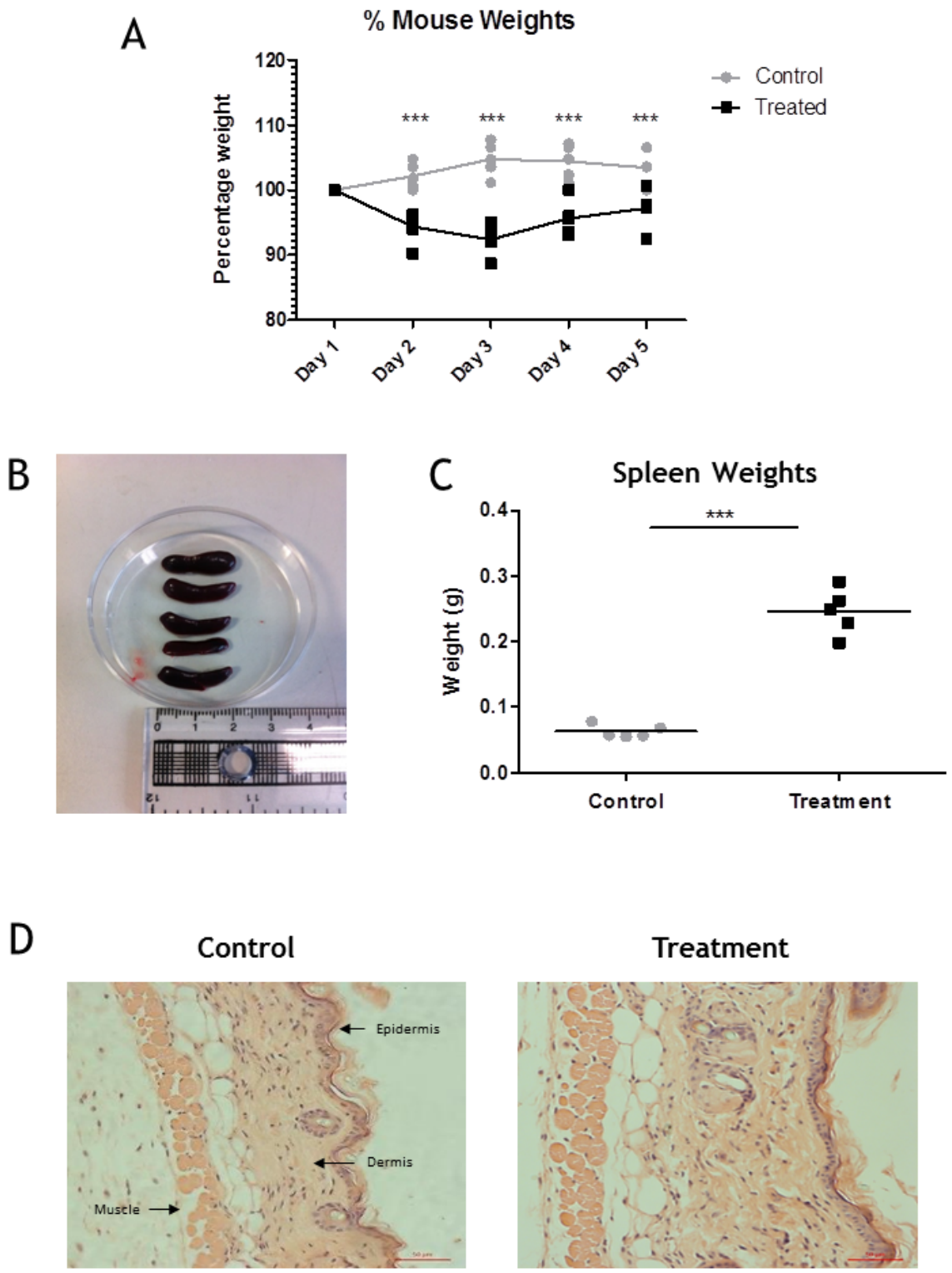
Figure 4-16 Evaluation of the phenotypic response to IMQ induced skin inflammation
Mice treated with 80mg IMQ cream (5% v:v in aqueous control cream), or equivalent volume control cream, were weighed following each application (A). In addition, spleens from IMQ-treated mice were photographed (B) and spleens from control and treated mice were weighed (C). H&E staining was performed using 5µm thick sections of IMQ- or control-treated skin which were imaged at 200X magnification. n = 5/group. Significance was measured using two-way ANOVA. *** = p ≤ 0.001.

4.6.1 QPCR analysis of ISG expression in response to topical cutaneous Imiquimod

To determine whether or not the topical administration of IMQ could stimulate the expression of ISGs in the brain and the periphery, QPCR was performed using RNA from brains and PBL isolated 24 hours after the final application. Each of the 15 ISGs were normalised to the housekeeping gene, *TBP*, and each treatment group was compared to the corresponding control group, which were normalised to a fold change value of 1. The fold change induction of each gene in the brain and PBL is shown in Figure 4-17.

4.6.1.1 QPCR analysis of the ISG response in the brain

To identify ISGs that were significantly induced in the brain following topical IMQ treatment, the brains from IMQ treated mice were compared with control brains. With the exception of *Ctsc*, all 15 ISGs were significantly upregulated in the brains of the IMQ treated group compared with the control group. The transcriptional induction in the brain was quite striking, with many of the genes exhibiting 10-100 fold change increases. *Sp100* was of particular note, with a fold change increase in excess of 1000-fold (Figure 4-17N). It was clear from these results that topical IMQ treatment can lead to a strong ISG response in the brain, indistinguishable from the brain response following topical Aldara application.

4.6.1.2 QPCR analysis of the ISG response in peripheral blood leukocytes

In order to identify whether or not topical IMQ treatment could also induce an ISG response in the periphery, the expression of the genes in the PBL was evaluated for both the treated group and the control group. Interestingly, 9 out of the 15 ISGs were significantly downregulated in the PBL of the IMQ treated group compared with the PBL of the control group. Only two genes, *Oasl2* and *Rtp4* (Figure 4-17L + M), were significantly induced in the PBL following topical IMQ treatment with an approximately 8-fold increase. The remaining genes, *Gbp3*, *IFIT1*, *Irgm* and *Lgals3bp*, remained consistent between the control PBL and the treated PBL. These results indicated that topically applied IMQ did not induce a distinct ISG response in the periphery.

4.6.1.3 Comparison of central brain response with the peripheral blood response

Two-way ANOVA was performed to determine the significance of the differential expression of the ISGs between the brain and the PBL. The fold-change induction of all 15 ISGs was significantly greater in the brain when compared with the PBL. With the exception of *Ctsc*, the differential expression between the ISGs in the brain and PBL was highly significant and satisfied a p-value <0.001. This confirmed that the ISG response in the brain was not the result of blood contamination. These findings also highlighted the differential nature of the peripheral response when compared with the central response, suggesting that ISG induction in the brain was not a general consequence of peripheral immune stimulation.

When compared with the other models, the ISG response following topically applied IMQ is similar to the ISG response following topical Aldara treatment, both of which were characterised by a distinct brain response and a mild PBL response. This implies that the actions of the TLR7 ligand, IMQ, and the initial localised skin response are important for the generation of the brain ISG response.

A. CTSC

B. CXCL10

C. Gbp2

D. Gbp3

E. Gbp4

F. Gbp6

G. IFIT1

H. IFITm3
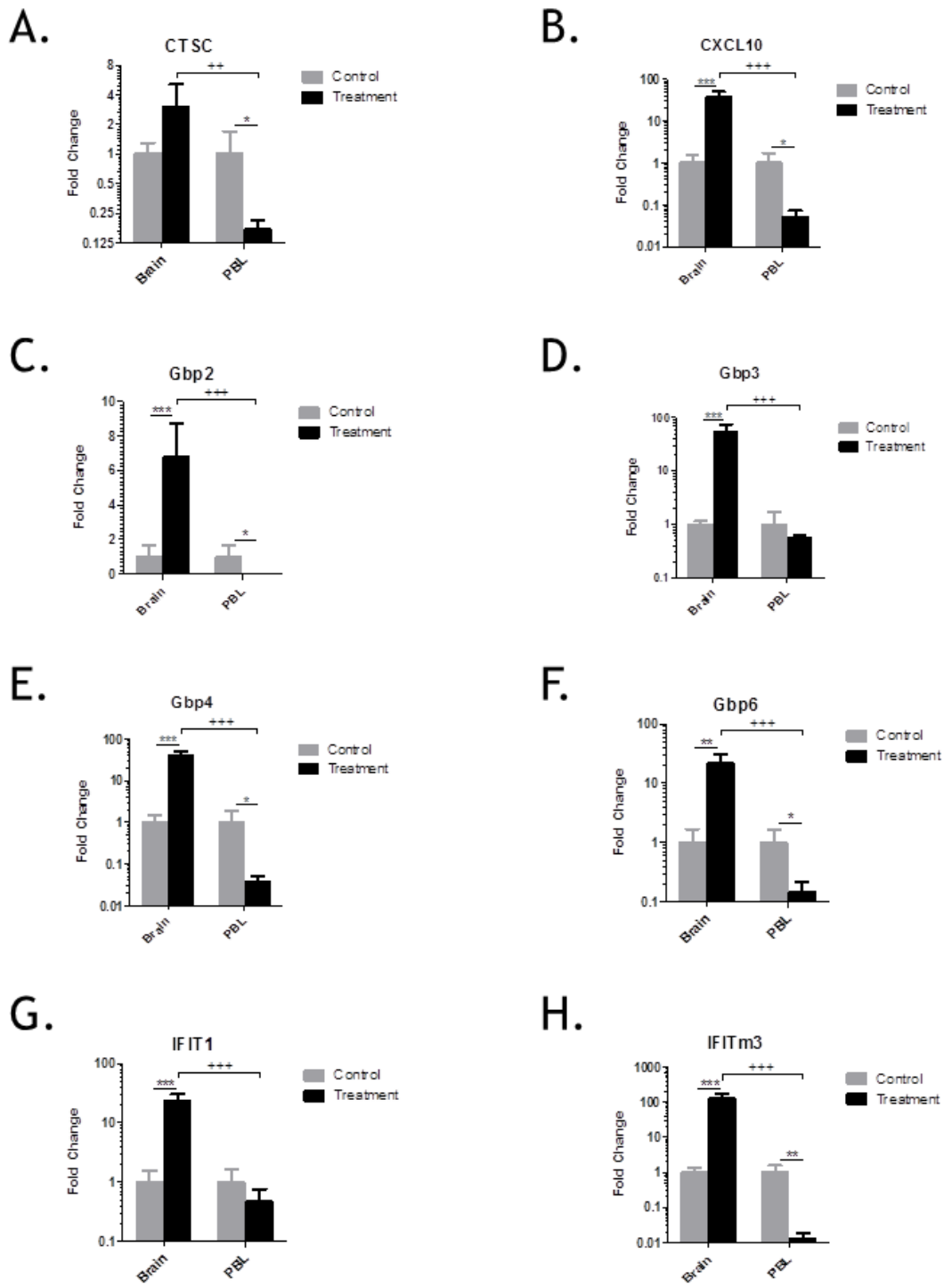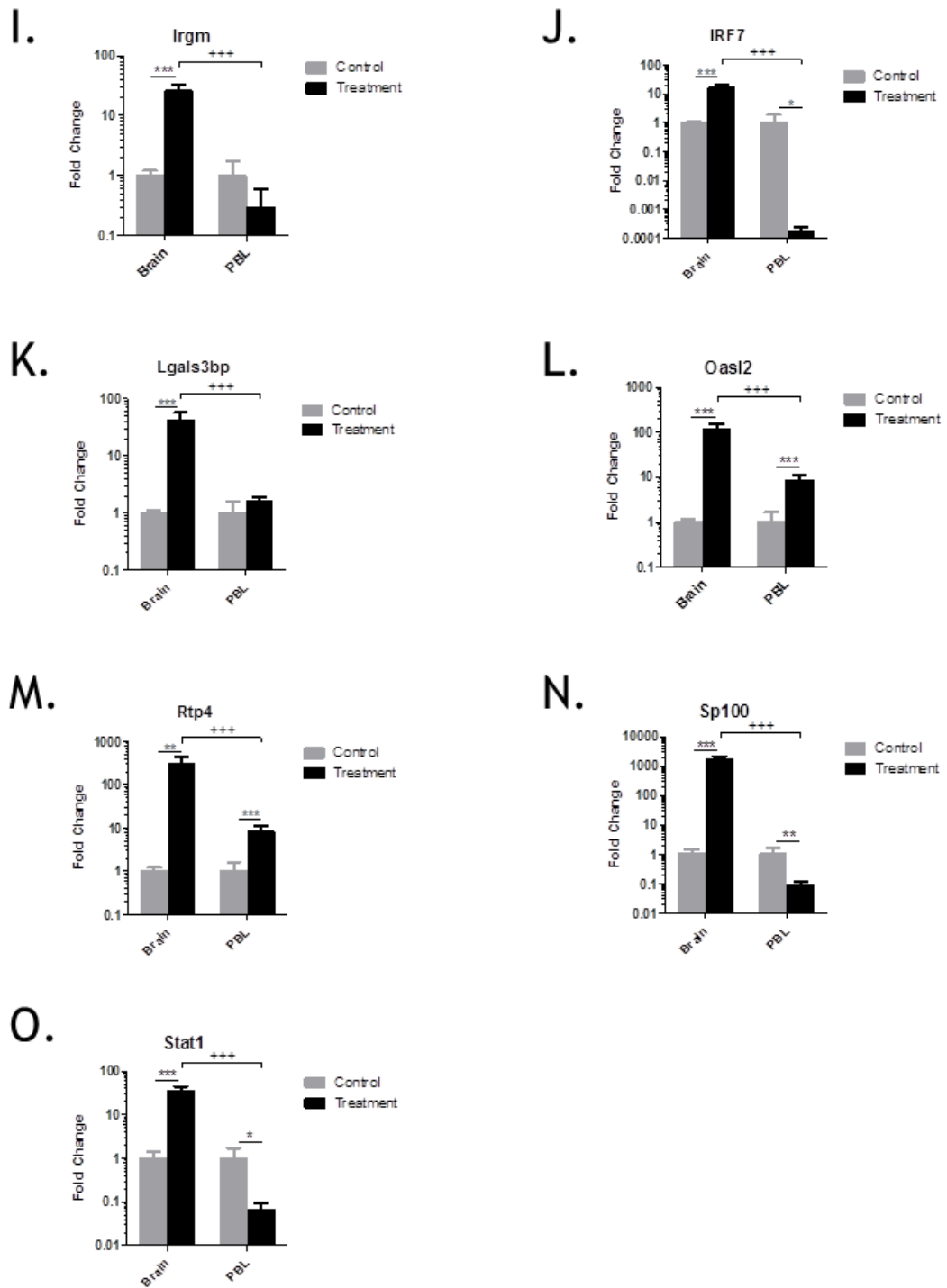
Figure 4-17 QPCR analysis of ISGs in the brain and PBL following topical IMQ application
Mice were treated with with 80mg IMQ cream (5% v:v in aqueous control cream), or equivalent volume control cream, every 24hrs for 5 consecutive days. Mice were euthanised 24hrs after the final application. Cardiac puncture was performed to retrieve PBLs and perfused brains were extracted. RNA was isolated from both tissues. QPCR analysis of the 15 target ISG genes was performed for both tissues (A-O). n= 5 mice per group. Significance was measured using individual unpaired students t tests for individual tissues (control vs treated) or two-way ANOVA with Bonferroni multiple comparison post-tests for comparisons between tissues (PBL vs brain). *** (+++) = p ≤ 0.001 **(++) = p ≤ 0.01 *(+) = p ≤ 0.05

4.7 Discussion

The results presented in Chapter 3, in which transcriptional profiling techniques were used, identified a distinct ISG response in the brain following topical cutaneous Aldara application. However, the mechanisms of induction remained to be fully understood. It was widely assumed that the response to Aldara cream was mediated through the actions of the active component, IMQ, which binds to TLR7/8. One signalling pathway initiated by TLR7/8 ligation is the activation of IRF7 and the production of Type I IFNs. Therefore, this mechanism seemed a likely candidate for driving the production of an ISG response in the brain following treatment. Recently, however, Walter et al. published a report showing that Aldara cream can also function in a TLR-independent mechanism, through the actions of isostearic acid, which is a component of the vehicle[372]. They propose that some features of the response may be driven by the ability of isostearic acid to activate the inflammasome. Thus, it seemed important to establish the involvement of TLR stimulation in the generation of the brain ISG response and to determine the individual roles of IMQ and isostearic acid. The aims of this chapter were to investigate the mechanisms driving the brain response following cutaneous inflammation and to determine the importance of TLR stimulation using a number of different inflammatory models.

Utilising a sterile model of skin inflammation, results suggested that TLR ligation was indispensable for the brain ISG response. Topical TPA administration induced a psoriasis-like skin inflammation consistent with that seen following Aldara application; however TPA failed to stimulate an ISG response. It has been shown that both Aldara and LPS administration[377] lead to the induction of an ISG response in the brain. Both of these TLR ligands can signal in an NF-κB-independent manner, leading to the production of Type I IFNs, thus making it a likely pathway in the generation of a downstream ISG response. This hypothesis is strengthened by results showing that a similar ISG response cannot be generated following sterile inflammation, in the form of TPA, or by the direct administration of inflammatory cytokines into the circulation[377]. Together, these results suggest that the ISG response following Aldara application is not simply a response to peripheral inflammation.

ISGs were not induced in the PBL following cutaneous Aldara or TPA stimulation; however these results were obtained following 5 consecutive applications. To better understand the temporal pattern of the responses, and to identify whether or not an ISG response is initiated in the periphery at an earlier time-point, time course models of Aldara treatment and TPA treatment were performed. The Aldara time course experiment revealed that the ISG response peaked in the brain following the third treatment, although the genes remained elevated in the brain after the fifth treatment. The model also showed that the ISG response was not mimicked in the PBL at any of the time-points. With regards to the PBL, several ISGs were induced at day 1; however the PBL response was short-lived and had largely dissipated by day 3. This also allowed us to confirm that the brain response was not due to contamination with peripheral blood. In contrast to the Aldara model, the TPA time course model confirmed that this sterile model of skin inflammation failed to induce an ISG response in the brain, even at the earlier time-points. These data strengthened the hypothesis that TLR stimulation may be important for the generation of a brain ISG response following cutaneous inflammation and highlight the difference in expression kinetics between the brain and the PBL. To confirm the role of TLR stimulation, it would be preferable to run both models using TLR7$^{-/-}$ or MyD88$^{-/-}$ mice.

To investigate the role of TLR stimulation further, and to rule out the effects of isostearic acid in the Aldara vehicle, two other inflammatory models were used. The first, which involved repeated intraperitoneal stimulation with IMQ, induced a relatively mild ISG response in the brain in comparison with the brain response to topical Aldara treatment. It did, however, cause a more pronounced response in the PBL, although there was a high degree of variability within the treated group. It is important to note that the dose of IMQ injected I.P was lower than the dose applied to the dorsal skin, which may be the reason we do not see a brain response with this model. It is also possible that IMQ could be sequestered in the gut, which would therefore prevent it from entering the circulation. The second model utilised soluble IMQ reconstituted into aqueous control cream as a vehicle, which was subsequently applied daily to the shaved dorsal skin of the mice. This model retained the route of administration used in previous models but eliminated any effects of isostearic acid. Following this treatment, a very

striking ISG response was seen in the brain, with fold-change inductions substantially greater than those seen following Aldara treatment. This response was not mimicked in the PBL, which showed a mixture of up- and down-regulations in the treated group. Intriguingly, this treatment did not appear to induce an inflammatory phenotype in the skin suggesting that, as reported in the literature, the IMQ and isostearic acid may be responsible for different aspects of the response. Walter et al suggested that, in the absence of IMQ, treatment with vehicle cream induced inflammasome activation, keratinocyte cell death and IL-1 production[372]. In keeping with our findings, they report that the local effects on the skin are largely due to IMQ-independent mechanisms, as they too failed to induce the full skin phenotype *in vivo* following treatment with IMQ in 'softcream'. These findings would explain why, in Section 4.6, H&E analysis of skin treated with IMQ reconstituted in aqueous control cream showed few signs of inflammation.

With such a potent brain response following topically administered IMQ; it would appear that the response was indeed TLR-driven. However, intraperitoneal administration of IMQ failed to induce an ISG response in the brain. Damm et al. used IMQ to investigate how TLR ligation, and different routes of administration, can cause the manifestation of inflammation at distant sites, including the brain[7]. They reported that a high dose of peripherally administered IMQ (subcutaneous and intraperitoneal) induced a moderate fever, peripheral and hypothalamic cytokine induction and inflammatory transcription factor activation. In keeping with our study, they found the response to be more pronounced with subcutaneous administration; however topical administration onto the dorsal skin was not investigated. Although an upregulation of inflammatory markers in the hypothalamus was reported, there was no change in brain levels of IFNs. It is difficult, however, to directly compare the results of their study to the results in this thesis as Damm et al focused on only one specific brain region at an earlier time point.

The results from this Chapter would suggest that the ISG response is TLR-driven but also dependent on some component of the localised skin response. The problem with this hypothesis is that, as I have already mentioned, the localised skin response is predominantly reliant on the effects of isostearic acid and not IMQ. Therefore this makes it hard to establish what, if any, aspect of the skin

response is necessary for the generation of the brain ISG response. To better understand the role of each component in the generation of the brain ISGs, isostearic acid alone should be used to treat the mice, which would allow for a direct comparison of the two active components of Aldara cream. In addition, it would be interesting to inject soluble IMQ subcutaneously, as this, in theory, should stimulate a similar response in the skin to topical application.

One proposed mechanism of peripheral immune signal transduction into the brain is via the activation of vascular endothelial cells by circulating cytokines, such as IL-1β and TNFα. To determine whether or not such cytokines were induced in the circulation following Aldara application, Luminex analysis was performed using plasma isolated from the time course model. According to the literature, TLR7 stimulation should lead to the production of inflammatory cytokines in the periphery, however it is also possible that cytokines, particularly IL-1β, could be produced as a result of inflammasome activation by isostearic acid. The Luminex data showed that four cytokines and four inflammatory chemokines were induced in the Aldara model following the first application; however IL-1β and TNFα were not detected. Luminex analysis was also performed using plasma from the TPA time course and the I.P. IMQ model, neither of which induced an ISG response in the brain. The Luminex results showed that the peripheral inflammatory cytokine response in both of these models was minimal, with very few cytokines being significantly induced. The lack of a peripheral cytokine response in a range of models, irrespective of their ability to induce an ISG response in the brain, indicated that the brain response was independent of the peripheral cytokine response and was driven by another mechanism. In addition, the expression of IFNγ was below the minimum level of detection of the kit in all of the models examined. This was interesting, since IFNs would normally be produced as a prerequisite to an ISG response. TLR7/8 stimulation does, however, lead to the production of IFNα, which unfortunately was not included in the panel of cytokines on the kit used in this study. Therefore, the production of Type I IFNs in the periphery following Aldara treatment cannot be ruled out. It is important to bear in mind however, that some cytokine expression may have been diluted out in this assay, and firm conclusions would require the assay to be repeated using undiluted samples.

The absence of an overt peripheral cytokine response indicated that cytokines may not be driving the brain response following Aldara treatment. An alternative mechanism for generating the ISG response in the brain is through TLR7/8 stimulation. This could occur in two ways; either by TLR ligation in the skin and the localised production of Type I IFNs that subsequently traffic to the brain and act in an endocrine fashion, or via the direct activation of TLR7/8 in the brain parenchyma or peripheral nerves. As mentioned, the ability of IMQ to cross the BBB is not known. Butchi et al have shown that intracerebroventricular inoculation of IMQ in developing mice leads to microglia and astrocyte activation[391]. They reported that protein levels of certain proinflammatory cytokines and chemokines, including CXCL10, IL-1β and IL-5, are upregulated in response to TLR7 ligation, as well as a strong IFNβ response. Their data suggest that, should IMQ be able to cross the BBB, it would induce a sufficiently strong inflammatory response to generate an ISG response. Interestingly, Damm et al have shown that, following IMQ administration, several transcription factors were activated in regions of the brain devoid of intact BBB, including the CVOs[7]. This suggests that areas protected by an intact BBB are less susceptible to IMQ, perhaps because it is not able to cross into the brain. According to the literature, dermal DCs, pDCs and Langerhans cells in the skin are activated following IMQ treatment and are the primary source of Type I IFN, specifically IFNα[368, 400, 401]. In addition, it has been reported that IFNα can mediate neurological effects by crossing the BBB by diffusion or by a facilitated saturable transport system[402, 403]. Therefore, if IMQ cannot cross the BBB, this would be a viable mechanism by which distal immune activation by Aldara/IMQ could mediate an ISG response in the brain. However, it does raise the question as to why an ISG response was not seen in the periphery if the response was induced by circulating Type I IFNs. As such, it may be the case that in this model, IFNs are produced directly in the brain. To test this hypothesis, QPCR and ELISA could be used to determine the expression of Type I IFNs in the brain at the various time-points following immune stimulation.

In summary, both topical Aldara and topical IMQ application to the skin induced a distinct ISG response in the brain. This response appeared to be dependent on TLR stimulation, and differed in kinetics and magnitude to the PBL response. In addition, this response was generated independently of an inflammatory

cytokine profile in the periphery. The results suggest that the remote brain response may be driven by the production of TLR-dependent Type I IFNs, highlighting a potential mechanism of transcriptional regulation in the brain following peripheral immune stimulation.

Chapter 5

Transcriptional chemokine response in the brain following cutaneous immune stimulation

5 Transcriptional chemokine response in the brain following cutaneous immune stimulation

5.1 Introduction

The results in Chapter 3 provided a transcriptional profile of the brain response following topical Aldara treatment. Microarray analysis revealed a number of ISGs that were induced in the brain following treatment, which were validated and assessed in a range of inflammatory models. However, the microarray also identified a number of other genes as being differentially expressed in the brain but these were not further investigated. DAVID ontology analysis of the microarray dataset identified the most enriched biological pathways, amongst which were 'Chemokine signalling pathway', 'Inflammation mediated by chemokine and cytokine signalling pathway' and 'Leukocyte transendothelial migration'. These pathways strongly implicated a chemokine response in the brain following Aldara treatment.

Chemokines, described in detail in Chapter 1, regulate cellular migration and are thought to be involved in maintaining certain homeostatic and developmental processes in the brain[109, 215]. In many inflammatory models, both peripheral and central, chemokines are commonly upregulated in the brain. It is thought that this induction not only drives immune cell infiltration into the brain, but perhaps also disrupts key homeostatic functions. It is therefore possible that chemokine induction in the brain could be a prerequisite for chronic neuroinflammation and changes in brain biology that lead to the onset of neuropsychiatric phenotypes.

To establish whether or not cutaneous Aldara treatment could lead to a chemokine response in the brain, the microarray dataset from Chapter 3 was revisited to identify the significantly induced chemokine genes. These genes were subsequently validated in the range of inflammatory models previously employed. Immunohistochemistry was performed to explore immune cell infiltration into the brain and finally, to try to correlate the chemokine response with a functional consequence, burrowing behaviour was investigated alongside the use of chemokine receptor antagonists.

5.2 Identifying the differential chemokine response in the brain following topical Aldara application

Upon revisiting the microarray data detailed in Chapter 0, 7 chemokines and 1 chemokine receptor were identified as being differentially expressed in the brains of the treatment group. GeneSpring GX software was used to generate a heat map showing the expression of the 8 genes, which is shown in Figure 5-1. The fold change induction and the p-value for each of the chemokine genes is shown in Table 5-1, where genes are presented in order of their fold-change induction.
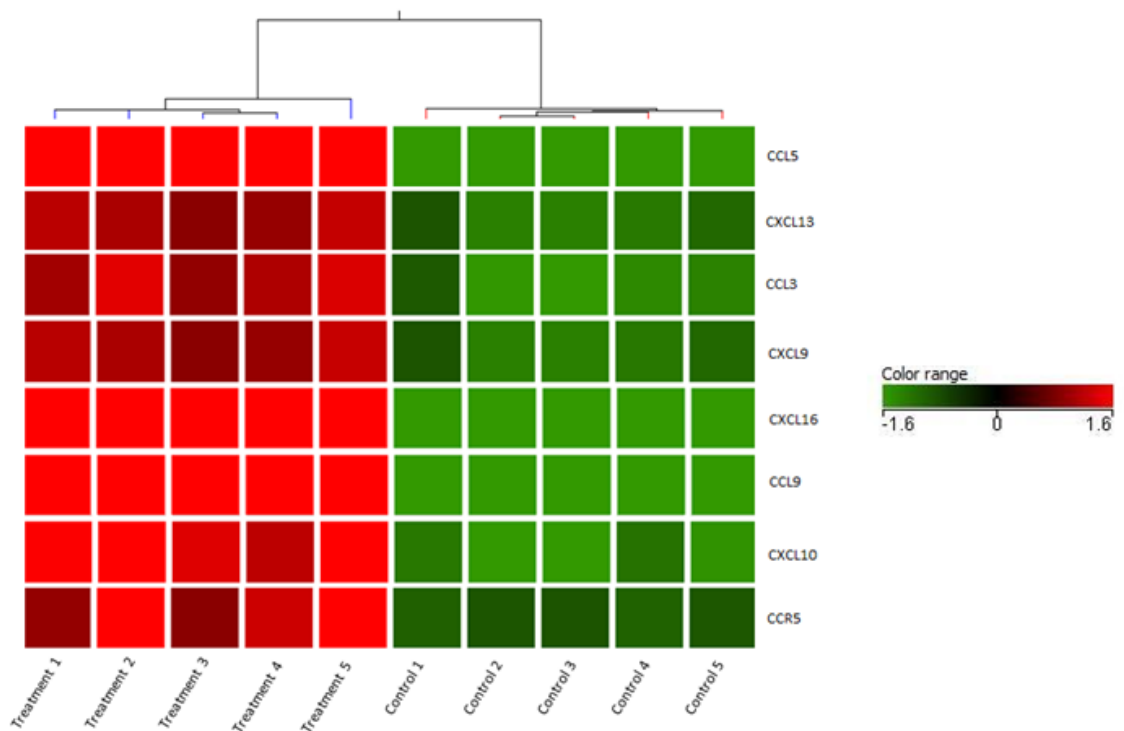
Figure 5-1 Heatmap of differentially expressed chemokines identified by microarray analysis
Microarray analysis was performed using RNA from brains of Aldara treated and control mice. Following statistical analysis, differentially expressed chemokine genes were identified. A heatmap was generated using GeneSpring GX software to depict the 7 differentially expressed chemokines and 1 chemokine receptor in Aldara treated and control brains. The five treatment samples are shown in red and the five control samples in green.

Table 5-1 A list of the chemokine genes that were upregulated in the Aldara model

Symbol	Gene name	Fold change	p-value
CCL5	chemokine (C-C motif) ligand 5	25.65	1.17E-09
CXCL13	chemokine (C-X-C motif) ligand 13	21.38	1.53E-09
CCL3	chemokine (C-C motif) ligand 3	18.67	4.10E-10
CXCL9	chemokine (C-X-C motif) ligand 9	6.40	1.57E-06
CXCL16	chemokine (C-X-C motif) ligand 16	5.46	1.30E-07
CCL9	chemokine (C-C motif) ligand 9	4.52	2.91E-07
CXCL10	chemokine (C-X-C motif) ligand 10	4.25	1.27E-04
CCR5	chemokine (C-C motif) receptor 5	3.74	4.31E-08

5.2.1 QPCR verification of the chemokine signature in the brain and PBL in response to Aldara treatment

To verify the expression of the 8 target chemokine genes following Aldara treatment, SYBR Green QPCR analysis was performed using RNA from brains and PBL isolated 24 hours after the final Aldara treatment. If a chemokine response was identified in the PBL, it may be that the expression found in the brain was the result of a contaminating signal from the blood. Therefore, by using the PBL as a comparator, this part of the study would ensure that blood contamination was not a factor in the brain response. Although the microarray data demonstrated significant induction of the gene encoding CXCL9, this appeared to be below the detection limit of the QPCR assay and could not be validated in the PBL and the brain (data not shown). It was therefore excluded from further analysis. Expression of each gene was normalised to that of the housekeeping gene, *TBP*, and each treatment group was compared to the corresponding control group, which were normalised to a fold change value of 1. The fold change induction of each gene in the brain and PBL is shown in Figure 5-2.

The results of the QPCR confirmed that the 6 chemokines and 1 chemokine receptor were significantly induced in the brains of Aldara treated mice when compared with the control brains. The fold-change induction of the genes ranged from around 2-fold to 200-fold. Both *CCL5* and its receptor, *CCR5*, exhibited the highest inductions in the brain, upwards of 200-fold (Figure 5-2B + G).

With regards to the PBL, only one of the genes, *CCL9*, was significantly induced following Aldara treatment (Figure 5-2C). In addition, one of the genes, *CXCL16*, was significantly downregulated in the PBL of the treated group when compared with the control group (Figure 5-2F). The expression levels of the remaining 5 genes were consistent between the control and treated groups.

To determine whether or not the response in the brain was significantly greater than the response in the PBL, data were analysed using two-way ANOVA. With the exception of CCL9, the induction of all of the genes was higher in the brain than in the PBL, with the most significant difference being seen with expression of *CXCL10* and *CXCL16*.

Together, the results of the QPCR analysis confirmed the presence of a distinct chemokine response in the brain following Aldara treatment when compared with controls. Although this treatment led to the induction of CCL9 in the periphery, the overall chemokine response was not mimicked in the PBL.

Figure 5-2 QPCR analysis of chemokines in brains and PBL following Aldara treatment
Mice were treated with 80mg Aldara cream or control cream every 24hrs for 5 consecutive days. Mice were euthanised 24hrs after the final application. Cardiac puncture was performed to retrieve PBLs and perfused brains were extracted. RNA was isolated from both tissues. QPCR analysis of the target chemokine genes identified in the microarray was performed for both tissues (A-G). n= 5 mice per group. Significance was measured within each tissue using individual students t test or between the tissues using two-way ANOVA with Bonferroni multiple comparison post-tests *** (+++) = p ≤ 0.001 **(++) = p ≤ 0.01 *(+) = p ≤ 0.05

5.3 QPCR analysis of the chemokine signature in the brain and PBL in response to TPA treatment

Having confirmed the induction of chemokine genes in the brain following Aldara treatment, the same genes were assessed following TPA treatment, to again establish whether or not TLR ligation was a prerequisite for this response. To determine the expression of the 7 chemokine genes following TPA treatment, SYBR Green QPCR analysis was performed using RNA from brains, and PBL, isolated 24 hours after the fifth and final treatment. Each gene was normalised to the housekeeping gene, *TBP*, and each treatment group was compared to the corresponding control group, which were normalised to a fold change value of 1. The fold change induction of each gene in the brain and PBL is shown in Figure 5-3.

The results of the QPCR showed that none of the chemokine genes were significantly induced in the brains of TPA-treated mice when compared with control mice. Some of the genes showed a slight downwards trend in the treated brains, including *CCL3*, *CCL5* and *CXCL10*, however none of these reached significance.

With regards to the PBL, again none of the chemokine genes was significantly induced in the treated mice when compared with the control mice. The cycle threshold values for many of the samples were high (data not shown) which is perhaps why there was such a high degree of variability within the groups, indicated by the size of the error bars. *CXCL16* expression in the PBL of both control and TPA treated mice was below the level of detection (Figure 5-3F).

Two-way ANOVA was used to compare the brain and the PBL to establish whether the responses were significantly different. *CCL9* was the only gene to reach significance, whereby the induction in the PBL following TPA treatment was significantly greater than the induction in the brain (Figure 5-3C). None of the other genes was significantly differentially expressed between the brain and the PBL.

Together, the results of the QPCR analysis showed that topical TPA treatment failed to induce a similar chemokine response in the brain, or in the PBL, to that

seen with Aldara. These results are consistent with the ISG expression in the brain, reported in Chapter 4, despite TPA application inducing a similar inflammatory skin phenotype. These results highlight the differential response between mice treated with an "infective" model versus a "sterile" model and strengthen the hypothesis that the brain response following Aldara treatment is TLR driven.
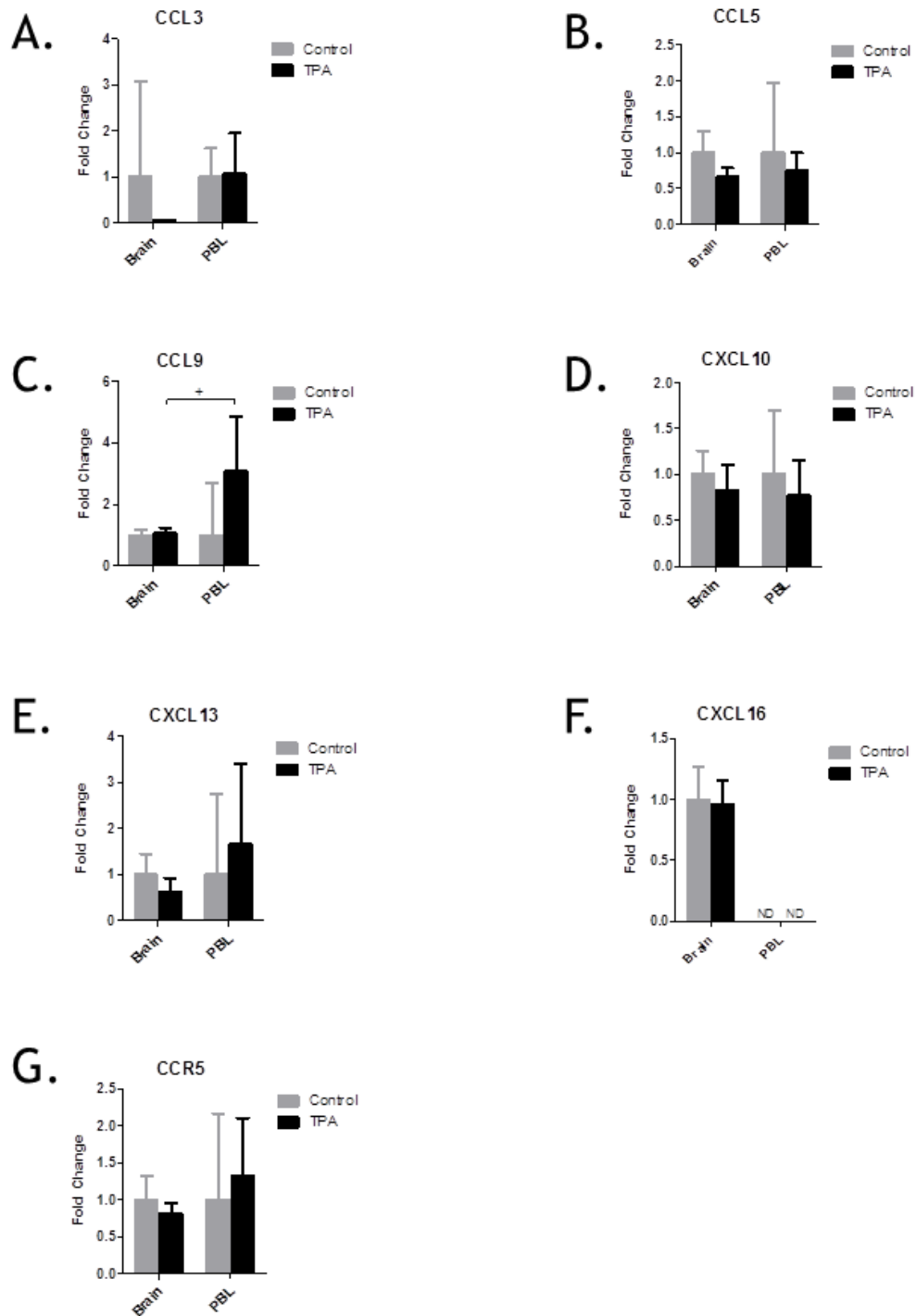
Figure 5-3 QPCR analysis of chemokines in brains and PBL following TPA treatment
Mice were treated with 150µl 100µM TPA, or equivalent volume of acetone, every 24hrs for 5 consecutive days. Mice were euthanised 24hrs after the final application. Cardiac puncture was performed to retrieve PBLs and perfused brains were extracted. RNA was isolated from both tissues. QPCR analysis of the target chemokine genes identified in the microarray was performed for both tissues (A-G). n= 5 mice per group. Significance was measured within each tissue using individual students t test or between the tissues using two-way ANOVA with Bonferroni multiple comparison post-tests *** (+++) = p ≤ 0.001 **(++) = p ≤ 0.01 *(+) = p ≤ 0.05

5.4 QPCR analysis of the chemokine signature in the brain and PBL during the Aldara time-course

The previous two sections confirmed the presence of a chemokine response in the brain following topical Aldara and established that such a response was not generated following TPA application. This differential pattern of expression between the two models mirrors the pattern of the ISG response that was reported in Chapter 4. It was also established that, rather than the day 5 time-point studied initially, the peak of the ISG response in the brain appeared to be day 3. Therefore, to determine whether or not the expression of the 7 chemokine genes followed the same temporal pattern as the ISGs, SYBR Green QPCR analysis was performed using RNA from brains and PBL isolated 24 hours after 1, 3 and 5 applications of Aldara. Each gene was normalised to the housekeeping gene, *TBP*, and each treatment group was compared to the corresponding control group, which were normalised to a fold change value of 1. The fold change induction of each gene in the brain and PBL is shown in Figure 5-4.

The results of the QPCR suggested that the chemokine response shared the same temporal pattern in the brain as the ISGs, as the peak of the response appeared to be at day 3. All 6 chemokines and 1 chemokine receptor analysed were significantly induced in the brains of Aldara treated mice at day 3 when compared with control mice. *CCL3*, *CCL5* and *CXCL10* (Figure 5-4A, B + D) showed striking upregulations, with around 1000-fold inductions in the brain at this time-point. None of the chemokine genes was significantly induced at day 1 and by day 5, 5 out of the 7 genes remained significantly induced in the brain. The induction of *CCL5* at day 5 was still very high, at around 800-fold, whereas all other genes were 100-fold or less.

With regards to the PBL, the response at all time-points remained below a 20-fold induction. *CCL3* was the only gene to be significantly induced in the PBL at all three time-points, with a consistent 3-4-fold upregulation (Figure 5-4A). Both *CXCL10* and *CCR5* were significantly induced at day 1 when compared with the PBL from control mice. At day 3, *CCL5* and *CCR5* were significantly induced in the treated group. With the exception of *CCL3*, none of the chemokine genes were significantly induced at day 5.

Statistical comparisons were performed to determine whether the induction in the brain was significantly different to the induction in the PBL in Aldara-treated mice. At day 3, the induction in the brain was significantly greater than the induction in the PBL for all 7 chemokine genes. With the exception of *CCL3* and *CXCL10*, this remained true for all genes at day 5. None of the genes was significantly induced in the brain at day 1 when compared with the induction in the PBL; however one gene, *CCR5*, was induced in the PBL to a significantly greater extent at day 1 than it was in the brain. This was the only gene to be more strongly induced in the PBL than the brain at any of the time-points analysed.

The results suggested that, like the ISG response detailed in Chapter 4, the chemokine response in the brain following Aldara treatment appeared to peak at day 3. This response, which was particularly strong with respect to CCL3, CCL5 and CXCL10 at day 3, persisted in the brain at day 5, in accordance with the results shown in Section 5.2.1. Aldara treatment did appear to induce a chemokine response in the PBL but, with the exception of CCR5, the chemokine response was significantly higher in the brain than it was in the PBL. These data highlighted how the response in the brain and PBL differed, both in kinetics and magnitude, and suggested that the brain response was independent of the PBL response.
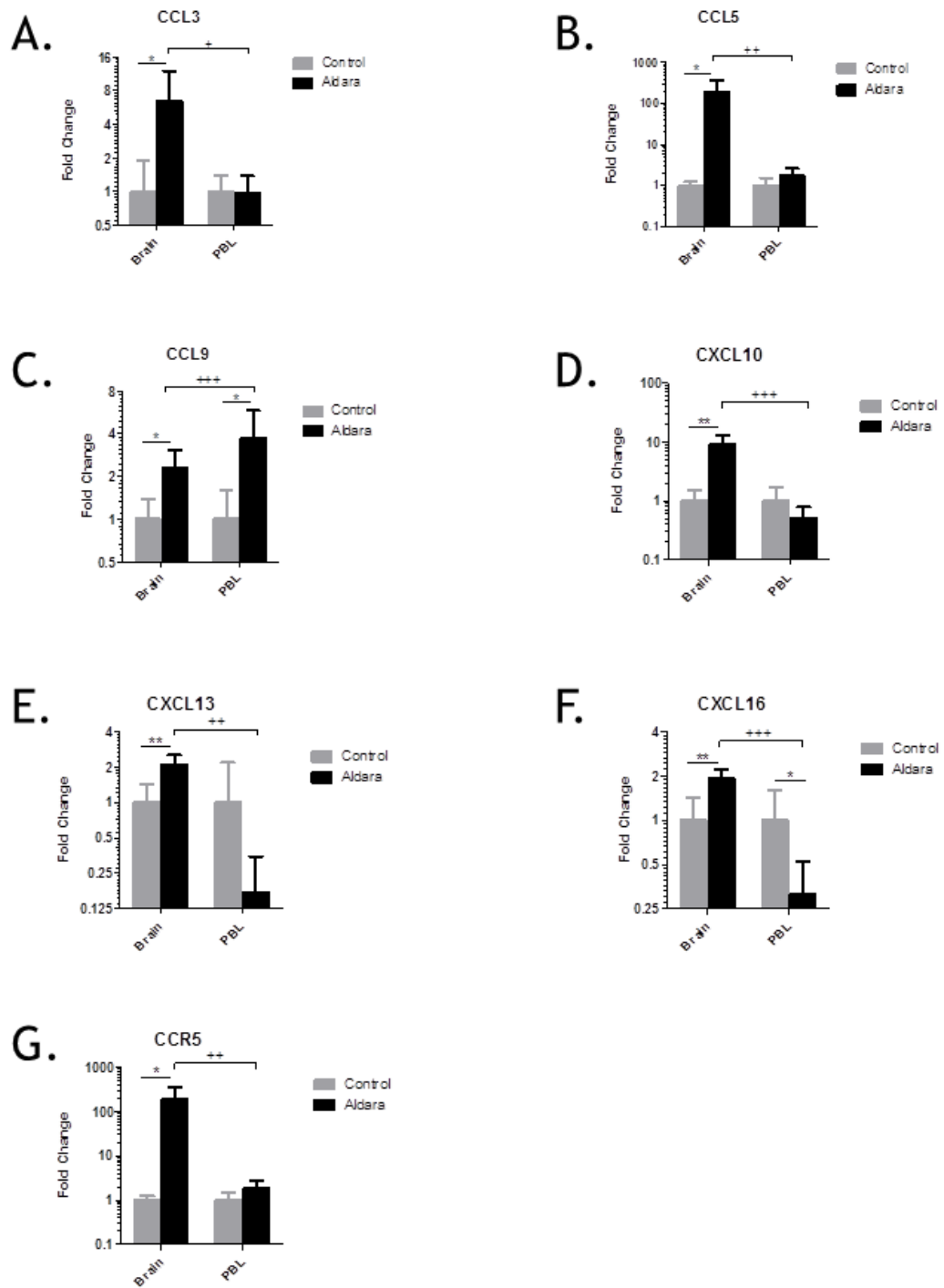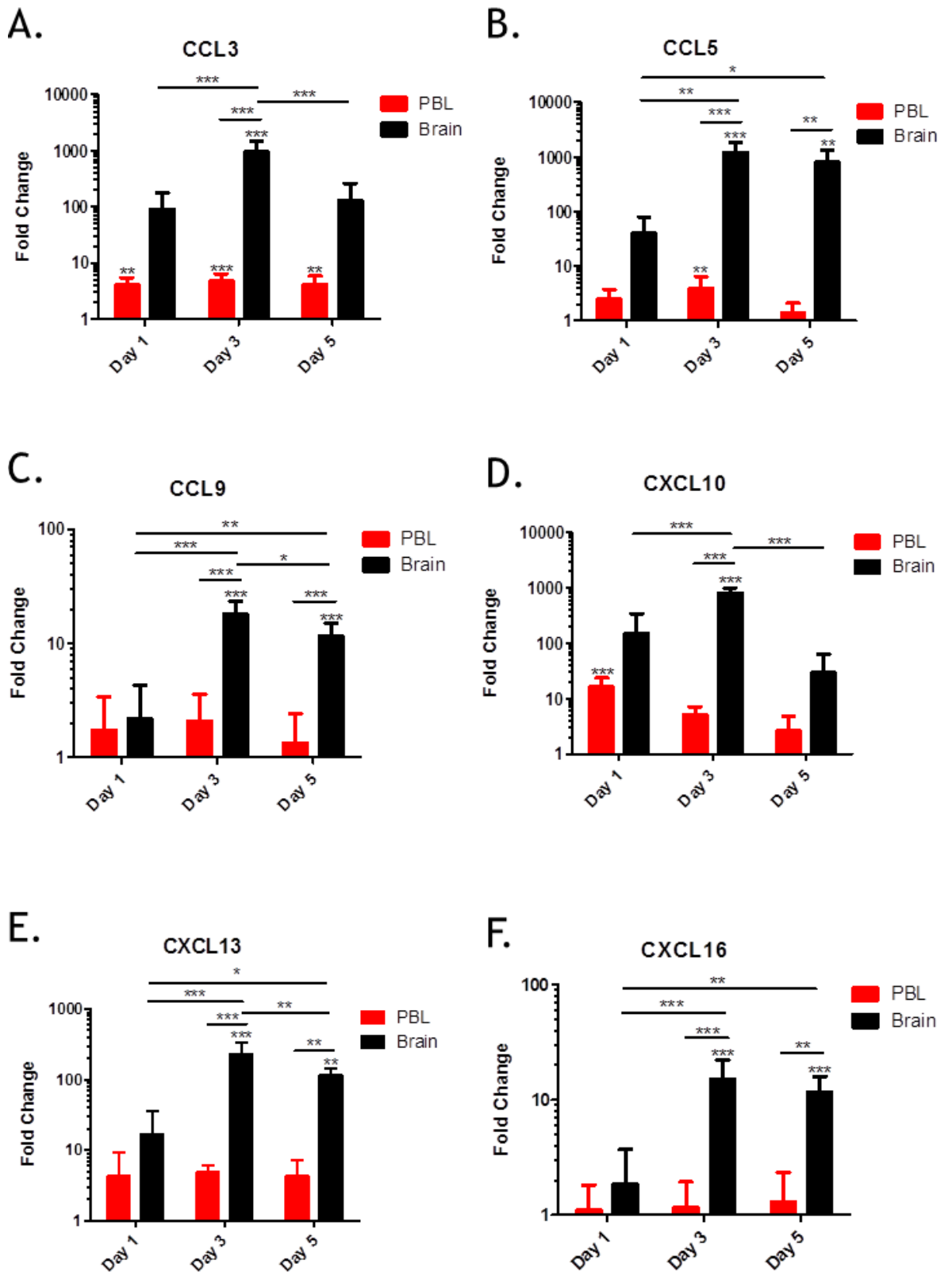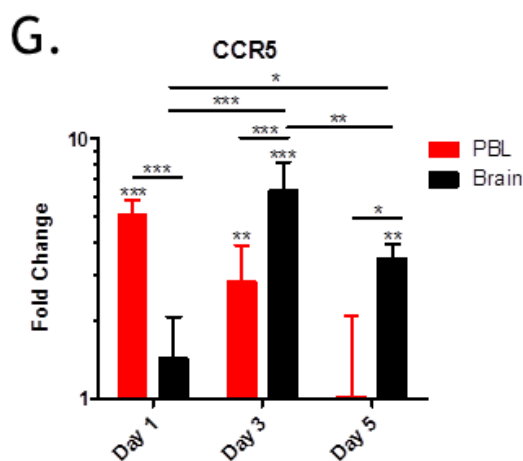
Figure 5-4 QPCR analysis of chemokines in brains and PBL following Aldara treatment
Mice were treated with 80mg Aldara cream or control cream every 24hrs for 1, 3 or 5 days. Mice were euthanised 24hrs after the final application. Cardiac puncture was performed to retrieve PBLs and perfused brains were extracted. RNA was isolated from both tissues. QPCR analysis of the target chemokine genes identified in the microarray was performed for both tissues (A-G). n= 4 mice per group. Significance was calculated for individual tissues (control vs treated), between tissues (treated only, PBL vs brain) and between time-points (treated only, d1 vs d3 vs d5) using two-way ANOVA with Bonferroni multiple comparison post-test. *** $p \leq 0.001$. ** $p \leq 0.01$, * $p \leq 0.05$

5.5 QPCR analysis of the chemokine signature in the brain and PBL during the TPA time-course

It has been demonstrated in this Chapter that peripheral Aldara treatment leads to a distinct transcriptional chemokine response in the brain, which peaks following the third application. This response does not appear to be induced following TPA treatment; however the earlier time-points were not investigated. Therefore, to determine whether or not any of the 7 chemokine genes could be found in the brain or PBL at an earlier time, SYBR Green QPCR analysis was performed using RNA from brains and PBL isolated 24 hours after 1, 3 and 5 applications of TPA or acetone. Each gene was normalised to the housekeeping gene, *TBP*, and each treatment group was compared to the corresponding control group, which were normalised to a fold change value of 1. The fold change induction of each gene in the brain and PBL is shown in Figure 5-5.

With regards to the brain, none of the chemokine genes was significantly induced in the TPA treated mice compared with the control mice at any of the time-points. Several of the genes showed a slight downregulation in the brain; however none of the reductions reached significance.

The same was true of the PBL analysis, where the QPCR results confirmed that none of the genes was significantly induced in the treated group when compared with the control group. Many of the apparent downwards trends in expression coincided with a high degree of error, suggesting that the expression levels were close to the minimum detection levels of the assay.

As none of the genes was significantly differentially expressed between the control and treated groups of each tissue, there was no significant difference between the treated groups of the brain and PBL. The expression levels were quite consistent 'across the board', both control versus treated and brain versus PBL.

These results confirmed that topical TPA application failed to induce a transcriptional chemokine response in the brain or PBL 1, 3 or 5 days following treatment. In addition, this experiment showed that the chemokine response appeared to be similar in kinetics to the ISG response identified in Chapter 4.
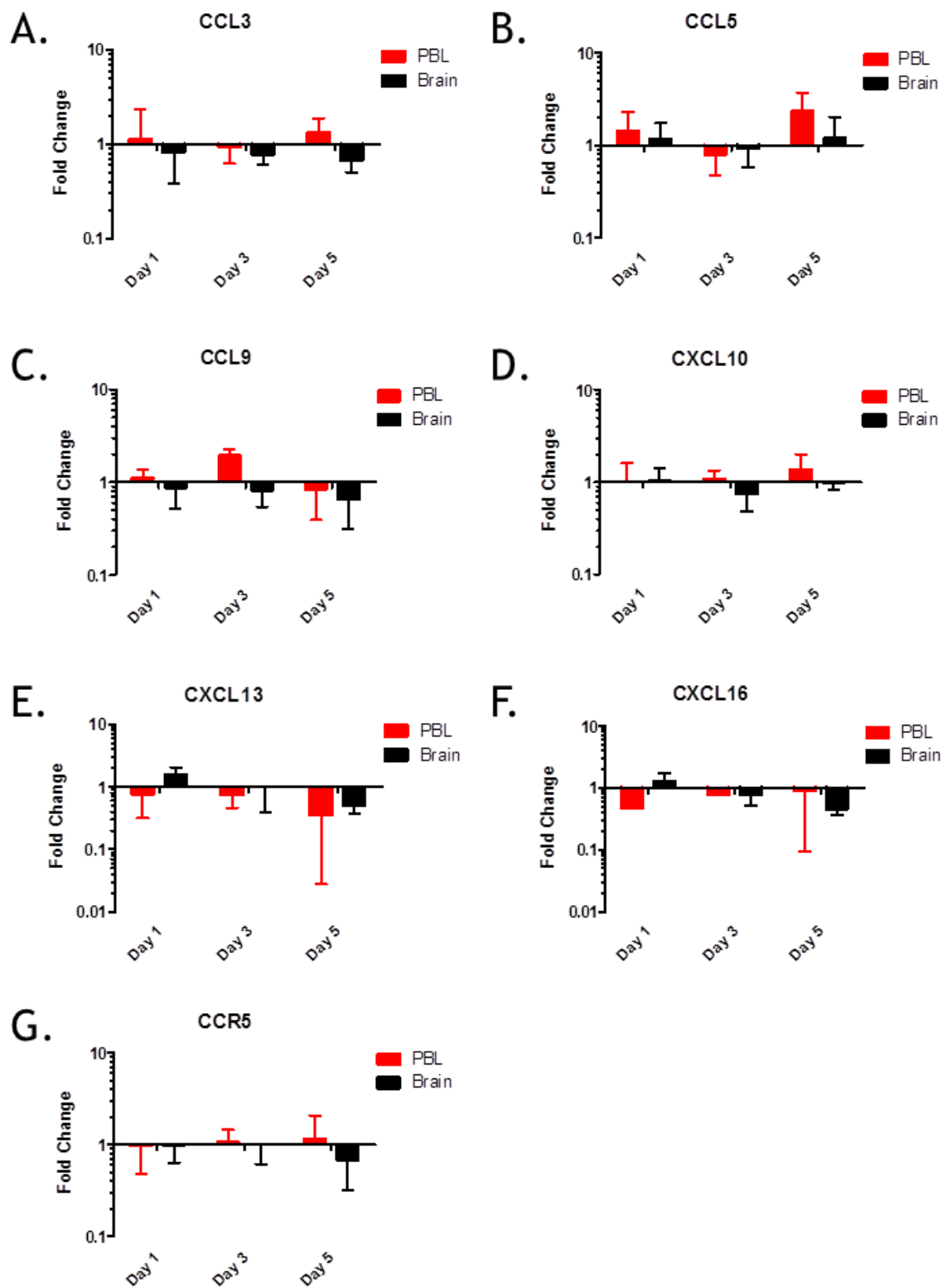
Figure 5-5 QPCR analysis of chemokines in brains and PBL following TPA treatment
Mice were treated with 150µl 100µM TPA, or equivalent volume of acetone, every 24hrs for 1, 3 or 5 days. Mice were euthanised 24hrs after the final application. Cardiac puncture was performed to retrieve PBLs and perfused brains were extracted. RNA was isolated from both tissues. QPCR analysis of the target chemokine genes identified in the microarray was performed for both tissues (A-G). n= 4 mice per group. Significance was calculated for individual tissues (control vs treated) and between tissues (treated only, PBL vs brain) using two-way ANOVA with Bonferroni multiple comparison post-test.

5.6 QPCR analysis of the chemokine signature in the brain and PBL following intraperitoneal IMQ treatment

To determine the importance of a localised skin response in the generation of a transcriptional chemokine response in the brain, the 7 chemokine genes were evaluated following the intraperitoneal injection of IMQ. SYBR Green QPCR analysis was performed using RNA from brains and PBL isolated 24 hours after the fifth administration of I.P. IMQ or saline. Each gene was normalised to the housekeeping gene, *TBP*, and each treatment group was compared to the corresponding control group, which were normalised to a fold change value of 1. The fold change induction of each gene in the brain and PBL is shown in Figure 5-6.

With regards to the brain, only two of the chemokine genes, *CCL5* and *CCR5* (Figure 5-6B + G, respectively), were significantly induced in the brains of IMQ-injected mice compared with the brains of saline-injected mice. The expression of many of the genes in the brain, particularly *CXCL10*, *CXCL13* and *CXCL16*, was highly variable, as shown by the large error bars, perhaps indicating that the expression of the genes was very low.

Only one gene was significantly induced in the PBL of the treated group when compared with the control group. *CCL5* was upregulated 3-fold in the PBL of the treated mice, an almost identical fold-induction to that of the brain (Figure 5-6B). Again, many of the chemokine genes had a high degree of error, suggesting that the expression levels were close to the minimum detection levels of the assay.

CCL9 was the only gene found to be significantly differentially expressed between the brain and the PBL (Figure 5-6C). The results suggested that the fold-change induction of *CCL9* in the brain was greater than the induction in the PBL; however the induction of this gene failed to reach significance in the individual tissues.

These results indicated that I.P. administered IMQ was not able to induce a transcriptional chemokine response in the brain or PBL similar to that seen following topical IMQ administration.
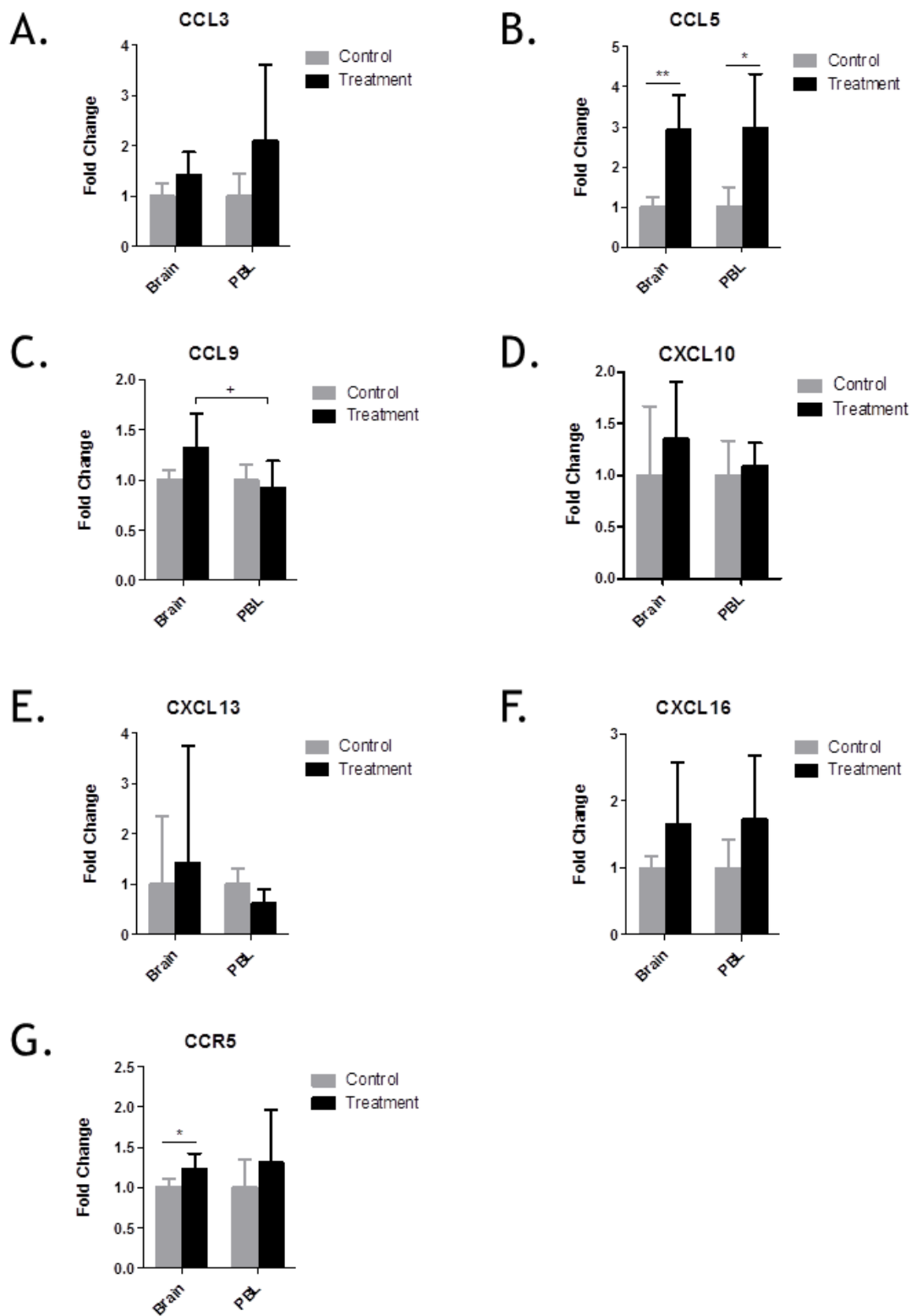
Figure 5-6 QPCR analysis of chemokines in brains and PBL following I.P IMQ injection
Mice were treated with 100µl 1mg/ml IMQ, or equivalent volume of saline, every 24hrs for 5 consecutive days. Mice were euthanised 24hrs after the final application. Cardiac puncture was performed to retrieve PBLs and perfused brains were extracted. RNA was isolated from both tissues. QPCR analysis of the target chemokine genes identified in the microarray was performed for both tissues (A-G). n= 5 mice per group. Significance was measured within each tissue using individual students t test or between the tissues using two-way ANOVA with Bonferroni multiple comparison post-tests *** (+++) = p ≤ 0.001 **(++) = p ≤ 0.01 *(+) = p ≤ 0.05

5.7 QPCR analysis of the chemokine signature in the brain and PBL following topical IMQ treatment

Results from Chapter 4 showed that I.P administration of IMQ failed to induce an ISG response in the brain. In agreement, section 5.6 of this chapter showed that this model also failed to induce the upregulation of the target chemokine genes. This could be due to the lack of isostearic acid; however topically applied IMQ did induce an ISG response in the brain (shown in Chapter 4); indicating that the more likely reason for the lack of a brain response was due to the route of administration. To determine whether IMQ alone could induce a chemokine response if it was applied topically, SYBR Green QPCR was performed on RNA from the brain and PBL of mice treated with topical IMQ in aqueous cream.

The results of the brain analysis showed that all seven of the chemokine genes were significantly induced in the brains of IMQ-treated mice compared with control mice. The induction of three of the genes, *CCL3*, *CCL5* and *CCR5*, was extremely high in the brain with increases of around 10,000-fold (Figure 5-7A, B + G).

In stark contrast, none of the genes was significantly induced in the PBL of the IMQ-treated mice. Interestingly, four of the seven genes, *CCL5*, *CCL9*, *CXCL10* and *CXCL16*, were significantly downregulated in the PBL, highlighting the difference between the response in the brain and the response in the periphery.

This difference was emphasised following statistical analysis of the brain response compared with the PBL response. Results showed that the fold-change induction in the brain was significantly greater than the induction in the PBL for all seven chemokine genes analysed.

Together, the results showed that topically applied IMQ induced a significant chemokine response in the brain that was not mimicked in the PBL. Along with ISG data from Chapter 4, the results indicated that this model was the most potent at inducing a transcriptional brain response out of all the models studied in this thesis.
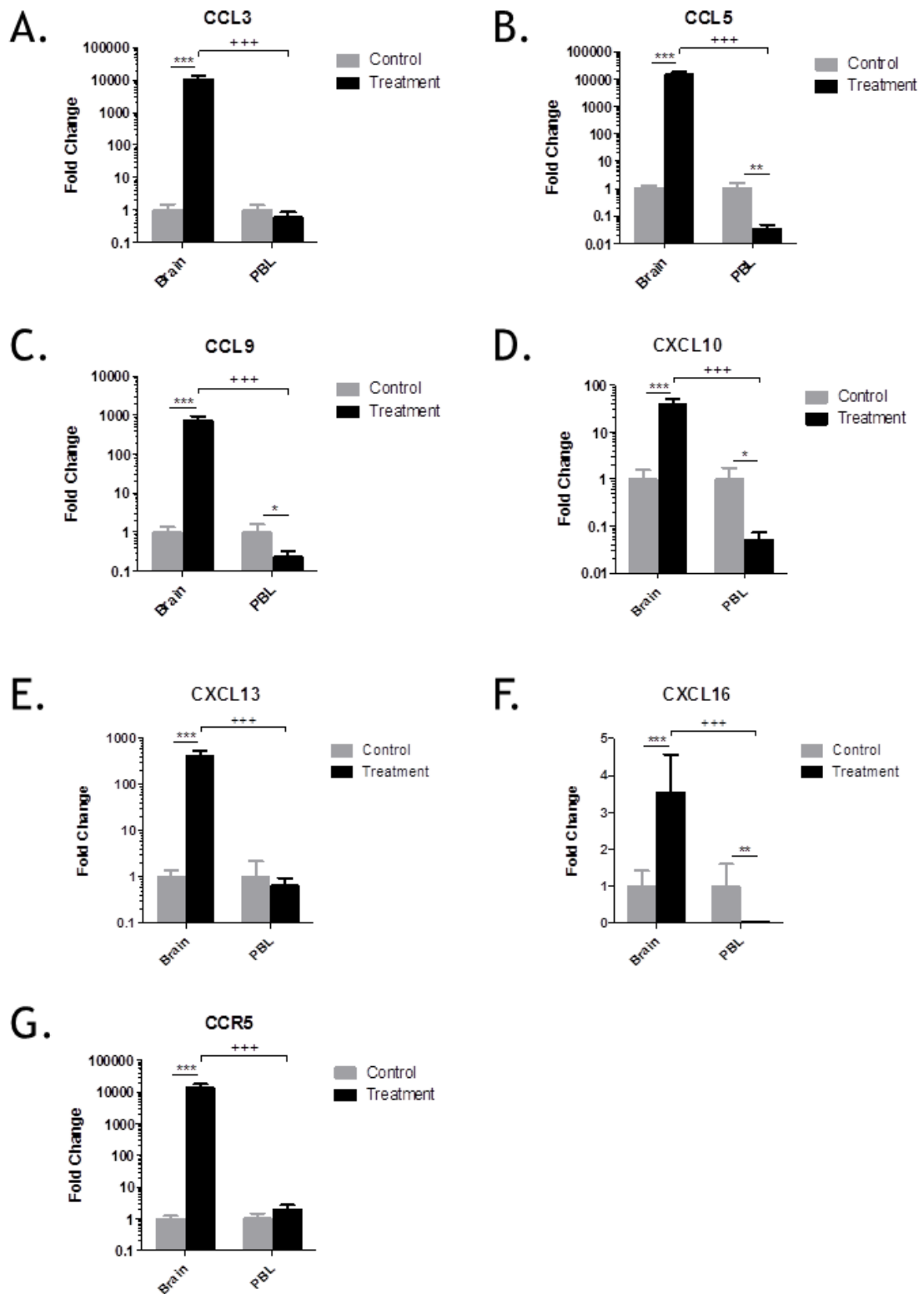
Figure 5-7 QPCR analysis of chemokines in brains and PBL following topical IMQ
Mice were treated with 80mg IMQ (5%v:v), or equivalent quantity of control cream, every 24hrs for 5 consecutive days. Mice were euthanised 24hrs after the final application. Cardiac puncture was performed to retrieve PBLs and perfused brains were extracted. RNA was isolated from both tissues. QPCR analysis of the target chemokine genes identified in the microarray was performed for both tissues (A-G). n= 5 mice per group. Significance was measured within each tissue using individual students t test or between the tissues using two-way ANOVA with Bonferroni multiple comparison post-tests *** (+++) = p ≤ 0.001 **(++) = p ≤ 0.01 *(+) = p ≤ 0.05

5.8 CD3 T cell infiltration into the brain following Aldara treatment

A fundamental function of chemokines is to mediate immune cell migration[404]. Chemokine expression in the brain has been shown to induce the influx of inflammatory cells including monocytes and T cells[229, 233, 234]. Following Aldara treatment, we have shown that several inflammatory chemokines have been significantly upregulated in the brain. Thus we next sought to investigate whether or not Aldara treatment led to immune cell infiltration into the brain. Several of the chemokines induced in the brain following treatment are ligands for chemokine receptors expressed by different subsets of CD3$^+$ T cells, therefore this was the cell type thought to be most likely recruited. To investigate this, mice were treated with Aldara cream or control cream every 24 hours for 1, 3 or 5 consecutive days. Perfused brains were extracted and formalin fixed before being sectioned and stained for CD3.

Representative images from control and Aldara-treated mice at the different time-points are shown for the cerebellum (Figure 5-8A) and hippocampus (Figure 5-8B). It was immediately clear that Aldara treatment induced the influx of CD3$^+$ cells after the third and fifth treatments. The positive cells were found throughout the brain parenchyma and did not appear to have any localised, region-specific anatomical distribution. Very few CD3$^+$ cells were seen in the control mice, as was expected. The number of CD3$^+$ cells in the brain was quantified by performing blind cell counts of whole brain sections. Three whole sagittal sections from the brain were counted for each mouse (Figure 5-8C). The cell counts confirmed that Aldara-treatment induced a significant influx of CD3$^+$ cells into the brain following the third and fifth applications, averaging around 300 cells on day 3 and 550 cells on day 5.

These data confirmed that topical Aldara treatment induced the influx of CD3$^+$ T cells into the brain parenchyma, which was likely due to the distinct chemokine response identified in the brain following treatment.
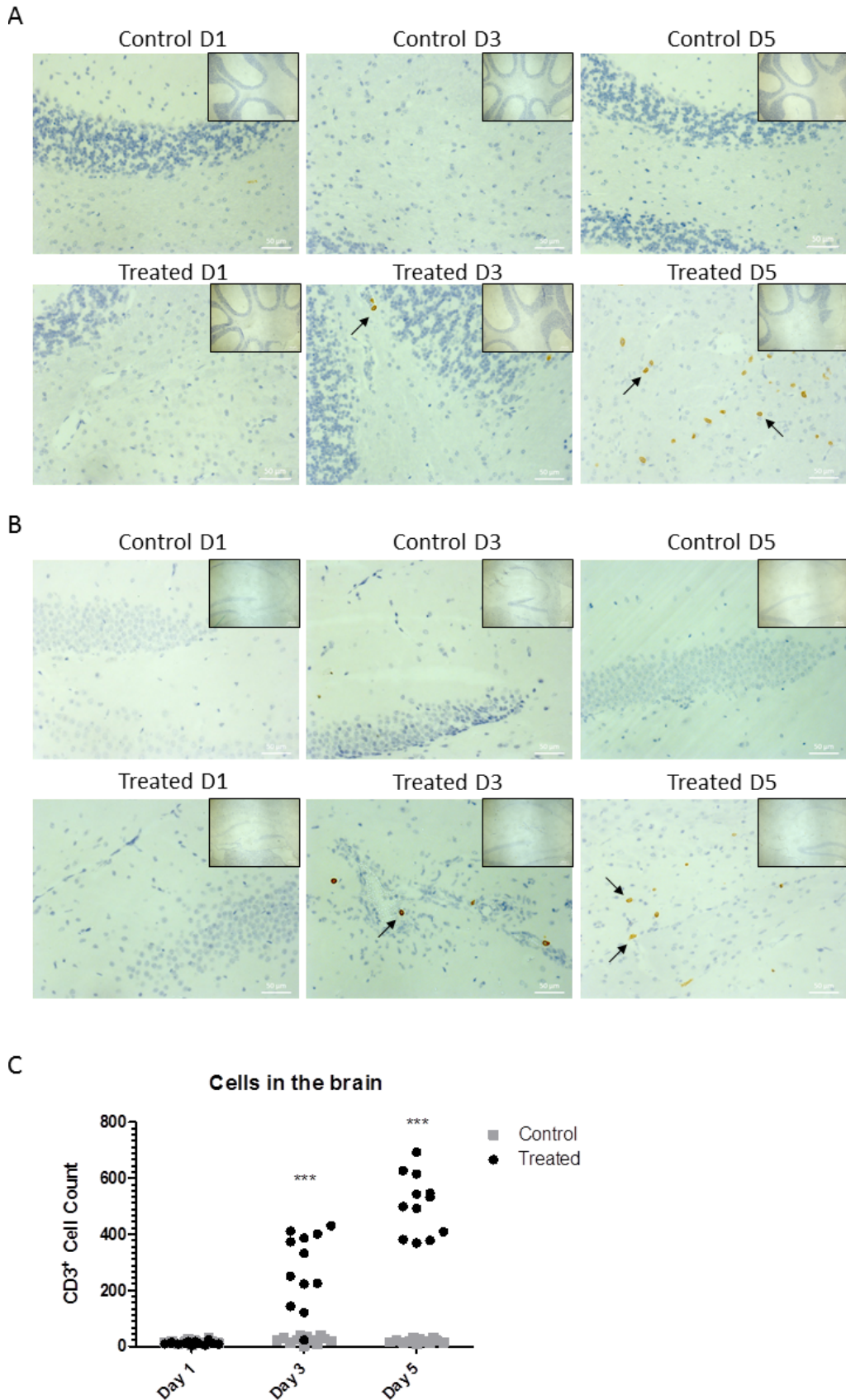
Figure 5-8 CD3$^+$ T cell infiltration into the brain following Aldara treatment
Mice were treated with 80mg Aldara cream or control cream every 24hrs for 5 consecutive days. Perfused brains were formalin fixed and embedded in wax. Brain sections were stained for CD3 and representative 200X magnified images from cerebellum (A) and hippocampus (B) are shown. Inserts on each image show respective field of view at 50X magnification. Cell counts were performed blind on 3 sections per brain (C). n=4 mice/group. Significance was measured using two-way ANOVA with Bonferroni multiple comparison post-tests *** = p ≤ 0.001

5.9 Assessment of burrowing behaviour with chemokine blockade

The results presented in this thesis have, so far, shown that topical Aldara treatment induced a chemokine response in the brain, the influx of immune cells into the brain parenchyma and a reduction in burrowing behaviour. Next, we wanted to determine whether blocking inflammatory chemokine responses would have an effect on burrowing behaviour to see if this functional output was being mediated by chemokine expression. If chemokines were mediating the behavioural changes, perhaps burrowing activity could be restored if responses to these chemokines were blocked.

Two different pharmaceutical agents were used to test this hypothesis, both of which have been used to investigate the role of chemokine receptors in viral encephalitis[405]. CCR5 blockade would inhibit the effects of CCL3, CCL4, CCL5 and CCL8, whereas CXCR3 blockade would inhibit CXCL9, CXCL10 and CXCL11 activity. Mice were treated with topical Aldara or control cream every 24 hours for 3 consecutive days. Aldara-treated mice were, in addition, treated with either CCR5 blocker, CXCR3 blocker or a CXCR3 mimic control. Burrowing behaviour was evaluated in each of the groups as previously described (Section 3.6).

The results showed that co-treatment with CCR5 blocker reduced burrowing behaviour in Aldara-treated mice (Figure 5-9A). By the second and third treatment days, mice burrowed very little. The withdrawal from burrowing behaviour appeared to be more rapidly induced than in Aldara-treated mice that did not receive the blocker, particularly at day 1; however the difference did not reach significance. As has been shown previously, the burrowing activity of control mice increased over the course of the treatment period. These data suggested that blocking the activity of CCR5, and its corresponding chemokine ligands, could not restore burrowing activity.

The same study was performed using a CXCR3 blocker (Compound 21). The results showed that mice treated with Aldara along with blocker experienced reduced burrowing activity (Figure 5-9B). However, the blocker itself had no effect on this response as the suppression of burrowing activity was in line with

that seen in Aldara-treated mice without blocker and in mice that received the CXCR3 mimic. These results again suggested that the activity of CXCR3, and its ligands, was not directly mediating the behavioural response to Aldara treatment.
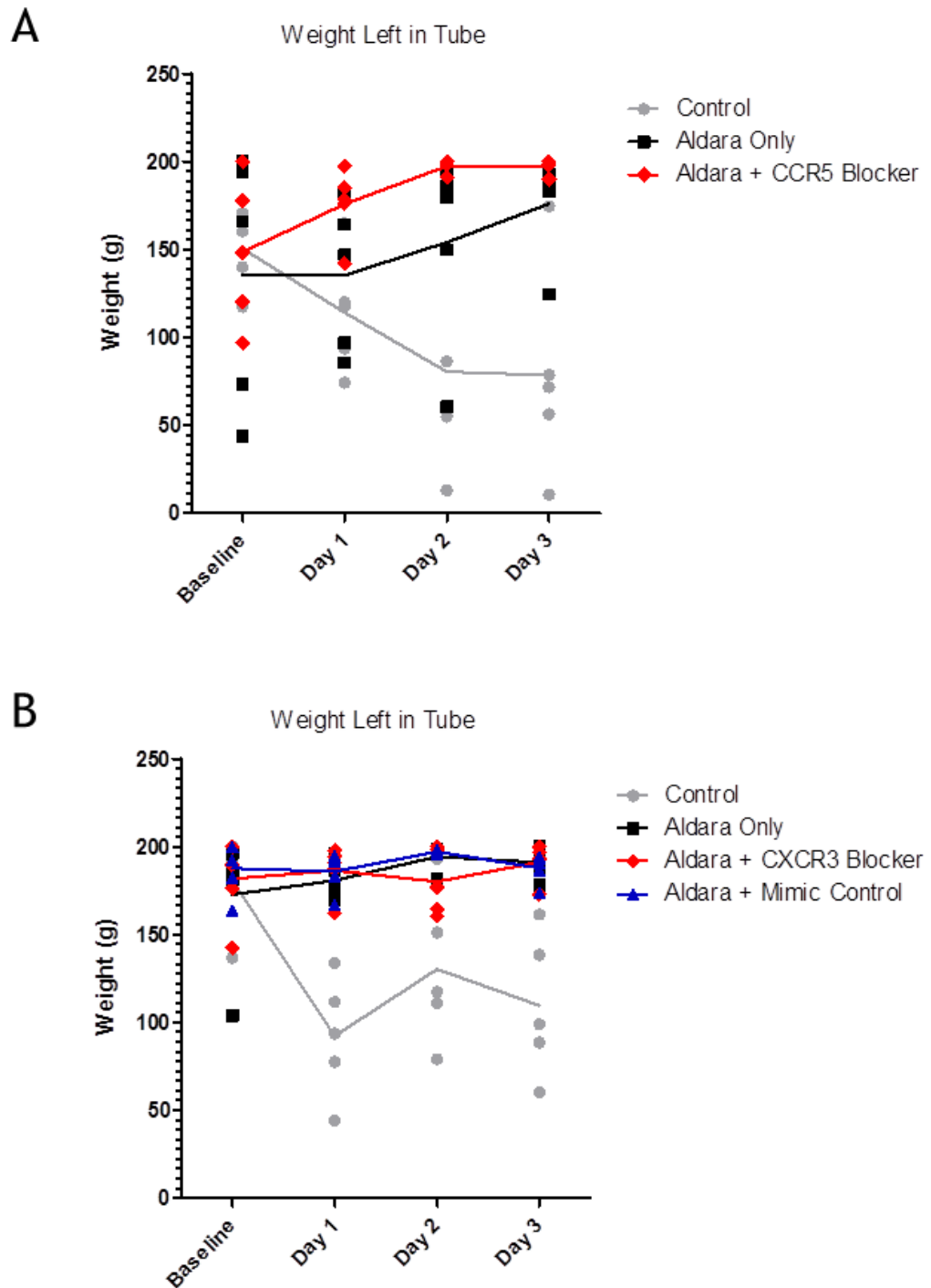
Figure 5-9 Burrowing activity of Aldara-treated mice with chemokine blockade
WT mice were treated with ~80mg Aldara cream, control cream or Aldara cream along with CCR5 blocker, CXCR3 blocker or mimic. Mice were assessed for burrowing activity on three consecutive days. Four hours following treatment application, mice were single caged with a burrowing tube containing 200g of food pellets for 2 hours. At the end of this time point, mice were caged again in groups and the remaining weight of food pellets in the tubes was recorded. The weight left in the tube following treatment with CCR5 blocker (A) and CXCR3 blocker (B) is shown. n=5 mice per group.

5.10 Discussion

The aim of this chapter was to investigate the chemokine response that was identified following microarray analysis and gene ontology clustering of brains from Aldara-treated mice. QPCR analysis was used to assess the chemokine response in the brain and PBL following Aldara treatment, TPA treatment, I.P. IMQ administration and topical IMQ treatment. In addition, immune cell infiltration into the brain parenchyma was assessed in Aldara-treated mice to determine whether or not peripheral cutaneous inflammation could induce the recruitment of cells. Finally, chemokine blockers were used in conjunction with the burrowing model to investigate whether inflammatory chemokines were driving the behavioural phenotype in response to cutaneous Aldara treatment.

The results of the QPCR analysis confirmed the presence of a distinct chemokine profile in the brain in response to Aldara treatment and topical IMQ treatment, but not in response to TPA or I.P. administered IMQ. This was in keeping with the ISG data shown in Chapter 4 and it would appear that ISG induction and chemokine induction were two aspects of a general brain response since they followed the same temporal pattern. Similar patterns of chemokine upregulation have been described in studies using LPS-induced immune stimulation. Both Erikson et al and Thomson et al report a specific chemokine response in the brain following peripheral inflammation which is not mimicked in the PBL[377, 406]. It is therefore possible that the transcriptional response we see in the brain may be the result of general TLR stimulation in the periphery.

Many of the inflammatory chemokines induced in the brain are involved in immune cell migration. Specifically, *CCL3, CCL5* and *CXCL10* are important in mediating CD4^{+} and CD8^{+} T cell migration, as these cells express the corresponding receptors, CCR5 and CXCR3. Several groups have shown that chemokine induction in the brain can induce immune cell infiltration, both under neuroinflammatory conditions[234, 244, 407-409] and in response to peripheral inflammation[230]. Here, we have shown that, consistent with the literature, peripheral immune stimulation led to the infiltration of CD3^{+} T cells into the brain parenchyma. To our knowledge, we are the first to show this following cutaneous inflammation. These infiltrating T cells were found throughout the brain parenchyma and did not appear to be restricted to any specific anatomical

region, or regions, of the brain. To confirm that this influx was the direct result of chemokine upregulation, the experiment would have to be repeated in the models that did not show a chemokine response in the brain or through the use of chemokine blockers. However, it is plausible to hypothesise that this response was a direct consequence of inflammatory chemokine expression in the brain.

We next sought to establish whether chemokine induction in the brain could be driving the behavioural phenotype described in Chapter 0. To investigate this, burrowing activity was assessed in Aldara-treated mice co-treated with chemokine blockers. Two different chemokine receptor antagonists were used in this experiment, a CCR5 blocker and a CXCR3 blocker. Neither was found to have an effect on the behavioural response to Aldara treatment as all groups, both with and without the administration of blocker, showed a similar suppression of burrowing activity. These blockers have been used previously to demonstrate the role of chemokines in viral encephalitis, with their administration leading to a reduction in immune cell infiltration into the brain[405]. It would therefore be useful to investigate whether the numbers of $CD3^+$ T cells in the brain is reduced following co-treatment with chemokine blockers. Nonetheless, the results from this experiment suggest that, although inflammatory chemokines may be important for initiating the response to Aldara treatment, modulating their function does not appear to affect the consequential phenotypes.

Although we can show that Aldara treatment caused a transcriptional chemokine response in the brain and T cell infiltration into the parenchyma, we have been unable to identify the exact mechanisms by which this response is generated. Further analysis would be required to try to better understand the relationship between the different aspects of this response.

In summary, the results in this Chapter have identified a distinct chemokine profile in the brain and have linked peripheral skin inflammation with immune cell infiltration into the brain and impaired burrowing activity that could not be rescued using chemokine blockers. This study has demonstrated that peripheral, tissue-specific skin inflammation can induce both a transcriptional and functional response in the brain and highlights the importance for further investigation into the role of inflammatory chemokines as potential mediators of ensuing CNS inflammation.

Chapter 6

ACKR2 in the brain

6 ACKR2 in the brain

6.1 Introduction

Data presented in Chapter 5 have shown that treatment with topical Aldara and topical IMQ induced a chemokine response in the brain. Amongst the chemokine genes induced, *CCL3* and *CCL5*, along with their receptor, *CCR5*, were the most highly upregulated in the brain following treatment. Both of these inflammatory chemokines bind to ACKR2, an atypical chemokine receptor which was described in detail in Chapter 1[115]. ACKR2 acts as a scavenger, binding to inflammatory CC chemokines and removing them from the microenvironment, and is therefore considered to have anti-inflammatory properties[114].

Interestingly, ACKR2 is expressed throughout the adult brain, as well as in specific structures including the dentate gyrus and the olfactory bulb (Figure 6-1). The distinct anatomical distribution of ACKR2 in the brain could suggest that the scavenging receptor is there to regulate inflammatory chemokine function. In addition, since these regions of expression are also sites of adult neurogenesis, ACKR2 may have a role to play in regulating the generation and maintenance of new neurons. Therefore, the aim of this Chapter was to investigate the regulatory role of ACKR2 in the brain response to cutaneous inflammation using ACKR2 KO mice. We hypothesised that the inflammatory response would be exacerbated in the absence of ACKR2.
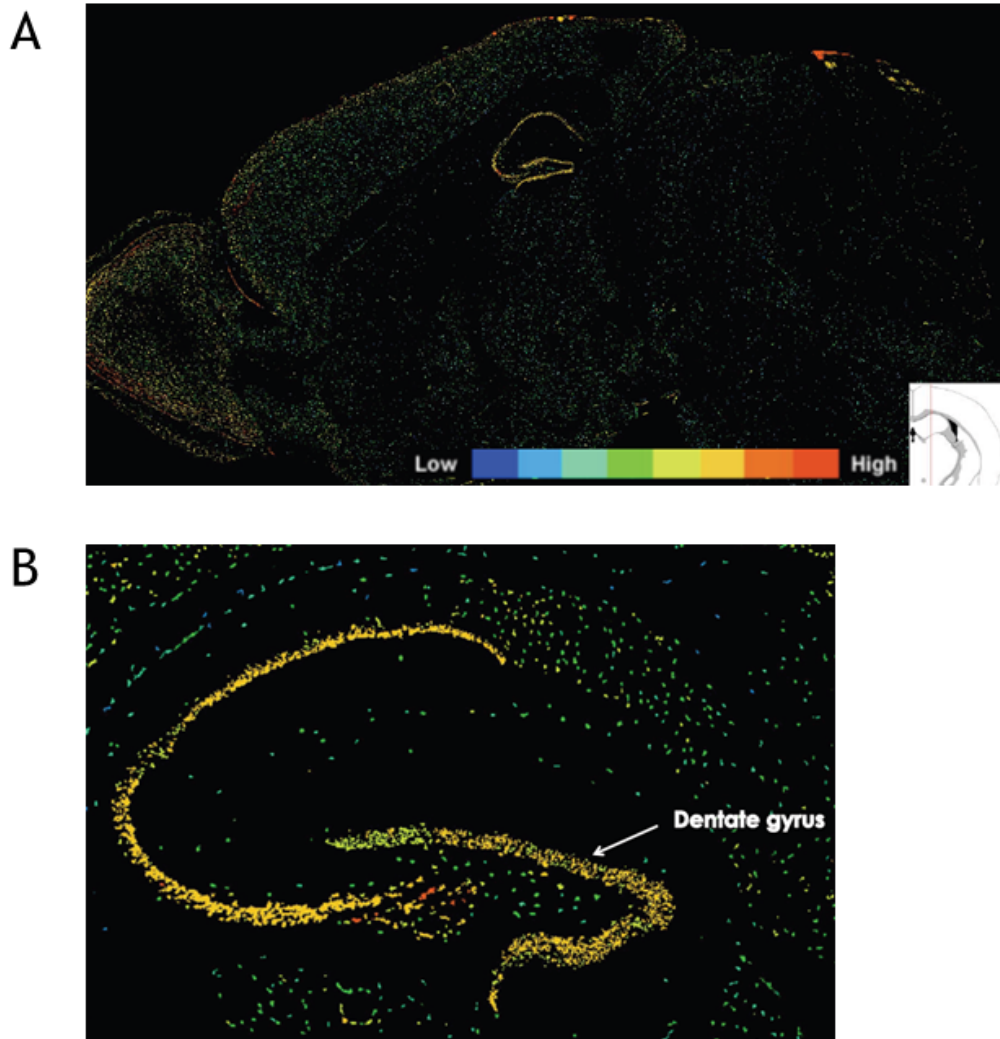
Figure 6-1 Expression of ACKR2 in the adult mouse brain
Images showing the anatomical distribution of ACKR2 in the mouse brain (A), highlighting the
concentrated expression in the dentate gyrus of the hippocampus (B). Images taken from the Allen
Brain Atlas http://www.brain-map.org/

6.2 Aldara model of skin inflammation in ACKR2 KO mice

The model was first validated, whereby mouse weights, spleen weights and
treated skin were evaluated in Aldara-treated wild-type mice and Aldara-treated
ACKR2 KO mice (Figure 6-2). The results showed that the weight loss was similar
between WT and ACKR2 KO mice for the first three treatment days; however
ACKR2 KO mice started to recover some weight between day 3 and day 4,
whereas WT mice continued to lose weight (A). ACKR2 KO mice were
significantly heavier than WT mice at day 5, suggesting that they recovered

more quickly than the WT mice. There was no significant difference between the spleen weights of WT and KO mice, although the WT spleens were more variable (B), and they were visually very similar in size (C). With regards to the treated skin, both WT and KO skin showed signs of inflammation with marked epidermal hyperplasia and hyperkeratosis (D). It should be noted that many hair follicles were seen in the skin, indicative of hair cycle, which can alter the response to inflammation, however the presence of hair follicles was consistent between the two strains of mice. As no overt differences between WT and KO mice were observed, these results suggested that ACKR2 was not integral to the regulation of the cutaneous response to Aldara treatment.
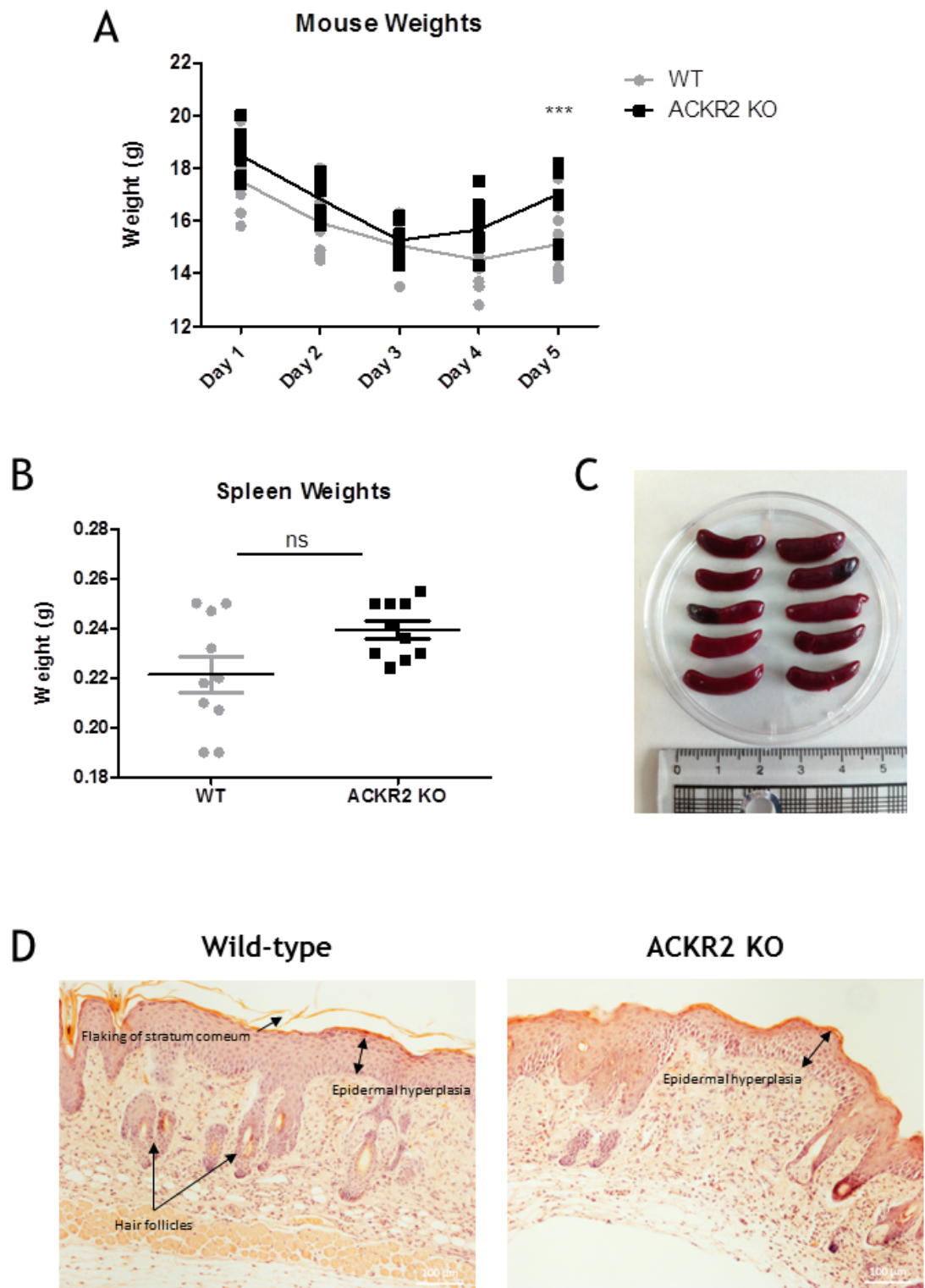
Figure 6-2 Evaluation of the response to Aldara treatment in WT and ACKR2 KO mice
WT mice and ACKR2 KO mice were treated with ~80mg Aldara cream every 24hrs for five consecutive days and were weighed following each application (A). In addition, spleens were removed and were weighed (B) and photographed (C). H&E staining was performed using 5µm thick sections of Aldara- or control- treated skin which were visualised at 200X magnification (D). (A & B) n = 10/ group from two independent experiments (C & D) n = 5/ group. Significance was measured using two-way ANOVA with Bonferroni multiple comparison post-tests *** = p ≤ 0.001.

6.2.1 QPCR analysis of the chemokine response to Aldara treatment in ACKR2 KO mice

Although ACKR2 did not appear to be regulating the response in terms of the phenotypes examined in Section 6.2, it may be regulating other aspects of the response. For example, immune cell infiltration into the skin is dependent on chemokines, which may be under the influence of ACKR2. Indeed, it has previously been shown that ACKR2 KO mice have an exacerbated skin response following TPA treatment[410, 411]. A heightened local response may result in an increased response in the brain, thus the panel of chemokine genes examined in Chapters 3 and 4 were evaluated in the brain and PBL of ACKR2 KO mice following topical Aldara treatment (Figure 6-3). ACKR2 should not directly influence chemokine transcript expression as it functions at the protein level; therefore the absence of ACKR2 should not, in theory, affect chemokine levels in the brain under steady state conditions. Any differences in chemokine expression would likely be a secondary effect as the result of a heightened inflammatory response.

The QPCR results showed that, with the exception of *CXCL10*, all of the chemokine genes were significantly induced in the brains of ACKR2 KO Aldara treated mice when compared with control ACKR2 KO mice. *CCL5* was the most highly induced, with an upregulation of around 100-fold (Figure 6-3B).

With regards to PBL, three of the genes, *CCL5*, *CCL9* and *CXCL13*, were significantly induced in the PBL of the treated mice. Interestingly, two of the genes, *CXCL10* and *CXCL16*, were significantly downregulated in the PBL of ACKR2 KO treated mice (Figure 6-3D + F).

When the two tissues were compared, the fold-change induction in the brain was significantly greater than that of the PBL for all seven genes analysed. Although *CXCL10* had not been significantly induced in the brain, it was significantly downregulated in the PBL, accounting for the differential expression between the two tissues.

These results suggested that topical Aldara treatment induced a chemokine response in the brains of ACKR2 KO mice, similar to that seen in WT mice.

Despite some of the genes being significantly induced in the PBL, this was to a lesser extent than in the brain. Although it has been reported that ACKR2 KO mice are more sensitive to inflammation in a number of models, and we would therefore expect to see a heightened response to Aldara treatment, if we look back to the results in Figure 5-2, the induction of chemokines in the brain appears to be somewhat comparable to that of the WT mice. This would suggest that the response to Aldara cream is not dependent on the actions of ACKR2, either as a modulator or an inducer.
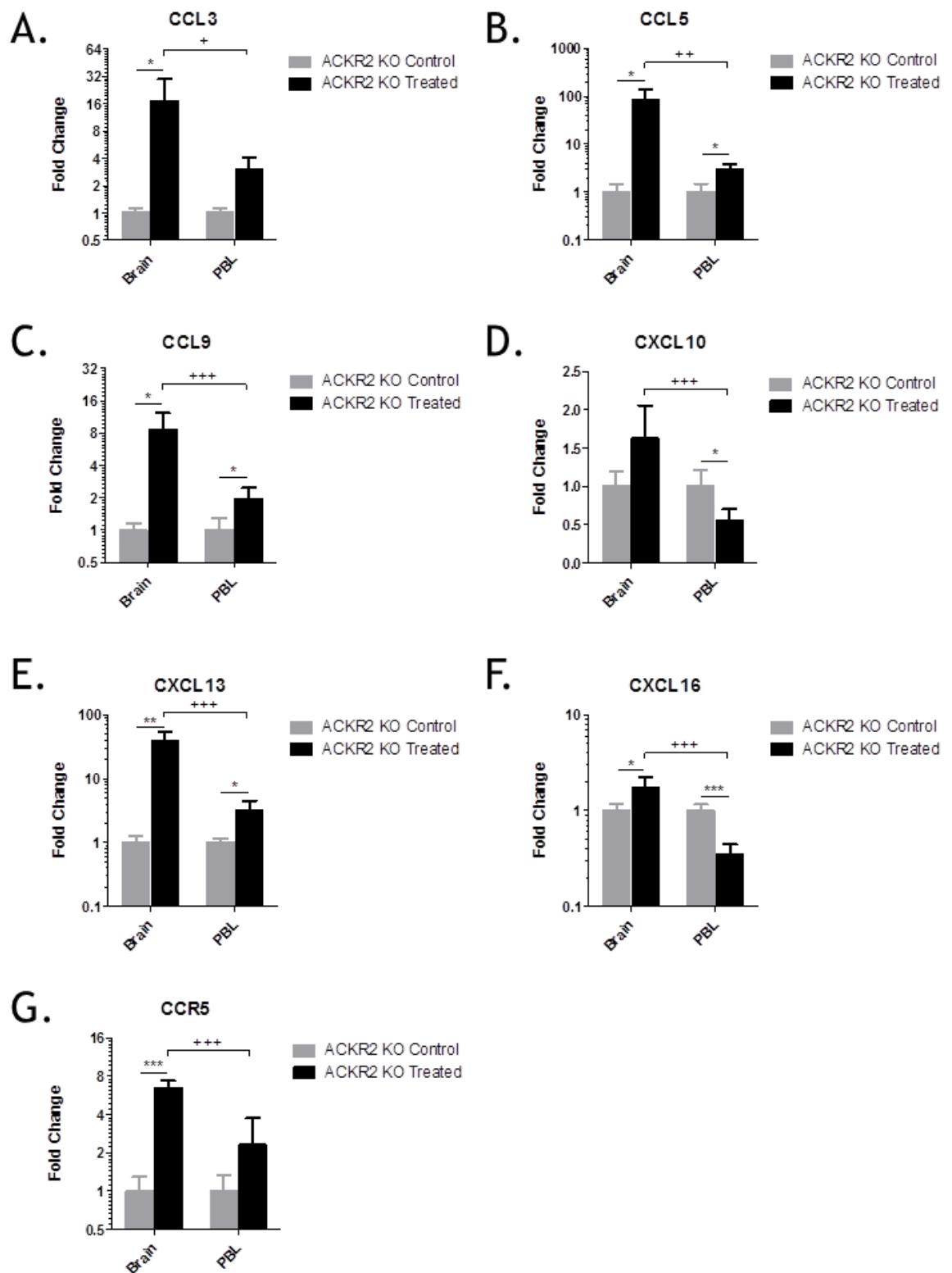
Figure 6-3 QPCR analysis of chemokines in brains and PBL of ACKR2 KO mice following Aldara treatment

ACKR2 KO mice were treated with 80mg Aldara cream, or equivalent quantity of control cream, every 24hrs for 5 consecutive days. Mice were euthanised 24hrs after the final application. Cardiac puncture was performed to retrieve PBLs and perfused brains were extracted. RNA was isolated from both tissues. QPCR analysis of the target chemokine genes identified in the microarray was performed for both tissues (A-G). n= 4 mice per group. Significance was measured within each tissue using individual students t test or between the tissues using two-way ANOVA with Bonferroni multiple comparison post-tests *** (+++) = p ≤ 0.001 **(++) = p ≤ 0.01 *(+) = p ≤ 0.05

6.2.2 The effect of Aldara treatment on neurogenesis in WT and ACKR2 KO mice

Neurogenesis continues throughout adult life at distinct anatomical locations within the brain, including the dentate gyrus and the olfactory bulb. It has been shown that this process is sensitive to inflammation, suggesting that disrupted neural generation and plasticity could be a mechanism by which immune stimulation can cause neurological phenotypes[412]. As shown in Figure 6-1, ACKR2 expression in the brain is centralised to the dentate gyrus and olfactory bulb; however its function in the CNS has yet to be identified. Such anatomical specificity highlighted the possibility that ACKR2 may function as a regulator of neurogenesis by minimising local inflammation. Therefore the aim of this section was two-fold. First, to investigate whether or not topical Aldara treatment impaired neurogenesis and, second, to determine the importance of ACKR2 in maintaining adult neurogenesis.

Doublecortin (DCX), which is expressed only by neural precursor cells, was assessed in the dentate gyrus of the hippocampus in WT and ACKR2 KO mice treated with topical Aldara or control cream. DAPI (blue) was used to stain the nuclei of the cells and FITC (green) was used to identify DCX-expressing cells. Figure 6-4A shows representative DCX staining of the dentate gyrus in WT control mice (I), WT Aldara-treated mice (II), ACKR2 KO control mice (III) and ACKR2 KO Aldara-treated mice (IV). A negative control and an isotype control were included to ensure the specificity of the staining and are shown in Figure 6-4B. It was immediately clear from the images that treated mice, both WT and ACKR2 KO, had reduced DCX staining, however quantification was required in order to determine whether the differences were significant.
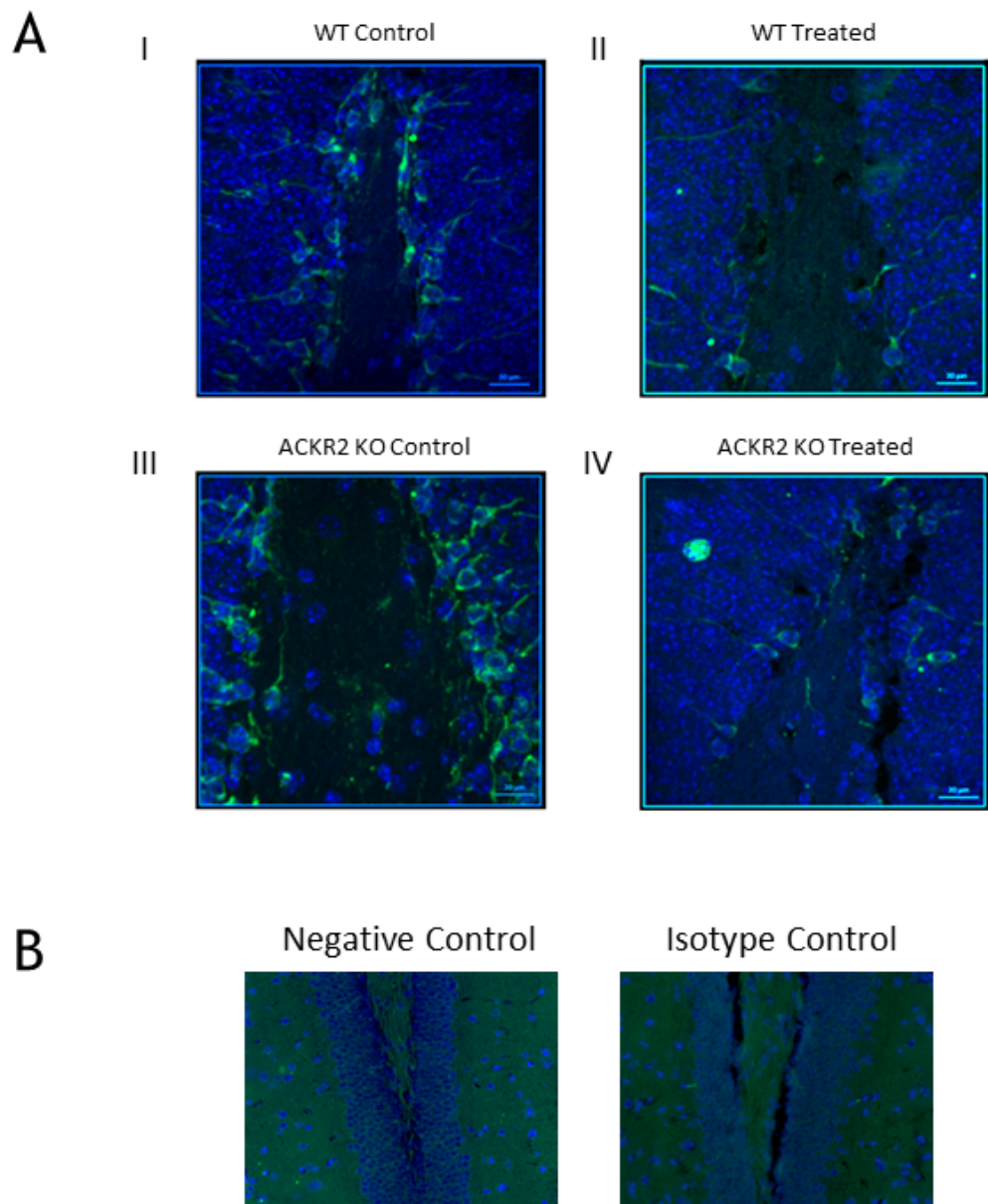
Figure 6-4 Doublecortin staining of the dentate gyrus
WT and ACKR2 KO mice were treated with ~80mg Aldara cream, or an equal volume of control cream, every 24 hours for 5 consecutive days. Perfused brains were extracted, formalin fixed and embedded in wax before being cut into 7µm sections. Sections were stained for DCX and were imaged at 400X magnification (A). Negative and isotype staining controls were included (B). n=4 mice per group.

6.2.2.2 Quantification of DCX staining

In order to quantify the DCX staining, slides were 'blinded' and a counting strategy was determined. As such, DCX$^+$ cells were counted in three areas of the dentate gyrus for each section, one from the top, one from the middle and one from the bottom, as indicated in Figure 6-5A. A mean of these three areas was then calculated. A minimum of 11 sections from at least 3 mice were counted for each group and the results are plotted in Figure 6-5B. The results showed that treatment with Aldara caused a significant reduction in the number of DCX$^+$ cells in both WT and ACKR2 KO mice. This indicated that peripheral immune stimulation with Aldara caused impaired neurogenesis in the dentate gyrus. However, there was no significant difference between the two mouse strains suggesting that ACKR2 is not a major regulator of this CNS process.
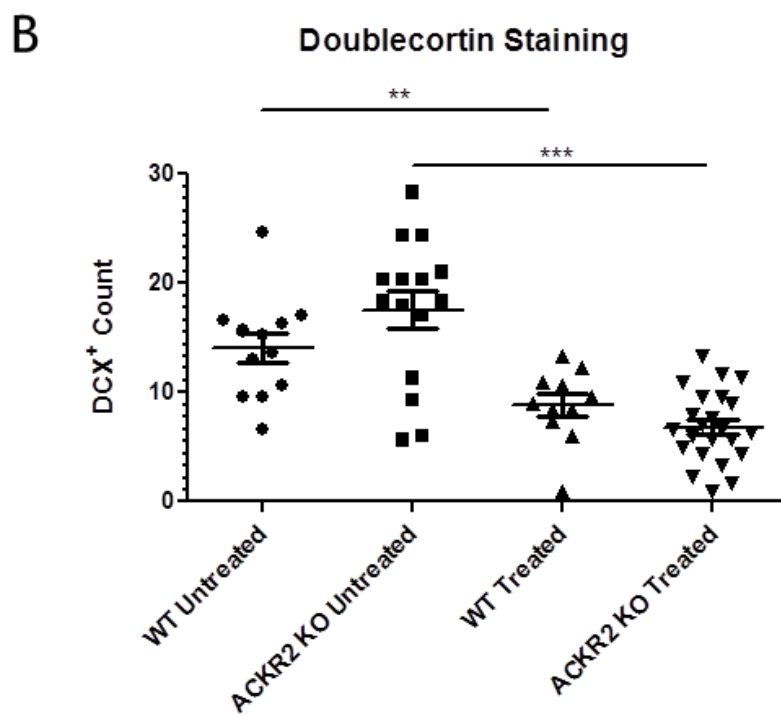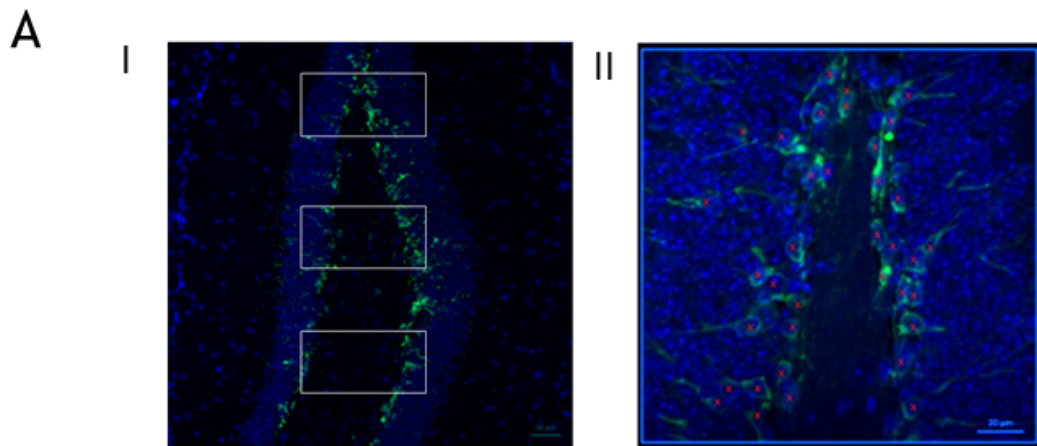
Figure 6-5 Counting strategy and DCX⁺ counts

WT and ACKR2 KO mice were treated with ~80mg Aldara cream, or an equal volume of control cream, every 24 hours for 5 consecutive days. Perfused brains were extracted and were stained for DCX. Cell counts were performed on 3 different areas of the dentate gyrus for each section (A) and a minimum of 11 sections from at least 3 mice were counted (B). Significance was measured using unpaired two-tailed student's t tests. ** $p \leq 0.01$ *** $p \leq 0.001$. n=3/4 mice per group.

6.2.4 Assessment of burrowing behaviour in Aldara-treated ACKR2 KO mice

Having established that ACKR2 KO mice responded to topical Aldara treatment in a similar fashion to WT mice in terms of the chemokine response in the brain and in terms of neurogenesis, we next sought to establish if this treatment could also diminish burrowing activity. As detailed in Chapter 3, this model was used to assess the extent to which mice burrow during a 2 hour window following treatment. ACKR2 KO mice were treated at the same time each morning with ~80mg of either Aldara cream or control cream, as described previously, and were then single-housed for the testing period 4 hours later.

The results showed that, as seen previously in WT mice, ACKR2 KO mice treated with Aldara cream burrowed less than those treated with control cream. Figure 6-6A shows that control mice burrowed more over time, as the weight of food left in the tubes declined over the three day period, whereas the burrowing activity of Aldara-treated mice was minimal. ACKR2 KO mice treated with Aldara appeared to burrow slightly more actively after the third application, a trend that was not seen with WT mice in Chapter 3; however this was still significantly less than the ACKR2 KO mice treated with control cream. The results were also portrayed as a percentage burrowing activity based on baseline measurements, which were considered 100% (B). This showed the variation in burrowing activity within the two groups and more clearly showed the increase in burrowing activity of the treated group after the third Aldara application. The results from the ACKR2 KO mice were compared with those from WT mice to determine if a lack of ACKR2 significantly affects the burrowing response to Aldara cream. Figure 6-6C shows a clear separation between the control mice and the treated mice; however there was no apparent difference between the WT mice and the ACKR2 KO mice. These results add to the evidence suggesting that the response of ACKR2 KO mice to Aldara treatment was very similar to that of WT mice. It would suggest that, whilst inflammatory CC chemokines may be important for generating the response to Aldara application, the response is not being overtly regulated by the scavenging receptor ACKR2.
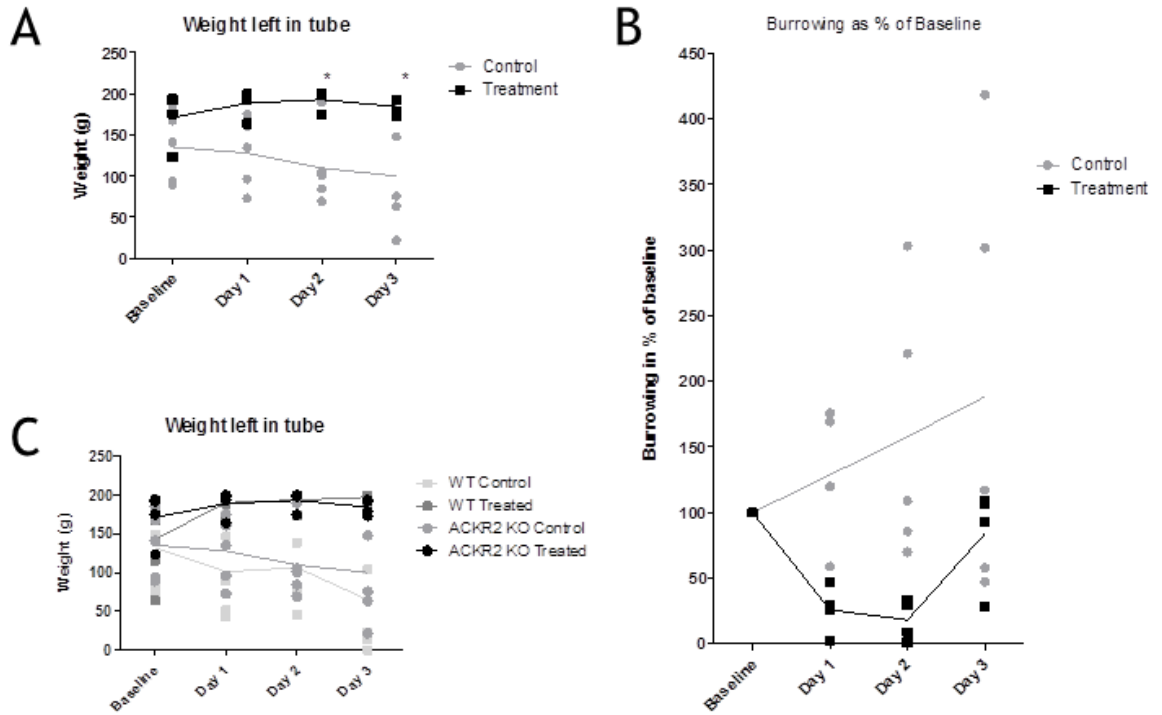
Figure 6-6 Burrowing activity of ACKR2 KO Aldara-treated mice
ACKR2 KO and WT mice were treated with ~80mg Aldara cream or control cream and were assessed for burrowing activity on three consecutive days. Four hours following treatment application, mice were single caged with a burrowing tube containing 200g of food pellets for 2 hours. At the end of this time point, mice were caged again in groups and the remaining weight of food pellets in the tubes was recorded. The weight left in the tube following the 2 hour period is shown (A) or presented as a percentage of baseline tests, where baseline readings were considered 100% (B). To identify differences in burrowing activity between the two strains of mice, ACKR2 KO mice were compared with WT mice (C). n=4/5 per group. Significance was measured using two-way ANOVA with Bonferroni posttests *= p ≤ 0.05.

6.4 Discussion

The results in Chapter 5 identified a distinct chemokine response in the brain following topical Aldara treatment. To further investigate the functional consequences of the response, and to determine whether inflammatory chemokines in the brain were regulated by scavenging receptor ACKR2, the Aldara model of cutaneous inflammation was repeated using ACKR2 KO mice. QPCR analysis was used to determine the chemokine response in the brain and burrowing behaviour was assessed as a functional output. In addition, due to the specific nature of ACKR2 expression in the brain, neurogenesis was measured in both WT, and ACKR2 KO, Aldara-treated mice.

The results suggested that the phenotypic, cutaneous response to topical Aldara application was similar between WT and ACKR2 KO, as no overt differences in skin pathology were identified. Subsequently, the transcriptional chemokine response in the brain and PBL was assessed in the mutant mice. Although this gene deletion should not directly affect the transcript levels of chemokines as it functions at the protein level, Jamieson et al and Baldwin et al have suggested that cutaneous inflammation is exacerbated in ACKR2 KO mice[410, 411]. Thus, the tissue-specific, or systemic, inflammatory response to Aldara treatment may be heightened in these mice, which may in turn cause a greater response in the brain. However, the results showed that the transcriptional chemokine upregulation in the brains of ACKR2 KO mice followed a similar pattern when compared with WT mice, suggesting that ACKR2 was not an essential regulator of the chemokine response in the brain.

The distinct anatomical distribution of ACKR2 in the brain, which is localised to the dentate gyrus and the olfactory bulb, indicated that it may be involved in regulating adult neurogenesis. As mentioned in Chapter 1, the process of neurogenesis is thought to be important for synaptic and neural plasticity and increased cognitive function[332, 413]. Therefore, using DCX staining, neurogenesis was assessed in Aldara-treated WT and ACKR2 KO mice. The results showed that neurogenesis was significantly impaired in mice treated with topical Aldara when compared with control mice. Although neurogenesis has been shown to be modulated by immune stimulation[414-416], this is the first report to show that distal, cutaneous inflammation can have a negative effect. However, the results

presented in this Chapter suggested that, whilst cutaneous inflammation significantly impaired neurogenesis, ACKR2 did not appear to regulate this response as neurogenesis was reduced to a similar extent in WT and KO mice.

In summary, the results in this Chapter suggest that ACKR2 KO mice respond in a similar fashion to topical Aldara-treatment as WT mice. The transcriptional chemokine response in the brain, the impairment of adult neurogenesis and the reduction in burrowing behaviour is consistent between the two different mouse strains. It may be that the scavenging effects of ACKR2 are subtle and the redundancy of the chemokine family and the magnitude of the brain response overwhelmed the regulatory effects of ACKR2 in this system. However, taken together, the results indicate that ACKR2-dependent regulation of inflammatory CC chemokines is not an essential mechanism in the brain response to peripheral inflammation.

Chapter 7

Discussion

7 Discussion

Neuropsychiatric conditions are commonly associated with chronic inflammatory diseases that affect the periphery[417, 418]. However, the mechanisms underpinning this relationship are unclear, not least because the brain is an 'immune-specialised' tissue[137, 179]. Studies have attempted to investigate this and, although our understanding of the communication between the brain and the periphery has increased in recent years, many unanswered questions remain. In addition, a large proportion of these studies have relied upon the administration of potent systemic inflammatory agents, inflammatory models that are unlike the tissue-specific conditions affecting humans. To try to further our knowledge with regards to the mechanisms underpinning the relationship between peripheral inflammation and the onset of neurological conditions, this thesis used a pathologically relevant mouse model of cutaneous inflammation to investigate the brain response to peripheral inflammation.

The Aldara model of psoriasis-like skin inflammation is well documented[363, 372, 401], but has never before been used to investigate the central response to peripheral inflammation. In the studies described in Chapter 3, this model was used to determine the brain response to cutaneous inflammation using transcriptional profiling techniques. The microarray analysis identified a distinct, and pronounced, ISG response in the brain following Aldara treatment. This brain response was confirmed using QPCR and was found to correlate with a reduction in burrowing behaviour, indicating behavioural dysfunction in Aldara-treated mice. In Chapter 4, the ISG response in the brain was evaluated in a number of different inflammatory models and was found to be induced following topical IMQ treatment, the TLR-specific active component of Aldara cream. The brain signature was not, however, identified following TPA-induced skin inflammation or following I.P. administration of IMQ. The temporal pattern of the response to Aldara application was also investigated and it was discovered that the brain response, which peaked following the third application, was not mimicked by a similar response in the PBL. In Chapter 5, the microarray dataset was revisited and a chemokine signature in the Aldara-treated brains was identified. When compared with the other models, we found that the chemokine response followed the same temporal expression pattern as the ISG response and was present in the topical IMQ model, but not in the TPA model or the I.P IMQ

model. In addition to the transcriptional response, topical Aldara treatment also induced the influx of CD3^{+} T cells into the brain parenchyma. We showed, through the use of two chemokine receptor blockers, that impaired burrowing behaviour did not appear to be dependent on the individual activity of chemokine receptors CCR5 or CXCR3. Finally, the role of ACKR2 was investigated through the use of ACKR2 KO mice. The data presented in Chapter 6 indicated that ACKR2 was not an important mediator in the response to cutaneous inflammation as results from the transcriptional analysis of the brain, and results from the two functional studies, were consistent between WT and KO strains. Although no strain difference was observed, analysis of emerging neurons in the dentate gyrus showed that cutaneous inflammation caused a reduction in adult neurogenesis. Whilst some debate remains as to the functional relevance of adult neurogenesis[413], it is thought to promote learning and memory and support cognition[419].

It is difficult to determine the role of an ISG and chemokine response in the brain, and whether or not their induction would be beneficial or detrimental to the host. Although we have shown that Aldara treatment, and the subsequent transcriptional response in the brain, correlate with decreased burrowing activity and impaired neurogenesis, we have been unable to identify the causal relationship between these observations. The role of many specific ISGs remains unknown; however their purpose as a whole is to mediate a potent anti-viral response. This has been shown following the intranasal administration of viruses and, although the viruses only infected the olfactory bulb, the subsequent ISG response was found throughout the brain and in distant, uninfected sites[393]. It is therefore possible that the brain ISG response that we see following cutaneous TLR7 stimulation is the same classic response to virus infection that one would expect to see in the localised area, but is somehow projected to this distant tissue. More recent studies performed in our lab have investigated the transcriptional response to topical Aldara treatment in other tissues including the liver, spleen and lungs. Interestingly, the gene induction in these tissues was minimal, which suggests enhanced chemokine expression following cutaneous inflammation may be unique to the brain (Louis Nerurkar, unpublished data). It would be interesting to determine if an ISG response is present in other tissues, such as the liver and spleen following Aldara and IMQ treatment. Evidence as to

how ISGs in the brain might affect homeostatic functions are limited, therefore it is difficult to hypothesise whether or not the ISGs are the direct cause of any of the functional outputs we observed.

It is likely that the induction of CCL3, CCL5, CXCL9 (identified in the microarray only) and CXCL10 were driving the influx of CD3^{+} T cells into the brain as these are ligands for chemokine receptors expressed by T cells. Indeed, this has been shown in a model of viral encephalitis[234]. If time had allowed, this mechanism could have been confirmed by performing CD3 immunohistochemistry on brains from Aldara-treated mice co-treated with the CXCR3 blocker and CCR5 blocker. It remains unclear as to whether or not chemokines in the brain could drive the behavioural changes and suppression of neurogenesis identified following Aldara treatment. Although the use of ACKR2 KO mice did not appear to alter the results in any way, this genetic modification would only impact on two of the chemokines induced in the brain, CCL3 and CCL5, as ACKR2 is a scavenging receptor for inflammatory CC chemokines. Chemokines are thought to be involved in the regulation of neurogenesis, both during development and in adulthood[153, 414]. In particular, CXCR4-directed migration of neuronal precursors and CX3CL1-dependent crosstalk between neurons and microglia are thought to be important[152, 210]. These data would suggest that if the levels of chemokines were altered in the brain, this in turn could impact the level of neurogenesis. However, none of the key chemokines reported to be involved in neurogenesis were identified as being differentially expressed in the brain following Aldara treatment. As mentioned in Chapter 1, it has been suggested that chemokines can act as neurotransmitters, supporting the communication between neurons and glial cells and modulating GABAergic neurotransmission[211, 215, 224]. However, there is a lot of contradictory literature regarding the role of chemokines within the healthy adult brain and CCL5 was the only chemokine upregulated in response to cutaneous Aldara treatment that has been reported to act as a neurotransmitter. Furthermore, despite numerous studies into the role of chemokines in neuropsychiatric conditions, findings are often inconsistent and mainly focus on two prototypical inflammatory chemokines, CXCL8 and CCL2[374], neither of which were induced in the brain following Aldara treatment. It would therefore appear that the chemokines induced in the brain in response to Aldara treatment have the primary role of promoting an inflammatory response through

the recruitment of immune cells into the brain. To link chemokines to the other functional outputs, the reduction in neurogenesis and impaired burrowing activity, would require further studies.

7.1 Hypotheses

The mechanisms by which tissue-specific cutaneous inflammation can affect the brain remain to be established, therefore we can only speculate as to the potential mechanisms based on the evidence we have obtained. The results in this thesis implicate TLR ligation and 'non-canonical' TLR signalling as one potential mechanism driving the brain response. For example, although a brain response was detected following topical Aldara and topical IMQ application, a similar but non-TLR based stimulus, TPA, failed to induce an ISG or chemokine response in the brain. These findings are in agreement with previous studies that have shown an ISG and chemokine response in the brain following LPS administration; a response which could not be reproduced following systemic cytokine administration[377]. As mentioned in Chapter 1, TLR ligation leads to a downstream signalling event which results in the activation of the transcription factor NF-κB and the production of inflammatory cytokines[33]. However, certain TLRs can signal through alternative pathways to activate different transcription factors[33, 387]. Interestingly, in addition to the 'classical' TLR signalling pathway, TLR4 and TLR7, which bind LPS and IMQ respectively, can also signal through non-canonical pathways which lead to the production of Type I IFNs (Figure 7-1)[420]. These 'alternative' signalling pathways provide us with a mechanism through which LPS and IMQ could mediate an ISG response in the brain following peripheral stimulation. We have shown that LTA, a ligand for TLR2, which can only signal through the 'classical' pathway, was unable to induce an ISG response in the brain, again suggesting that the ISG response is the result of the 'alternative' TLR signalling pathways[377].
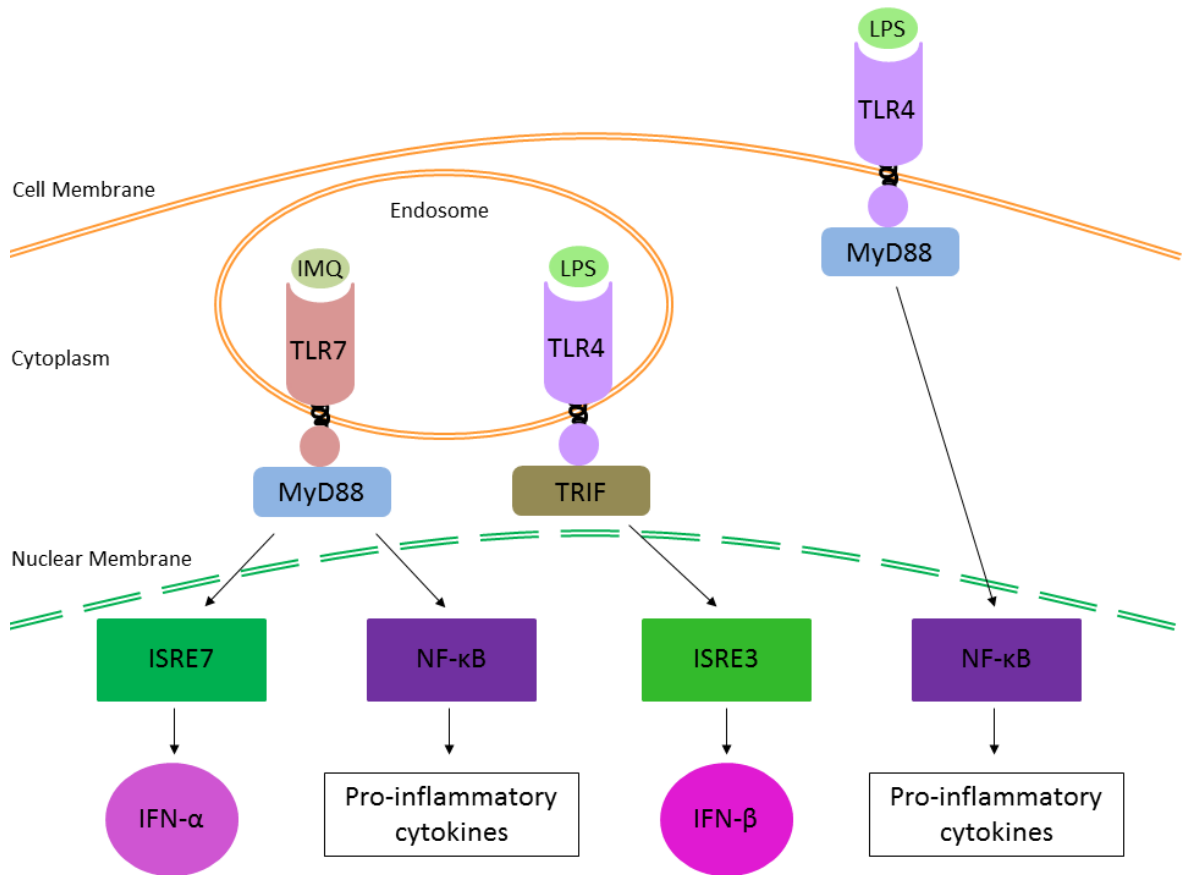
Figure 7-1 TLR4 and TLR7 signalling pathways
Diagram showing the signalling pathways following TLR4 and TLR7 ligation. Both signal through 'alternative' signalling pathways that lead to Type I IFN production, in addition to the the NF-κB-dependent 'classical' pathway that leads to the production of inflammatory cytokines.

However, the results presented in this thesis provide a number of caveats that need to be considered. For example, the plasma levels of inflammatory cytokines following topical Aldara and topical IMQ treatment were low and variable and diminished over the course of the treatments. It was apparent from the results that the brain response did not correlate with a strong inflammatory cytokine profile in the periphery and, most notably, we did not find high expression of IFNγ, although Type I IFNs were not assessed. This was surprising as pro-inflammatory cytokines and Type I IFNs are classically induced following TLR7 stimulation. Some cytokines may be produced early in the acute response and it may be the case that expression levels would be higher had they been assessed at an earlier time point; however, if we propose that circulating cytokines are driving the brain response we see at day 3 and day 5, we would expect detectable levels in the blood plasma.

In addition, if the brain response was dependent on non-canonical TLR signalling, we would have expected to see a similar brain response following intraperitoneal administration of IMQ to that seen following topical IMQ. However, only a very mild response was detected in the brain following I.P. IMQ compared with mice treated with topical IMQ. This less severe response to intraperitoneal TLR7 agonists has also been reported in the literature[421] and, although it could simply be a consequence of the dose used in this thesis, it could imply that the brain response to IMQ was dependent on the localised skin response. However, we have also shown that topical IMQ failed to induce cutaneous inflammation as this aspect of the response was likely caused by the vehicle component, isostearic acid. Independently of overt tissue inflammation in the skin, topical IMQ treatment induced the most striking brain response out of all of the models investigated. In light of this, we propose a second hypothesis to serve as an alternative mechanism by which the effects of topical IMQ are being mediated; through the inflammatory reflex[291].

One way in which the presence of IMQ in the skin might be detected is through the activation of the vagus nerve. Like all tissues highly exposed to the external environment, the skin is innervated with sensory nerve fibres that are sensitive to heat, pain and touch. These sensory neurons are responsive to danger and inflammatory stimuli via the expression of three different types of receptor, 1) receptors that recognise PAMPS, including TLRs and NLRs 2) receptors that recognise DAMPS and 3) receptors for inflammatory cytokines[422]. As mentioned in Chapter 1, the afferent branches of the vagus nerve are also surrounded by macrophages and DCs that can be activated in response to inflammatory cytokines or PAMPs[282]. Through the use of vagotomy studies, it has been shown that, in order to sense inflammatory stimuli in the periphery, an intact vagus nerve is required[288, 423, 424]. This transmits signals directly to the brain and can mediate responses including cytokine-induced fever[425] and sickness behaviours[423] and is therefore considered key in maintaining immunological homeostasis. In addition, electrical stimulation of the vagus nerve has been shown to attenuate inflammation through the cholinergic anti-inflammatory pathways[284, 424]. This mechanism of immune-to-brain communication might help explain our findings, that topically applied IMQ induced a brain response without the need for an overt inflammatory response in the periphery. If IMQ was directly activating the

peripheral nervous system, there would not be the need for high levels of inflammatory cytokines or for a localised inflammatory response in the skin. In this way, the response would still rely on the function of TLR7, but the action of local inflammatory mediators would be complemented by the direct communication with the brain.

7.2 Conclusions

The results in this thesis demonstrate that peripheral inflammation can induce a profound response in the brain. We have shown that cutaneous inflammation leads to the induction of an ISG and chemokine response in the brain, along with impaired dentate neurogenesis, a reduction in burrowing behaviour and the influx of inflammatory cells into the brain parenchyma. We hypothesise that these functional changes may be mediated through the TLR7-dependent activation of the afferent vagus nerve, conferring direct communicating with the brain. Despite being considered an 'immune-specialised' tissue, these findings highlight the sensitivity of the brain to peripheral, tissue-specific immune stimulus. These results could help forward our understanding as to how peripheral inflammatory diseases are so commonly associated with the onset of neuropsychiatric conditions. However, to fully understand the mechanisms that define this relationship, further investigations would be required.

7.3 Future directions

The work in this thesis has generated some interesting and novel data; however many of the findings are observational and would require further investigation to clarify the relationships and identify the underlying mechanisms. Several experiments could be performed to help advance our understanding.

The results have relied upon the analysis of global gene expression in the brain, rather than focusing on distinct brain regions and specific neural cell types. To my knowledge, this was the first study to investigate the brain response to cutaneous Aldara treatment; therefore it made sense to begin with an unbiased, broad-spectrum approach. However, these results would be complemented with the use of fluorescent *in-situ* hybridisation (FISH) techniques that would allow us to identify the regional and cellular specificity of the gene expression, focusing

on our identified panel of genes of interest. This would help us to determine whether the transcriptional response was the result of infiltrating immune cells or whether it was the direct activation of glial cells. It would also be beneficial to look for a wider panel of infiltrating immune cells in the brains of Aldara-treated mice. Although our focus was CD3^{+} T cells, the chemokines induced in the brain also regulate the chemotaxis of other immune cells, particularly neutrophils and monocytes.

To test our hypotheses, that the brain response is mediated by non-canonical TLR signalling through the activation of the vagus nerve, several studies could be performed. To identify the involvement of the different TLR signalling pathways, IRF7-deficient mice or NF-κB inhibition could be used[426, 427]. In addition, the role of Type I IFNs in behaviour and neurogenesis could be assessed using IFNAR-deficient mice[428]. To determine whether or not the brain response to cutaneous inflammation was generated via the afferent vagus nerve, vagotomy experiments could be performed. Alternatively, the vagus nerve could be directly, and specifically, stimulated using IMQ and a non-TLR stimulus in order to compare the responses.

Finally, this study would benefit from more in depth behavioural analyses to fully profile the functional output of topical Aldara treatment. The burrowing behavioural test is a basic model that was selected for this thesis as it satisfied the constraints of our animal license. However, there are other models that could be used in order to identify specific impairments in memory, learning, cognitive function and depression-like sickness behaviours[55, 429, 430].

Appendices

Appendix 1 List of genes identified using microarray analysis

Gene Symbol	Gene Name	Fold Change	p-value
Cd72	CD72 antigen	28.13216	2.30E-11
Ccl5	chemokine (C-C motif) ligand 5	25.649666	1.17E-09
Gm11428	predicted gene 11428	23.267797	1.74E-10
Ms4a6c	membrane-spanning 4-domains, subfamily A, member 6C	22.076183	1.19E-09
Cxcl13	chemokine (C-X-C motif) ligand 13	21.38037	1.53E-09
Ccl3	chemokine (C-C motif) ligand 3	18.673525	4.10E-10
Ms4a7	membrane-spanning 4-domains, subfamily A, member 7	16.419401	1.11E-09
Clec4a1	C-type lectin domain family 4, member a1	15.462207	6.18E-10
Oasl2	2'-5' oligoadenylate synthetase-like 2	14.909811	1.68E-08
Ifi44	interferon-induced protein 44	14.84326	8.11E-07
Ifit1	interferon-induced protein with tetratricopeptide repeats 1	14.1490965	2.26E-07
AI607873		13.953218	4.32E-09
Ifit3	interferon-induced protein with tetratricopeptide repeats 3	13.801712	3.73E-08
Irf7	interferon regulatory factor 7	13.696917	3.23E-08
Cybb	cytochrome b-245, beta polypeptide	13.394899	7.46E-11
Emr1	EGF-like module containing, mucin-like, hormone receptor-like sequence 1	12.654873	6.06E-10
Usp18	ubiquitin specific peptidase 18	12.629435	8.64E-07
H2-K1	histocompatibility 2, K1, K region	12.393708	4.71E-11
Cd52	CD52 antigen	12.29611	1.60E-09
Lyz2	lysozyme 2	12.252241	4.53E-10
0	MHC class I like protein GS10	histocompatibility 2, Q region locus 5	11.900996	8.21E-09
Ms4a6d	membrane-spanning 4-domains, subfamily A, member 6D	11.575372	7.73E-09
Ms4a4c	membrane-spanning 4-domains, subfamily A, member 4C	11.117746	1.64E-06
Plbd1	phospholipase B domain containing 1	10.889762	6.35E-09
Fcgr4	Fc receptor, IgG, low affinity IV	10.599809	1.14E-08
C3ar1	complement component 3a receptor 1	10.397596	3.88E-10
H2-Q6|LOC68395	histocompatibility 2, Q region locus 6	histocompatibility 2, Q region locus 6-like	10.238313	2.92E-08
Clec12a	C-type lectin domain family 12, member a	9.760899	1.91E-10
Clec4a3	C-type lectin domain family 4, member a3	9.502658	1.55E-08
Trim30	tripartite motif-containing 30	9.322903	7.06E-07
Lgals3bp	lectin, galactoside-binding, soluble, 3 binding protein	8.6376915	5.24E-09

Fcer1g	Fc receptor, IgE, high affinity I, gamma polypeptide	8.5139475	8.67E-11
Gm885	predicted gene 885	8.477824	1.39E-09
Ptprc	protein tyrosine phosphatase, receptor type, C	8.296488	3.43E-09
Tgfbi	transforming growth factor, beta induced	8.292485	4.72E-09
Cd180	CD180 antigen	7.9570346	6.19E-10
Sirpb1b|Sirpb1a|LOC100038947|LOC630976|LOC641195	signal-regulatory protein beta 1B | signal-regulatory protein beta 1A | signal-regulatory protein beta 1-like | similar to SIRP beta 1 isoform 3 | similar to SIRP beta 1 isoform 1	7.933538	8.64E-09
Ifitm3	interferon induced transmembrane protein 3	7.9153414	6.25E-09
I830012O16Rik	RIKEN cDNA I830012O16 gene	7.8779535	2.29E-05
Fyb	FYN binding protein	7.656857	2.61E-10
Pilra	paired immunoglobin-like type 2 receptor alpha	7.5580826	9.62E-10
H2-D1|H2-L	histocompatibility 2, D region locus 1	7.542797	6.61E-11
Rtp4	receptor transporter protein 4	7.315761	3.52E-07
Pld4	phospholipase D family, member 4	7.2694716	2.81E-10
AW112010		7.258376	2.05E-10
Ctsc	cathepsin C	7.220582	2.65E-10
Saa3	serum amyloid A 3	7.173075	2.25E-06
Apobec1	apolipoprotein B mRNA editing enzyme, catalytic polypeptide 1	7.168513	5.67E-10
Acp5	acid phosphatase 5, tartrate resistant	7.1567636	4.93E-08
C4b|C4a	complement component 4B (Childo blood group) | complement component 4A (Rodgers blood group)	7.0189023	2.26E-10
Irgm1	immunity-related GTPase family M member 1	6.9834146	4.35E-07
Gbp3	guanylate binding protein 3	6.911741	3.71E-06
Ms4a6b	membrane-spanning 4-domains, subfamily A, member 6B	6.896093	4.91E-08
Ifi204|Mnda	interferon activated gene 204 | myeloid cell nuclear differentiation antigen	6.8321	1.04E-05
Gbp2	guanylate binding protein 2	6.5060687	3.34E-06
Serpina3n	serine (or cysteine) peptidase inhibitor, clade A, member 3N	6.447621	1.85E-10
Cxcl9	chemokine (C-X-C motif) ligand 9	6.4027085	1.57E-06
Gm4951	predicted gene 4951	6.300047	2.04E-05
		6.2691884	7.58E-06
Igsf6	immunoglobulin superfamily, member 6	6.205959	1.68E-09
Mpa2l|Gbp10|EG634650|Gbp8	macrophage activation 2 like | guanylate-binding protein 10 | predicted gene, EG634650 | guanylate-binding protein 8	6.181138	1.17E-06
Lilrb4	leukocyte immunoglobulin-like receptor, subfamily B, member 4	6.1702504	3.61E-07
Mpeg1	macrophage expressed gene 1	6.138617	1.42E-11
Oas1g|Oas1a	2'-5' oligoadenylate synthetase 1G | 2'-5' oligoadenylate synthetase 1A	5.8706975	1.18E-05

Gene	Description	Value	p-value
H2-Q7|H2-Q6|H2-Q8	histocompatibility 2, Q region locus 7 | histocompatibility 2, Q region locus 6 | histocompatibility 2, Q region locus 8	5.8335204	2.45E-11
Ifi27l2a	interferon, alpha-inducible protein 27 like 2A	5.8044176	8.40E-07
Tlr13	toll-like receptor 13	5.718304	6.51E-09
Ddx58	DEAD (Asp-Glu-Ala-Asp) box polypeptide 58	5.7036858	3.45E-06
Ctsh	cathepsin H	5.6594315	8.12E-10
		5.598447	1.10E-05
Cxcl16|Zmynd15	chemokine (C-X-C motif) ligand 16 | zinc finger, MYND-type containing 15	5.4621305	1.30E-07
Rnf213	ring finger protein 213	5.451237	5.37E-06
		5.329549	9.26E-06
Gpnmb	glycoprotein (transmembrane) nmb	5.3048334	6.56E-07
Cd53	CD53 antigen	5.291279	2.81E-10
Cyp4f18	cytochrome P450, family 4, subfamily f, polypeptide 18	5.2113914	2.80E-07
Stat1	signal transducer and activator of transcription 1	5.2003345	2.13E-06
		5.1890216	1.68E-05
Pik3ap1	phosphoinositide-3-kinase adaptor protein 1	5.1737046	1.50E-09
Klra2	killer cell lectin-like receptor, subfamily A, member 2	5.165078	2.34E-08
Ctss	cathepsin S	5.161943	1.94E-10
AI451617		5.0858283	1.23E-05
Il2rg	interleukin 2 receptor, gamma chain	5.0607347	1.28E-07
Ms4a4a	membrane-spanning 4-domains, subfamily A, member 4A	4.9973893	1.52E-08
		4.9876914	1.59E-05
		4.9528537	1.64E-05
		4.9109077	3.17E-05
Irgm2|Igtp	immunity-related GTPase family M member 2 | interferon gamma induced GTPase	4.905407	1.01E-06
Lcp1	lymphocyte cytosolic protein 1	4.82637	1.62E-08
		4.824545	1.84E-05
H2-T22|H2-T9|H2-T10	histocompatibility 2, T region locus 22 | histocompatibility 2, T region locus 9 | histocompatibility 2, T region locus 10	4.7803392	2.80E-07
Iigp1	interferon inducible GTPase 1	4.7393727	5.79E-05
Oas1b	2'-5' oligoadenylate synthetase 1B	4.6943526	2.57E-05
Sirpb1a|Sirpb1b|LOC100038947|LOC630976	signal-regulatory protein beta 1A | signal-regulatory protein beta 1B | signal-regulatory protein beta 1-like | similar to SIRP beta 1 isoform 3	4.6814513	1.42E-08
Samd9l	sterile alpha motif domain containing 9-like	4.6794043	2.95E-05
Ddx60	DEAD (Asp-Glu-Ala-Asp) box polypeptide 60	4.6703634	2.19E-05
Itgb2	integrin beta 2	4.578407	6.79E-08
Ly86	lymphocyte antigen 86	4.5482535	1.10E-09

Sh2d1b1	SH2 domain protein 1B1	4.548108	1.29E-06
		4.5266757	2.33E-05
Ccl9	chemokine (C-C motif) ligand 9	4.517743	2.91E-07
Aoah	acyloxyacyl hydrolase	4.4741716	6.13E-09
D14Ertd668e	DNA segment, Chr 14, ERATO Doi 668, expressed	4.4590044	7.04E-04
C3	complement component 3	4.4247837	2.86E-08
Lcn2	lipocalin 2	4.392422	2.19E-09
Ms4a14	membrane-spanning 4-domains, subfamily A, member 14	4.35078	2.38E-06
Gbp4	guanylate binding protein 4	4.3316245	1.37E-06
Hck	hemopoietic cell kinase	4.327205	1.56E-07
Eif2ak2	eukaryotic translation initiation factor 2-alpha kinase 2	4.2970195	3.46E-05
		4.283881	7.76E-05
Rnf213	ring finger protein 213	4.264224	1.62E-05
Cxcl10	chemokine (C-X-C motif) ligand 10	4.246946	1.27E-04
Sirpb1b|Sirpb1a|LOC100038947|LOC641195	signal-regulatory protein beta 1B | signal-regulatory protein beta 1A | signal-regulatory protein beta 1-like | similar to SIRP beta 1 isoform 1	4.2158923	1.83E-08
Gpr65	G-protein coupled receptor 65	4.1929426	1.23E-09
Psmb8	proteasome (prosome, macropain) subunit, beta type 8 (large multifunctional peptidase 7)	4.1857376	6.08E-06
Vav1	vav 1 oncogene	4.172101	3.47E-08
H2-Q8	histocompatibility 2, Q region locus 8	4.132269	6.47E-07
Tgtp1|Tgtp2|Gm12185	T-cell specific GTPase 1 | T-cell specific GTPase 2 | predicted gene 12185	4.123084	3.62E-05
Ube2l6	ubiquitin-conjugating enzyme E2L 6	4.117248	4.18E-05
Tgtp1|Tgtp2|Gm12185	T-cell specific GTPase 1 | T-cell specific GTPase 2 | predicted gene 12185	4.114396	2.22E-05
Ifit2	interferon-induced protein with tetratricopeptide repeats 2	4.1017013	9.34E-05
Gbp6	guanylate binding protein 6	4.0850587	1.01E-05
Unc93b1	unc-93 homolog B1 (C. elegans)	4.079613	5.62E-10
Rac2	RAS-related C3 botulinum substrate 2	4.0723453	6.72E-08
Lgals9	lectin, galactose binding, soluble 9	4.061534	3.03E-06
H2-t9|EG547347	MHC class Ib T9 | predicted gene, EG547347	4.0322742	7.58E-09
H2-T23|C920025E04Rik	histocompatibility 2, T region locus 23 | RIKEN cDNA C920025E04 gene	3.994959	4.41E-07
Naip2	NLR family, apoptosis inhibitory protein 2	3.9914474	1.63E-07
Rsad2	radical S-adenosyl methionine domain containing 2	3.9893818	9.71E-05
Cd48	CD48 antigen	3.9850123	7.09E-08
Xaf1	XIAP associated factor 1	3.9349377	1.86E-05
Arhgdib	Rho, GDP dissociation inhibitor (GDI) beta	3.9166377	4.25E-08
Bst2	bone marrow stromal cell antigen 2	3.9156516	1.18E-05

Casp8	caspase 8	3.900089	7.32E-09
Ifih1	interferon induced with helicase C domain 1	3.8993988	4.05E-05
Irf9	interferon regulatory factor 9	3.8860035	7.60E-08
Slfn4	schlafen 4	3.8827317	5.75E-04
Cd68	CD68 antigen	3.8816974	1.55E-09
Itgam	integrin alpha M	3.8755326	5.37E-08
Ifi30	interferon gamma inducible protein 30	3.872788	4.07E-07
Tyrobp	TYRO protein tyrosine kinase binding protein	3.807827	3.37E-11
Pyhin1	pyrin and HIN domain family, member 1	3.7786415	4.61E-06
9930111J21Rik2 | 9930111J21Rik1 | Gm5431	RIKEN cDNA 9930111J21 gene 2 | RIKEN cDNA 9930111J21 gene 1 | predicted gene 5431	3.7734895	7.22E-08
Slc11a1	solute carrier family 11 (proton-coupled divalent metal ion transporters), member 1	3.761288	3.36E-07
Ifi203	interferon activated gene 203	3.7605247	1.28E-05
Gm5431	predicted gene 5431	3.750554	3.24E-06
Ccr5|Ccr2	chemokine (C-C motif) receptor 5 | chemokine (C-C motif) receptor 2	3.7445805	4.31E-08
Tap1	transporter 1, ATP-binding cassette, sub-family B (MDR/TAP)	3.7434745	3.13E-07
Ccr5|Ccr2	chemokine (C-C motif) receptor 5 | chemokine (C-C motif) receptor 2	3.7419653	4.14E-08
C1qc	complement component 1, q subcomponent, C chain	3.691437	9.21E-09
Cyba	cytochrome b-245, alpha polypeptide	3.6912851	2.94E-08
Fcrl5	Fc receptor-like 5	3.6699855	2.10E-05
Sp100		3.6670215	4.49E-07
Sfpi1	SFFV proviral integration 1	3.6336854	5.97E-08
9930111J21Rik2 | 9930111J21Rik1 | Gm5431	RIKEN cDNA 9930111J21 gene 2 | RIKEN cDNA 9930111J21 gene 1 | predicted gene 5431	3.624132	5.27E-08
Cd84	CD84 antigen	3.619827	6.09E-08
Parp12	poly (ADP-ribose) polymerase family, member 12	3.6093345	4.74E-06
C1qa	complement component 1, q subcomponent, alpha polypeptide	3.5933928	1.21E-09
Lcp2	lymphocyte cytosolic protein 2	3.5550501	1.57E-08
Dock2	dedicator of cyto-kinesis 2	3.542894	2.29E-07
Tagap	T-cell activation Rho GTPase-activating protein	3.5305424	4.78E-08
C1qb	complement component 1, q subcomponent, beta polypeptide	3.4979184	2.85E-10
Laptm5	lysosomal-associated protein transmembrane 5	3.4805212	8.98E-10
Itgax	integrin alpha X	3.4801943	3.22E-06
Nckap1l	NCK associated protein 1 like	3.4672332	1.23E-09

Cd93	CD93 antigen	3.434816	5.93E-07
Tlr1	toll-like receptor 1	3.4326348	8.31E-07
Slamf7	SLAM family member 7	3.408035	3.06E-05
AB124611		3.40638	1.79E-07
Pik3cg	phosphoinositide-3-kinase, catalytic, gamma polypeptide	3.3917887	1.08E-07
Glipr1|Krr1	GLI pathogenesis-related 1 (glioma) | KRR1, small subunit (SSU) processome component, homolog (yeast)	3.3862197	6.39E-08
Serping1	serine (or cysteine) peptidase inhibitor, clade G, member 1	3.3831935	2.65E-07
		3.3748608	0.001022
Grn	granulin	3.3616664	1.59E-09
Ly6a	lymphocyte antigen 6 complex, locus A	3.3566322	6.88E-09
Slfn8	schlafen 8	3.346721	1.03E-04
Gfap	glial fibrillary acidic protein	3.312322	8.63E-11
Arpc1b|Gm5637	actin related protein 2/3 complex, subunit 1B | predicted pseudogene 5637	3.3091986	5.15E-09
Dtx3l|Parp9	deltex 3-like (Drosophila) | poly (ADP-ribose) polymerase family, member 9	3.2979794	2.54E-06
Alox5ap	arachidonate 5-lipoxygenase activating protein	3.2976754	5.21E-09
Gp49a|Lilrb4	glycoprotein 49 A | leukocyte immunoglobulin-like receptor, subfamily B, member 4	3.2844298	1.17E-04
Il10ra	interleukin 10 receptor, alpha	3.2723858	1.31E-08
Dhx58	DEXH (Asp-Glu-X-His) box polypeptide 58	3.2714343	6.17E-05
Slamf9	SLAM family member 9	3.2574503	1.06E-06
Tlr7	toll-like receptor 7	3.2499063	1.90E-07
Apobec3	apolipoprotein B mRNA editing enzyme, catalytic polypeptide 3	3.2438989	7.50E-08
		3.2321565	2.57E-05
Neurl3	neuralized homolog 3 homolog (Drosophila)	3.2239246	5.04E-08
Nkg7	natural killer cell group 7 sequence	3.2131076	1.10E-05
Myo1f	myosin IF	3.205457	1.74E-08
Isg20	interferon-stimulated protein	3.1826715	4.01E-04
Bcl2a1a|Bcl2a1d|Bcl2a1b|Bcl2a1c	B-cell leukemia/lymphoma 2 related protein A1a | B-cell leukemia/lymphoma 2 related protein A1d | B-cell leukemia/lymphoma 2 related protein A1b | B-cell leukemia/lymphoma 2 related protein A1c	3.1532354	6.08E-05
Gm11711|Clm3	predicted gene 11711 | CMRF-35-like molecule 3	3.1490738	2.86E-08
Fcgr1	Fc receptor, IgG, high affinity I	3.1478186	8.17E-07
Oas2	2'-5' oligoadenylate synthetase 2	3.1414037	5.05E-05
Trim12|LOC100048060	tripartite motif-containing 12 | similar to tripartite motif protein TRIM12	3.1135898	5.97E-05
Aif1	allograft inflammatory factor 1	3.112917	2.21E-06
BC013712		3.102906	7.42E-08

F11r	F11 receptor	3.092533	5.43E-10
Herc5	hect domain and RLD 5	3.0876677	4.30E-05
Lyn	Yamaguchi sarcoma viral (v-yes-1) oncogene homolog	3.0821068	6.15E-09
Top2a	topoisomerase (DNA) II alpha	3.0800803	4.27E-07
Ly9	lymphocyte antigen 9	3.0745974	8.18E-09
Arpc1b	actin related protein 2/3 complex, subunit 1B	3.0633452	3.34E-09
Tlr8	toll-like receptor 8	3.0540376	4.50E-07
Mki67	antigen identified by monoclonal antibody Ki 67	3.0507367	7.68E-08
Gm11711|Clm3	predicted gene 11711	CMRF-35-like molecule 3	3.0498946	4.06E-08
Fcgr2b	Fc receptor, IgG, low affinity IIb	3.0432014	9.66E-08
Msn	moesin	3.0280933	2.14E-09
Parp9|Dtx3l	poly (ADP-ribose) polymerase family, member 9	deltex 3-like (Drosophila)	3.0247502	1.85E-05

Appendix 2

JOURNAL OF
NEUROINFLAMMATION

RESEARCH   Open Access

Peripheral inflammation is associated with remote global gene expression changes in the brain

Carolyn A Thomson[1], Alison McColl[1], Jonathan Cavanagh[2*†] and Gerard J Graham[1*†]

Abstract

Background: Although the central nervous system (CNS) was once considered an immunologically privileged site, in recent years it has become increasingly evident that cross talk between the immune system and the CNS does occur. As a result, patients with chronic inflammatory diseases, such as rheumatoid arthritis, inflammatory bowel disease or psoriasis, are often further burdened with neuropsychiatric symptoms, such as depression, anxiety and fatigue. Despite the recent advances in our understanding of neuroimmune communication pathways, the precise effect of peripheral immune activation on neural circuitry remains unclear. Utilizing transcriptomics in a well-characterized murine model of systemic inflammation, we have started to investigate the molecular mechanisms by which inflammation originating in the periphery can induce transcriptional modulation in the brain.

Methods: Several different systemic and tissue-specific models of peripheral toll-like-receptor-(TLR)-driven (lipopolysaccharide (LPS), lipoteichoic acid and Imiquimod) and sterile (tumour necrosis factor (TNF) and 12-O-tetradecanoylphorbol-13-acetate (TPA)) inflammation were induced in C57BL/6 mice. Whole brain transcriptional profiles were assessed and compared 48 hours after intraperitoneal injection of lipopolysaccharide or vehicle, using Affymetrix GeneChip microarrays. Target gene induction, identified by microarray analysis, was validated independently using qPCR. Expression of the same panel of target genes was then investigated in a number of sterile and other TLR-dependent models of peripheral inflammation.

Results: Microarray analysis of whole brains collected 48 hr after LPS challenge revealed increased transcription of a range of interferon-stimulated genes (ISGs) in the brain. In addition to acute LPS challenge, ISGs were induced in the brain following both chronic LPS-induced systemic inflammation and Imiquimod-induced skin inflammation. Unique to the brain, this transcriptional response is indicative of peripherally triggered, interferon-mediated CNS inflammation. Similar models of sterile inflammation and lipoteichoic-acid-induced systemic inflammation did not share the capacity to trigger ISG induction in the brain.

Conclusions: These data highlight ISG induction in the brain as being a consequence of a TLR-induced type I interferon response. As considerable evidence links type I interferons to psychiatric disorders, we hypothesize that interferon production in the brain could represent an important mechanism, linking peripheral TLR-induced inflammation with behavioural changes.

Keywords: cytokines, innate immunity, interferons, interferon-stimulated genes, lipopolysaccharide, neuroimmune communication, neuroinflammation, systemic inflammation, toll-like-receptor ligation

* Correspondence: Jonathan.Cavanagh@glasgow.ac.uk;
Gerard.Graham@glasgow.ac.uk
†Equal contributors
[2]Institute of Health & Wellbeing, College of Medical & Veterinary Life Sciences, University of Glasgow, Southern General Hospital, Glasgow G51 4TF, UK
[1]Institute of Infection, Immunity & Inflammation, College of Medical & Veterinary Life Sciences, University of Glasgow, 120 University Place, Glasgow G12 8TA, UK

BioMed Central

Background

By mechanisms that remain to be fully established, systemic infection or inflammation can have a profound effect on the central nervous system (CNS), manifesting in a number of behavioural adaptations, as well as fever and increased neuroendocrine activation. Promoting energy conservation and minimizing heat loss, these sickness behaviours represent a sound strategy designed to help an organism overcome infection. Symptoms include fever, malaise, anorexia, lethargy and, in severe cases, neuropsychiatric disorders, such as depression and anxiety [1]. Sickness behaviours occur during acute bacterial or viral infections, but also during chronic inflammatory diseases, such as rheumatoid arthritis, inflammatory bowel disease and psoriasis [2-4]. In the case of the latter, what would be a beneficial, self-limiting, system can become dysregulated. The prolonged depression and anxiety that ensues represents a major burden to patients, not least because these detrimental comorbidities lead to a poorer clinical outcome.

It is becoming increasingly evident that sickness behaviours are triggered as a result of biological, inflammatory, pathways. In particular, inflammatory cytokines, such as tumour necrosis factor α (TNFα), interleukin-1 β (IL-1β) and interleukin-6 (IL-6) play a pivotal role in inducing symptoms of sickness behaviour. Although not a prerequisite for any of the psychiatric symptoms, IL-6 is required for the induction of a fever response [5], whereas behavioural changes are thought to be attributable to IL-1β and TNFα. Using animal models, it has been demonstrated that most behavioural symptoms can be induced by peripheral, or central, administration of either IL-1β or TNFα [6,7]. Furthermore, several cytokines have been implicated in the manifestation of major depressive disorders in patients with chronic inflammatory diseases. For example, in a phase III clinical trial in which patients with moderate-to-severe psoriasis were treated with the soluble TNFα receptor etanercept, improvement in depression scores preceded the improvements seen in terms of psoriasis severity [4]. Supporting the notion of cytokine-induced depression, patients receiving interferon (IFN) α or IFNβ therapy face a risk of experiencing depression as a side effect of treatment [8-12]. Moreover, patients with major depressive disorders, and no clinical signs of inflammation, often present with elevated levels of circulating inflammatory cytokines [13]. Therefore, significant quantities of literature back the immune system, in particular inflammatory cytokine production, as a key contributor to sickness-induced behavioural changes.

Once considered an immunologically privileged site, the CNS is well fortified against changes in the periphery. However, cross talk does occur and, as a result, much research has gone into elucidating putative routes of immune-to-brain communication. In spite of this, the precise effect of peripheral immune activation on neural circuitry remains unclear. With the aim of better unravelling neuroimmune communication pathways, and the downstream consequences of peripheral inflammation on the brain, we compared gene expression in the brains of mice following several different sterile (tumour necrosis factor (TNF) and 12-O-tetradecanoylphorbol-13-acetate (TPA) and toll-like-receptor-(TLR)-dependent (lipopolysaccharide (LPS), lipoteichoic acid (LTA) and Imiquimod) models of peripheral inflammation. We also compared gene expression in the brain with that of peripheral blood leucocytes (PBLs). Lastly, we explored a potential molecular mechanism by which inflammation originating in the periphery can induce transcriptional modulation in the brain.

Methods

Mice

Wild type C57BL/6 mice (7 to 8 weeks old, 20 to 25 g) were purchased from Harlan Laboratories. Mice were maintained in specific pathogen-free conditions in standard caging in the Central Research Facility at the University of Glasgow and treated with sterile (TNF and TPA) and TLR ligand-based (LPS, LTA and Imiquimod) inflammatory agents as described. For microarray experiments, a minimum of three biological replicates are required to allow statistical analysis of the data [14]. Three mice were used per study arm for all our microarray experiments and four or five mice each for qPCR-based experiments, to ensure the statistical robustness of the data. All experiments received ethical approval and were performed under the auspices of UK Home Office Licences.

Acute inflammatory models

For acute LPS-induced inflammation, mice were injected intraperitoneally (i.p.) with 100 µl of 1 mg/ml LPS ($\approx$4 mg/kg), derived from *Escherichia coli* serotype 055:B5 (Sigma, St. Louis, MO, USA, or an equivalent volume of vehicle (PBS). For TNFα- or LTA-induced inflammation, mice were injected intravenously (i.v.) with two doses of 1 µg recombinant TNFα (Peprotech, Rocky Hill, NJ, USA), two doses of 500 µg LTA (Sigma, St. Louis, MO, USA) or two doses of an equivalent volume (100 µl) of vehicle (sterile H_2O) at 0 and 24 hours. Mice were euthanized by CO_2 exposure 48 hours after initial injection and perfused for 5 minutes with 20 ml PBS.

Chronic inflammatory models

For chronic LPS-induced inflammation, and induction of endotoxin tolerance, mice received a daily i.p. injection of 100 µl of 0.5 mg/ml LPS ($\approx$2 mg/kg) (Sigma, St. Louis, MO, USA) or an equivalent volume (100 µl) of vehicle (PBS) for 2, 5 or 7 consecutive days. For skin-inflammation models, mice were shaved on their dorsal skin 24 hours

prior to receiving daily applications of ≈ 80 mg of 5% Imi-quimod (Aldara™, MEDA Ab, Stockholm, Sweden) cream [15], 150 μl of 100 μM TPA, or an equivalent volume of Vaseline (Unilever, Leatherhead, UK) or acetone control. Mice were treated for 5 consecutive days as described previously [15]. All mice were euthanized by CO_2 exposure 24 hours after final treatment and perfused for 5 minutes with 20 ml PBS.

ELISA

Blood was collected from tail veins (approximately 300 μl) prior to termination of the mice. Plasma was isolated from whole blood by centrifugation. Throughout the study, plasma concentrations of soluble mediators, IL-1β, TNFα and IL-6, were determined using DuoSet ELISA kits (R&D Systems, Minneapolis, MN, USA) according to the manufacturer's instructions.

RNA isolation from tissue and peripheral blood leucocytes

Whole brain tissue was snap frozen and stored at −80°C until use. Under RNase-free conditions, brains were homogenized using the TissueLyser LT (Qiagen, Hilden, Germany). RNA was extracted from homogenized tissue using Trizol® (Life Technologies, Invitrogen, Carlsbad, CA, USA) as described by the manufacturers. Isolated RNA was further purified and genomic DNA removed using an RNeasy Mini Kit (Qiagen, Hilden, Germany). Red blood cells were lysed from blood samples using red blood cell lysis buffer (Miltenyi, Cologne, Germany). Under RNase-free conditions, RNA was isolated and genomic DNA was removed from PBLs using an RNeasy Micro Kit (Qiagen, Hilden, Germany).

GeneChip microarray analysis

Microarray assays were performed in the Glasgow Polyomics Facility at the University of Glasgow [16]. Briefly, 1 μg of purified total RNA was amplified by *in-vitro* transcription and converted to sense-strand cDNA using a WT Expression kit (Life Technologies, Invitrogen, Carlsbad, CA, USA). cDNA was then fragmented and labelled using a GeneChip WT Terminal Labelling kit (Affymetrix, Santa Clara, CA, USA). Fragmented cDNA samples were then hybridized to GeneChip Mouse Gene 1.0 ST Arrays (Affymetrix, Santa Clara, CA, USA). Procedures were carried out as described by the manufacturers.

To maximize the identification of key differentially expressed genes we utilized two separate software analysis packages (Partek and GeneSpring) and focused on gene expression differences identified using both approaches. As shown in the results section, this reduced the number of genes requiring analysis and provided increased confidence in their validity.

Data generated using Partek Genomics Suite were normalized using the robust multichip average (RMA) method, adjusted for GC content. The normalized data were subsequently analyzed using one-way analysis of variance (ANOVA) to determine the significance of each gene in LPS-treated mice compared with vehicle-treated controls. Data generated using GeneSpring GX software were normalized using RMA 16. Normalized data were analyzed using unpaired *t* tests to determine the significance of gene expression differences in LPS-treated mice compared with vehicle-treated controls. In both analyses, *P* values were adjusted for multiple comparisons using the Benjamini-Hochberg multiple testing correction.

Gene ontology terms were assigned to differentially expressed genes using the Database for Annotation, Visualization and Integrated Discovery (DAVID) Bioinformatics Resources v6.7 [17]. Analysis was performed in accordance with two protocols outlined by Huang *et al.* [18,19]. Significance of enrichment was determined using a modified Fisher's exact test and a Benjamini-Hochberg multiple testing correction was used to correct for the rate of type I errors. Co-expression of a gene cluster was considered significant for $P ≤ 0.05$.

Genes were grouped into canonical pathways using Ingenuity Pathway Analysis software (Ingenuity® Systems [20]). Significance of differentially altered pathways was determined using a Fisher's exact test and a Benjamini-Hochberg multiple testing correction was used to correct for the rate of type I errors. Enrichment of a pathway was considered significant for $P ≤ 0.05$.

qPCR

Total RNA was reverse transcribed using Quantitect® Reverse Transcription kit (Qiagen, Hilden, Germany) using random primers. Quantitative real-time PCR (QPCR) amplifications were performed in triplicate using PerfeCTa® SYBR® Green FastMix® (Quanta Biosystems, Gaithersburg, MD, USA). A 500 μM mix of forward and reverse primers was used per reaction. Primers were designed using Primer3 Input software (version 0.4.0) and generated by IDT technologies. Primer sequences are listed in Additional file 1: Table S1. qPCR reactions were performed using a Prism® 7500HT Sequence Detection System (Life Technologies, Invitrogen, CA, USA) for 40 cycles, in accordance with the manufacturer's guidelines. The absolute copy number was calculated from a standard curve and normalized to a reference gene, TATA binding protein (TBP), as previously described [21]. Fold change values were calculated by comparing the normalized copy number of individual samples with the mean of the control samples.

Histology

Skin samples were fixed in 10% buffered formalin prior to processing and paraffin embedding. Processing was

232

performed using the Shandon Citadel 1000 automated tissue processor (Thermo scientific). Embedded tissue was then cut into 5 μm sections and stained with (H & E) to discern morphology.

Results

Peripheral LPS challenge triggers an inflammatory response in the brain

To induce systemic inflammation, mice were injected with a single high dose of LPS (100 μg i.p.); 6 hours following injection, plasma from all mice injected with LPS displayed significantly elevated levels of IL-1β and IL-6 (Figure 1A). Although TNFα was not elevated, it has previously been shown that TNFα levels peak in the circulation of C57BL/6 mice 2 hours following LPS injection

(100 μg i.p.) and then rapidly decline [22]. Levels of IL-1β returned to baseline between 6 and 12 hours following injection and IL-6 levels remained elevated until 48 hours. Thus, systemic LPS injection triggers a potent and rapid inflammatory response in the periphery.

Systemic administration of high doses of LPS is known to activate the innate immune system in the CNS, occurring throughout the circumventricular organs, the meninges and the parenchyma [23,24]. To determine what downstream effects this has on global gene expression throughout the brain, Affymetrix GeneChip microarrays were used to compare transcriptional profiles of brain tissue 48 hours after LPS or vehicle injection. The time point of 48 hours was selected to allow time for the transcription and translation of peripheral responses to LPS
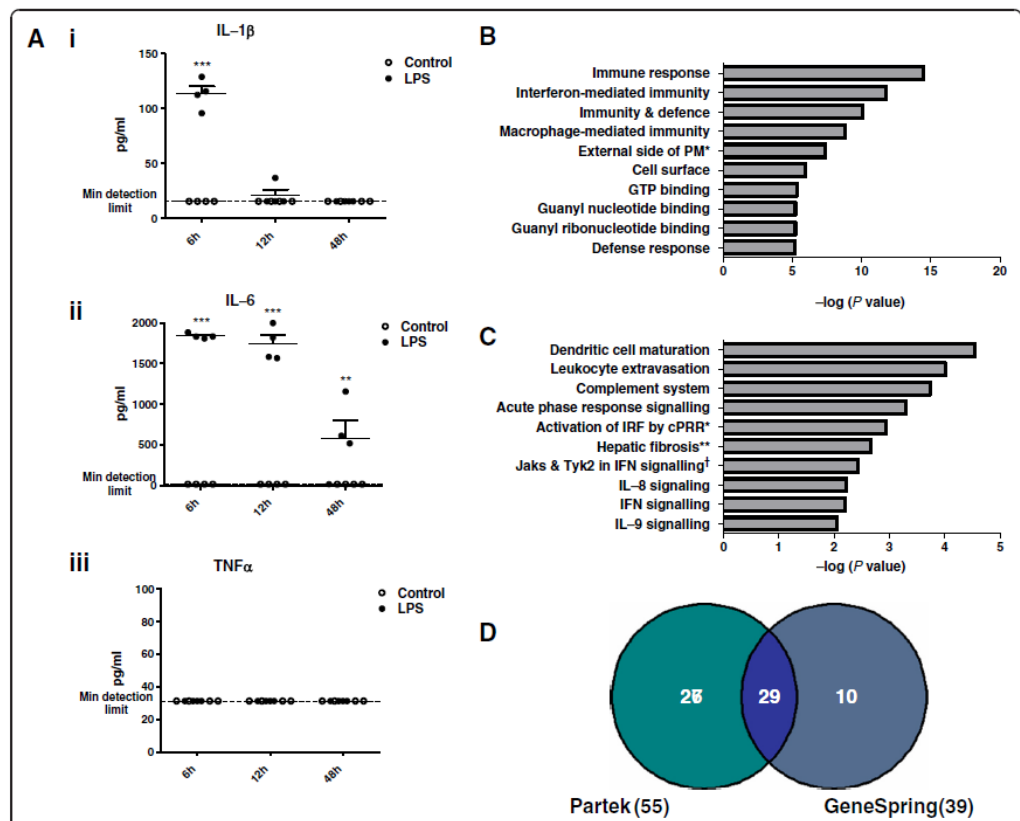
Figure 1 Systemic LPS injection results in an inflammatory response in the periphery and brain. (A) Plasma concentrations of (i) IL-1β, (ii) IL-6 and (iii) TNFα, 6, 12 and 48 hours following injection with LPS (100 μg i.p.) or vehicle. Data represent the mean ± the standard error of the mean (SEM). Significance was determined using two-way ANOVA: **$P \leq 0.01$, ***$P \leq 0.001$; $n = 4$/group. **(B)** Top enriched gene ontology classifications determined using DAVID Bioinformatics Resources. **(C)** Top significantly altered pathways determined using Ingenuity Pathway Analysis software. **(B,C)** Significance was calculated using Fisher's exact test. **(D)** Comparison of entities identified using Partek Genomics Suite and Genespring GX software packages as being differentially expressed by $\geq$ 2-fold.

and the subsequent initiation of transcriptional responses in the brain. Whilst it is not possible to define rigorously when these processes will have been completed, 48 hours was selected as a plausible time point. All mice were perfused extensively (20 ml over 5 minutes) with PBS to remove contaminating peripheral blood from the harvested brains. When analyzed using Partek Genomics Suite, 85 entities were differentially expressed in the brains by at least 1.5-fold (Additional file 2: Table S2). Therefore, 48 hours after challenge, the transcriptional profile of the brain is altered in response to systemic LPS-induced inflammation.

Differentially expressed genes with a fold change value of 1.5 or greater were subjected to gene ontology clustering using the DAVID Bioinformatics Resources. Amongst the most significantly enriched biological processes are: 'immune response', 'immunity and defence', 'macrophage-mediated immunity' and 'interferon-mediated immunity' (Figure 1B). This strongly implies the presence of a remotely triggered immune or inflammatory response in the brain.

To complement and validate the data generated using DAVID, the putative interactions and functional relationships between the protein products of the significantly altered genes were assessed using Ingenuity Pathway Analysis software. Significantly altered pathways included: 'activation of interferon regulatory factors (IRFs) by cytosolic pattern recognition receptors (cPRRs)', 'Jak1, Jak2 and Tyk2 in interferon signalling' and 'interferon signalling' (Figure 1C). The transcriptional enhancement of IFN signalling pathway components, coupled with the enrichment of genes involved in IFN-mediated immunity, suggests that systemic LPS challenge might induce an IFN response in the brain.

Analyzing the Affymetrix dataset using Partek Genomics Suite returned a list of 55 differentially expressed entities that satisfied a more stringent fold change cut-off of 2 (Additional file 2: Table S2). Prior to qPCR validation, with the aim of focusing only on the genes that are most robustly differentially expressed, the Affymetrix dataset was reanalyzed using GeneSpring GX analysis software, and the resulting list of significantly regulated genes was compared with that generated using Partek. The 39 entities identified by GeneSpring as being upregulated by at least 2-fold (Additional file 3: Table S3) were then compared with those identified using Partek (Figure 1D). Of the 29 entities that were common to both lists, 24 are known genes. These are grouped according to biological function in Table 1. Strikingly, over half of the genes in this list are interferon-stimulated genes (ISGs). This supports the hypothesis generated from the Ingenuity Pathway analysis; that IFN signalling is induced in the brain following peripheral LPS injection. As they have been simultaneously validated using two

Table 1 Functional properties of differentially expressed target genes

Gene symbol	Gene name
Interferon-stimulated genes	
Ctsc	Cathepsin C
Gbp2	Guanylate-binding protein 2
Gbp3	Guanylate-binding protein 3
Gbp6	Guanylate-binding protein 6
Gbp7	Guanylate-binding protein 7
Ifit1	Interferon-induced protein with tetratricopeptide repeats
Ifitm3	Interferon-induced transmembrane protein
Irgm1	Immunity-related GTPase, family M, member 1
Lgals3bp	Lectin, galactoside-binding, soluble, 3 binding protein
Oasl2	2'-5' Oligoadenylate synthetase-like 2
Rnf213	Ring finger protein 213
Rtp4	Receptor transporter protein 4
Sp100	Nuclear antigen Sp100
Stat1	Signal transducer and activator of transcription 1
Acute phase reactants	
Lcn2	Lipocalin 2
Saa3	Serum amyloid A3
Serpina3n	Serine (or cysteine) peptidase inhibitor, clade A
Immunity system components	
C4b |*C4a*	Complement component 4B (Childo blood group) | complement 4A (Rodgers blood group)
Fcgr4	Fc receptor, IgG, low affinity IV
H2-K1	Histocompatibility 2, K1, K region
Pglyrp1	Peptidoglycan recognition protein 1
Cell surface molecules	
Il2rg	Interleukin 2 receptor, gamma chain
Ly6a	Lymphocyte antigen 6 complex, locus A
mRNA editing	
Apobec3	Apolipoprotein B mRNA editing enzyme

bioinformatics approaches, ISGs from this sub-list of genes (Table 1) have subsequently been focused on for the remainder of the study, with the assumption that these genes are most likely to be biologically relevant.

Differential expression of ISGs was confirmed using qPCR

Using RNA isolated from an independent experiment, ISG upregulation in the brain following LPS injection was then validated using qPCR. Even though brains were perfused, to control for the possibility of a residual contaminating signal coming from the peripheral blood, the expression of ISGs was compared in the brain and PBLs. In addition to target ISGs (Table 1), upregulation of genes encoding the classic interferon-inducible chemokine

CXCL10, and IRF7, were also validated by qPCR, as was the upregulation of the gene encoding the negative regulator of IRF7, guanylate-binding protein (GBP) 4. Owing to the relatively high proportion of GBPs in the dataset, *Gbp6* and *Gbp7* were arbitrarily excluded from validation. With the exception of *Sp100* and *Stat1*, all ISGs assayed were significantly upregulated in the brains of mice challenged with systemic LPS compared with vehicle controls (Figure 2A, Table 2). Although many of the genes were upregulated to a similar extent in both the brain and PBLs, in terms of fold change, *Cxcl10, Irf7, Gbp3* and *Gbp4* were upregulated independently in the brain. Thus, our data demonstrate a differential pattern of gene expression in the brain from that of the PBLs. Not only do these crucial observations provide evidence of a brain-specific inflammatory response as a result of systemic

LPS injection, but they support the validity of the dataset; confirming an upregulation of target genes whilst simultaneously verifying that the observed fold changes in the brain are not a secondary effect of blood contamination.

ISGs are rapidly induced in the brain following systemic LPS injection

In the immediate hours following a single injection of LPS, the response in the brain is well characterized. Largely encompassing an acute phase response, the majority of reported effects in the brain are known to peak within 12 hours following peripheral LPS injection [24-26]. To determine whether the upregulation of ISGs is a remnant of an earlier response, we looked at expression levels of a selection of ISGs in the brain 6 hours and 12 hours following injection and compared them

Figure 2 ISG induction in the brain and blood of LPS-treated mice. (A) Relative expression of ISGs in the brain and PBLs, 48 hours after LPS injection (100 μg i.p.) compared with vehicle injection. **(B)** Relative expression of ISGs in the brain, 6, 12 and 48 hours after LPS injection compared with vehicle injection. Gene expression normalized to TBP. Fold change calculated by comparing the normalized copy number in each sample with the mean of the vehicle-injected controls. Data represent mean ± SEM. Statistical significance was determined using two-way ANOVA: *$P \leq 0.05$, **$P \leq 0.01$, ***$P \leq 0.001$; $n = 4$/group.

Table 2 Significance of differentially expressed target genes following acute inflammatory models

Gene	Significance of fold change in treatment group compared to vehicle control group (↑, upregulated; ↓, downregulated)					
	LPS (*P*)		TNFα (*P*)		LTA (*P*)	
	Brain	PBLs	Brain	PBLs	Brain	PBLs
Ctsc	↑ 0.0332	↑ 0.0283	Not significant	Not significant	Not significant	Not significant
Cxcl10	↑ 0.0122	↑ 0.0329	Not significant	↓ 0.0016	Not significant	Not significant
Gbp2	↑ 0.0160	Not significant	Not significant	↓ 0.0288	Not significant	Not significant
Gbp3	↑ 0.0197	Not significant	Not significant	↓ 0.0179	Not significant	Not significant
Gbp4	↑ 0.0030	Not significant	↑ 0.0334	↓ 0.0478	Not significant	Not significant
Ifit1	↑ 0.0027	↑ 0.0010	Not significant	Not significant	Not significant	Not significant
Ifitm3	↑ 0.0016	↑ 0.0001	Not significant	Not significant	Not significant	↑ 0.0481
Igrm1	↑ 0.0343	↑ 0.0311	Not significant	Not significant	Not significant	Not significant
Irf7	↑ 0.0004	Not significant	Not significant	Not significant	Not significant	Not significant
Lgals3bp	↑ 0.0012	↑ 0.0055	Not significant	Not significant	Not significant	↑ 0.0030
Oasl2	↑ 0.0075	↑ 0.0008	Not significant	Not significant	Not significant	Not significant
Rtp4	↑ 0.0044	↑ 0.0010	Not significant	Not significant	Not significant	Not significant
Sp100	Not significant	↓ 0.0101	Not significant	↓ 0.0062	Not significant	Not significant
Stat1	Not significant	Not significant	↑ 0.0252	↓ 0.0371	Not significant	Not significant

Significance of differential gene expression was calculated separately for individual genes in each tissue using an unpaired *t* test.

with the expression levels at 48 hours (Figure 2B). With the exception of *Cxcl10*, the expression levels of which are significantly reduced at 48 hours, no significant differences were observed in the expression levels of ISGs at 48 hours, compared with either 6 hours or 12 hours. Thus, ISGs are induced in the brain by 6 hours following systemic LPS injection and this response persists until 48 hours after injection.

ISGs were not induced in the brain following peripheral TNFα-induced inflammation

One of the accepted routes of brain sensitization following systemic LPS challenge is the activation of endothelial cells in the brain vasculature by circulating cytokines [26]. To determine whether circulating cytokines were sufficient to induce the expression of ISGs in the brain, mice were challenged with recombinant murine TNFα (1 µg i.v. at 0 and 24 hours). After 48 hours, the expression of the target ISGs was quantified by qPCR. *Gbp4* and *Stat1* were the only ISGs to show slight but significant elevation (1.59- and 1.26-fold, respectively) in the brain following TNFα-injection (Figure 3, Table 2). In fact, several ISGs were significantly downregulated in matched PBLs. Given that the concentrations of systemic TNFα that would result from the intravenous injection of 1 µg would be considerably higher than those induced by systemic LPS (levels were undetectable, as shown in Figure 1), these data collectively suggest that central ISG induction following LPS challenge cannot be accounted for simply on the basis of elevated TNFα in the circulation.

Inflammatory cytokines and ISGs remain elevated in the brain during endotoxin tolerance

Although ISGs were not induced in the brain in response to circulating TNFα, the previous experiment did not rule out the contribution of other inflammatory cytokines. With the aim of establishing the temporal pattern of ISG expression in the brain and PBLs in the context of endotoxin tolerance, when inflammatory cytokine production is known to be ameliorated in the periphery, we injected mice with a single dose of LPS (50 µg i.p.) daily for 2, 5 or 7 consecutive days. This contrasts with the use of a single application of 100 µg for the initiation of acute LPS effects. Endotoxin tolerance is an important defence mechanism designed to protect the host against endotoxic shock. In addition to eliciting expression of a number of proinflammatory genes, initial cellular exposure to LPS triggers the simultaneous downregulation of TLR expression and the induction of several inhibitory molecules that negatively regulate TLR signalling [27]. This culminates in a transient inactivation of various proinflammatory genes by leucocytes in the periphery, including genes encoding the inflammatory cytokines TNFα, IL-1β and IL-6. At the same time, less potentially pathogenic genes are primed, such as antimicrobial effectors [28]. As a consequence, repeated exposure to TLR ligands leads to a dampening of the proinflammatory milieu without compromising host defence. Conversely, cytokine expression has been shown to continue in the brain during endotoxin tolerance [29,30].

Consistent with previous reports, *Il1b* and *Tnfa* were independently upregulated in the brain following multiple LPS challenges (Figure 4A). As anticipated, under

Figure 3 Response in the brain to systemic administration of TNF. Mice were injected with two doses of TNFα (1 µg i.v.) or vehicle at 0 and 24 hours and relative expression of interferon-stimulated genes (ISGs) in the brain and peripheral blood leucocytes (PBLs) was determined 48 hours after initial injection. Gene expression was normalized to TBP. Fold change was calculated by comparing the normalized copy number in each sample with the mean of the vehicle-injected control group. Data represent mean ± SEM.

these conditions, inflammatory cytokine transcripts were not induced in PBLs. Interestingly, whilst ISG expression is rapidly dampened in the periphery, expression continues in the brain, gradually decreasing between days 2 and 7 (Figure 4B). At day 2, all ISGs were significantly upregulated in the brains of the LPS-challenged mice. At the same time point, most ISGs were similarly upregulated in PBLs as in brain, with the exception of *GBP4*, which was downregulated. On day 5, ISGs remained induced in the brain. All but *Cxcl10* were significantly upregulated at this time point. In contrast, the same genes were significantly downregulated by PBLs. By day 7, ISG transcript levels began to return to baseline, with the exception of *Irf7*, which remained significantly induced. Thus, in comparison with PBLs, it would appear that the brain exhibits a specific and prolonged response to repeated LPS challenge. Not only does this further suggests that LPS-induced ISG expression in the brain is unlikely to be a downstream consequence of peripheral inflammatory cytokines, it again suggests differential mechanism of gene regulation in the brain and the PBLs.

Systemic administration of LTA was unable to induce an IFN response in the brain

LPS binds to TLR4 and exerts its effects via one of two downstream signalling pathways (Figure 5): activation of NFκB through the classical MyD88-dependent pathway, which results in inflammatory cytokine induction, or IRF3 activation through the domain-containing-adaptor-protein-(TRIF)-dependent pathway, which triggers IFNβ production [31]. As many of the genes upregulated in response to LPS can be regulated by IFNs, it is possible that they are being expressed downstream of LPS-induced

IFNβ production. To further investigate this possibility, mice were challenged systemically with two high doses of the TLR2 ligand, LTA (500 µg i.v. at 0 and 24 hours). TLR2 ligation can only activate NFκB through the classical pathway [31], thereby eliminating the possibility of TRIF-dependent signalling (Figure 5). As we hypothesized, no significant ISG induction was detected in the brain following LTA-injections (Figure 6, Table 2). *Ifitm3* and *Lgals3bp* were the only ISGs to be significantly induced in PBL. Consequently, activation of the MyD88-dependent pathway alone is insufficient to mimic the brain inflammation that occurs following systemic LPS challenge.

Brain-specific ISG induction is seen following induction of psoriasis-like skin inflammation

Our data demonstrate that following acute or chronic LPS challenge, the response in the brain culminates in the transcription of a panel of ISGs. To determine whether TLR-induced inflammation could induce ISG expression in a tissue-specific peripheral, but not systemic, model of inflammation, we decided to assess the expression of target ISGs in mouse brains obtained following topical, cutaneous administration of a TLR7 agonist. Mice were challenged daily with topical applications of Imiquimod (IMQ) cream on their dorsal skin for five consecutive days and sacrificed for tissue harvesting 24 hours later. This is a standard method used to create a psoriasis-like pathology [15]. After two applications, all IMQ-treated mice showed signs of psoriasis-like skin inflammation, characterized by skin thickening, erythema and scaling. The severity of the symptoms peaked after the fourth application (data not shown). Figure 7A shows representative histological images of the skin inflammation

Figure 4 ISG induction in the brain and PBL of mice treated daily with LPS. Mice were injected daily with LPS (50 µg i.p.) or vehicle. **(A,B)** Relative gene expression in the brains and PBLs of mice, 2, 5 and 7 days following initial injection. **(A)** Relative expression of cytokines; (i) Il1b, (ii) Il6 and (iii) Tnfa. **(B)** Relative expression of target ISGs; (i) Cxcl10, (ii) Ifit1, (iii) Irf7, (iv) Oasl2 and (v) Gbp4. Gene expression normalized to TBP. Fold change was calculated by comparing the normalized copy number in each sample with the mean of the vehicle-injected controls. Data represent mean ± SEM. Statistical significance was determined using two-way ANOVA: *$P \leq 0.05$, **$P \leq 0.01$, ***$P \leq 0.001$; $n = 4$/group.

present after five applications of IMQ or control cream. Like human psoriasis lesions, dorsal skin samples from IMQ-treated mice display epidermal hyperplasia. No signs of inflammation were observed following control cream (Vaseline)-treatment. The concentration of circulating IL-1β, IL-6 and TNFα was measured by ELISA. No significant increase in circulating cytokines was detected 24 hours after the final application of IMQ (Figure 7B). Thus, daily applications of IMQ induce a psoriasis-like skin pathology that causes local, but not systemic, inflammation.

At 24 hours after the final application, all target ISGs were significantly upregulated in the brains of IMQ-treated mice (Figure 7C, Table 3). Importantly, these data identify a common transcriptional signature in the brains of LPS- and IMQ-treated mice. Strikingly, in contrast with the brain, ISG expression in the PBLs did not significantly deviate from baseline. The difference in ISG regulation in the brain and PBLs following IMQ-treatment again highlights a brain-specific response to peripheral inflammation that does not appear to be mediated by circulating inflammatory cytokines.

Figure 5 TLR-induced signalling pathways. When activated, toll-like receptors (TLRs) either heterodimerize, such as TLR2 with either TLR1 or TLR6, or homodimerize to induce signalling pathway activation. Signalling is regulated by adaptor molecules. MyD88 is an adaptor used by all TLRs aside from TLR3. TLR7 recruits MyD88 directly, whereas TLR4 and TLR2 recruit MyD88 through bridging adapter TIRAP. MyD88 recruitment ultimately leads to the activation of nuclear transcription factor NFκB by releasing the p50 and p65 subunits from the NFκB inhibitor IκB. Activated NFκB then translocates to the nucleus to induce the expression of inflammatory cytokines. When activated by TLR7, MyD88 can also induce the phosphorylation and dimerization of interferon regulatory factor 7 (IRF7). This activation of IRF7 triggers the induction of IFNα. An alternative signalling pathway downstream of TLR4 involves the recruitment of adaptor molecule TRIF through bridging protein TRAM. This ultimately leads to activation of IRF3 and subsequent IFNβ induction (For review see [31]). Note that for simplicity the full complement of extracellular proteins involved in TLR for function are not represented in this diagram. Specifically, TLR4 requires MD-2, CD14 and LPS binding protein to bind LPS efficiently.

Lack of ISG induction following sterile psoriasis-like skin inflammation

Central ISG expression was also measured in a sterile model of skin inflammation to determine the importance of TLR ligation. Mice were challenged daily with topical applications of 12-O-tetradecanoylphorbol-13-acetate (TPA) on their dorsal skin for five consecutive days. Like human psoriasis and IMQ-treatment, TPA is thought to induce skin inflammation in an IL-17 and IL-23-dependent manner [32]. However, unlike IMQ,

Figure 6 Response in the brain to systemic administration of LTA. Mice were injected with two doses of LTA (500 µg i.v.) or vehicle at 0 and 24 hours and relative expression of interferon-stimulated genes (ISGs) in the brain and peripheral blood leucocytes (PBLs) was determined 48 hours after initial injection. Gene expression was normalized to TBP. Fold change was calculated by comparing the normalized copy number in each sample with the mean of the vehicle-injected control group. Data represent mean ± SEM; $n = 4$/group.

Figure 7 (See legend on next page.)

(See figure on previous page.)
Figure 7 Response in the brain to IMQ-induced skin inflammation. Mice were treated daily with IMQ or control cream (Vaseline). Samples taken 24 hours after the fifth application. **(A)** H & E stains of (i) IMQ-treated and (ii) Vaseline-treated skin. Scale bar: 100 μm. Arrow points to epidermal hyperplasia. **(B)** Plasma concentrations of (i) IL-1β, (ii) IL-6 and (iii) TNFα. **(C)** Relative expression of ISGs, normalized to TBP, in brain and PBLs of IMQ-treated compared with Vaseline-treated mice. Fold change was calculated by comparing the normalized copy number in each sample to the mean of the vehicle-injected control group. Data represent mean ± SEM; n = 5/group.

TPA does not result in TLR ligation. After two applications, all TPA-treated mice displayed psoriasis-like skin thickening, lesioning and erythema. Symptoms gradually worsened until the end of the model (data not shown). Figure 8A shows histological images of the skin inflammation present after five applications of TPA or vehicle. Like those from the IMQ model, dorsal skin samples taken from TPA-treated mice displayed epidermal hyperplasia. Only mild signs of inflammation were observed when mice were treated with the vehicle. At 24 hours after the final application, no inflammatory cytokines were detected in the circulation (Figure 8B). Therefore, topical applications of TPA induce a psoriasis-like pathology with similar characteristics to the inflammatory skin condition induced by IMQ.

Despite both the IMQ- and TPA-treated mice displaying similar skin pathology, no upregulated ISG expression was detected in the brains of the TPA-treated mice compared with the vehicle-treated control group (Figure 8C, Table 3). This is in stark contrast to the significant induction of all target ISGs that was detected in the brains of the IMQ-treated group. *Gbp4* was the only ISG to be significantly upregulated in the PBL. The lack of response in the brain following TPA-treatment suggests that ISG induction in

the brains of IMQ-treated mice is not a generic effect of skin inflammation.

Discussion
Here we demonstrate that systemic administration of LPS or topical administration of IMQ alters the gene expression profile in the brain, inducing the expression of a common panel of ISGs. Differing in kinetics and magnitude, this response is distinct from that of the PBLs. We also highlight ISG induction as a consequence of a TLR-induced type I IFN response. As considerable evidence links type I IFNs to psychiatric disorders [8-12], IFN production in the brain may represent a significant mechanism, linking peripheral TLR-induced inflammation with neuropsychiatric symptoms.

The differential response of brain and PBLs provides evidence of a brain-specific inflammatory response resulting from both acute and chronic LPS challenge and IMQ-induced skin inflammation. This was not a downstream by-product of peripheral inflammatory cytokine production as similar sterile models of inflammation failed to induce the same response. Furthermore, ISG expression remained elevated in the brain following daily LPS or IMQ administration, long after the peripheral cytokine

Table 3 Significance of differentially expressed target genes following chronic inflammatory models

Gene	Significance of fold change in treatment group compared to vehicle control group (↑, upregulated; ↓, downregulated)			
	IMQ (*P*)		TPA (*P*)	
	Brain	PBLs	Brain	PBLs
Ctsc	↑ 0.0187	Not significant	↓ 0.0026	Not significant
Cxcl10	↑ 0.0156	Not significant	Not significant	Not significant
Gbp2	↑ 0.0177	Not significant	↓ 0.0401	Not significant
Gbp3	↑ 0.0032	Not significant	Not significant	Not significant
Gbp4	↑ 0.0254	Not significant	Not significant	↓ 0.0490
Ifit1	↑ 0.0053	Not significant	Not significant	Not significant
Ifitm3	↑ 0.0010	Not significant	Not significant	Not significant
Igrm1	↑ 0.0005	Not significant	Not significant	Not significant
Irf7	↑ 0.0029	Not significant	Not significant	Not significant
Lgals3bp	↑ 0.0003	Not significant	Not significant	Not significant
Oasl2	↑ 0.0015	Not significant	Not significant	Not significant
Rtp4	↑ 0.0002	Not significant	Not significant	Not significant
Sp100	↑ 0.0087	Not significant	Not significant	Not significant
Stat1	↑ 0.0043	Not significant	↓ 0.0241	Not significant

Significance of differential gene expression was calculated separately for individual genes in each tissue using an unpaired *t* test.

Figure 8 (See legend on next page.)
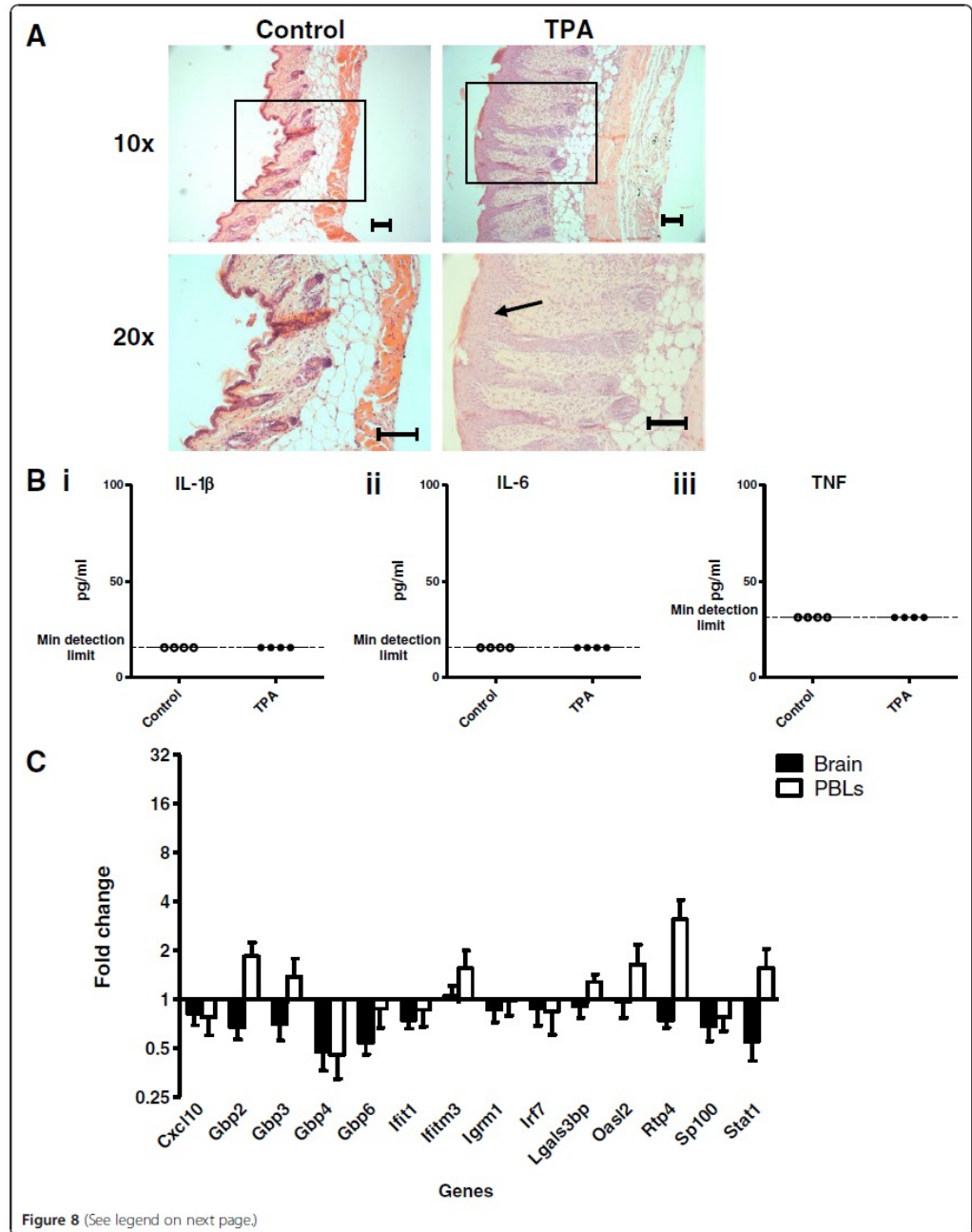
(See figure on previous page.)
Figure 8 Response in the brain to TPA-induced skin inflammation. Mice were treated daily with five topical applications of TPA or acetone. Samples were taken 24 hours after fifth application. **(A)** H & E stains of (i) TPA-treated and (ii) acetone-treated skin. Scale bar: 100 μm. Arrow points to epidermal hyperplasia. **(B)** Plasma concentrations of (i) IL-1β, (ii) IL-6 and (iii) TNFα. **(C)** Relative expression of ISGs, normalized to TBP, in brain and PBLs of TPA-treated compared to acetone-treated mice. Fold change was calculated by comparing the normalized copy number in each sample to the mean of the vehicle-injected control group. Data represent mean ± SEM; *n* = 5/group.

response was attenuated. Thus, ISG induction was brain-specific and not mediated by peripheral inflammatory cytokines in either the skin or the circulation.

As type I IFN production is a classic hallmark of both TLR4-induced IRF3 activation and TLR7-induced IRF7 activation, it would be attractive to propose that a TLR-induced IFN response is responsible for the induction of ISGs in the brain. Supporting this hypothesis, Skelly and colleagues documented a central induction of IFNβ within 2 hours of systemic LPS challenge [33]. No central or peripheral type I IFN induction was observed following systemic TNFα or IL-1β injection. Furthermore, Leung and colleagues demonstrated that, following systemic administration of a TLR7 agonist, IFNα was induced in the brain in an IRF7-dependent manner [34]. Both TLR4 and TLR7 are widely expressed in the brain. Although, to our knowledge, the capacity of IMQ to cross the blood–brain barrier (BBB) has not been investigated, a study with radiolabelled LPS suggested that negligible levels cross the intact BBB [35]. Therefore, it is possible that the upregulation of target ISGs, following peripheral LPS or IMQ challenge, occurs via an indirect route downstream of IRF activation in the periphery. This may involve the direct action of peripherally produced IFNs on the CNS, the BBB or afferent nerves. Alternatively, introducing high or repeated doses of LPS or IMQ to the periphery may cause BBB breakdown, facilitating the direct action of these TLR ligands on the brain.

To further investigate the involvement of IRF activation in the neuroinflammation induced by systemic LPS injection, mice were challenged with the TLR2 ligand LTA. Consistent with previous reports [36], no response was detectable in the brains of mice following peripheral LTA injection. This lack of response may be due to the inability of TLR2 ligands to stimulate IRF-dependent signalling. Conversely, peripheral stimulation with TLR3 ligands is known to trigger brain inflammation [37,38]. Like the MyD88-independent pathway downstream of TLR4, TLR3 signals through the adaptor molecule TRIF to activate IRF3, ultimately triggering IFNβ production [31]. Subsequently, it would appear that IRF-dependent signalling, whether it occurs in the periphery or the brain, may be a requirement of ISG induction in the brain following systemic administration of TLR ligands.

As described, type I IFN therapy is intrinsically linked to severe neuropsychiatric disorders, mainly major depression [8-12]. It is well known that injecting rodents with LPS initiates a number of behavioural adaptations, including a depression-like behaviour that perseveres after the other sickness behaviours have resolved [1]. A recent report has also linked IMQ-treatment to the development of sickness behaviours in rats [39]. The elevated transcription of type I ISGs in the brain following LPS or IMQ challenge is a strong indication that type I IFNs are produced during these models. As this family of cytokines are well known for their effects on behaviour, type I IFN production in either the periphery or in the brain, following peripheral LPS or IMQ challenge could contribute to the onset of depression-like behaviours in rodents. Formal demonstration of this will require the use of rodent behavioural models in conjunction with appropriate gene-deficient mice.

Conclusions

Toll-like receptor ligands have the capacity to modulate ISG expression distally in a manner that may be dependent on TLR-induced type I IFN production. Whether type I IFNs are produced in the brain or whether peripherally induced IFNs directly access the brain to modulate ISG expression remains open to further investigation; as does the downstream effects of central ISG induction. Owing to the well-established link between type I IFNs and depression, TLR-induced IFN production is worth investigating as a potential key mechanism, linking peripheral inflammation with sickness behaviour.

Additional files

Additional file 1: Table S1. Primer sequences.

Additional file 2: Table S2. Analysis of differentially expressed entities identified using Partek.

Additional file 3: Table S3. Analysis of differentially expressed entities identified using GeneSpring.

Abbreviations

ANOVA: analysis of variance; BBB: blood–brain barrier; CNS: central nervous system; cPRR: cytosolic pattern recognition receptor; DAVID: Database for Annotation, Visualization and Integrated discovery; ELISA: enzyme-linked immunosorbent assay; GBP: guanylate-binding protein; H & E: haematoxylin and eosin; IFN: interferon; IL: interleukin; IMQ: Imiquimod; i.p.: intraperitoneally; IRF: interferon regulatory factor; ISG: interferon-stimulated gene; i.v.: intravenously; IκB: NFκB inhibitor; LPS: lipopolysaccharide; LTA: lipoteichoic acid; NFκB: nuclear factor κ-light-chain-enhancer of activated B cells; PBL: peripheral blood leucocyte; PBS: phosphate-buffered saline; qPCR: quantitative polymerase chain reaction; RMA: robust multichip average; SEM: standard error of the mean; TBP: TATA

binding protein; TIR: Toll/interleukin-1 receptor; TLR: toll-like receptor; TNF: tumour necrosis factor; TPA: 12-O-tetradecanoylphorbol-13-acetate; TRIF: domain-containing adaptor protein.

References
1. Dantzer R, O'Connor JC, Freund GG, Johnson RW, Kelley KW: From inflammation to sickness and depression: when the immune system subjugates the brain. *Nat Rev Neurosci* 2008, **9**:46–56.
2. Addolorato G, Capristo E, Stefanini GF, Gasbarrini G: Inflammatory bowel disease: a study of the association between anxiety and depression, physical morbidity, and nutritional status. *Scand J Gastroenterol* 1997, **32**:1013–1021.
3. Dickens C, McGowan L, Clark-Carter D, Creed F: Depression in rheumatoid arthritis: a systematic review of the literature with meta-analysis. *Psychosom Med* 2002, **64**:52–60.
4. Tyring S, Gottlieb A, Papp K, Gordon K, Leonardi C, Wang A, Lalla D, Woolley M, Jahreis A, Zitnik R, Cella D, Krishnan R, Tyring S, Gottlieb A, Papp K, Gordon K, Leonardi C, Wang A: Etanercept and clinical outcomes, fatigue, and depression in psoriasis: double-blind placebo-controlled randomised phase III trial. *Lancet* 2007, **367**:29–35.
5. Chai Z, Gatti S, Toniatti C, Poli V, Bartfai T: Interleukin (IL)-6 gene expression in the central nervous system is necessary for fever response to lipopolysaccharide or IL-1 β: a study on IL-6-deficient mice. *J Exp Med* 1996, **183**:311–316.
6. Bluthé RM, Pawlowski M, Suarez S, Parnet P, Pittman Q, Kelley KW, Dantzer R: Synergy between tumor necrosis factor α and interleukin-1 in the induction of sickness behavior in mice. *Psychoneuroendocrinology* 1994, **19**:197–207.
7. Dantzer R: Cytokine-induced sickness behavior: where do we stand? *Brain Behav Immun* 2001, **15**:7–24.
8. Kraus MR, Schäfer A, Faller H, Csef H, Scheurlen M: Psychiatric symptoms in patients with chronic hepatitis C receiving interferon alfa-2b therapy. *J Clin Psychiatry* 2003, **64**:708–714.
9. Kraus MR, Schäfer A, Schöttker K, Keicher C, Weissbrich B, Hofbauer I, Scheurlen M: Therapy of interferon-induced depression in chronic hepatitis C with citalopram: a randomised, double-blind, placebo-controlled study. *Gut* 2008, **57**:531–536.
10. Miyaoka H, Otsubo T, Kamijima K, Ishii M, Onuki M, Mitamura K: Depression from interferon therapy in patients with hepatitis C. *Am J Psychiatry* 1999, **156**:1120.
11. Musselman DL, Lawson DH, Gumnick JF, Manatunga AK, Penna S, Goodkin RS, Greiner K, Nemeroff CB, Miller AH: Paroxetine for the prevention of depression induced by high-dose interferon alfa. *N Engl J Med* 2001, **344**:961–966.
12. Neilley LK, Goodin DS, Goodkin DE, Hauser SL: Side effect profile of interferon beta-1b in MS: results of an open label trial. *Neurology* 1996, **46**:552–553.
13. Raison CL, Capuron L, Miller AH: Cytokines sing the blues: inflammation and the pathogenesis of depression. *Trends Immunol* 2006, **27**:24–31.
14. How to Design a Successful Microarray Experiment. [www.brc.dcs.gla.ac.uk/~rb106x/microarray_tips.htm]
15. van der Fits L, Mourits S, Voerman JS, Kant M, Boon L, Laman JD, Cornelissen F, Mus AM, Florencia E, Prens EP, Lubberts E: Imiquimod-induced psoriasis-like skin inflammation in mice is mediated via the IL-23/IL-17 axis. *J Immunol* 2009, **182**:5836–5845.
16. Glasgow Polyomics: Glasgow Polyomics. [www.gla.ac.uk/colleges/mvls/researchinstitutes/gpf]
17. DAVID Bioinformatics Resources 6.7. [http://david.abcc.ncifcrf.gov/]
18. Huang DW, Sherman BT, Lempicki RA: Systematic and integrative analysis of large gene lists using DAVID Bioinformatics Resources. *Nat Protocols* 2008, **4**:44–57.
19. Huang DW, Sherman BT, Lempicki RA: Bioinformatics enrichment tools: paths toward the comprehensive functional analysis of large gene lists. *Nucleic Acids Res* 2009, **37**:1–13.
20. Ingenuity®. [www.ingenuity.com]
21. McKimmie CS, Fazakerley JK: In response to pathogens, glial cells dynamically and differentially regulate toll-like receptor gene expression. *J Neuroimmunol* 2005, **169**:116–125.
22. Jones KL, Mansell A, Patella S, Scott BJ, Hedger MP, de Kretser DM, Phillips DJ: Activin A is a critical component of the inflammatory response, and its binding protein, follistatin, reduces mortality in endotoxemia. *Proc Natl Acad Sci* 2007, **104**:16239–16244.
23. Nadeau S, Rivest S: Effects of circulating tumor necrosis factor on the neuronal activity and expression of the genes encoding the tumor necrosis factor receptors (p55 and p75) in the rat brain: a view from the blood–brain barrier. *Neuroscience* 1999, **93**:1449–1464.
24. Quan N, Whiteside M, Herkenham M: Time course and localization patterns of interleukin-1β messenger RNA expression in brain and pituitary after peripheral administration of lipopolysaccharide. *Neuroscience* 1998, **83**:281–293.
25. Buttini M, Boddeke H: Peripheral lipopolysaccharide stimulation induces interleukin-1β messenger RNA in rat brain microglial cells. *Neuroscience* 1995, **65**:523–530.
26. Serrats J, Schiltz JC, García-Bueno B, van Rooijen N, Reyes TM, Sawchenko PE: Dual roles for perivascular macrophages in immune-to-brain signaling. *Neuron* 2010, **65**:94–106.
27. Liew FY, Xu D, Brint EK, O'Neill LA: Negative regulation of toll-like receptor-mediated immune responses. *Nat Rev Immunol* 2005, **5**:446–458.
28. Foster SL, Hargreaves DC, Medzhitov R: Gene-specific control of inflammation by TLR-induced chromatin modifications. *Nature* 2007, **447**:972–978.
29. Chen R, Zhou H, Beltran J, Malellari L, Chang SL: Differential expression of cytokines in the brain and serum during endotoxin tolerance. *J Neuroimmunol* 2005, **163**:53–72.
30. Faggioni R, Fantuzzi G, Villa P, Buurman W, van Tits LJ, Ghezzi P: Independent down-regulation of central and peripheral tumor necrosis factor production as a result of lipopolysaccharide tolerance in mice. *Infect Immun* 1995, **63**:1473–1477.
31. Akira S, Takeda K: Toll-like receptor signalling. *Nat Rev Immunol* 2004, **4**:499–511.
32. Nakajima K, Kanda T, Takaishi M, Shiga T, Miyoshi K, Nakajima H, Kamijima R, Tarutani M, Benson JM, Elloso MM, Gutshall LL, Naso MF, Iwakura Y, DiGiovanni J, Sano S: Distinct roles of IL-23 and IL-17 in the development of psoriasis-like lesions in a mouse model. *J Immunol* 2011, **186**:4481–4489.
33. Skelly DT, Hennessy E, Dansereau MA, Cunningham C: A systematic analysis of the peripheral and CNS effects of systemic LPS, IL-1β, TNF-α and IL-6 challenges in C57BL/6 mice. *PLoS One* 2013, **8**:e69123.
34. Leung PY, Stevens SL, Packard AE, Lessov NS, Yang T, Conrad VK, van den Dungen NN, Simon RP, Stenzel-Poore MP: Toll-like receptor 7 preconditioning induces robust neuroprotection against stroke by a novel type I interferon-mediated mechanism. *Stroke* 2012, **43**:1383–1389.
35. Banks WA, Robinson SM: Minimal penetration of lipopolysaccharide across the murine blood–brain barrier. *Brain Behav Immun* 2010, **24**:102–109.
36. Laflamme N, Soucy GV, Rivest S: Circulating cell wall components derived from Gram-negative, not Gram-positive, bacteria cause a profound induction of the gene-encoding Toll-like receptor 2 in the CNS. *J Neurochem* 2001, **79**:648–657.
37. Field R, Campion S, Warren C, Murray C, Cunningham C: Systemic challenge with the TLR3 agonist poly I:C induces amplified IFNα/β and IL-1β responses in the diseased brain and exacerbates chronic neurodegeneration. *Brain Behav Immun* 2010, **24**:996–1007.

38. Konat GW, Borysiewicz E, Fil D, James I: Peripheral challenge with double-stranded RNA elicits global up-regulation of cytokine gene expression in the brain. *J Neurosci Res* 2009, **87**:1381–1388.
39. Damm J, Wiegand F, Harden LM, Gerstberger R, Rummel C, Roth J: Fever, sickness behavior, and expression of inflammatory genes in the hypothalamus after systemic and localized subcutaneous stimulation of rats with the toll-like receptor 7 agonist Imiquimod. *Neuroscience* 2012, **201**:166–183.

List of References

1.   Stovner, L.J., Hoff, J.M., Svalheim, S. & Gilhus, N.E. Neurological disorders in the Global Burden of Disease 2010 study. *Acta neurologica Scandinavica. Supplementum*, 1-6 (2014).
2.   Morris, N. (The Independent, www.independent.co.uk; 2011).
3.   Psychiatrists, R.C.o. 48 www.rcpsyche.co.uk; 2010).
4.   Miller, A.H., Maletic, V. & Raison, C.L. Inflammation and its discontents: the role of cytokines in the pathophysiology of major depression. *Biological psychiatry* **65**, 732-741 (2009).
5.   Schiepers, O.J., Wichers, M.C. & Maes, M. Cytokines and major depression. *Progress in neuro-psychopharmacology & biological psychiatry* **29**, 201-217 (2005).
6.   Dantzer, R., O'Connor, J.C., Freund, G.G., Johnson, R.W. & Kelley, K.W. From inflammation to sickness and depression: when the immune system subjugates the brain. *Nature reviews. Neuroscience* **9**, 46-56 (2008).
7.   Damm, J. *et al*. Fever, sickness behavior, and expression of inflammatory genes in the hypothalamus after systemic and localized subcutaneous stimulation of rats with the Toll-like receptor 7 agonist imiquimod. *Neuroscience* **201**, 166-183 (2012).
8.   Burton, M.D., Sparkman, N.L. & Johnson, R.W. Inhibition of interleukin-6 trans-signaling in the brain facilitates recovery from lipopolysaccharide-induced sickness behavior. *Journal of neuroinflammation* **8**, 54 (2011).
9.   Girard, J.P., Moussion, C. & Forster, R. HEVs, lymphatics and homeostatic immune cell trafficking in lymph nodes. *Nature reviews. Immunology* **12**, 762-773 (2012).
10.   Murphy, K. *Immunobiology*, Edn. 8th Edition. (Garland Science, New York; 2011).
11.   Pober, J.S. & Sessa, W.C. Evolving functions of endothelial cells in inflammation. *Nature reviews. Immunology* **7**, 803-815 (2007).
12.   Iwasaki, H. & Akashi, K. Myeloid lineage commitment from the hematopoietic stem cell. *Immunity* **26**, 726-740 (2007).
13.   Kolaczkowska, E. & Kubes, P. Neutrophil recruitment and function in health and inflammation. *Nature reviews. Immunology* **13**, 159-175 (2013).
14.   Brinkmann, V. *et al*. Neutrophil extracellular traps kill bacteria. *Science* **303**, 1532-1535 (2004).
15.   Steinberg, B.E. & Grinstein, S. Unconventional roles of the NADPH oxidase: signaling, ion homeostasis, and cell death. *Science's STKE : signal transduction knowledge environment* **2007**, pe11 (2007).
16.   Brinkmann, V. & Zychlinsky, A. Neutrophil extracellular traps: is immunity the second function of chromatin? *The Journal of cell biology* **198**, 773-783 (2012).
17.   Swirski, F.K. *et al*. Identification of splenic reservoir monocytes and their deployment to inflammatory sites. *Science* **325**, 612-616 (2009).
18.   Aziz, A., Soucie, E., Sarrazin, S. & Sieweke, M.H. MafB/c-Maf deficiency enables self-renewal of differentiated functional macrophages. *Science* **326**, 867-871 (2009).
19.   Stout, R.D. *et al*. Macrophages sequentially change their functional phenotype in response to changes in microenvironmental influences. *Journal of immunology* **175**, 342-349 (2005).

20. Mylonas, K.J., Nair, M.G., Prieto-Lafuente, L., Paape, D. & Allen, J.E. Alternatively activated macrophages elicited by helminth infection can be reprogrammed to enable microbial killing. *Journal of immunology* **182**, 3084-3094 (2009).

21. Kapsenberg, M.L. Dendritic-cell control of pathogen-driven T-cell polarization. *Nature reviews. Immunology* **3**, 984-993 (2003).

22. Merad, M., Sathe, P., Helft, J., Miller, J. & Mortha, A. The dendritic cell lineage: ontogeny and function of dendritic cells and their subsets in the steady state and the inflamed setting. *Annual review of immunology* **31**, 563-604 (2013).

23. Adib-Conquy, M., Scott-Algara, D., Cavaillon, J.M. & Souza-Fonseca-Guimaraes, F. TLR-mediated activation of NK cells and their role in bacterial/viral immune responses in mammals. *Immunology and cell biology* **92**, 256-262 (2014).

24. Broz, P. & Monack, D.M. Newly described pattern recognition receptors team up against intracellular pathogens. *Nature reviews. Immunology* **13**, 551-565 (2013).

25. Takeuchi, O. & Akira, S. Pattern recognition receptors and inflammation. *Cell* **140**, 805-820 (2010).

26. Fukata, M., Vamadevan, A.S. & Abreu, M.T. Toll-like receptors (TLRs) and Nod-like receptors (NLRs) in inflammatory disorders. *Seminars in immunology* **21**, 242-253 (2009).

27. Carneiro, L.A., Magalhaes, J.G., Tattoli, I., Philpott, D.J. & Travassos, L.H. Nod-like proteins in inflammation and disease. *The Journal of pathology* **214**, 136-148 (2008).

28. Geijtenbeek, T.B. & Gringhuis, S.I. Signalling through C-type lectin receptors: shaping immune responses. *Nature reviews. Immunology* **9**, 465-479 (2009).

29. Janeway, C.A., Jr. Approaching the asymptote? Evolution and revolution in immunology. *Cold Spring Harbor symposia on quantitative biology* **54 Pt 1**, 1-13 (1989).

30. Janeway, C.A., Jr. Pillars article: approaching the asymptote? Evolution and revolution in immunology. Cold spring harb symp quant biol. 1989. 54: 1-13. *Journal of immunology* **191**, 4475-4487 (2013).

31. Medzhitov, R., Preston-Hurlburt, P. & Janeway, C.A., Jr. A human homologue of the Drosophila Toll protein signals activation of adaptive immunity. *Nature* **388**, 394-397 (1997).

32. Takeda, K. & Akira, S. TLR signaling pathways. *Seminars in immunology* **16**, 3-9 (2004).

33. Akira, S. & Takeda, K. Toll-like receptor signalling. *Nature reviews. Immunology* **4**, 499-511 (2004).

34. Akira, S., Uematsu, S. & Takeuchi, O. Pathogen recognition and innate immunity. *Cell* **124**, 783-801 (2006).

35. Schnare, M. *et al*. Toll-like receptors control activation of adaptive immune responses. *Nature immunology* **2**, 947-950 (2001).

36. Guermonprez, P., Valladeau, J., Zitvogel, L., Thery, C. & Amigorena, S. Antigen presentation and T cell stimulation by dendritic cells. *Annual review of immunology* **20**, 621-667 (2002).

37. Geginat, J. *et al*. The CD4-centered universe of human T cell subsets. *Seminars in immunology* **25**, 252-262 (2013).

38. Zhu, J. & Paul, W.E. Heterogeneity and plasticity of T helper cells. *Cell research* **20**, 4-12 (2010).

39. Eyerich, S. & Zielinski, C.E. Defining Th-cell subsets in a classical and tissue-specific manner: Examples from the skin. *European journal of immunology* **44**, 3475-3483 (2014).

40. Trifari, S., Kaplan, C.D., Tran, E.H., Crellin, N.K. & Spits, H. Identification of a human helper T cell population that has abundant production of interleukin 22 and is distinct from T(H)-17, T(H)1 and T(H)2 cells. *Nature immunology* **10**, 864-871 (2009).

41. Duhen, T., Geiger, R., Jarrossay, D., Lanzavecchia, A. & Sallusto, F. Production of interleukin 22 but not interleukin 17 by a subset of human skin-homing memory T cells. *Nature immunology* **10**, 857-863 (2009).

42. Eyerich, S. *et al.* Th22 cells represent a distinct human T cell subset involved in epidermal immunity and remodeling. *The Journal of clinical investigation* **119**, 3573-3585 (2009).

43. Veldhoen, M. *et al.* Transforming growth factor-beta 'reprograms' the differentiation of T helper 2 cells and promotes an interleukin 9-producing subset. *Nature immunology* **9**, 1341-1346 (2008).

44. Dardalhon, V. *et al.* IL-4 inhibits TGF-beta-induced Foxp3+ T cells and, together with TGF-beta, generates IL-9+ IL-10+ Foxp3(-) effector T cells. *Nature immunology* **9**, 1347-1355 (2008).

45. Licona-Limon, P. *et al.* Th9 Cells Drive Host Immunity against Gastrointestinal Worm Infection. *Immunity* **39**, 744-757 (2013).

46. Kagi, D. *et al.* Cytotoxicity mediated by T cells and natural killer cells is greatly impaired in perforin-deficient mice. *Nature* **369**, 31-37 (1994).

47. Garraud, O. *et al.* Revisiting the B-cell compartment in mouse and humans: more than one B-cell subset exists in the marginal zone and beyond. *BMC immunology* **13**, 63 (2012).

48. Dinarello, C.A. Historical insights into cytokines. *European journal of immunology* **37 Suppl 1**, S34-45 (2007).

49. Paul, W.E. Pleiotropy and redundancy: T cell-derived lymphokines in the immune response. *Cell* **57**, 521-524 (1989).

50. Brocker, C., Thompson, D., Matsumoto, A., Nebert, D.W. & Vasiliou, V. Evolutionary divergence and functions of the human interleukin (IL) gene family. *Human genomics* **5**, 30-55 (2010).

51. Marcus, B.C., Wyble, C.W., Hynes, K.L. & Gewertz, B.L. Cytokine-induced increases in endothelial permeability occur after adhesion molecule expression. *Surgery* **120**, 411-416; discussion 416-417 (1996).

52. Saper, C.B. & Breder, C.D. The neurologic basis of fever. *The New England journal of medicine* **330**, 1880-1886 (1994).

53. Castell, J.V. *et al.* Interleukin-6 is the major regulator of acute phase protein synthesis in adult human hepatocytes. *FEBS letters* **242**, 237-239 (1989).

54. Kopf, M. *et al.* Impaired immune and acute-phase responses in interleukin-6-deficient mice. *Nature* **368**, 339-342 (1994).

55. Dantzer, R. Cytokine, sickness behavior, and depression. *Immunology and allergy clinics of North America* **29**, 247-264 (2009).

56. Bluthe, R.M. *et al.* Lipopolysaccharide induces sickness behaviour in rats by a vagal mediated mechanism. *Comptes rendus de l'Academie des sciences. Serie III, Sciences de la vie* **317**, 499-503 (1994).

57. Maier, S.F., Wiertelak, E.P., Martin, D. & Watkins, L.R. Interleukin-1 mediates the behavioral hyperalgesia produced by lithium chloride and endotoxin. *Brain research* **623**, 321-324 (1993).

58.	Isaacs, A. & Lindenmann, J. Virus interference. I. The interferon. *Proceedings of the Royal Society of London. Series B, Containing papers of a Biological character. Royal Society* **147**, 258-267 (1957).

59.	Dussurget, O., Bierne, H. & Cossart, P. The bacterial pathogen Listeria monocytogenes and the interferon family: type I, type II and type III interferons. *Frontiers in cellular and infection microbiology* **4**, 50 (2014).

60.	Schreiber, R.D., Farrar, M.A., Hershey, G.K. & Fernandez-Luna, J. The structure and function of interferon-gamma receptors. *International journal of immunopharmacology* **14**, 413-419 (1992).

61.	Dalton, D.K. *et al*. Multiple defects of immune cell function in mice with disrupted interferon-gamma genes. *Science* **259**, 1739-1742 (1993).

62.	Kaplan, D.H. *et al*. Demonstration of an interferon gamma-dependent tumor surveillance system in immunocompetent mice. *Proceedings of the National Academy of Sciences of the United States of America* **95**, 7556-7561 (1998).

63.	Harty, J.T. & Bevan, M.J. Specific immunity to Listeria monocytogenes in the absence of IFN gamma. *Immunity* **3**, 109-117 (1995).

64.	Jouanguy, E. *et al*. IL-12 and IFN-gamma in host defense against mycobacteria and salmonella in mice and men. *Current opinion in immunology* **11**, 346-351 (1999).

65.	van Pesch, V., Lanaya, H., Renauld, J.C. & Michiels, T. Characterization of the murine alpha interferon gene family. *Journal of virology* **78**, 8219-8228 (2004).

66.	Mancuso, G. *et al*. Type I IFN signaling is crucial for host resistance against different species of pathogenic bacteria. *Journal of immunology* **178**, 3126-3133 (2007).

67.	Auerbuch, V., Brockstedt, D.G., Meyer-Morse, N., O'Riordan, M. & Portnoy, D.A. Mice lacking the type I interferon receptor are resistant to Listeria monocytogenes. *The Journal of experimental medicine* **200**, 527-533 (2004).

68.	Carrero, J.A., Calderon, B. & Unanue, E.R. Type I interferon sensitizes lymphocytes to apoptosis and reduces resistance to Listeria infection. *The Journal of experimental medicine* **200**, 535-540 (2004).

69.	O'Connell, R.M. *et al*. Type I interferon production enhances susceptibility to Listeria monocytogenes infection. *The Journal of experimental medicine* **200**, 437-445 (2004).

70.	Robinson, N. *et al*. Type I interferon induces necroptosis in macrophages during infection with Salmonella enterica serovar Typhimurium. *Nature immunology* **13**, 954-962 (2012).

71.	Martin, F.J. *et al*. Staphylococcus aureus activates type I IFN signaling in mice and humans through the Xr repeated sequences of protein A. *The Journal of clinical investigation* **119**, 1931-1939 (2009).

72.	Hertzog, P., Forster, S. & Samarajiwa, S. Systems biology of interferon responses. *Journal of interferon & cytokine research : the official journal of the International Society for Interferon and Cytokine Research* **31**, 5-11 (2011).

73.	Trinchieri, G. Type I interferon: friend or foe? *The Journal of experimental medicine* **207**, 2053-2063 (2010).

74.	Gonzalez-Navajas, J.M., Lee, J., David, M. & Raz, E. Immunomodulatory functions of type I interferons. *Nature reviews. Immunology* **12**, 125-135 (2012).

75. Sommereyns, C., Paul, S., Staeheli, P. & Michiels, T. IFN-lambda (IFN-lambda) is expressed in a tissue-dependent fashion and primarily acts on epithelial cells in vivo. *PLoS pathogens* **4**, e1000017 (2008).

76. Prokunina-Olsson, L. *et al*. A variant upstream of IFNL3 (IL28B) creating a new interferon gene IFNL4 is associated with impaired clearance of hepatitis C virus. *Nature genetics* **45**, 164-171 (2013).

77. Schoggins, J.W. *et al*. A diverse range of gene products are effectors of the type I interferon antiviral response. *Nature* **472**, 481-485 (2011).

78. Der, S.D., Zhou, A., Williams, B.R. & Silverman, R.H. Identification of genes differentially regulated by interferon alpha, beta, or gamma using oligonucleotide arrays. *Proceedings of the National Academy of Sciences of the United States of America* **95**, 15623-15628 (1998).

79. Schoggins, J.W. & Rice, C.M. Interferon-stimulated genes and their antiviral effector functions. *Current opinion in virology* **1**, 519-525 (2011).

80. Diamond, M.S. & Farzan, M. The broad-spectrum antiviral functions of IFIT and IFITM proteins. *Nature reviews. Immunology* **13**, 46-57 (2013).

81. Bailey, C.C., Zhong, G., Huang, I.C. & Farzan, M. IFITM-Family Proteins: The Cell's First Line of Antiviral Defense. *Annual review of virology* **1**, 261-283 (2014).

82. Cong, X.L. *et al*. Usp18 promotes conventional CD11b+ dendritic cell development. *Journal of immunology* **188**, 4776-4781 (2012).

83. Yoshimura, A., Naka, T. & Kubo, M. SOCS proteins, cytokine signalling and immune regulation. *Nature reviews. Immunology* **7**, 454-465 (2007).

84. Sadler, A.J. & Williams, B.R. Interferon-inducible antiviral effectors. *Nature reviews. Immunology* **8**, 559-568 (2008).

85. Rot, A. & von Andrian, U.H. Chemokines in innate and adaptive host defense: basic chemokinese grammar for immune cells. *Annual review of immunology* **22**, 891-928 (2004).

86. Zlotnik, A. & Yoshie, O. Chemokines: a new classification system and their role in immunity. *Immunity* **12**, 121-127 (2000).

87. Walz, A., Peveri, P., Aschauer, H. & Baggiolini, M. Purification and amino acid sequencing of NAF, a novel neutrophil-activating factor produced by monocytes. *Biochemical and biophysical research communications* **149**, 755-761 (1987).

88. Van Damme, J., Van Beeumen, J., Opdenakker, G. & Billiau, A. A novel, NH2-terminal sequence-characterized human monokine possessing neutrophil chemotactic, skin-reactive, and granulocytosis-promoting activity. *The Journal of experimental medicine* **167**, 1364-1376 (1988).

89. Schroder, J.M., Mrowietz, U., Morita, E. & Christophers, E. Purification and partial biochemical characterization of a human monocyte-derived, neutrophil-activating peptide that lacks interleukin 1 activity. *Journal of immunology* **139**, 3474-3483 (1987).

90. Yoshimura, T. *et al*. Purification of a human monocyte-derived neutrophil chemotactic factor that has peptide sequence similarity to other host defense cytokines. *Proceedings of the National Academy of Sciences of the United States of America* **84**, 9233-9237 (1987).

91. Owen, J.L. & Mohamadzadeh, M. Macrophages and chemokines as mediators of angiogenesis. *Frontiers in physiology* **4**, 159 (2013).

92. Raz, E. & Mahabaleshwar, H. Chemokine signaling in embryonic cell migration: a fisheye view. *Development* **136**, 1223-1229 (2009).

93. Behm, B., Babilas, P., Landthaler, M. & Schreml, S. Cytokines, chemokines and growth factors in wound healing. *Journal of the European Academy of Dermatology and Venereology : JEADV* **26**, 812-820 (2012).

94. Feng, Y., Broder, C.C., Kennedy, P.E. & Berger, E.A. HIV-1 entry cofactor: functional cDNA cloning of a seven-transmembrane, G protein-coupled receptor. *Science* **272**, 872-877 (1996).
95. Deng, H. *et al.* Identification of a major co-receptor for primary isolates of HIV-1. *Nature* **381**, 661-666 (1996).
96. Doranz, B.J. *et al.* A dual-tropic primary HIV-1 isolate that uses fusin and the beta-chemokine receptors CKR-5, CKR-3, and CKR-2b as fusion cofactors. *Cell* **85**, 1149-1158 (1996).
97. Dragic, T. *et al.* HIV-1 entry into CD4+ cells is mediated by the chemokine receptor CC-CKR-5. *Nature* **381**, 667-673 (1996).
98. Alkhatib, G. *et al.* CC CKR5: a RANTES, MIP-1alpha, MIP-1beta receptor as a fusion cofactor for macrophage-tropic HIV-1. *Science* **272**, 1955-1958 (1996).
99. Sugiyama, T., Kohara, H., Noda, M. & Nagasawa, T. Maintenance of the hematopoietic stem cell pool by CXCL12-CXCR4 chemokine signaling in bone marrow stromal cell niches. *Immunity* **25**, 977-988 (2006).
100. Ohl, L. *et al.* Cooperating mechanisms of CXCR5 and CCR7 in development and organization of secondary lymphoid organs. *The Journal of experimental medicine* **197**, 1199-1204 (2003).
101. Scandella, E. *et al.* CCL19/CCL21-triggered signal transduction and migration of dendritic cells requires prostaglandin E2. *Blood* **103**, 1595-1601 (2004).
102. Forster, R. *et al.* CCR7 coordinates the primary immune response by establishing functional microenvironments in secondary lymphoid organs. *Cell* **99**, 23-33 (1999).
103. Britschgi, M.R., Favre, S. & Luther, S.A. CCL21 is sufficient to mediate DC migration, maturation and function in the absence of CCL19. *European journal of immunology* **40**, 1266-1271 (2010).
104. Ohl, L. *et al.* CCR7 governs skin dendritic cell migration under inflammatory and steady-state conditions. *Immunity* **21**, 279-288 (2004).
105. Shirozu, M. *et al.* Structure and chromosomal localization of the human stromal cell-derived factor 1 (SDF1) gene. *Genomics* **28**, 495-500 (1995).
106. Zou, Y.R., Kottmann, A.H., Kuroda, M., Taniuchi, I. & Littman, D.R. Function of the chemokine receptor CXCR4 in haematopoiesis and in cerebellar development. *Nature* **393**, 595-599 (1998).
107. Nagasawa, T. *et al.* Defects of B-cell lymphopoiesis and bone-marrow myelopoiesis in mice lacking the CXC chemokine PBSF/SDF-1. *Nature* **382**, 635-638 (1996).
108. Tzeng, Y.S. *et al.* Loss of Cxcl12/Sdf-1 in adult mice decreases the quiescent state of hematopoietic stem/progenitor cells and alters the pattern of hematopoietic regeneration after myelosuppression. *Blood* **117**, 429-439 (2011).
109. Murdoch, C. & Finn, A. Chemokine receptors and their role in inflammation and infectious diseases. *Blood* **95**, 3032-3043 (2000).
110. Murphy, P.M. *et al.* International union of pharmacology. XXII. Nomenclature for chemokine receptors. *Pharmacological reviews* **52**, 145-176 (2000).
111. Lacotte, S., Brun, S., Muller, S. & Dumortier, H. CXCR3, inflammation, and autoimmune diseases. *Annals of the New York Academy of Sciences* **1173**, 310-317 (2009).
112. Siehler S, M.G. 430 (Cambridge University Press, USA; 2011).

113. Zlotnik, A., Yoshie, O. & Nomiyama, H. The chemokine and chemokine receptor superfamilies and their molecular evolution. *Genome biology* **7**, 243 (2006).

114. Graham, G.J. D6 and the atypical chemokine receptor family: novel regulators of immune and inflammatory processes. *European journal of immunology* **39**, 342-351 (2009).

115. Bachelerie, F. *et al*. New nomenclature for atypical chemokine receptors. *Nature immunology* **15**, 207-208 (2014).

116. Nibbs, R., Graham, G. & Rot, A. Chemokines on the move: control by the chemokine "interceptors" Duffy blood group antigen and D6. *Seminars in immunology* **15**, 287-294 (2003).

117. Borroni, E.M. *et al*. beta-arrestin-dependent activation of the cofilin pathway is required for the scavenging activity of the atypical chemokine receptor D6. *Science signaling* **6**, ra30 31-11, S31-33 (2013).

118. Rajagopal, S. *et al*. Beta-arrestin- but not G protein-mediated signaling by the "decoy" receptor CXCR7. *Proceedings of the National Academy of Sciences of the United States of America* **107**, 628-632 (2010).

119. Nibbs, R.J., Wylie, S.M., Pragnell, I.B. & Graham, G.J. Cloning and characterization of a novel murine beta chemokine receptor, D6. Comparison to three other related macrophage inflammatory protein-1alpha receptors, CCR-1, CCR-3, and CCR-5. *The Journal of biological chemistry* **272**, 12495-12504 (1997).

120. Nibbs, R.J., Wylie, S.M., Yang, J., Landau, N.R. & Graham, G.J. Cloning and characterization of a novel promiscuous human beta-chemokine receptor D6. *The Journal of biological chemistry* **272**, 32078-32083 (1997).

121. Weber, M. *et al*. The chemokine receptor D6 constitutively traffics to and from the cell surface to internalize and degrade chemokines. *Molecular biology of the cell* **15**, 2492-2508 (2004).

122. Martinez de la Torre, Y. *et al*. Increased inflammation in mice deficient for the chemokine decoy receptor D6. *European journal of immunology* **35**, 1342-1346 (2005).

123. Nibbs, R.J. *et al*. The atypical chemokine receptor D6 suppresses the development of chemically induced skin tumors. *The Journal of clinical investigation* **117**, 1884-1892 (2007).

124. Barre-Sinoussi, F. *et al*. Isolation of a T-lymphotropic retrovirus from a patient at risk for acquired immune deficiency syndrome (AIDS). *Science* **220**, 868-871 (1983).

125. Lusso, P. HIV and the chemokine system: 10 years later. *The EMBO journal* **25**, 447-456 (2006).

126. Cocchi, F. *et al*. Identification of RANTES, MIP-1 alpha, and MIP-1 beta as the major HIV-suppressive factors produced by CD8+ T cells. *Science* **270**, 1811-1815 (1995).

127. Choe, H. *et al*. The beta-chemokine receptors CCR3 and CCR5 facilitate infection by primary HIV-1 isolates. *Cell* **85**, 1135-1148 (1996).

128. Berkowitz, R.D. *et al*. CCR5- and CXCR4-utilizing strains of human immunodeficiency virus type 1 exhibit differential tropism and pathogenesis in vivo. *Journal of virology* **72**, 10108-10117 (1998).

129. Karlsson, I. *et al*. Differential pathogenesis of primary CCR5-using human immunodeficiency virus type 1 isolates in ex vivo human lymphoid tissue. *Journal of virology* **79**, 11151-11160 (2005).

130. Stephens, J.C. *et al*. Dating the origin of the CCR5-Delta32 AIDS-resistance allele by the coalescence of haplotypes. *American journal of human genetics* **62**, 1507-1515 (1998).

131. Glass, W.G. *et al*. CCR5 deficiency increases risk of symptomatic West Nile virus infection. *The Journal of experimental medicine* **203**, 35-40 (2006).

132. Karussis, D. The diagnosis of multiple sclerosis and the various related demyelinating syndromes: a critical review. *Journal of autoimmunity* **48-49**, 134-142 (2014).

133. Baxter, A.G. The origin and application of experimental autoimmune encephalomyelitis. *Nature reviews. Immunology* **7**, 904-912 (2007).

134. Reboldi, A. *et al*. C-C chemokine receptor 6-regulated entry of TH-17 cells into the CNS through the choroid plexus is required for the initiation of EAE. *Nature immunology* **10**, 514-523 (2009).

135. Elhofy, A., Depaolo, R.W., Lira, S.A., Lukacs, N.W. & Karpus, W.J. Mice deficient for CCR6 fail to control chronic experimental autoimmune encephalomyelitis. *Journal of neuroimmunology* **213**, 91-99 (2009).

136. Gaupp, S., Pitt, D., Kuziel, W.A., Cannella, B. & Raine, C.S. Experimental autoimmune encephalomyelitis (EAE) in CCR2(-/-) mice: susceptibility in multiple strains. *The American journal of pathology* **162**, 139-150 (2003).

137. Ghersi-Egea, J.F., Leininger-Muller, B., Cecchelli, R. & Fenstermacher, J.D. Blood-brain interfaces: relevance to cerebral drug metabolism. *Toxicology letters* **82-83**, 645-653 (1995).

138. Matyszak, M.K. & Perry, V.H. The potential role of dendritic cells in immune-mediated inflammatory diseases in the central nervous system. *Neuroscience* **74**, 599-608 (1996).

139. Weller, R.O., Galea, I., Carare, R.O. & Minagar, A. Pathophysiology of the lymphatic drainage of the central nervous system: Implications for pathogenesis and therapy of multiple sclerosis. *Pathophysiology : the official journal of the International Society for Pathophysiology / ISP* **17**, 295-306 (2010).

140. Louveau, A. *et al*. Structural and functional features of central nervous system lymphatic vessels. *Nature* **523**, 337-341 (2015).

141. Eriksson, P.S. *et al*. Neurogenesis in the adult human hippocampus. *Nature medicine* **4**, 1313-1317 (1998).

142. Migaud, M. *et al*. Emerging new sites for adult neurogenesis in the mammalian brain: a comparative study between the hypothalamus and the classical neurogenic zones. *The European journal of neuroscience* **32**, 2042-2052 (2010).

143. Rock, R.B. *et al*. Role of microglia in central nervous system infections. *Clinical microbiology reviews* **17**, 942-964, table of contents (2004).

144. Ginhoux, F. *et al*. Fate mapping analysis reveals that adult microglia derive from primitive macrophages. *Science* **330**, 841-845 (2010).

145. Simard, A.R. & Rivest, S. Bone marrow stem cells have the ability to populate the entire central nervous system into fully differentiated parenchymal microglia. *FASEB journal : official publication of the Federation of American Societies for Experimental Biology* **18**, 998-1000 (2004).

146. Boche, D., Perry, V.H. & Nicoll, J.A. Review: activation patterns of microglia and their identification in the human brain. *Neuropathology and applied neurobiology* **39**, 3-18 (2013).

147. Jack, C.S. *et al*. TLR signaling tailors innate immune responses in human microglia and astrocytes. *Journal of immunology* **175**, 4320-4330 (2005).

148. Jenmalm, M.C., Cherwinski, H., Bowman, E.P., Phillips, J.H. & Sedgwick, J.D. Regulation of myeloid cell function through the CD200 receptor. *Journal of immunology* **176**, 191-199 (2006).

149. Gorczynski, R.M. CD200 and its receptors as targets for immunoregulation. *Current opinion in investigational drugs* **6**, 483-488 (2005).

150. Hoek, R.M. *et al*. Down-regulation of the macrophage lineage through interaction with OX2 (CD200). *Science* **290**, 1768-1771 (2000).

151. Cardona, A.E. *et al*. Control of microglial neurotoxicity by the fractalkine receptor. *Nature neuroscience* **9**, 917-924 (2006).

152. Rogers, J.T. *et al*. CX3CR1 deficiency leads to impairment of hippocampal cognitive function and synaptic plasticity. *The Journal of neuroscience : the official journal of the Society for Neuroscience* **31**, 16241-16250 (2011).

153. Bachstetter, A.D. *et al*. Fractalkine and CX 3 CR1 regulate hippocampal neurogenesis in adult and aged rats. *Neurobiology of aging* **32**, 2030-2044 (2011).

154. Volterra, A. & Meldolesi, J. Astrocytes, from brain glue to communication elements: the revolution continues. *Nature reviews. Neuroscience* **6**, 626-640 (2005).

155. Wallraff, A. *et al*. The impact of astrocytic gap junctional coupling on potassium buffering in the hippocampus. *The Journal of neuroscience : the official journal of the Society for Neuroscience* **26**, 5438-5447 (2006).

156. Schousboe, A. Role of astrocytes in the maintenance and modulation of glutamatergic and GABAergic neurotransmission. *Neurochemical research* **28**, 347-352 (2003).

157. Takano, T. *et al*. Astrocyte-mediated control of cerebral blood flow. *Nature neuroscience* **9**, 260-267 (2006).

158. Stobart, J.L., Lu, L., Anderson, H.D., Mori, H. & Anderson, C.M. Astrocyte-induced cortical vasodilation is mediated by D-serine and endothelial nitric oxide synthase. *Proceedings of the National Academy of Sciences of the United States of America* **110**, 3149-3154 (2013).

159. Zamanian, J.L. *et al*. Genomic analysis of reactive astrogliosis. *The Journal of neuroscience : the official journal of the Society for Neuroscience* **32**, 6391-6410 (2012).

160. Johann, S. *et al*. Expression of enzymes involved in the prostanoid metabolism by cortical astrocytes after LPS-induced inflammation. *Journal of molecular neuroscience : MN* **34**, 177-185 (2008).

161. Park, J. *et al*. Reactive oxygen species mediate chloroquine-induced expression of chemokines by human astroglial cells. *Glia* **47**, 9-20 (2004).

162. Perez, J.L. *et al*. Soluble oligomeric forms of beta-amyloid (Abeta) peptide stimulate Abeta production via astrogliosis in the rat brain. *Experimental neurology* **223**, 410-421 (2010).

163. Pineau, I., Sun, L., Bastien, D. & Lacroix, S. Astrocytes initiate inflammation in the injured mouse spinal cord by promoting the entry of neutrophils and inflammatory monocytes in an IL-1 receptor/MyD88-dependent fashion. *Brain, behavior, and immunity* **24**, 540-553 (2010).

164. Bauer, N.G., Richter-Landsberg, C. & Ffrench-Constant, C. Role of the oligodendroglial cytoskeleton in differentiation and myelination. *Glia* **57**, 1691-1705 (2009).

165. Wakao, S., Matsuse, D. & Dezawa, M. Mesenchymal Stem Cells as a Source of Schwann Cells: Their Anticipated Use in Peripheral Nerve Regeneration. *Cells, tissues, organs* (2015).

166. Bercury, K.K. & Macklin, W.B. Dynamics and Mechanisms of CNS Myelination. *Developmental cell* **32**, 447-458 (2015).
167. Lucchinetti, C. *et al.* Heterogeneity of multiple sclerosis lesions: implications for the pathogenesis of demyelination. *Annals of neurology* **47**, 707-717 (2000).
168. Love, S. Demyelinating diseases. *Journal of clinical pathology* **59**, 1151-1159 (2006).
169. Petty, M.A. & Lo, E.H. Junctional complexes of the blood-brain barrier: permeability changes in neuroinflammation. *Progress in neurobiology* **68**, 311-323 (2002).
170. Bradbury, M.W.B. Ultrastructure of Brain Endothelium, in *Physiology and Pharmacology of the Blood-Brain Barrier*, Vol. 103 1-22 (Springer- Verlag, Berlin; 1992).
171. Anderson, J.M. & Van Itallie, C.M. Physiology and function of the tight junction. *Cold Spring Harbor perspectives in biology* **1**, a002584 (2009).
172. Stevenson, B.R. & Keon, B.H. The tight junction: morphology to molecules. *Annual review of cell and developmental biology* **14**, 89-109 (1998).
173. Mitic, L.L. & Anderson, J.M. Molecular architecture of tight junctions. *Annual review of physiology* **60**, 121-142 (1998).
174. Minagar, A. & Alexander, J.S. Blood-brain barrier disruption in multiple sclerosis. *Multiple sclerosis* **9**, 540-549 (2003).
175. Zlokovic, B.V. The blood-brain barrier in health and chronic neurodegenerative disorders. *Neuron* **57**, 178-201 (2008).
176. Johanson, C.E., Stopa, E.G. & McMillan, P.N. The blood-cerebrospinal fluid barrier: structure and functional significance. *Methods in molecular biology* **686**, 101-131 (2011).
177. Hogan, Q.H. *et al.* Magnetic resonance imaging of cerebrospinal fluid volume and the influence of body habitus and abdominal pressure. *Anesthesiology* **84**, 1341-1349 (1996).
178. Arango, C. *et al.* Patterns of cranial, brain and sulcal CSF volumes in male and female deficit and nondeficit patients with schizophrenia. *Psychiatry research* **162**, 91-100 (2008).
179. Engelhardt, B. & Sorokin, L. The blood-brain and the blood-cerebrospinal fluid barriers: function and dysfunction. *Seminars in immunopathology* **31**, 497-511 (2009).
180. Edsbagge, M., Tisell, M., Jacobsson, L. & Wikkelso, C. Spinal CSF absorption in healthy individuals. *American journal of physiology. Regulatory, integrative and comparative physiology* **287**, R1450-1455 (2004).
181. Ganong, W.F. Circumventricular organs: definition and role in the regulation of endocrine and autonomic function. *Clinical and experimental pharmacology & physiology* **27**, 422-427 (2000).
182. Decimo, I., Fumagalli, G., Berton, V., Krampera, M. & Bifari, F. Meninges: from protective membrane to stem cell niche. *American journal of stem cells* **1**, 92-105 (2012).
183. Mercier, F. & Hatton, G.I. Connexin 26 and basic fibroblast growth factor are expressed primarily in the subpial and subependymal layers in adult brain parenchyma: roles in stem cell proliferation and morphological plasticity? *The Journal of comparative neurology* **431**, 88-104 (2001).
184. Borrell, V. & Marin, O. Meninges control tangential migration of hem-derived Cajal-Retzius cells via CXCL12/CXCR4 signaling. *Nature neuroscience* **9**, 1284-1293 (2006).

185. Siegenthaler, J.A. *et al*. Retinoic acid from the meninges regulates cortical neuron generation. *Cell* **139**, 597-609 (2009).
186. Ousman, S.S. & Kubes, P. Immune surveillance in the central nervous system. *Nature neuroscience* **15**, 1096-1101 (2012).
187. Williams, K., Alvarez, X. & Lackner, A.A. Central nervous system perivascular cells are immunoregulatory cells that connect the CNS with the peripheral immune system. *Glia* **36**, 156-164 (2001).
188. Hickey, W.F. & Kimura, H. Perivascular microglial cells of the CNS are bone marrow-derived and present antigen in vivo. *Science* **239**, 290-292 (1988).
189. Serafini, B., Columba-Cabezas, S., Di Rosa, F. & Aloisi, F. Intracerebral recruitment and maturation of dendritic cells in the onset and progression of experimental autoimmune encephalomyelitis. *The American journal of pathology* **157**, 1991-2002 (2000).
190. Kivisakk, P. *et al*. Localizing central nervous system immune surveillance: meningeal antigen-presenting cells activate T cells during experimental autoimmune encephalomyelitis. *Annals of neurology* **65**, 457-469 (2009).
191. McMenamin, P.G. Distribution and phenotype of dendritic cells and resident tissue macrophages in the dura mater, leptomeninges, and choroid plexus of the rat brain as demonstrated in wholemount preparations. *The Journal of comparative neurology* **405**, 553-562 (1999).
192. McMenamin, P.G., Wealthall, R.J., Deverall, M., Cooper, S.J. & Griffin, B. Macrophages and dendritic cells in the rat meninges and choroid plexus: three-dimensional localisation by environmental scanning electron microscopy and confocal microscopy. *Cell and tissue research* **313**, 259-269 (2003).
193. O'Keefe, G.M., Nguyen, V.T. & Benveniste, E.N. Regulation and function of class II major histocompatibility complex, CD40, and B7 expression in macrophages and microglia: Implications in neurological diseases. *Journal of neurovirology* **8**, 496-512 (2002).
194. Baruch, K. *et al*. CNS-specific immunity at the choroid plexus shifts toward destructive Th2 inflammation in brain aging. *Proceedings of the National Academy of Sciences of the United States of America* **110**, 2264-2269 (2013).
195. Hawke, S., Stevenson, P.G., Freeman, S. & Bangham, C.R. Long-term persistence of activated cytotoxic T lymphocytes after viral infection of the central nervous system. *The Journal of experimental medicine* **187**, 1575-1582 (1998).
196. Wei, C.H. *et al*. Tissue-resident memory CD8+ T cells can be deleted by soluble, but not cross-presented antigen. *Journal of immunology* **175**, 6615-6623 (2005).
197. Becher, B., Bechmann, I. & Greter, M. Antigen presentation in autoimmunity and CNS inflammation: how T lymphocytes recognize the brain. *Journal of molecular medicine* **84**, 532-543 (2006).
198. Wekerle, H., Sun, D., Oropeza-Wekerle, R.L. & Meyermann, R. Immune reactivity in the nervous system: modulation of T-lymphocyte activation by glial cells. *The Journal of experimental biology* **132**, 43-57 (1987).
199. Walter, B.A., Valera, V.A., Takahashi, S. & Ushiki, T. The olfactory route for cerebrospinal fluid drainage into the peripheral lymphatic system. *Neuropathology and applied neurobiology* **32**, 388-396 (2006).
200. Mathieu, E., Gupta, N., Macdonald, R.L., Ai, J. & Yucel, Y.H. In vivo imaging of lymphatic drainage of cerebrospinal fluid in mouse. *Fluids and barriers of the CNS* **10**, 35 (2013).

201. Laman, J.D. & Weller, R.O. Drainage of cells and soluble antigen from the CNS to regional lymph nodes. *Journal of neuroimmune pharmacology : the official journal of the Society on NeuroImmune Pharmacology* **8**, 840-856 (2013).

202. Kida, S., Pantazis, A. & Weller, R.O. CSF drains directly from the subarachnoid space into nasal lymphatics in the rat. Anatomy, histology and immunological significance. *Neuropathology and applied neurobiology* **19**, 480-488 (1993).

203. Carare, R.O. *et al.* Solutes, but not cells, drain from the brain parenchyma along basement membranes of capillaries and arteries: significance for cerebral amyloid angiopathy and neuroimmunology. *Neuropathology and applied neurobiology* **34**, 131-144 (2008).

204. Louveau, A., Harris, T.H. & Kipnis, J. Revisiting the Mechanisms of CNS Immune Privilege. *Trends in immunology* **36**, 569-577 (2015).

205. Rostene, W. *et al.* Neurochemokines: a menage a trois providing new insights on the functions of chemokines in the central nervous system. *Journal of neurochemistry* **118**, 680-694 (2011).

206. Ubogu, E.E., Cossoy, M.B. & Ransohoff, R.M. The expression and function of chemokines involved in CNS inflammation. *Trends in pharmacological sciences* **27**, 48-55 (2006).

207. Callewaere, C., Banisadr, G., Rostene, W. & Parsadaniantz, S.M. Chemokines and chemokine receptors in the brain: implication in neuroendocrine regulation. *Journal of molecular endocrinology* **38**, 355-363 (2007).

208. Li, M. & Ransohoff, R.M. Multiple roles of chemokine CXCL12 in the central nervous system: a migration from immunology to neurobiology. *Progress in neurobiology* **84**, 116-131 (2008).

209. Klein, R.S. *et al.* SDF-1 alpha induces chemotaxis and enhances Sonic hedgehog-induced proliferation of cerebellar granule cells. *Development* **128**, 1971-1981 (2001).

210. Lu, M., Grove, E.A. & Miller, R.J. Abnormal development of the hippocampal dentate gyrus in mice lacking the CXCR4 chemokine receptor. *Proceedings of the National Academy of Sciences of the United States of America* **99**, 7090-7095 (2002).

211. Banisadr, G. *et al.* Neuroanatomical distribution of CXCR4 in adult rat brain and its localization in cholinergic and dopaminergic neurons. *The European journal of neuroscience* **16**, 1661-1671 (2002).

212. Warf, B.C., Fok-Seang, J. & Miller, R.H. Evidence for the ventral origin of oligodendrocyte precursors in the rat spinal cord. *The Journal of neuroscience : the official journal of the Society for Neuroscience* **11**, 2477-2488 (1991).

213. Tsai, H.H. *et al.* The chemokine receptor CXCR2 controls positioning of oligodendrocyte precursors in developing spinal cord by arresting their migration. *Cell* **110**, 373-383 (2002).

214. Rostene, W. & Buckingham, J.C. Chemokines as modulators of neuroendocrine functions. *Journal of molecular endocrinology* **38**, 351-353 (2007).

215. Rostene, W., Kitabgi, P. & Parsadaniantz, S.M. Chemokines: a new class of neuromodulator? *Nature reviews. Neuroscience* **8**, 895-903 (2007).

216. Davatelis, G. *et al.* Macrophage inflammatory protein-1: a prostaglandin-independent endogenous pyrogen. *Science* **243**, 1066-1068 (1989).

217. Minano, F.J., Fernandez-Alonso, A., Myers, R.D. & Sancibrian, M. Hypothalamic interaction between macrophage inflammatory protein-1

alpha (MIP-1 alpha) and MIP-1 beta in rats: a new level for fever control? *The Journal of physiology* **491 (Pt 1)**, 209-217 (1996).

218.	Machado, R.R., Soares, D.M., Proudfoot, A.E. & Souza, G.E. CCR1 and CCR5 chemokine receptors are involved in fever induced by LPS (E. coli) and RANTES in rats. *Brain research* **1161**, 21-31 (2007).

219.	Zampronio, A.R., Souza, G.E., Silva, C.A., Cunha, F.Q. & Ferreira, S.H. Interleukin-8 induces fever by a prostaglandin-independent mechanism. *The American journal of physiology* **266**, R1670-1674 (1994).

220.	Plata-Salaman, C.R. & Borkoski, J.P. Chemokines/intercrines and central regulation of feeding. *The American journal of physiology* **266**, R1711-1715 (1994).

221.	Myers, R.D., Paez, X., Roscoe, A.K., Sherry, B. & Cerami, A. Fever and feeding: differential actions of macrophage inflammatory protein-1 (MIP-1), MIP-1 alpha and MIP-1 beta on rat hypothalamus. *Neurochemical research* **18**, 667-673 (1993).

222.	Purves D, A.G., Fitzpatrick D, Katz LC, LaMantia AS, McNamara JO, Williams SM *Neuroscience*, Edn. 2nd. (Sinauer Associates Inc, 2001).

223.	Banisadr, G., Skrzydelski, D., Kitabgi, P., Rostene, W. & Parsadaniantz, S.M. Highly regionalized distribution of stromal cell-derived factor-1/CXCL12 in adult rat brain: constitutive expression in cholinergic, dopaminergic and vasopressinergic neurons. *The European journal of neuroscience* **18**, 1593-1606 (2003).

224.	Banisadr, G. *et al*. Highly regionalized neuronal expression of monocyte chemoattractant protein-1 (MCP-1/CCL2) in rat brain: evidence for its colocalization with neurotransmitters and neuropeptides. *The Journal of comparative neurology* **489**, 275-292 (2005).

225.	Harrison, J.K. *et al*. Role for neuronally derived fractalkine in mediating interactions between neurons and CX3CR1-expressing microglia. *Proceedings of the National Academy of Sciences of the United States of America* **95**, 10896-10901 (1998).

226.	Guyon, A., Rovere, C., Cervantes, A., Allaeys, I. & Nahon, J.L. Stromal cell-derived factor-1alpha directly modulates voltage-dependent currents of the action potential in mammalian neuronal cells. *Journal of neurochemistry* **93**, 963-973 (2005).

227.	Gosselin, R.D. *et al*. Constitutive expression of CCR2 chemokine receptor and inhibition by MCP-1/CCL2 of GABA-induced currents in spinal cord neurones. *Journal of neurochemistry* **95**, 1023-1034 (2005).

228.	Callewaere, C. *et al*. The chemokine SDF-1/CXCL12 modulates the firing pattern of vasopressin neurons and counteracts induced vasopressin release through CXCR4. *Proceedings of the National Academy of Sciences of the United States of America* **103**, 8221-8226 (2006).

229.	Takeshita, Y. & Ransohoff, R.M. Inflammatory cell trafficking across the blood-brain barrier: chemokine regulation and in vitro models. *Immunological reviews* **248**, 228-239 (2012).

230.	D'Mello, C., Le, T. & Swain, M.G. Cerebral microglia recruit monocytes into the brain in response to tumor necrosis factoralpha signaling during peripheral organ inflammation. *The Journal of neuroscience : the official journal of the Society for Neuroscience* **29**, 2089-2102 (2009).

231.	Trifilo, M.J., Bergmann, C.C., Kuziel, W.A. & Lane, T.E. CC chemokine ligand 3 (CCL3) regulates CD8(+)-T-cell effector function and migration following viral infection. *Journal of virology* **77**, 4004-4014 (2003).

232.	Simpson, J.E., Newcombe, J., Cuzner, M.L. & Woodroofe, M.N. Expression of monocyte chemoattractant protein-1 and other beta-chemokines by

resident glia and inflammatory cells in multiple sclerosis lesions. *Journal of neuroimmunology* **84**, 238-249 (1998).

233. Glass, W.G. *et al.* Chemokine receptor CCR5 promotes leukocyte trafficking to the brain and survival in West Nile virus infection. *The Journal of experimental medicine* **202**, 1087-1098 (2005).

234. Michlmayr, D. *et al.* Defining the chemokine basis for leukocyte recruitment during viral encephalitis. *Journal of virology* **88**, 9553-9567 (2014).

235. Haeberle, H.A. *et al.* Inducible expression of inflammatory chemokines in respiratory syncytial virus-infected mice: role of MIP-1alpha in lung pathology. *Journal of virology* **75**, 878-890 (2001).

236. Palma, J.P. & Kim, B.S. Induction of selected chemokines in glial cells infected with Theiler's virus. *Journal of neuroimmunology* **117**, 166-170 (2001).

237. Zhou, J., Stohlman, S.A., Hinton, D.R. & Marten, N.W. Neutrophils promote mononuclear cell infiltration during viral-induced encephalitis. *Journal of immunology* **170**, 3331-3336 (2003).

238. Hosking, M.P. & Lane, T.E. The role of chemokines during viral infection of the CNS. *PLoS pathogens* **6**, e1000937 (2010).

239. Marro, B.S., Hosking, M.P. & Lane, T.E. CXCR2 signaling and host defense following coronavirus-induced encephalomyelitis. *Future virology* **7**, 349-359 (2012).

240. Holman, D.W., Klein, R.S. & Ransohoff, R.M. The blood-brain barrier, chemokines and multiple sclerosis. *Biochimica et biophysica acta* **1812**, 220-230 (2011).

241. Kivisakk, P. *et al.* Expression of CCR7 in multiple sclerosis: implications for CNS immunity. *Annals of neurology* **55**, 627-638 (2004).

242. Hickey, W.F. Leukocyte traffic in the central nervous system: the participants and their roles. *Seminars in immunology* **11**, 125-137 (1999).

243. Izikson, L., Klein, R.S., Charo, I.F., Weiner, H.L. & Luster, A.D. Resistance to experimental autoimmune encephalomyelitis in mice lacking the CC chemokine receptor (CCR)2. *The Journal of experimental medicine* **192**, 1075-1080 (2000).

244. Fife, B.T., Huffnagle, G.B., Kuziel, W.A. & Karpus, W.J. CC chemokine receptor 2 is critical for induction of experimental autoimmune encephalomyelitis. *The Journal of experimental medicine* **192**, 899-905 (2000).

245. Mahad, D.J. & Ransohoff, R.M. The role of MCP-1 (CCL2) and CCR2 in multiple sclerosis and experimental autoimmune encephalomyelitis (EAE). *Seminars in immunology* **15**, 23-32 (2003).

246. Bay-Richter, C., Janelidze, S., Hallberg, L. & Brundin, L. Changes in behaviour and cytokine expression upon a peripheral immune challenge. *Behavioural brain research* **222**, 193-199 (2011).

247. Ley, K., Laudanna, C., Cybulsky, M.I. & Nourshargh, S. Getting to the site of inflammation: the leukocyte adhesion cascade updated. *Nature reviews. Immunology* **7**, 678-689 (2007).

248. Stamatovic, S.M., Keep, R.F. & Andjelkovic, A.V. Brain endothelial cell-cell junctions: how to "open" the blood brain barrier. *Current neuropharmacology* **6**, 179-192 (2008).

249. Plumb, J., McQuaid, S., Mirakhur, M. & Kirk, J. Abnormal endothelial tight junctions in active lesions and normal-appearing white matter in multiple sclerosis. *Brain pathology* **12**, 154-169 (2002).

250. Gronberg, N.V., Johansen, F.F., Kristiansen, U. & Hasseldam, H. Leukocyte infiltration in experimental stroke. *Journal of neuroinflammation* **10**, 115 (2013).

251. Israelsson, C. *et al.* Distinct cellular patterns of upregulated chemokine expression supporting a prominent inflammatory role in traumatic brain injury. *Journal of neurotrauma* **25**, 959-974 (2008).

252. Roe, K., Orillo, B. & Verma, S. West Nile virus-induced cell adhesion molecules on human brain microvascular endothelial cells regulate leukocyte adhesion and modulate permeability of the in vitro blood-brain barrier model. *PloS one* **9**, e102598 (2014).

253. Carlos, T.M., Clark, R.S., Franicola-Higgins, D., Schiding, J.K. & Kochanek, P.M. Expression of endothelial adhesion molecules and recruitment of neutrophils after traumatic brain injury in rats. *Journal of leukocyte biology* **61**, 279-285 (1997).

254. O'Sullivan, J.B., Ryan, K.M., Harkin, A. & Connor, T.J. Noradrenaline reuptake inhibitors inhibit expression of chemokines IP-10 and RANTES and cell adhesion molecules VCAM-1 and ICAM-1 in the CNS following a systemic inflammatory challenge. *Journal of neuroimmunology* **220**, 34-42 (2010).

255. Whalen, M.J. *et al.* Reduced brain edema after traumatic brain injury in mice deficient in P-selectin and intercellular adhesion molecule-1. *Journal of leukocyte biology* **67**, 160-168 (2000).

256. Tang, T., Frenette, P.S., Hynes, R.O., Wagner, D.D. & Mayadas, T.N. Cytokine-induced meningitis is dramatically attenuated in mice deficient in endothelial selectins. *The Journal of clinical investigation* **97**, 2485-2490 (1996).

257. Wong, D. & Dorovini-Zis, K. Upregulation of intercellular adhesion molecule-1 (ICAM-1) expression in primary cultures of human brain microvessel endothelial cells by cytokines and lipopolysaccharide. *Journal of neuroimmunology* **39**, 11-21 (1992).

258. Cannella, B. & Raine, C.S. The adhesion molecule and cytokine profile of multiple sclerosis lesions. *Annals of neurology* **37**, 424-435 (1995).

259. Allport, J.R., Muller, W.A. & Luscinskas, F.W. Monocytes induce reversible focal changes in vascular endothelial cadherin complex during transendothelial migration under flow. *The Journal of cell biology* **148**, 203-216 (2000).

260. Reijerkerk, A. *et al.* Diapedesis of monocytes is associated with MMP-mediated occludin disappearance in brain endothelial cells. *FASEB journal : official publication of the Federation of American Societies for Experimental Biology* **20**, 2550-2552 (2006).

261. Minagar, A. *et al.* Serum from patients with multiple sclerosis downregulates occludin and VE-cadherin expression in cultured endothelial cells. *Multiple sclerosis* **9**, 235-238 (2003).

262. Czigner, A. *et al.* Kinetics of the cellular immune response following closed head injury. *Acta neurochirurgica* **149**, 281-289 (2007).

263. Satoh, S. *et al.* Inhibition of neutrophil migration by a protein kinase inhibitor for the treatment of ischemic brain infarction. *Japanese journal of pharmacology* **80**, 41-48 (1999).

264. Denes, A. *et al.* Proliferating resident microglia after focal cerebral ischaemia in mice. *Journal of cerebral blood flow and metabolism : official journal of the International Society of Cerebral Blood Flow and Metabolism* **27**, 1941-1953 (2007).

265. Yilmaz, G., Arumugam, T.V., Stokes, K.Y. & Granger, D.N. Role of T lymphocytes and interferon-gamma in ischemic stroke. *Circulation* **113**, 2105-2112 (2006).

266. Campanella, M., Sciorati, C., Tarozzo, G. & Beltramo, M. Flow cytometric analysis of inflammatory cells in ischemic rat brain. *Stroke; a journal of cerebral circulation* **33**, 586-592 (2002).

267. Fassbender, K. *et al.* Inflammatory leukocyte infiltration in focal cerebral ischemia: unrelated to infarct size. *Cerebrovascular diseases* **13**, 198-203 (2002).

268. Zhang, R.L., Chopp, M., Chen, H. & Garcia, J.H. Temporal profile of ischemic tissue damage, neutrophil response, and vascular plugging following permanent and transient (2H) middle cerebral artery occlusion in the rat. *Journal of the neurological sciences* **125**, 3-10 (1994).

269. Stevens, S.L. *et al.* The use of flow cytometry to evaluate temporal changes in inflammatory cells following focal cerebral ischemia in mice. *Brain research* **932**, 110-119 (2002).

270. Banks, W.A., Kastin, A.J. & Gutierrez, E.G. Penetration of interleukin-6 across the murine blood-brain barrier. *Neuroscience letters* **179**, 53-56 (1994).

271. Banks, W.A., Ortiz, L., Plotkin, S.R. & Kastin, A.J. Human interleukin (IL) 1 alpha, murine IL-1 alpha and murine IL-1 beta are transported from blood to brain in the mouse by a shared saturable mechanism. *The Journal of pharmacology and experimental therapeutics* **259**, 988-996 (1991).

272. Gutierrez, E.G., Banks, W.A. & Kastin, A.J. Murine tumor necrosis factor alpha is transported from blood to brain in the mouse. *Journal of neuroimmunology* **47**, 169-176 (1993).

273. Pan, W., Banks, W.A. & Kastin, A.J. Permeability of the blood-brain and blood-spinal cord barriers to interferons. *Journal of neuroimmunology* **76**, 105-111 (1997).

274. Marchi, N. *et al.* The etiological role of blood-brain barrier dysfunction in seizure disorders. *Cardiovascular psychiatry and neurology* **2011**, 482415 (2011).

275. Anderson, V.C., Lenar, D.P., Quinn, J.F. & Rooney, W.D. The blood-brain barrier and microvascular water exchange in Alzheimer's disease. *Cardiovascular psychiatry and neurology* **2011**, 615829 (2011).

276. Dantzer, R., Konsman, J.P., Bluthe, R.M. & Kelley, K.W. Neural and humoral pathways of communication from the immune system to the brain: parallel or convergent? *Autonomic neuroscience : basic & clinical* **85**, 60-65 (2000).

277. Serrats, J. *et al.* Dual roles for perivascular macrophages in immune-to-brain signaling. *Neuron* **65**, 94-106 (2010).

278. Lin, C.C. *et al.* Upregulation of COX-2/PGE2 by ET-1 mediated through Ca2+-dependent signals in mouse brain microvascular endothelial cells. *Molecular neurobiology* **49**, 1256-1269 (2014).

279. Bullitt, E. Expression of c-fos-like protein as a marker for neuronal activity following noxious stimulation in the rat. *The Journal of comparative neurology* **296**, 517-530 (1990).

280. Herkenham, M., Lee, H.Y. & Baker, R.A. Temporal and spatial patterns of c-fos mRNA induced by intravenous interleukin-1: a cascade of non-neuronal cellular activation at the blood-brain barrier. *The Journal of comparative neurology* **400**, 175-196 (1998).

281. Saijo, K. & Glass, C.K. Microglial cell origin and phenotypes in health and disease. *Nature reviews. Immunology* **11**, 775-787 (2011).
282. Pavlov, V.A. & Tracey, K.J. The vagus nerve and the inflammatory reflex--linking immunity and metabolism. *Nature reviews. Endocrinology* **8**, 743-754 (2012).
283. McCorry, L.K. Physiology of the autonomic nervous system. *American journal of pharmaceutical education* **71**, 78 (2007).
284. Bernik, T.R. *et al.* Pharmacological stimulation of the cholinergic antiinflammatory pathway. *The Journal of experimental medicine* **195**, 781-788 (2002).
285. Reyes, E.P. *et al.* LPS-induced c-Fos activation in NTS neurons and plasmatic cortisol increases in septic rats are suppressed by bilateral carotid chemodenervation. *Advances in experimental medicine and biology* **758**, 185-190 (2012).
286. Marvel, F.A., Chen, C.C., Badr, N., Gaykema, R.P. & Goehler, L.E. Reversible inactivation of the dorsal vagal complex blocks lipopolysaccharide-induced social withdrawal and c-Fos expression in central autonomic nuclei. *Brain, behavior, and immunity* **18**, 123-134 (2004).
287. Wan, W., Wetmore, L., Sorensen, C.M., Greenberg, A.H. & Nance, D.M. Neural and biochemical mediators of endotoxin and stress-induced c-fos expression in the rat brain. *Brain research bulletin* **34**, 7-14 (1994).
288. Bluthe, R.M., Michaud, B., Kelley, K.W. & Dantzer, R. Vagotomy attenuates behavioural effects of interleukin-1 injected peripherally but not centrally. *Neuroreport* **7**, 1485-1488 (1996).
289. Bluthe, R.M., Michaud, B., Kelley, K.W. & Dantzer, R. Vagotomy blocks behavioural effects of interleukin-1 injected via the intraperitoneal route but not via other systemic routes. *Neuroreport* **7**, 2823-2827 (1996).
290. Hansen, M.K., O'Connor, K.A., Goehler, L.E., Watkins, L.R. & Maier, S.F. The contribution of the vagus nerve in interleukin-1beta-induced fever is dependent on dose. *American journal of physiology. Regulatory, integrative and comparative physiology* **280**, R929-934 (2001).
291. Tracey, K.J. The inflammatory reflex. *Nature* **420**, 853-859 (2002).
292. Shytle, R.D. *et al.* Cholinergic modulation of microglial activation by alpha 7 nicotinic receptors. *Journal of neurochemistry* **89**, 337-343 (2004).
293. Kawashima, K. & Fujii, T. Expression of non-neuronal acetylcholine in lymphocytes and its contribution to the regulation of immune function. *Frontiers in bioscience : a journal and virtual library* **9**, 2063-2085 (2004).
294. Borovikova, L.V. *et al.* Vagus nerve stimulation attenuates the systemic inflammatory response to endotoxin. *Nature* **405**, 458-462 (2000).
295. Konsman, J.P., Luheshi, G.N., Bluthe, R.M. & Dantzer, R. The vagus nerve mediates behavioural depression, but not fever, in response to peripheral immune signals; a functional anatomical analysis. *The European journal of neuroscience* **12**, 4434-4446 (2000).
296. Bellavance, M.A. & Rivest, S. The HPA - Immune Axis and the Immunomodulatory Actions of Glucocorticoids in the Brain. *Frontiers in immunology* **5**, 136 (2014).
297. Goldstein, D.S. Adrenal responses to stress. *Cellular and molecular neurobiology* **30**, 1433-1440 (2010).
298. Silverman, M.N. & Sternberg, E.M. Glucocorticoid regulation of inflammation and its functional correlates: from HPA axis to

glucocorticoid receptor dysfunction. *Annals of the New York Academy of Sciences* **1261**, 55-63 (2012).

299. Lee, S.W. *et al.* Glucocorticoids selectively inhibit the transcription of the interleukin 1 beta gene and decrease the stability of interleukin 1 beta mRNA. *Proceedings of the National Academy of Sciences of the United States of America* **85**, 1204-1208 (1988).

300. Goujon, E., Laye, S., Parnet, P. & Dantzer, R. Regulation of cytokine gene expression in the central nervous system by glucocorticoids: mechanisms and functional consequences. *Psychoneuroendocrinology* **22 Suppl 1**, S75-80 (1997).

301. Maes, M., Calabrese, J. & Meltzer, H.Y. The relevance of the in- versus outpatient status for studies on HPA-axis in depression: spontaneous hypercortisolism is a feature of major depressed inpatients and not of major depression per se. *Progress in neuro-psychopharmacology & biological psychiatry* **18**, 503-517 (1994).

302. Liu, Y., Ho, R.C. & Mak, A. Interleukin (IL)-6, tumour necrosis factor alpha (TNF-alpha) and soluble interleukin-2 receptors (sIL-2R) are elevated in patients with major depressive disorder: a meta-analysis and meta-regression. *Journal of affective disorders* **139**, 230-239 (2012).

303. Dahl, J. *et al.* The plasma levels of various cytokines are increased during ongoing depression and are reduced to normal levels after recovery. *Psychoneuroendocrinology* **45**, 77-86 (2014).

304. Maes, M. *et al.* Relationships between interleukin-6 activity, acute phase proteins, and function of the hypothalamic-pituitary-adrenal axis in severe depression. *Psychiatry research* **49**, 11-27 (1993).

305. Berkenbosch, F., van Oers, J., del Rey, A., Tilders, F. & Besedovsky, H. Corticotropin-releasing factor-producing neurons in the rat activated by interleukin-1. *Science* **238**, 524-526 (1987).

306. Andreis, P.G. *et al.* Interleukin-1 beta enhances corticosterone secretion by acting directly on the rat adrenal gland. *Endocrinology* **129**, 53-57 (1991).

307. Samuels, B.A. *et al.* Modeling treatment-resistant depression. *Neuropharmacology* **61**, 408-413 (2011).

308. Sainio, E.L., Pulkki, K. & Young, S.N. L-Tryptophan: Biochemical, nutritional and pharmacological aspects. *Amino acids* **10**, 21-47 (1996).

309. Fukui, S., Schwarcz, R., Rapoport, S.I., Takada, Y. & Smith, Q.R. Blood-brain barrier transport of kynurenines: implications for brain synthesis and metabolism. *Journal of neurochemistry* **56**, 2007-2017 (1991).

310. Heyes, M.P. *et al.* Quinolinic acid and kynurenine pathway metabolism in inflammatory and non-inflammatory neurological disease. *Brain : a journal of neurology* **115 (Pt 5)**, 1249-1273 (1992).

311. Alberati-Giani, D., Ricciardi-Castagnoli, P., Kohler, C. & Cesura, A.M. Regulation of the kynurenine metabolic pathway by interferon-gamma in murine cloned macrophages and microglial cells. *Journal of neurochemistry* **66**, 996-1004 (1996).

312. Rossler, W., Salize, H.J., van Os, J. & Riecher-Rossler, A. Size of burden of schizophrenia and psychotic disorders. *European neuropsychopharmacology : the journal of the European College of Neuropsychopharmacology* **15**, 399-409 (2005).

313. Lapin, I.P. Neurokynurenines (NEKY) as common neurochemical links of stress and anxiety. *Advances in experimental medicine and biology* **527**, 121-125 (2003).

314. Saito, K., Crowley, J.S., Markey, S.P. & Heyes, M.P. A mechanism for increased quinolinic acid formation following acute systemic immune stimulation. *The Journal of biological chemistry* **268**, 15496-15503 (1993).
315. Taylor, M.W. & Feng, G.S. Relationship between interferon-gamma, indoleamine 2,3-dioxygenase, and tryptophan catabolism. *FASEB journal : official publication of the Federation of American Societies for Experimental Biology* **5**, 2516-2522 (1991).
316. Muller, N. & Schwarz, M.J. The immune-mediated alteration of serotonin and glutamate: towards an integrated view of depression. *Molecular psychiatry* **12**, 988-1000 (2007).
317. Musso, T., Gusella, G.L., Brooks, A., Longo, D.L. & Varesio, L. Interleukin-4 inhibits indoleamine 2,3-dioxygenase expression in human monocytes. *Blood* **83**, 1408-1411 (1994).
318. Mellor, A.L. & Munn, D.H. IDO expression by dendritic cells: tolerance and tryptophan catabolism. *Nature reviews. Immunology* **4**, 762-774 (2004).
319. Munn, D.H. *et al.* Inhibition of T cell proliferation by macrophage tryptophan catabolism. *The Journal of experimental medicine* **189**, 1363-1372 (1999).
320. Christmas, D.M., Potokar, J. & Davies, S.J. A biological pathway linking inflammation and depression: activation of indoleamine 2,3-dioxygenase. *Neuropsychiatric disease and treatment* **7**, 431-439 (2011).
321. Potvin, S. *et al.* Inflammatory cytokine alterations in schizophrenia: a systematic quantitative review. *Biological psychiatry* **63**, 801-808 (2008).
322. Reichenberg, A. *et al.* Cytokine-associated emotional and cognitive disturbances in humans. *Archives of general psychiatry* **58**, 445-452 (2001).
323. Hauser, P. *et al.* A prospective study of the incidence and open-label treatment of interferon-induced major depressive disorder in patients with hepatitis C. *Molecular psychiatry* **7**, 942-947 (2002).
324. Kraus, M.R., Schafer, A., Faller, H., Csef, H. & Scheurlen, M. Psychiatric symptoms in patients with chronic hepatitis C receiving interferon alfa-2b therapy. *The Journal of clinical psychiatry* **64**, 708-714 (2003).
325. Udina, M. *et al.* Interferon-induced depression in chronic hepatitis C: a systematic review and meta-analysis. *The Journal of clinical psychiatry* **73**, 1128-1138 (2012).
326. Malaguarnera, M. *et al.* Neuropsychiatric effects and type of IFN-alpha in chronic hepatitis C. *Journal of interferon & cytokine research : the official journal of the International Society for Interferon and Cytokine Research* **21**, 273-278 (2001).
327. Amodio, P. *et al.* Mood, cognition and EEG changes during interferon alpha (alpha-IFN) treatment for chronic hepatitis C. *Journal of affective disorders* **84**, 93-98 (2005).
328. Capuron, L. *et al.* Neurobehavioral effects of interferon-alpha in cancer patients: phenomenology and paroxetine responsiveness of symptom dimensions. *Neuropsychopharmacology : official publication of the American College of Neuropsychopharmacology* **26**, 643-652 (2002).
329. Tyring, S. *et al.* Etanercept and clinical outcomes, fatigue, and depression in psoriasis: double-blind placebo-controlled randomised phase III trial. *Lancet* **367**, 29-35 (2006).
330. Reichenberg, A. *et al.* Endotoxin-induced changes in food consumption in healthy volunteers are associated with TNF-alpha and IL-6 secretion. *Psychoneuroendocrinology* **27**, 945-956 (2002).

331. Ming, G.L. & Song, H. Adult neurogenesis in the mammalian brain: significant answers and significant questions. *Neuron* **70**, 687-702 (2011).
332. Sahay, A. *et al*. Increasing adult hippocampal neurogenesis is sufficient to improve pattern separation. *Nature* **472**, 466-470 (2011).
333. Snyder, J.S., Soumier, A., Brewer, M., Pickel, J. & Cameron, H.A. Adult hippocampal neurogenesis buffers stress responses and depressive behaviour. *Nature* **476**, 458-461 (2011).
334. Akers, K.G. *et al*. Hippocampal neurogenesis regulates forgetting during adulthood and infancy. *Science* **344**, 598-602 (2014).
335. Mongiat, L.A. & Schinder, A.F. Neuroscience. A price to pay for adult neurogenesis. *Science* **344**, 594-595 (2014).
336. Phillips, W., Michell, A.W. & Barker, R.A. Neurogenesis in diseases of the central nervous system. *Stem cells and development* **15**, 359-379 (2006).
337. Sheline, Y.I., Wang, P.W., Gado, M.H., Csernansky, J.G. & Vannier, M.W. Hippocampal atrophy in recurrent major depression. *Proceedings of the National Academy of Sciences of the United States of America* **93**, 3908-3913 (1996).
338. Campbell, S. & MacQueen, G. An update on regional brain volume differences associated with mood disorders. *Current opinion in psychiatry* **19**, 25-33 (2006).
339. Malberg, J.E., Eisch, A.J., Nestler, E.J. & Duman, R.S. Chronic antidepressant treatment increases neurogenesis in adult rat hippocampus. *The Journal of neuroscience : the official journal of the Society for Neuroscience* **20**, 9104-9110 (2000).
340. van Praag, H., Kempermann, G. & Gage, F.H. Running increases cell proliferation and neurogenesis in the adult mouse dentate gyrus. *Nature neuroscience* **2**, 266-270 (1999).
341. Olson, A.K., Eadie, B.D., Ernst, C. & Christie, B.R. Environmental enrichment and voluntary exercise massively increase neurogenesis in the adult hippocampus via dissociable pathways. *Hippocampus* **16**, 250-260 (2006).
342. Waterhouse, E.G. *et al*. BDNF promotes differentiation and maturation of adult-born neurons through GABAergic transmission. *The Journal of neuroscience : the official journal of the Society for Neuroscience* **32**, 14318-14330 (2012).
343. Sakata, K. *et al*. Effects of antidepressant treatment on mice lacking brain-derived neurotrophic factor expression through promoter IV. *The European journal of neuroscience* **37**, 1863-1874 (2013).
344. Lang, U.E. & Borgwardt, S. Molecular mechanisms of depression: perspectives on new treatment strategies. *Cellular physiology and biochemistry : international journal of experimental cellular physiology, biochemistry, and pharmacology* **31**, 761-777 (2013).
345. Gemma, C. & Bachstetter, A.D. The role of microglia in adult hippocampal neurogenesis. *Frontiers in cellular neuroscience* **7**, 229 (2013).
346. Neumann, H., Kotter, M.R. & Franklin, R.J. Debris clearance by microglia: an essential link between degeneration and regeneration. *Brain : a journal of neurology* **132**, 288-295 (2009).
347. Nakamura, Y., Si, Q.S. & Kataoka, K. Lipopolysaccharide-induced microglial activation in culture: temporal profiles of morphological change and release of cytokines and nitric oxide. *Neuroscience research* **35**, 95-100 (1999).

348. Pinkernelle, J., Fansa, H., Ebmeyer, U. & Keilhoff, G. Prolonged minocycline treatment impairs motor neuronal survival and glial function in organotypic rat spinal cord cultures. *PloS one* **8**, e73422 (2013).
349. Nair, R.P. *et al.* Evidence for two psoriasis susceptibility loci (HLA and 17q) and two novel candidate regions (16q and 20p) by genome-wide scan. *Human molecular genetics* **6**, 1349-1356 (1997).
350. Cargill, M. *et al.* A large-scale genetic association study confirms IL12B and leads to the identification of IL23R as psoriasis-risk genes. *American journal of human genetics* **80**, 273-290 (2007).
351. Capon, F. *et al.* Sequence variants in the genes for the interleukin-23 receptor (IL23R) and its ligand (IL12B) confer protection against psoriasis. *Human genetics* **122**, 201-206 (2007).
352. Trembath, R.C. *et al.* Identification of a major susceptibility locus on chromosome 6p and evidence for further disease loci revealed by a two stage genome-wide search in psoriasis. *Human molecular genetics* **6**, 813-820 (1997).
353. Lee, E. *et al.* Increased expression of interleukin 23 p19 and p40 in lesional skin of patients with psoriasis vulgaris. *The Journal of experimental medicine* **199**, 125-130 (2004).
354. Zheng, Y. *et al.* Interleukin-22, a T(H)17 cytokine, mediates IL-23-induced dermal inflammation and acanthosis. *Nature* **445**, 648-651 (2007).
355. Fujita, H. The role of IL-22 and Th22 cells in human skin diseases. *Journal of dermatological science* **72**, 3-8 (2013).
356. Wolk, K. *et al.* IL-22 regulates the expression of genes responsible for antimicrobial defense, cellular differentiation, and mobility in keratinocytes: a potential role in psoriasis. *European journal of immunology* **36**, 1309-1323 (2006).
357. Skroza, N. *et al.* Correlations between psoriasis and inflammatory bowel diseases. *BioMed research international* **2013**, 983902 (2013).
358. Szeimies, R.M. *et al.* Imiquimod 5% cream for the treatment of actinic keratosis: results from a phase III, randomized, double-blind, vehicle-controlled, clinical trial with histology. *Journal of the American Academy of Dermatology* **51**, 547-555 (2004).
359. Karnes, J.B. & Usatine, R.P. Management of external genital warts. *American family physician* **90**, 312-318 (2014).
360. Geisse, J. *et al.* Imiquimod 5% cream for the treatment of superficial basal cell carcinoma: results from two phase III, randomized, vehicle-controlled studies. *Journal of the American Academy of Dermatology* **50**, 722-733 (2004).
361. Fanti, P.A., Dika, E., Vaccari, S., Miscial, C. & Varotti, C. Generalized psoriasis induced by topical treatment of actinic keratosis with imiquimod. *International journal of dermatology* **45**, 1464-1465 (2006).
362. Patel, U., Mark, N.M., Machler, B.C. & Levine, V.J. Imiquimod 5% cream induced psoriasis: a case report, summary of the literature and mechanism. *The British journal of dermatology* **164**, 670-672 (2011).
363. Vinter, H., Iversen, L., Steiniche, T., Kragballe, K. & Johansen, C. Aldara-induced skin inflammation - studies of psoriasis patients. *The British journal of dermatology* (2014).
364. Gudjonsson, J.E., Johnston, A., Dyson, M., Valdimarsson, H. & Elder, J.T. Mouse models of psoriasis. *The Journal of investigative dermatology* **127**, 1292-1308 (2007).

365.	Ueyama, A. *et al.* Mechanism of pathogenesis of imiquimod-induced skin inflammation in the mouse: a role for interferon-alpha in dendritic cell activation by imiquimod. *The Journal of dermatology* **41**, 135-143 (2014).

366.	van der Fits, L. *et al.* Imiquimod-induced psoriasis-like skin inflammation in mice is mediated via the IL-23/IL-17 axis. *Journal of immunology* **182**, 5836-5845 (2009).

367.	Kadowaki, N. *et al.* Subsets of human dendritic cell precursors express different toll-like receptors and respond to different microbial antigens. *The Journal of experimental medicine* **194**, 863-869 (2001).

368.	Palamara, F. *et al.* Identification and characterization of pDC-like cells in normal mouse skin and melanomas treated with imiquimod. *Journal of immunology* **173**, 3051-3061 (2004).

369.	Gibson, S.J. *et al.* Plasmacytoid dendritic cells produce cytokines and mature in response to the TLR7 agonists, imiquimod and resiquimod. *Cellular immunology* **218**, 74-86 (2002).

370.	Ito, T. *et al.* Interferon-alpha and interleukin-12 are induced differentially by Toll-like receptor 7 ligands in human blood dendritic cell subsets. *The Journal of experimental medicine* **195**, 1507-1512 (2002).

371.	Wohn, C. *et al.* Langerin(neg) conventional dendritic cells produce IL-23 to drive psoriatic plaque formation in mice. *Proceedings of the National Academy of Sciences of the United States of America* **110**, 10723-10728 (2013).

372.	Walter, A. *et al.* Aldara activates TLR7-independent immune defence. *Nature communications* **4**, 1560 (2013).

373.	Deacon, R.M. Burrowing in rodents: a sensitive method for detecting behavioral dysfunction. *Nature protocols* **1**, 118-121 (2006).

374.	Stuart, M.J. & Baune, B.T. Chemokines and chemokine receptors in mood disorders, schizophrenia, and cognitive impairment: a systematic review of biomarker studies. *Neuroscience and biobehavioral reviews* **42**, 93-115 (2014).

375.	Fu, X. *et al.* Central administration of lipopolysaccharide induces depressive-like behavior in vivo and activates brain indoleamine 2,3 dioxygenase in murine organotypic hippocampal slice cultures. *Journal of neuroinflammation* **7**, 43 (2010).

376.	Nakajima, K. *et al.* Distinct roles of IL-23 and IL-17 in the development of psoriasis-like lesions in a mouse model. *Journal of immunology* **186**, 4481-4489 (2011).

377.	Thomson, C.A., McColl, A., Cavanagh, J. & Graham, G.J. Peripheral inflammation is associated with remote global gene expression changes in the brain. *Journal of neuroinflammation* **11**, 73 (2014).

378.	Ransohoff, R.M. *et al.* Astrocyte expression of mRNA encoding cytokines IP-10 and JE/MCP-1 in experimental autoimmune encephalomyelitis. *FASEB journal : official publication of the Federation of American Societies for Experimental Biology* **7**, 592-600 (1993).

379.	Takada, H. *et al.* Increased serum levels of interferon-gamma-inducible protein 10 and monokine induced by gamma interferon in patients with haemophagocytic lymphohistiocytosis. *Clinical and experimental immunology* **133**, 448-453 (2003).

380.	Simpson, J.E., Newcombe, J., Cuzner, M.L. & Woodroofe, M.N. Expression of the interferon-gamma-inducible chemokines IP-10 and Mig and their receptor, CXCR3, in multiple sclerosis lesions. *Neuropathology and applied neurobiology* **26**, 133-142 (2000).

381. Amin, D.N. *et al*. Expression and role of CXCL10 during the encephalitic stage of experimental and clinical African trypanosomiasis. *The Journal of infectious diseases* **200**, 1556-1565 (2009).
382. Klein, R.S. *et al*. Neuronal CXCL10 directs CD8+ T-cell recruitment and control of West Nile virus encephalitis. *Journal of virology* **79**, 11457-11466 (2005).
383. Chai, Q., She, R., Huang, Y. & Fu, Z.F. Expression of Neuronal CXCL10 Induced by Rabies Virus Infection Initiates Infiltration of Inflammatory Cells, Production of Chemokines and Cytokines, and Enhancement of Blood-Brain Barrier Permeability. *Journal of virology* **89**, 870-876 (2015).
384. Teeling, J.L., Cunningham, C., Newman, T.A. & Perry, V.H. The effect of non-steroidal anti-inflammatory agents on behavioural changes and cytokine production following systemic inflammation: Implications for a role of COX-1. *Brain, behavior, and immunity* **24**, 409-419 (2010).
385. Cunningham, C. *et al*. Systemic inflammation induces acute behavioral and cognitive changes and accelerates neurodegenerative disease. *Biological psychiatry* **65**, 304-312 (2009).
386. Lund, J.M. *et al*. Recognition of single-stranded RNA viruses by Toll-like receptor 7. *Proceedings of the National Academy of Sciences of the United States of America* **101**, 5598-5603 (2004).
387. Puig, M. *et al*. TLR9 and TLR7 agonists mediate distinct type I IFN responses in humans and nonhuman primates in vitro and in vivo. *Journal of leukocyte biology* **91**, 147-158 (2012).
388. Diebold, S.S., Kaisho, T., Hemmi, H., Akira, S. & Reis e Sousa, C. Innate antiviral responses by means of TLR7-mediated recognition of single-stranded RNA. *Science* **303**, 1529-1531 (2004).
389. Hemmi, H. *et al*. Small anti-viral compounds activate immune cells via the TLR7 MyD88-dependent signaling pathway. *Nature immunology* **3**, 196-200 (2002).
390. Perry, A.K., Chen, G., Zheng, D., Tang, H. & Cheng, G. The host type I interferon response to viral and bacterial infections. *Cell research* **15**, 407-422 (2005).
391. Butchi, N.B., Woods, T., Du, M., Morgan, T.W. & Peterson, K.E. TLR7 and TLR9 trigger distinct neuroinflammatory responses in the CNS. *The American journal of pathology* **179**, 783-794 (2011).
392. Wacher, C. *et al*. Coordinated regulation and widespread cellular expression of interferon-stimulated genes (ISG) ISG-49, ISG-54, and ISG-56 in the central nervous system after infection with distinct viruses. *Journal of virology* **81**, 860-871 (2007).
393. van den Pol, A.N., Ding, S. & Robek, M.D. Long-distance interferon signaling within the brain blocks virus spread. *Journal of virology* **88**, 3695-3704 (2014).
394. Mostafavi, S. *et al*. Type I interferon signaling genes in recurrent major depression: increased expression detected by whole-blood RNA sequencing. *Molecular psychiatry* **19**, 1267-1274 (2014).
395. Malek-Ahmadi, P. Mood disorders associated with interferon treatment: theoretical and practical considerations. *The Annals of pharmacotherapy* **35**, 489-495 (2001).
396. Dieperink, E., Willenbring, M. & Ho, S.B. Neuropsychiatric symptoms associated with hepatitis C and interferon alpha: A review. *The American journal of psychiatry* **157**, 867-876 (2000).
397. Constant, A. *et al*. Mood alterations during interferon-alfa therapy in patients with chronic hepatitis C: evidence for an overlap between

manic/hypomanic and depressive symptoms. *The Journal of clinical psychiatry* **66**, 1050-1057 (2005).

398. Stanley, P.L., Steiner, S., Havens, M. & Tramposch, K.M. Mouse skin inflammation induced by multiple topical applications of 12-O-tetradecanoylphorbol-13-acetate. *Skin pharmacology : the official journal of the Skin Pharmacology Society* **4**, 262-271 (1991).

399. Wen-Sheng, W. & Jun-Ming, H. Activation of protein kinase C alpha is required for TPA-triggered ERK (MAPK) signaling and growth inhibition of human hepatoma cell HepG2. *Journal of biomedical science* **12**, 289-296 (2005).

400. Aspord, C. *et al*. Imiquimod inhibits melanoma development by promoting pDC cytotoxic functions and impeding tumor vascularization. *The Journal of investigative dermatology* **134**, 2551-2561 (2014).

401. Wohn, C.T., Pantelyushin, S., Ober-Blobaum, J.L. & Clausen, B.E. Aldara-induced psoriasis-like skin inflammation: isolation and characterization of cutaneous dendritic cells and innate lymphocytes. *Methods in molecular biology* **1193**, 171-185 (2014).

402. Greig, N.H., Fredericks, W.R., Holloway, H.W., Soncrant, T.T. & Rapoport, S.I. Delivery of human interferon-alpha to brain by transient osmotic blood-brain barrier modification in the rat. *The Journal of pharmacology and experimental therapeutics* **245**, 581-586 (1988).

403. Fioravanti, J. *et al*. The fusion protein of IFN-alpha and apolipoprotein A-I crosses the blood-brain barrier by a saturable transport mechanism. *Journal of immunology* **188**, 3988-3992 (2012).

404. Baggiolini, M. Chemokines and leukocyte traffic. *Nature* **392**, 565-568 (1998).

405. Michlmayr, D. & Lim, J.K. Chemokine receptors as important regulators of pathogenesis during arboviral encephalitis. *Frontiers in cellular neuroscience* **8**, 264 (2014).

406. Erickson, M.A. & Banks, W.A. Cytokine and chemokine responses in serum and brain after single and repeated injections of lipopolysaccharide: multiplex quantification with path analysis. *Brain, behavior, and immunity* **25**, 1637-1648 (2011).

407. Marques, C.P. *et al*. Prolonged microglial cell activation and lymphocyte infiltration following experimental herpes encephalitis. *Journal of immunology* **181**, 6417-6426 (2008).

408. Dufour, J.H. *et al*. IFN-gamma-inducible protein 10 (IP-10; CXCL10)-deficient mice reveal a role for IP-10 in effector T cell generation and trafficking. *Journal of immunology* **168**, 3195-3204 (2002).

409. Karpus, W.J. & Ransohoff, R.M. Chemokine regulation of experimental autoimmune encephalomyelitis: temporal and spatial expression patterns govern disease pathogenesis. *Journal of immunology* **161**, 2667-2671 (1998).

410. Jamieson, T. *et al*. The chemokine receptor D6 limits the inflammatory response in vivo. *Nature immunology* **6**, 403-411 (2005).

411. Baldwin, H.M. *et al*. Microarray analyses demonstrate the involvement of type I interferons in psoriasiform pathology development in D6-deficient mice. *The Journal of biological chemistry* **288**, 36473-36483 (2013).

412. Kohman, R.A. & Rhodes, J.S. Neurogenesis, inflammation and behavior. *Brain, behavior, and immunity* **27**, 22-32 (2013).

413. Kempermann, G., Wiskott, L. & Gage, F.H. Functional significance of adult neurogenesis. *Current opinion in neurobiology* **14**, 186-191 (2004).

414. Ekdahl, C.T., Claasen, J.H., Bonde, S., Kokaia, Z. & Lindvall, O. Inflammation is detrimental for neurogenesis in adult brain. *Proceedings of the National Academy of Sciences of the United States of America* **100**, 13632-13637 (2003).

415. Liu, Q. *et al.* Interleukin-17 inhibits Adult Hippocampal Neurogenesis. *Scientific reports* **4**, 7554 (2014).

416. Monje, M.L., Toda, H. & Palmer, T.D. Inflammatory blockade restores adult hippocampal neurogenesis. *Science* **302**, 1760-1765 (2003).

417. Dickens, C., McGowan, L., Clark-Carter, D. & Creed, F. Depression in rheumatoid arthritis: a systematic review of the literature with meta-analysis. *Psychosomatic medicine* **64**, 52-60 (2002).

418. Russo, P.A., Ilchef, R. & Cooper, A.J. Psychiatric morbidity in psoriasis: a review. *The Australasian journal of dermatology* **45**, 155-159; quiz 160-151 (2004).

419. Neves, G., Cooke, S.F. & Bliss, T.V. Synaptic plasticity, memory and the hippocampus: a neural network approach to causality. *Nature reviews. Neuroscience* **9**, 65-75 (2008).

420. Kagan, J.C. *et al.* TRAM couples endocytosis of Toll-like receptor 4 to the induction of interferon-beta. *Nature immunology* **9**, 361-368 (2008).

421. Yokogawa, M. *et al.* Epicutaneous application of toll-like receptor 7 agonists leads to systemic autoimmunity in wild-type mice: a new model of systemic Lupus erythematosus. *Arthritis & rheumatology* **66**, 694-706 (2014).

422. Chiu, I.M., von Hehn, C.A. & Woolf, C.J. Neurogenic inflammation and the peripheral nervous system in host defense and immunopathology. *Nature neuroscience* **15**, 1063-1067 (2012).

423. Goehler, L.E. *et al.* Vagal immune-to-brain communication: a visceral chemosensory pathway. *Autonomic neuroscience : basic & clinical* **85**, 49-59 (2000).

424. Kox, M. *et al.* Effects of vagus nerve stimulation and vagotomy on systemic and pulmonary inflammation in a two-hit model in rats. *PloS one* **7**, e34431 (2012).

425. Watkins, L.R. *et al.* Blockade of interleukin-1 induced hyperthermia by subdiaphragmatic vagotomy: evidence for vagal mediation of immune-brain communication. *Neuroscience letters* **183**, 27-31 (1995).

426. Honda, K. *et al.* IRF-7 is the master regulator of type-I interferon-dependent immune responses. *Nature* **434**, 772-777 (2005).

427. Gerondakis, S., Grossmann, M., Nakamura, Y., Pohl, T. & Grumont, R. Genetic approaches in mice to understand Rel/NF-kappaB and IkappaB function: transgenics and knockouts. *Oncogene* **18**, 6888-6895 (1999).

428. Muller, U. *et al.* Functional role of type I and type II interferons in antiviral defense. *Science* **264**, 1918-1921 (1994).

429. Walf, A.A. & Frye, C.A. The use of the elevated plus maze as an assay of anxiety-related behavior in rodents. *Nature protocols* **2**, 322-328 (2007).

430. Horner, A.E. *et al.* The touchscreen operant platform for testing learning and memory in rats and mice. *Nature protocols* **8**, 1961-1984 (2013).